

**DEVELOPMENT OF A CELL
ENCAPSULATION TECHNOLOGY FOR
THE PRODUCTION OF FUNCTIONAL,
MICRO-ENCAPSULATED
PANCREATIC ISLETS FOR
TRANSPLANTATION**

by

DIRK JAN CORNELISSEN

2019

THE THESIS IS SUBMITTED IN PARTIAL FULFILMENT
FOR THE DEGREE OF

**DOCTOR OF PHILOSOPHY IN
BIOMEDICAL ENGINEERING**

DEPARTMENT OF BIOMEDICAL ENGINEERING
UNIVERSITY OF STRATHCLYDE

This thesis is the result of the author's original research. It has been composed by the author and has not been previously submitted for examination which has led to the award of a degree.

The copyright of this thesis belongs to the author under the terms of the United Kingdom Copyright Acts as qualified by University of Strathclyde Regulation 3.50. Due acknowledgement must always be made of the use of any material contained in, or derived from, this thesis.

Signed:

Date: 14-05-2019

Abstract

Diabetes type 1 is an autoimmune disease in which the patient's own immune system destroys the insulin producing β -cells, located in the pancreatic islets. Without enough insulin production, the blood glucose levels of the patient rise, which can lead to damages of blood vessels and nerves, blindness or even seizures and comas. For some patients that have trouble maintaining normoglycaemia allogeneic islet transplantation has become an alternative treatment option. Patients with these transplanted islets are no longer prone to hypoglycaemic episodes and can sometimes become completely insulin independent. However, this success is not long-lived. The life span of the transplanted islets is limited due to the host's immune responses and the toxicity of modern immunosuppressive agents. In this thesis, islet encapsulation for clinical transplantation is investigated and further developed. Islet encapsulation can protect the islets from the immune system, without the aid of the immunosuppressants. The construction and optimization of a micro-encapsulator that can be used to create encapsulations is described, as well as the multiple parameters to create small, uniform encapsulations. To further enhance the biocompatibility and immunoprotective properties of alginate hydrogel, alginate was purified to eliminate most of the impurities and tested for its permeability. Encapsulating pancreatic islets in this purified alginate showed encouraging results, with the islets remaining viable and functional longer than their control counterparts. Larger islets can develop necrotic cores within encapsulations, due to the lack of vascularization. To create smaller islets out of dissociated larger islets, a single-step encapsulation and aggregation method was developed, that unfortunately was not suitable for islet cells, but was capable of developing functional hepatic organoids out of HepaRG cells, that could be used for drug testing. Finally, a proof of principle was given for the creation of pancreatic islet patches using 3D bioprinting methods.

Acknowledgements

I would like to thank everyone who helped me throughout my PhD. Whether it was through assisting me scientifically, or just being there for a coffee and a chat, this work would have been so much harder without you!

Foremost thanks to my supervisor Professor Will Shu. Your enthusiasm, creativity and encouragements really helped to move this research along. You always managed to see opportunities when I saw failure and the collection of weekly updates in my dropbox made the writing up so much easier! I would furthermore like to thank my colleagues from our lab, both at Heriot Watt and at Strathclyde. Alan, Atabak, Valentina, Chris, Gregor, Ian, Gareth, Ross, Jack, Ian and Jiezhong; Being able to both discuss my work with you guys and find some much needed distraction made my PhD a lot more bearable.

I would like to thank Medical Research Scotland for their funding of this project, as well as for their Commercial training days. I found these to be very informative and fun, but they also helped me to network with my peers, some who I now call my friends. In particular I would like to thank Alex Graham for organizing these days and always keeping in touch with me, even if it took me weeks to reply.

I would also like to thank my other supervisors. John Casey, your enthusiasm about my work was not unrecognised. Your input during our monthly meetings was a great help for the directions my research was taking. Jason King, your knowledge about all the different cell assays (and scientific practice in general) helped me to shape the experiments, and create better figures. Aidan Courtney, your different take on things was refreshing, and helped me to think more practical at times. I would also like to thank Professor Helen Grant for the

uplifting pep-talks and very useful tips and tricks. Your experience and knowledge have truly helped me, especially in the final stages of my PhD.

I would like to thank all the supporting staff at both Heriot-Watt and Strathclyde; Cameron Smith, Krystena Callaghan and Katie Henderson, thank you for keeping our lab working smoothly and helping me with my experiments. Linda Horan, thank you so much for teaching me about *in vivo* experiments and helping me with the eggs!

I would like to thank all my friends in PoBBBs for the fun and the coffee and Heriot Watt. Miguel and Isabel, buying the unlimited card with you guys was one of the better choices during my PhD. I would also like to thank my friends at Strathclyde, in particular my office-buddies Laura, Chaz and Kirsty. The coffee breaks and short talks with you guys kept me sane. Christine and Jock, you two were the best roommates a guy could ask for, I really enjoyed living with you guys, and was really sad when I had to move.

Natuurlijk wil ik ook mijn familie bedanken, en voornamelijk mijn ouders. Jullie steun en vertrouwen heeft me de mogelijkheid gegeven om deze kans te pakken, en jullie bezoeken maakten me altijd blij! Tim en Rens, bedankt dat jullie zulke goede grote broer/zus voor me geweest zijn! Walerie, ik hoop dat dit onderzoek jou ooit kan helpen! Bedankt voor het zijn van een inspiratiebron!

Miranda, Richte, Tom en Elise, de paar daagjes in het jaar dat ik jullie zag (of het nou hier of in Nederlands was) waren altijd de dagen waar ik naar uit keek in het jaar. *At Nauseam!*

Heren van V.S.G. Silenus (jullie zijn ondertussen met teveel om bij naam te noemen), ik heb veel dingen moeten overslaan afgelopen jaren, maar de dispuutsapp zorgde toch voor flink wat gemakkelijke afleiding. Als ik dan toch weer een keer langs kon komen voelde ik me meteen weer helemaal thuis! Ik vond het ook echt supertof dat zoveel van jullie de tijd

hebben genomen om mij op te zoeken in Schotland! Rob en Rien, bedankt dat ik bij jullie kon crashen bij deze gelegenheden. Peter, bedankt voor alle keren dat ik met je mee kon rijden. Thomas, super bedankt voor het ontwerp van de omslag! *Vacua Cupa, Venter Senatus!*

PAVO Realis, hetzelfde geldt natuurlijk voor jullie! Ik maakte graag tijd vrij voor de jaarlijkse dinertjes en jullie bezoek aan Glasgow deed me echt heel goed! *HUWEEEEEEH!*

Jolien en Suzan, team awesome heeft zijn naam waargemaakt dankzij jullie!

Petra, je weet het misschien niet, maar het stalken jouw goodreads account heeft mij veel boeken gegeven om te lezen/luisteren!

Ryanne, jouw bezoeken waren niet alleen gezellig, maar hebben me ook Edinburgh en Glasgow beter leren kennen.

En tot slot, maar misschien wel het belangrijkste, mijn lieve vriendje Patrick. Jij hebt al die jaren achter me gestaan, ook al zat er zo'n 700 km tussen ons. Bedankt dat ik altijd op je kon steunen, en dat je me altijd op wist te beuren als dingen tegen zaten, en ik mijn frustraties altijd bij jou kwijt kon.

Table of contents

Abstract	II
Acknowledgments	III
Table of Contents	VI
Abbreviations and Nomenclature	X
List of Publications by the Candidate	XIII
1 Introduction	1
1.1. Background and Motivation	2
1.2. Literature Review	3
1.2.1. Diabetes	3
1.2.1.1. Isolated Islet Transplantation	5
1.2.1.2. Islet Encapsulation.....	8
1.2.1.3. The Transplantation Area	11
1.2.2. Cell Encapsulation Techniques	11
1.2.2.1. Macro-encapsulation.....	11
1.2.2.2. Micro-encapsulation.....	13
1.2.3. Biomaterials for Cell Encapsulation	18
1.2.3.1. Synthetic Hydrogels for Encapsulation:	19
1.2.3.2. Natural Occurring Hydrogels for Encapsulation.....	21
1.3. Summary, Aims and Objectives	26
1.4. Structure of the Thesis	30
1.5. References	32
2 Materials and Methods	46
2.1. Designing and Production of the Micro-encapsulator.....	47
2.1.1. Frame	47
2.1.2. Laser Cutting.....	47
2.1.3. 3D Printing.....	48
2.2. Solutions.....	49
2.2.1. Alginate	49
2.2.2. Crosslinking Solutions.....	49
2.2.3. Pluronic Hydrogel	50
2.2.4. Collagen Hydrogel	51
2.3. Alginate Purification	52

2.3.1.	Purification Protocol.....	52
2.3.2.	Measuring Impurities	52
2.3.3.	Measuring Viscosity.....	53
2.4.	Micro-encapsulation and Bead Fabrication.....	53
2.4.1.	Single Nozzle Bead Fabrication and Micro-encapsulation	53
2.4.2.	Coaxial Core-Shell Bead Fabrication and Micro-encapsulation	55
2.4.3.	Determining Alginate Permeability Using Confocal Microscopy	56
2.5.	Cell Culture.....	58
2.5.1.	Adipose Derived Stem Cells and HepaRG cells	58
2.5.2.	Aggregate Creation.....	58
2.5.3.	Donated Human Pancreatic Islets	60
2.5.4.	Islet Dissociation.....	61
2.5.5.	3D Culture	61
2.6.	Cell Function Assays	62
2.6.1.	Islet Function.....	62
2.6.2.	HepaRG Function.....	62
2.7.	3D Bioprinting	63
2.7.1.	3D Bioprinting Cells and Beads.....	64
2.7.2.	3D Biofabrication Using Pluronic Moulds	65
2.8.	Chorioallantoic Membrane Assay.....	66
2.9.	Imaging.....	67
2.9.1.	Live / Dead Assay.....	67
2.9.2.	Immunohistochemistry	67
2.9.3.	Microscopes	69
2.10.	Statistical analysis.....	70
2.11.	References.....	71
3	Design, Construction and Optimisation of the Micro-encapsulator.....	72
3.1.	Introduction	73
3.2.	Design.....	73
3.3.	Optimisation of the System.....	76
3.3.1.	Syringe Pump	76
3.3.2.	Ground Electrode	80
3.3.3.	Top Panel.....	83
3.4.	Parameters Influencing the Bead Size and Morphology.....	83

3.4.1.	Voltage	84
3.4.2.	Dispensing Flow Rate	85
3.4.3.	Distance Between Dispensing Needle and Bath	86
3.4.4.	Alginate Concentration.....	87
3.4.5.	Dispensing Nozzle.....	90
3.4.6.	Gelling Bath	91
3.5.	Conclusion.....	93
3.6.	References	94
4	Purified Alginate for Clinical Cell Encapsulation.....	95
4.1.	Introduction	96
4.2.	Purification of Alginate.....	97
4.2.1.	Creating the Shortened Purification Protocol.....	97
4.2.2.	Measuring Impurities	100
4.2.2.1.	Protein Contaminants.....	100
4.2.2.2.	Polyphenol Contaminants	102
4.2.2.3.	Endotoxin Contaminants	103
4.2.3.	Viscosity	105
4.3.	Measuring Permeability Using Confocal Microscopy	105
4.4.	Antibody Resistance.....	112
4.5.	Conclusion.....	114
4.6.	References	115
5	One-step Encapsulated Organoid Formation.....	118
5.1.	Introduction	119
5.2.	Coaxial Encapsulation.....	121
5.2.1.	Influence of Viscosity Difference on Bead Morphology.....	121
5.3.	Coaxial Encapsulating HepaRG Cells.....	128
5.3.1.	HepaRG Viability.....	131
5.3.2.	Histology.....	131
5.3.3.	HepaRG Organoid Function	135
5.3.4.	Medium-core Encapsulations	137
5.4.	Conclusion.....	140
5.5.	References	142
6	Islet Encapsulation.....	144

6.1.	Introduction	145
6.2.	Islet dissociation.....	146
6.3.	Encapsulating in Alginate Hydrogel	148
6.4.	Coaxial Encapsulation of Islets	156
6.5.	Conclusion.....	170
6.6.	References	171
7	Towards a Pancreatic Islet Patch.....	172
7.1.	Introduction	173
7.2.	3D Bioprinting Patches	175
7.3.	3D Moulding Patches	181
7.4.	Testing Vascularization Using the CAM Model	186
7.5.	Conclusion.....	191
7.6.	References	193
8	Summary and Future Work.....	196
8.1.	Research Assessment	197
8.2.	Conclusions Summary	198
8.3.	Recommendations and Future Work	202
8.3.1.	The Micro-encapsulator	202
8.3.2.	Core-shell Encapsulation of Pancreatic Islets	203
8.3.3.	Pancreatic Islet Patch	204
8.3.4.	<i>In Vivo</i> Testing	205
8.4.	References	207
	Supplementary Data.....	208

Abbreviations and Nomenclature

ABS	Acrylonitrile Butadiene Styrene
ADB	Antibody diluent buffer
ADSC	Adipose derived stem cells
BCA	Bicinchoninic acid
CAM	Chorioallantoic membrane
CC	Coaxially encapsulated islet cells
CI	Coaxially encapsulated islets
CK19	Cytokeratin 19
CMC	carboxymethylcellulose
CSLM	Confocal Scanning Laser Microscope
CYP2D6	Cytochrome P450 2D6
CYP3A4	Cytochrome P450 3A4
DC	direct current
DIC	differential interference contrast
DMEM	Dulbecco's Modified Eagle Medium
DMSO	Dimethyl sulfoxide
DTZ	Dithizone
EC	Encapsulated islet cells
EDTA	Ethylenediaminetetraacetic acid
EI	Encapsulated islets
ELISA	enzyme-linked immunosorbent assay
Eu	endotoxin units
FBS	Foetal Bovine Serum

FDA	Fluorescein diacetate
FDM	fused deposition modelling
FFF	fused filament fabrication
FITC	Fluorescein isothiocyanate
G	α -l-guluronic acid
G-block	a pattern within alginate polymer consisting only out of successive G-monomers
GMP	Good manufacturing practice
HEPES	4-(2-hydroxyethyl)-1-piperazineethanesulfonic acid
HLA	Human Leukocyte antigen
HNF4 α	Hepatocyte nuclear factor 4 alpha
IBMIR	instant blood-mediated inflammatory reaction
ITA	Islet transplantation alone
KRBH	Krebs Ringer Bicarbonate
LAF-Hood	Laminar air flow hood
LAL	<i>Limulus</i> Amoebocyte Lysate (LAL)
M	β -d-mannuronic acid
MB	Microcarrier beads
M-block	A pattern within alginate polymer consisting only out of successive M-monomers
MEM	Minimum Essential Medium
MG-block	A pattern within alginate polymer consisting only out of alternating M and G-monomers
MW	Molecular weight
NGS	Normal goat serum

PBS	Phosphate buffered saline
PBST	PBS with 0,1% added Tween20
PEG	Polyethylene glycol
PI	Propidium Iodide
pNA	p-nitroaniline (pNA)
RLU	Relative Light Units
ROI	Region of Interest
RPM	rounds per minute
SD	Standard deviation
SNBTS	Scottish National Blood Transfusion Services
SPK	Simultaneous Pancreas-kidney transplantation
TCP	Tissue culture plastic
Tx	transplantation
ULA	Ultra low adhesion
ULI	Islets cultured on ULA-plates
VEGF	Vascular endothelial growth factor

List of Publications by the Candidate

2018 Cornelissen, D.J., Casey, J., King, J., Courtney, A., Shu, W., *Tuneable porosity of purified alginate hydrogels for clinical cell encapsulation and bioprinting*. *Advanced Healthcare Materials* (Submitted manuscript)

2017, Cornelissen, D.J., A. Faulkner-Jones, and W. Shu, *Current developments in 3D bioprinting for tissue engineering*. *Current Opinion in Biomedical Engineering*. **2**: p.76-82

2017-07-05 Cornelissen, D.J., Casey, J., King, J., Courtney, A., Shu, W., *Creating Encapsulated Islets*, Poster, Tissue and Cell Engineering Society Conference, Manchester, United Kingdom

2016 Buitinga, M., Janeczek Portalska, K., Cornelissen, D. J., Plass, J., Hanegraaf, M., Carlotti, F., de Koning, E., Engelse, M., van Blitterswijk, C., Karperien, M., van Apeldoorn, A., de Boer, J., *Coculturing Human Islets with Proangiogenic Support Cells to Improve Islet Revascularization at the Subcutaneous Transplantation Site*. *Tissue Eng Part A*, 2016. **22**(3-4): p. 375-85.

2016-01-26, Faulkner-Jones, A., Fyfe, C., Cornelissen, D. J., Gardner, J., King, J., Courtney, A., Shu, W., *Print your heart out*, Presenting Author, Oral Presentation, 3D Bioprinting Conference, Maastricht, The Netherlands.

2015 Faulkner-Jones, A., Fyfe, C., Cornelissen, D. J., Gardner, J., King, J., Courtney, A., Shu, W., *Bioprinting of human pluripotent stem cells and their directed differentiation into hepatocyte-like cells for the generation of mini-livers in 3D*. *Biofabrication*, 2015. **7**(4): p. 044102.

2015-10-08, Cornelissen, D.J., Casey, J., King, J., Courtney, A., Shu, W., *Bioprinting of encapsulated pancreatic islets*, Oral Presentation, Biofabrication Conference, Utrecht, The Netherlands

2015-09-20, Cornelissen, D.J., Casey, J., King, J., Courtney, A., Shu, W., *Bioprinting Encapsulated Islets*, Poster, Bayreuth Polymer Symposium, Bayreuth, Germany

Chapter 1

Introduction

1.1. Background and Motivation

Worldwide, an estimated 425 million people live with diabetes.^[1] Diabetes is a group of metabolic diseases in which defects are found in insulin action, secretion, or both, resulting in hyperglycaemia.^[11] In the long term, raised glucose levels can lead to atherosclerotic diseases, retinopathy, nephropathy and neuropathy.^[16] Type I diabetes, where patients are incapable of creating enough of their own insulin due to autoimmune destruction of their Islets of Langerhans, accounts for approximately 10% of the diabetic population.^[17] The conventional therapy for these patients is the administration of exogenous insulin. However, despite strict insulin regimens, the blood glucose levels cannot be adequately controlled in some patients. For these patients allogeneic islet transplantation or whole pancreas transplantation has become an alternative treatment option.^[18, 19] Shapiro *et al.* showed that by isolating pancreatic islets and injecting them into the liver patients could become insulin free.^[20] This is a successful procedure, with >80% of the patients being protected from hypoglycaemic episodes, and >60% being completely insulin independent after transplantation.^[18, 21] However, insulin independence is not long-lasting; after 5 years, 90 percent of the patients require insulin again to control their blood glucose levels.^[22] The wider application of islet transplantation is limited, however, by the need for large numbers of cells from human donor organs, limited life span of islets due to host innate and adaptive immune responses and the toxicity of modern immunosuppressive agents.^[23] Encapsulating the islets in a hydrogel may protect them from the immune-system, reducing the need for the administration of immunosuppressants, thereby solving 2 of the 3 main problems. The encapsulation of pancreatic islets is a tested method,^[24, 25] but it is only now being tested for clinical use.^[19, 25, 26] So far, these trials have been unsuccessful, although the reasons why remain unclear; the poor outcome of microencapsulated islets could be caused by an initial insufficient beta cell mass, or by the compromised survival of the implants. In the case of

macroencapsulated islets the researchers report that the islets survived, but that the bulk alginate material hampered their function.^[19] The research detailed in this thesis will be focused on further developing islet micro-encapsulation for clinical transplantation.

1.2. Literature Review

In this multi-disciplinary thesis different topics and research areas are discussed, all necessary for the encapsulation of pancreatic islets for clinical transplantation. The chapters in this thesis range from engineering topics like equipment development to more chemical topics like biomaterial science to biological topics like cell culture and function. This literature review focusses on the different options that were available when starting this research and will hopefully support the choices made during the course of this research. In section 1.2.1 an in-depth look is taken into the background problem, diabetes. In section 1.2.2 a selection of different cell encapsulation methods is given, which could be used to shield islets from the immune system. In section 1.2.3 biomaterials (mainly hydrogels) are discussed that could be used for the encapsulation of cells and other biofabrication methods. Finally, in section 1.3 the findings are summarized and the conclusion are used to create the aims and objectives for this thesis.

1.2.1. Diabetes

An estimated 425 million people suffer from Diabetes Mellitus,^[1] a group of metabolic diseases in which defects in insulin action, secretion, or both, result in hyperglycaemia.^[11] Diabetes is a disease revealing both short-term and long-term complications. Short term, patients will feel an increased hunger, thirst, and tiredness due to the high glucose levels in the blood. However, on long term, the raised glucose levels can lead to atherosclerotic diseases, retinopathy, nephropathy and neuropathy.^[16] Most cases of diabetes can be categorized within one of two categories: type 1 or type 2 diabetes.

Type-2 diabetes is the more common form of diabetes, covering roughly 90% of diabetic people.^[27] Patients with diabetes type 2 become less sensitive to insulin. Their body can either not make enough insulin to maintain normal blood glucose levels, or their cells become so resistant to the insulin that the glucose is not taken up anymore.^[28] Factors influencing this insulin resistance include physical activity,^[29] genetics^[30] (including ethnicity^[31]), carbohydrate intake,^[32] pregnancy^[33] and age.^[34] Diabetes type 2 is linked to obesity, with 80-90% of people suffering from diabetes type 2 being obese.^[35] In most cases of diabetes type 2, a change in lifestyle (losing weight, more physical activity) increases the chance of reversing the diabetes.^[36]

In this thesis a focus is placed on diabetes type 1. Patients suffering from type 1 diabetes have an absolute deficiency in insulin secretion, mainly caused by an autoimmune destruction of the β -cells within the islets of Langerhans. The islets of Langerhans are the areas of the pancreas that include hormone producing cells (Figure 1.1). The main function of the islets is to secrete glucagon (α -cells) and insulin (β -cells) to regulate the blood glucose levels.^[37] The rate of the autoimmune destruction of the β -cell in type 1 diabetes is variable. Fast degrading β -cell mass is mainly found in infants, while slow degrading β -cell mass can be found in adults, which can take up to more than 10 years.^[38] The exact cause of type 1 diabetes remains unknown. When this disease is affecting a homozygotic twin, a pairwise concordance only exists in less than 40% of the cases, indicating that exogenous factors contribute to the development of the disease.^[38, 39] However, genetic predisposition has also shown to be an important factor, with genetic variability in the human leukocyte antigen (HLA) region accounting for more than half of the genetic influence in diabetes type 1, and over 50 different non-HLA polymorphisms accounting for the other half.^[40] There are indications that among the exogenous factors, diet and viral infections play a part in the development of this autoimmune disease.^[41]

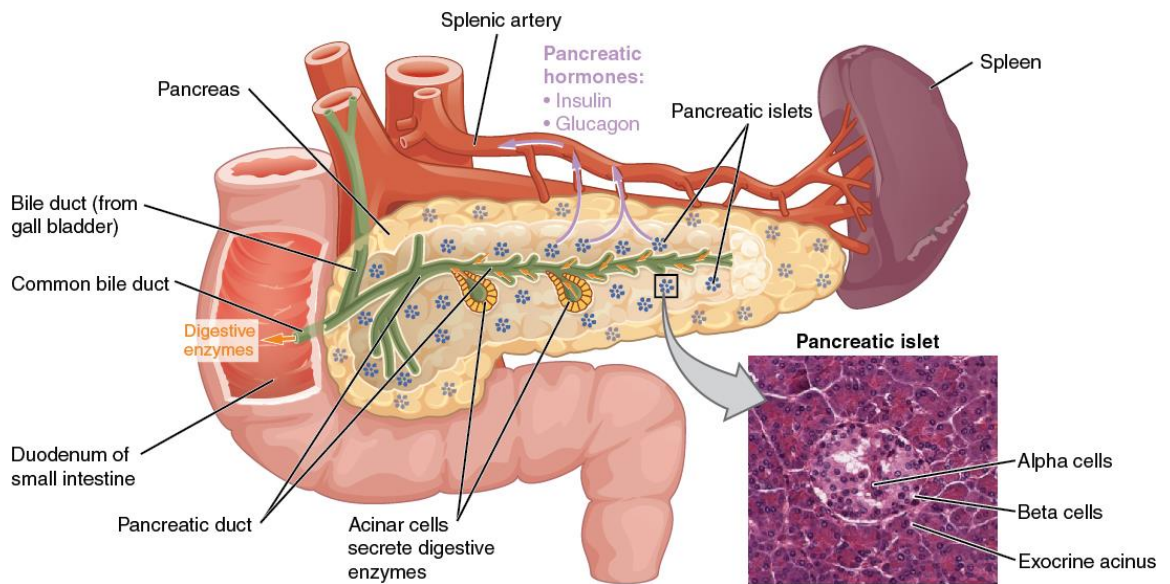


Figure 1.1: A schematic overview of the pancreas, in which the islets of Langerhans (pancreatic islets) can be found. [2]

1.2.1.1. Isolated Islet Transplantation

The conventional therapy for diabetes type 1 is the administration of exogenous insulin.

Patients have to be careful with the self-administration, as too little can make them hyperglycaemic, which can result in the beforementioned complications, and too much can result into a hypoglycaemic episode. During these, there is not enough glucose in the blood for the major organs to perform their function. For instance, the brain can no longer take up enough oxygen, which can lead to dizziness, passing out or even a coma.^[42, 43] The fear of these hypoglycaemic episodes can be a huge strain on the patients, stopping them for instance from partaking into physical activity.^[44] Patients who can not control their blood glucose levels despite these strict insulin regiments, whole pancreas or allogeneic isolated islet transplantation might be an alternative treatment option.^[18, 45] Whole pancreas transplantation is a major surgery, usually performed in combination with a kidney transplant, leading to a long hospitalization of the patient and a higher risk of

complications for the patient (table 1.1). Its success rate is relatively high, with 75% of the patients maintaining insulin independence for more than 5 years. However, when something does go wrong, the entire organ fails, making the patient completely dependent again.^[46] On the other hand, isolated islet transplantation is a minor operation, with a smaller chance of complications. For this transplantation method, human islets are isolated from the pancreas of a donor and injected into the portal vein of the patients liver, after which the islets engraft locally (Figure 1.2).^[20]

Table 1.1: Synopsis of pancreas vs. islet transplantation, adopted from Berney et al.^[46]

	Pancreas Tx	Islet Tx
First case performed	1966 (Mineapolis)	1974 (Minneapolis)
Total world experience	~28.000 cases	~1500 cases
Surgical approach	Laparotomy, major surgery	Interventional radiology, minimally invasive
Operative time (h)	4-6	1
Complications	Frequent/Severe: Thrombosis, pancreatitis, peritonitis	Less frequent/less severe: Bleeding, portal thrombosis
Hospital stay	1-3 weeks	3-7 days
Mortality	Low (4%)	Exceptional (~0%)
Insulin indepence (%)		
1 year	85	75
5 years	70	15-50 ^a
Graft function after 5 years^b (%)	70	70
No. donors required for success	1	1-4
Currently preferred indication	SPK	ITA
<p>^aFive-year insulin independence rates are available only from the early cohort from the University of Alberta and were reported as 15(%). In the latest collaborative islet transplant registry report insulin independence rates of 4 years are shown. In two recent single-centre series, insulin independence rates more than 50% at more than 3 years have been shown</p> <p>^bFor pancreas transplantation, graft function is defined as insulin independence; for islet transplantation, graft function is defined as detection of circulating C-peptide more than 0.5 ng/ml.</p> <p>SPK: simultaneous pancreas-kidney transplantation; ITA: islet transplantation alone, Tx, transplantation</p>		

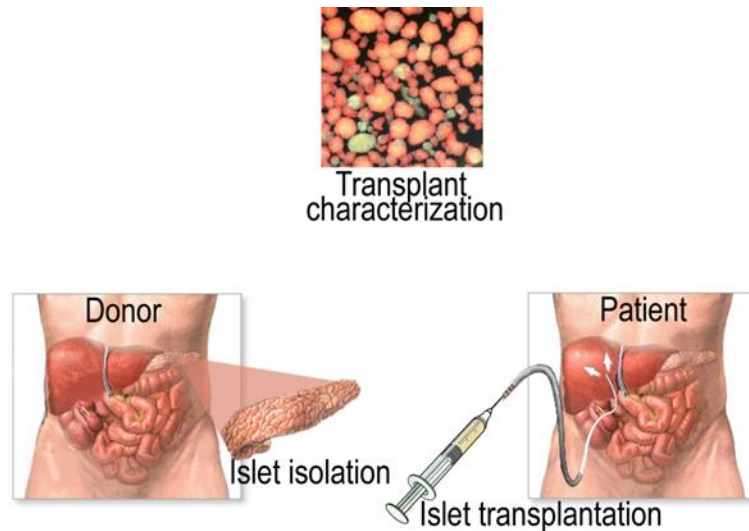


Figure 1.2: For isolated islet transplantation, islets are isolated from a donated pancreas, and injected into the patients' portal vein.

The cost of this operation is roughly £30,000, of which a third can be attributed to the isolation expenses.^[47, 48] This is a successful procedure with >80% of the patients being protected from hypoglycaemic episodes, and >60% being completely insulin independent after transplantation.^[18, 21] However, the insulin independency is not long-lasting; after 5 years, 90 percent of the patients requires insulin again to control their blood glucose levels.^[49] It is estimated that the insulin production after transplantation is only 20-40 percent of that of a healthy person, even when islets from multiple donors are transplanted.^[18] Even though islet loss seems unavoidable, only part of the islets are lost while the other islets remain functional, preventing patients from hypoglycaemic episodes, even if they are not completely insulin independent. Thus, the safety of the procedure and the relative short amount of after-care necessary for this type of transplantation (Table 1.1), make isolated islet transplantation a viable clinical transplantation, even with its islet loss.

1.2.1.2. Islet Encapsulation

As stated before, long-lasting insulin independence is not reached in patients with transplanted islets. Adverse factors hampering this procedure include the requirement of too many islets to achieve substantial functional effects, low life span of islets due to immune reactions and the toxicity of commonly used immunosuppressants to the islets.^[50] All these factors also lead to a very poor cost-effectiveness of this transplantation method. Encapsulating the islets may protect them from the immune-system, reducing the need for the administration of immunosuppressants, thereby solving 2 of the 3 main problems (Figure 1.3).

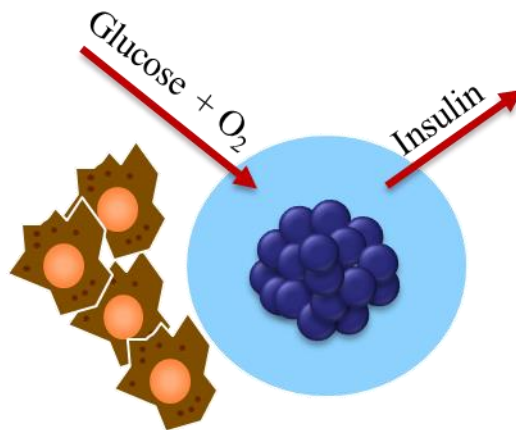


Figure 1.3: Encapsulating islets with an immunoprotective barrier can save them from the patients' own immune system, thereby eradicating the need for immunosuppressants. The barrier should shield the islets from any white blood cells and antibodies, while still allowing oxygen and nutrients through for the survival of the islets, as well as allowing the islet to sense the glucose concentration and excrete insulin accordingly.

Encapsulation is a technique using the envelopment of tissues or cells in a non-toxic polymeric membrane to protect them from the immune system. This technique was first described in 1932 by Rezzesi, who created a physical barrier between a mice-carcinoma transplanted in a guinea-pig, to increase its survival time.^[51] In the 1950s, a series of publications by Algire used the same technique to prove that xenografts survive longer when they are separated from the host tissue by a barrier that only allows small molecules, like

oxygen and nutrients, to pass. Thereby, he proved that the cell to cell contact from white blood cells to the donated tissue, plays a substantial part in immunology.^[52, 53] In current research, the immune-protection of the encapsulated cells is still an important characteristic of the materials used for encapsulation. Encapsulation is used to transplant cells without the use of immunosuppressants.^[54] Even in autografts it can be necessary to protect the transplanted cells from the immune system, for instance in the case of autografting patients with diabetes type 1. The immune system of the patient is the cause of the destruction of the insulin producing β -cells.^[55] To prevent the immune system of destroying auto- or allografted islets, the materials chosen for encapsulation should prevent large entities, like antibodies (150,000 MW)^[56] and white blood cells (7-30 μm),^[57] to reach the transplanted cells.^[58] However, small molecules, like oxygen, insulin(5,734 MW)^[59] and glucose (180 MW)^[60] should still be able to pass through the barrier.

However, immune-protection is not the only characteristic an encapsulating material should have. The observation that the graft survival rates of microencapsulated allografts and autografts are similar^[61] suggests that allograft recognition is not the only factor that influences the reaction. Biocompatibility of the material itself is necessary to prevent a non-specific foreign body reaction, where proteins adsorb to the surface of the capsule and a fibrotic overgrowth can be observed, leading to the necrosis of the islet inside.^[62-65] About 40% of transplanted encapsulated islets die due to fibrotic overgrowth.^[66] A recent research by Veisheh et al. seems to indicate that the size of the capsules is actually of influence on the chance of fibrotic overgrowth, with larger beads attracting less overgrowth.^[67]

Encapsulation of islets has one major drawback; it increases the distance between the blood vessels and the β -cells, increasing the diffusion distance and thereby decreasing the insulin production^[68-70] and increasing the β -cells necrosis due to hypoxia.^[66, 71, 72] With the size of

capsules historically being 600-800 μm ,^[50] the diffusion distance is relatively large, taking into account that *in vivo* every cell in the body is within 200 μm of a capillary vessel.^[73] Pancreatic islets have an even higher capillary density, with every cell being within 1 cell distance to a capillary vessel.^[74] As said before, a larger diffusion distance could lead to an increase of necrosis due to hypoxia. When necrosis occurs, the islets release chemokines, which in turn attract macrophages. Small islets (less than 150 μm in size) do not suffer from this adverse effect (Figure 1.4).^[10] Since it is known that the size of islets does not majorly influence the amount of insulin being created per islet,^[15, 75] controlling the size of the islets as well as the size of the encapsulation would be very beneficial for the engineering of encapsulated islets. Therefore, this thesis will show experiments dissociating islets, trying to use the cells to reconstitute islets of a certain (smaller) size. This will all be done in a one-step procedure, combined with the encapsulation of the islets.

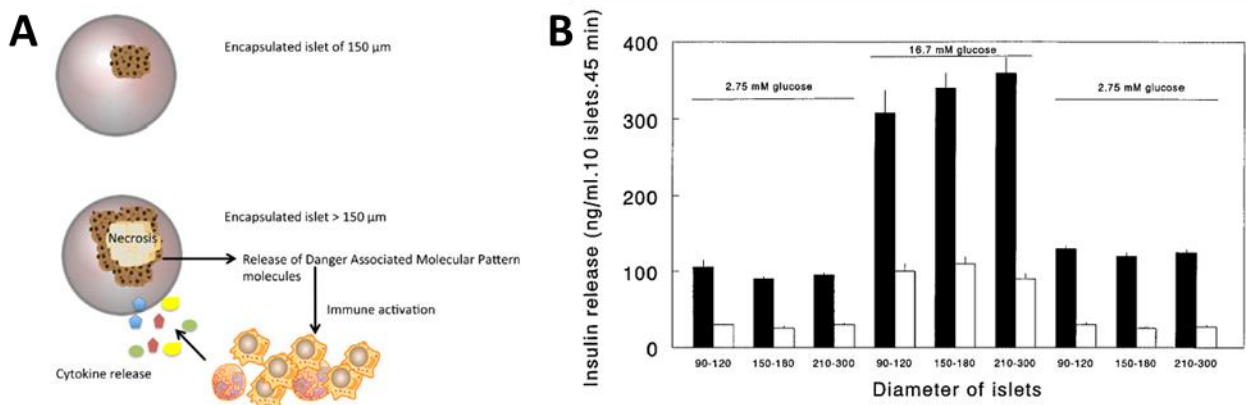


Figure 1.4: Islet size is important when encapsulating islets. A: Since the encapsulated islets will not be vascularized, they have to get all their nutrients and oxygen through diffusion. Larger islets will develop a necrotic core due to their lack of nutrients, which in turn can set off the immune system.^[10] B: there is no significant difference between the insulin released by smaller (<120 μm) or larger (>210 μm) islets, even though the larger islets have a lot more cells.^[15]

1.2.1.3. The Transplantation Area

One factor relating to the high islet loss might be the transplantation site. In the liver, islets are exposed to several stress factors like high levels of (immunosuppressive) drugs, hyperglycemia, the instant blood-mediated inflammatory reaction (IBMIR) and low oxygen tension.^[76] Multiple sites have been proposed as an alternative (spleen, gastrointestinal wall, omentum), however the success rate of islet transplantation mainly depends on vascularity of the transplantation site.^[77] Subcutaneous and intramuscular transplantation sites are favourable, since these sites are easily accessible, and transplantation can be performed with minimally invasive techniques, reducing the chance of life threatening complications.^[78] A drawback of these sites is that they are hypoxic and hypovascularic, which can result in poor transplantation outcomes. In this thesis a proof of concept is given of the creation of a biofabricated pancreatic patch. Creating a bioartificial transplantation site using hydrogels allows for the creation of a microenvironment that can be specifically tailored to support islet survival, function and increases vascularization around the encapsulated islets. Furthermore, by immobilizing the islets in a scaffold, transplantation procedures and retrieving the device can be made easier.

1.2.2. Cell Encapsulation Techniques

Cell encapsulation is the act of enveloping cells into a material that will shield them from the immune system.^[79] Different encapsulation methods can be found, depending on the final form of the encapsulation. All encapsulations can be divided into two main groups, macro-encapsulation and micro-encapsulation (Figure 1.5).^[80]

1.2.2.1. Macro-encapsulation

Macro-encapsulation usually consists of a large bulk of material encapsulating all islets in the same device. A great advantage of macro-encapsulation is that the devices are easy to transplant and might be retrieved or reloaded. Furthermore, macro-encapsulation allows for

a greater mechanical strength than micro-encapsulation. Macro-encapsulation devices can be divided into two main groups: intra-vascular and extra-vascular.^[81]

Intravascular macro-encapsulation devices are directly attached to the hosts vascular system, for instance in the form of a shunt, or in a diffusion chamber surrounding a semi-permeable membrane, which is surgically attached to the hosts blood vessels.^[82] A major advantage of

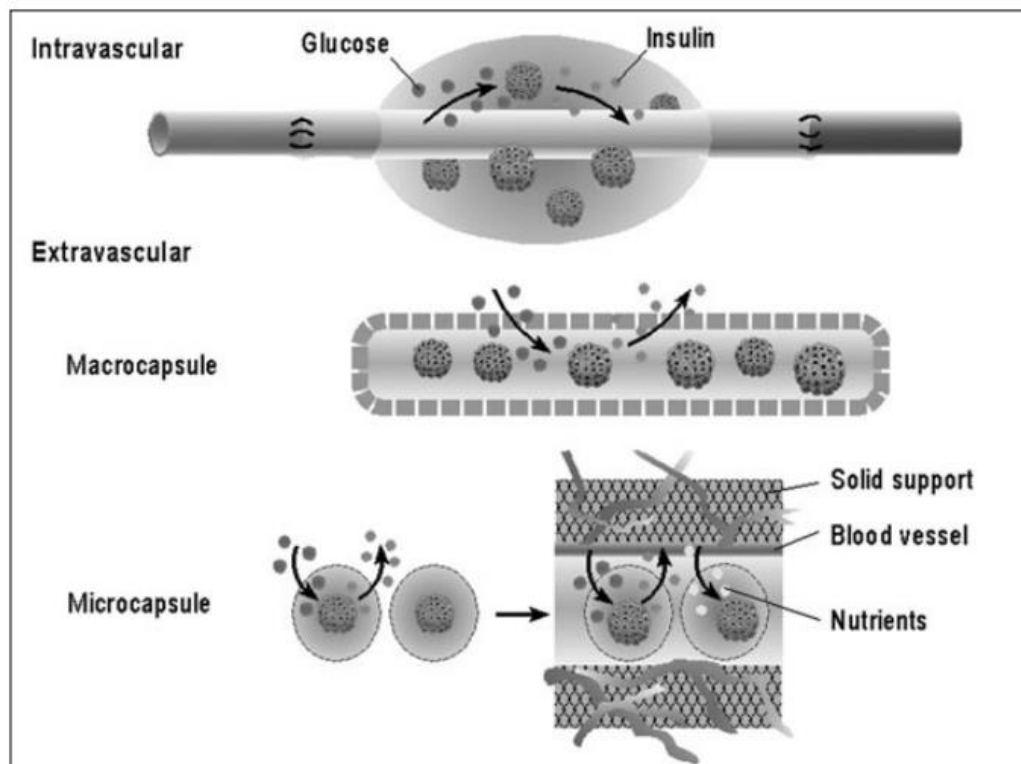


Figure 1.5: Encapsulations of cells come in different sorts and sizes. They can be divided in either micro- or macro-encapsulations, with the macro-encapsulations being either intra- or extravascular devices.^[3]

these type of encapsulations is that they are very close to the blood stream, which allows the islets to react to changes in the blood glucose levels almost immediately. A major drawback of this system is the chance of blood leakage, thrombosis, or even clogging of the device, if the chosen biomaterials are not biocompatible enough, which is a serious risk for the patient.^[83]

Extravascular macro-encapsulation devices mainly consist either out of diffusion chambers containing a large amount of islets, shielded from the host tissue by some sort of membrane, or a large amount of hydrogel holding the islets.^[84] These devices can easily be transplanted in highly vascularised transplantation sites, like the peritoneal cavity, an omental pocket, or a subcutaneous site.^[81] A major drawback of these type of systems are the diffusion of oxygen and nutrition into the devices.^[77] Scientist have tried to circumvent this problem by creating chambers with their own oxygen supply, which can be refuelled trans-dermally.^[19, 85, 86] Due to the size of these macro-encapsulation devices, the large diffusion distance between the islets and the blood vessels either delays insulin release after blood glucose levels rise, or results in the complete absence of glucose mediated insulin release,^[19] which is a drawback to this system.^[83]

1.2.2.2. Micro-encapsulation

The micro-encapsulation of islets involves the (individual) enveloping of the islet in an immunoprotective material.^[10, 87, 88] The smaller encapsulation leads to a favourable surface/volume ratio, which leads to better diffusion characteristics,^[89] compared to the macro-encapsulated islets. Furthermore, the manufacturing of micro-encapsulated islets usually doesn't involve complex or expensive manufacturing procedures, and the small size of the individual devices allows implantation through a minimally invasive injection.^[83] In almost all cases of micro-encapsulation, the islets are encapsulated in a hydrogel. However, the method of encapsulating the islets can greatly differ.

1.2.2.2.1. Droplet Generators

The most common used device for islet encapsulation (in alginate hydrogels) is an air based droplet generator (Figure 1.6). Alginate is pushed through a nozzle, and is aided by an airflow surrounding the nozzle to separate from the tip.^[90, 91] The droplets, usually around 600 μm in diameter, will fall in a gelling bath where the alginate will crosslink into a hydrogel.

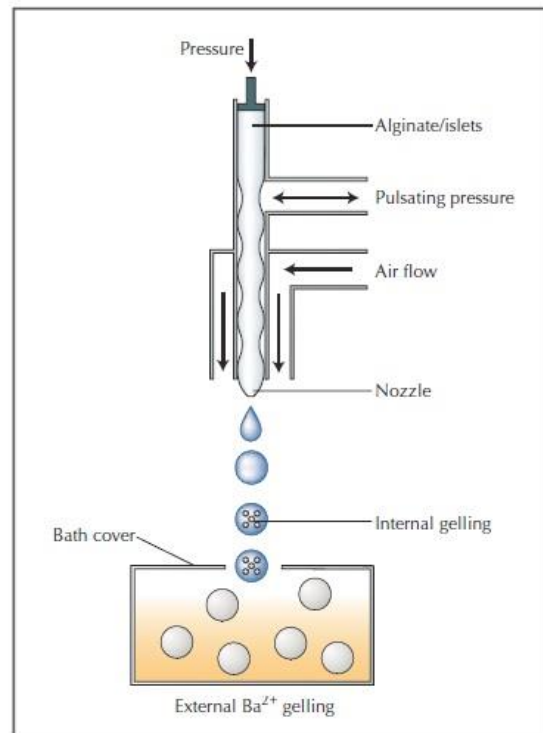


Figure 1.6: An air based droplet generator utilizes oscillating air pressure to aid droplets to separate at the tip of a nozzle.^[4]

1.2.2.2.2. Emulsion Encapsulation

Another method of encapsulating cells is through the creation of emulsions. The cells, suspended in a liquid of choice are mixed into an oil at high speed, creating an emulsion (Figure 1.7). The cell suspension is then allowed to gel. For crosslinkable hydrogels, this is done by adding the crosslinker (Ca²⁺ ions, for alginate)^[92] while thermoresponsive hydrogels like agarose only have to cool down.^[6] This method allows for the creation of thousands of encapsulations at the same time, in a short amount of time. However, an oily residue could be left behind on the beads. Furthermore, this method creates encapsulations in a wide variety of sizes. Hoesli et al. reported a size distribution of 200-1500 μm .^[14]

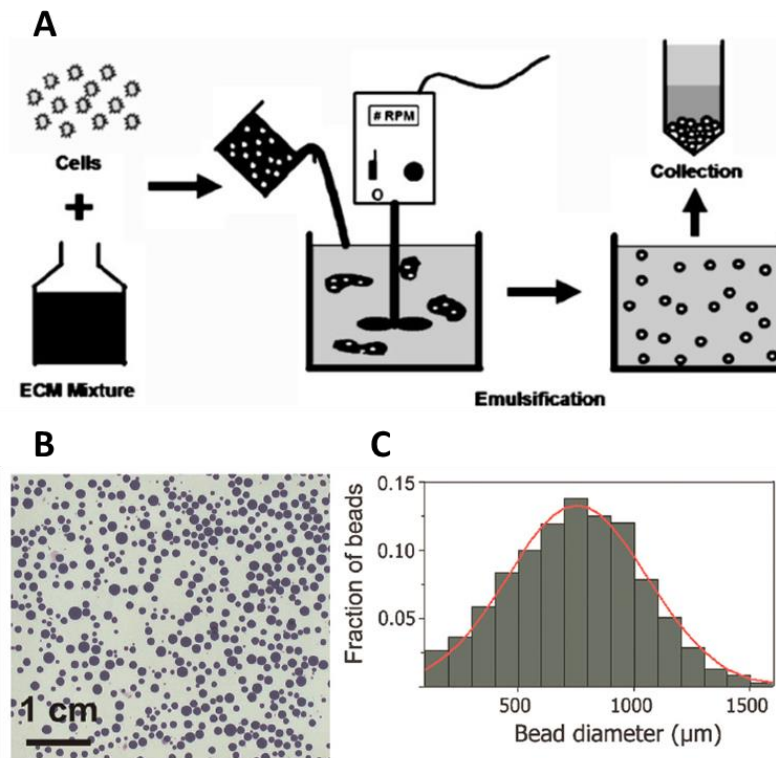


Figure 1.7: Using emulsification can be another method to encapsulate cells. A: Cells in an aqueous solution are mixed into an oil, and emulsified. The encapsulation solidify, and can be retrieved from the emulsion.^[6] B: A microscopic picture of encapsulations created through emulsion. C: Encapsulating through emulsification results in wide range of bead sizes.^[14]

1.2.2.2.3. Microfluidics

Another way of encapsulating islets is by using microfluidics (Figure 1.8).^[7] The advantages of microfluidics over air-nozzle based devices or emulsions is that the size of the beads are more uniform, and there is less chance of clogging up the system with islets. The most common microfluidic approaches bring together multiple streams of liquids in a chip, and use the shear stress of the faster flowing liquid to shear off small quantities of the slower flowing liquid.^[93] There are two major approaches: flow-focussing and T-junction bead formation. With flow-focussing, a coaxial stream is created, where the slower flowing core stream is sheared into multiple beads by the sheath stream. In the T-junction method (Figure 1.8 A) beads are directly sheared of the slower flowing liquid.^[94] Disadvantages are that apart from

the encapsulation material, a secondary material like mineral oil is necessary to create the droplets, which can leave residues on the encapsulation. A novel method of microfluidic encapsulation is in-air microfluidics.^[13] instead of having a chip based microfluidic device, this method utilizes two jets of fluids that meet in-air, creating small, uniform beads. An advantage of this method is the increased speed rate, and the fact that it can be combined with other biofabrication methods to immediately use the created encapsulations for 3D bioprinting. (Figure 1.8 B)

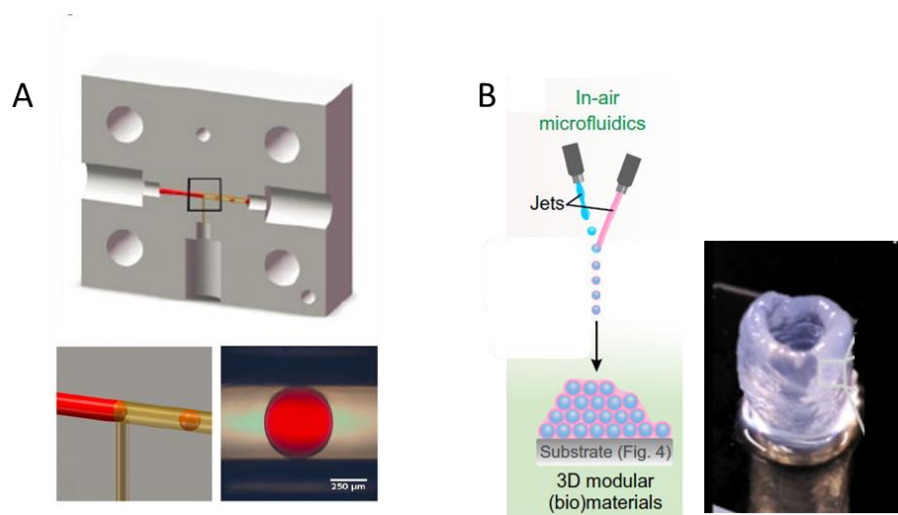


Figure 1.8 A: A microfluidic device for islet encapsulation. Islets suspended in an aqueous hydrogel solution are split into microdroplets by shearing them off with a mineral oil, before crosslinking them.^[7] B: In air microfluidics does not rely on a chip to create microdroplets, and can be used immediately for 3D bioprinting.^[13]

1.2.2.2.4. Electro-spraying

In this report a novel method for islet micro-encapsulation, based on electro-spraying, is further developed. Electro-spraying is a technique used to generate small, mono-sized droplets from viscous fluids.^[95] By applying an electrical pulling force, it is possible to elongate, and eventually separate, a viscous fluid at the end of a nozzle (Figure 1.9).^[96] This can be used to create very uniform droplets, which can range in size from hundreds of micrometers for cell encapsulation, to nanometer sized droplets used in the pharmaceutical industry.^[97] When this research was started, only 1 study by Ma et al., 2013^[98] used this method to

encapsulate rat pancreatic islets, which was then followed by another study by Veisheh et al., 2015, also encapsulating rat pancreatic islets.^[67] However, this technique has been used by other researchers to encapsulate other cells. Neuronal cells,^[99] cardiac cells,^[100] hepatocytes^[101] and even mesenchymal stem cells^[102] have successfully been encapsulated using the electro-spray technique.

Another interesting variation on electro-spraying uses a coaxial nozzle to create coaxial encapsulations.^[103] This could for instance be used to create encapsulations with a gelled shell, but a liquid core.^[104] The liquid core allows cells to migrate and form aggregates. The possible uses of this technology are described in the article by Lu et al.,^[105] and include the ability to research co-cultured cells in 3D, *in situ* aggregation and the possibility to translate 3D cultures to micro-array types of research. By double coating with alginate hydrogels, Ma et al. showed increased immune-protection properties using this coaxial method.^[98]

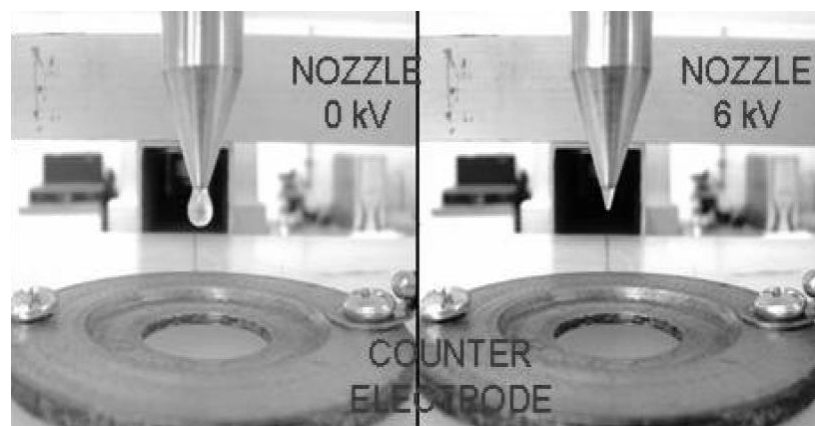


Figure 1.9: The electro-spray technologies utilizes electrical pulling forces to separate a viscous fluid into small droplets.^[5]

1.2.3. Biomaterials for Cell Encapsulation

Probably one of the most important aspects of cell encapsulation is the choice of material to encapsulate the cells or islets. A rough division can be made between synthetic biomaterials and natural occurring biomaterials for cell-encapsulation. Natural materials have the advantage of a high biocompatibility and can often be degraded by naturally occurring chemical processes or enzymatic reactions.^[106, 107] This can be useful as a temporary scaffold for the cells, that might be resorbed into the body. Another big advantage to natural materials are the natural occurring ligands in some of the materials, that allow cells to attach and can even help with cell signalling without any further modification.^[108]

Naturally occurring polymers for hydrogels can be harvested from plants, like Alginate from algae, and agarose from seaweed, or from the mammalian extracellular matrix, like Collagen, fibrin and matrigel. Advantages of using natural occurring polymers is the availability and biocompatibility. Disadvantages are that these natural occurring polymers usually have batch to batch variability, and it is nearly impossible to completely control their physico-chemical properties.^[106]

Synthetic materials on the other hand are tailor-made. Since most of the currently used synthetic materials show no biological activity on their own, combining them with specific bioactive molecules can improve cell adhesion and viability.^[8] However, creating these synthetic materials can be time consuming and expensive.

In this section, the materials most commonly used in combination with islet transplantation are discussed.

1.2.3.1. Synthetic Hydrogels for Encapsulation:

1.2.3.1.1. PEG Hydrogel

Poly(ethylene glycol) (PEG) is a widely used biomaterial, due to its hydrophilicity, biocompatibility, and resistance to protein adhesion and cell attachment.^[109] It is used for surface modification, bioconjugation and drug and cell-delivery.^[8] PEG hydrogel building blocks usually consist of a linear or branched PEG structure (multiarm or star) with hydroxyl end groups, which can be converted into different functional groups (Figure 1.10).^[8] The multitude of different functional groups that can be incorporated makes PEG hydrogels very versatile. For instance, it is possible to make a degradable gel by incorporating hydrolysable materials like lactide^[110, 111] or caprolactone,^[112, 113] or by incorporating enzyme sensitive peptide sequences that will allow cells to degrade the hydrogel themselves by secreting enzymes, as they would also normally do.^[114] Furthermore, the gel can be functionalized with peptides to increase cell adhesion, or to bind or release growth factors.^[8] PEG hydrogels can further be modified in such a way that they become actively immunoprotective.^[115] Cheung *et al.* have tethered the apoptosis inducing anti-Fas monoclonal anti-body to the surface of the PEG hydrogels, actively fighting the immune system by inducing apoptosis in T-Cells.^[116] Other advantages of PEG include high water content and high diffusion speed.^[10] PEG

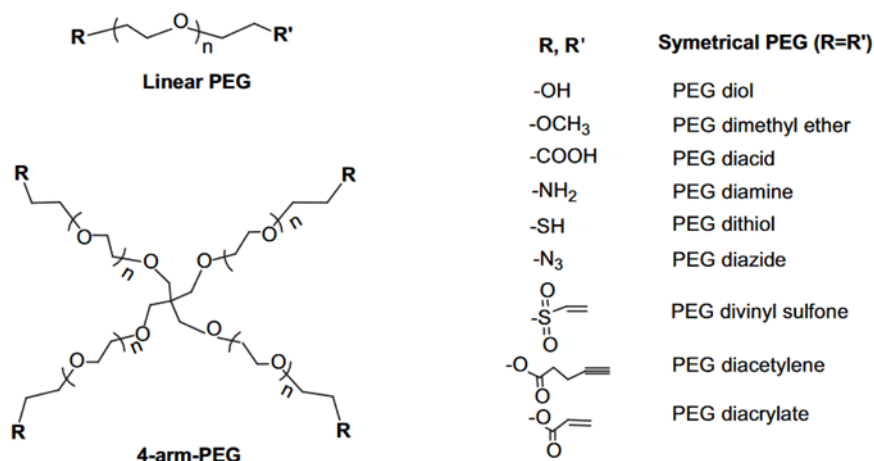


Figure 1.10: A structural representation of a linear PEG and 4-arm PEG. The variability of functional end groups make this hydrogel very versatile and allow it to be tailored for specific functions.^[8]

hydrogels have been used as a scaffold for the culture and differentiation of stem cells,^[117-119] smooth muscle cells,^[109] cartilage tissue engineering^[120, 121] and islet encapsulation.^[122-124]

1.2.3.1.2. Peptide Hydrogels

Self-assembling peptides are a relatively new set of molecules, which could be used to form hydrogels for the encapsulation of cells.^[125] These peptides are usually completely synthetically manufactured, nullifying the possible pathogenicity related with animal derived materials.^[126] By changing the (order of the) amino-acids within the material, mechanical characteristics and cell-material binding properties can be tailored.^[125] Depending on the peptides chosen, these gels are biocompatible^[127] and biodegradable.^[128] Li *et al.* for instance created a polypeptide hydrogel that crosslinks using DNA linkers, making this hydrogel both biodegradable by proteases and nucleases (Figure 1.11).^[9] The ability to customise these hydrogels can make them excellent micro-environments for use with chondrocytes,^[125] stem cells,^[129] islets^[127] and blood vessels.^[130]

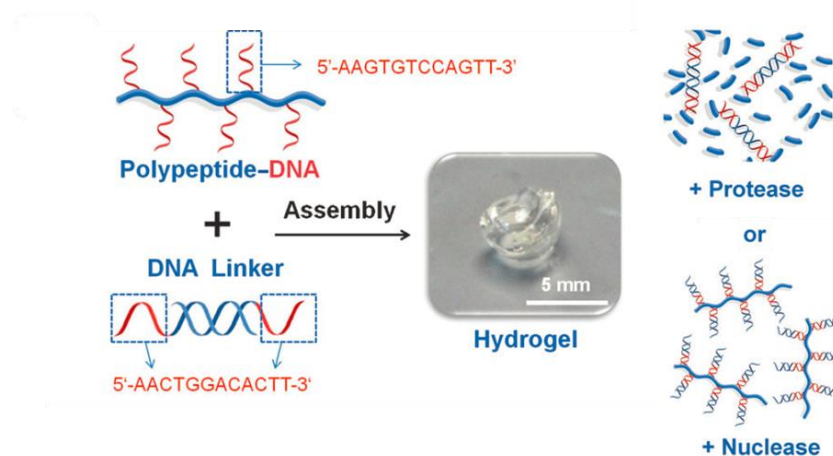


Figure 1.11: Peptide hydrogels are highly versatile. Li *et al.* created a hydrogel that crosslinks using DNA, making it biodegradable using either proteases or nucleases.^[9]

1.2.3.2. Naturally Occurring Hydrogels for Encapsulation

1.2.3.2.1. *Fibrin*

Fibrin is a polymer which occurs abundantly in the human body, as it is part of the wound healing process.^[131] Once the protease thrombin is activated, it cleaves fibrinogen, an abundant protein in the plasma, removing the parts that prevent spontaneous polymerization. The fibrin proteins start sticking together, creating a 3D hydrogel. The RGD motifs within the fibrin proteins allow platelets and other cells necessary for wound healing, to stick to the hydrogel.^[132] Fibrin hydrogels can be degraded by enzymatic reactions, which makes it a good temporary scaffold for tissue engineering,^[133] or a carrier for drugs^[134] and cells.^[135] Fibrin hydrogels are very versatile in their use within tissue engineering.^[136] They have been used for the engineering of cartilage,^[137] cardiac tissue,^[138] blood vessels,^[139] dermis,^[140] etc. Even though fibrin hydrogels cannot be used for immunoprotection of islets, they have been used before for the transplantation of islets. It increased vascularisation post-implantation, thereby increasing the survival and function of the non-encapsulated islets. ^[141, 142]

1.2.3.2.2. *Collagen*

Collagen is the most abundant structural protein within mammals and can be found throughout the human body.^[143] Collagen is widely used as a biomaterial for drug delivery,^[144] tissue engineering^[145] and cell encapsulation.^[146] Even though there are 29 found types of collagen described, 90% of the collagen found is type 1 collagen.^[10] The abundance of type 1 collagen, as well as its low antigenicity and biodegradability make it an excellent biomaterial for use as a temporary scaffold for cell transplantation.^[143] Although Islets react to collagen with an increase of insulin secretion,^[147, 148] the degradability of collagen makes it unsuitable as an encapsulation material for the immunoprotection of islets.

1.2.3.2.4. *Alginate*

The most commonly applied polymer in cellular encapsulation is alginate.^[10] Alginate is harvested from brown algae (Phaeophyta). It is found in extra-, and intracellular regions, making up 20-40% of the dry-weight of the algae.^[90] It is a polymer consisting mainly out of 2 monomers: β -d-mannuronic acid (M) and α -l-guluronic acid (G). These monomers are 1,4'-linked in different sequences and can be cross linked by adding a cation rich solution (mostly, Ca^{2+}).^[161] The sequences are not random, but form patterns of homopolymeric blocks (M-blocks or G-blocks) or alternating heteropolymeric blocks (MG-blocks).^[162] The guluronic acid blocks within the polymer are responsible for the selective binding of cations, crosslinking in an "egg-box" patterned way (Figure 1.13). This means that the stiffness of the gel increases with more G-blocks, and elasticity increases with more M-blocks.^[162] A higher concentration of G-blocks usually result in a lower biocompatibility,^[64] but better immunoprotective properties.^[163]

The stability of the created hydrogels also depend on the chosen cations for gelation, and decreases in the following order: $\text{Ba}^{2+} > \text{Cd}^{2+} > \text{Cu}^{2+} > \text{Sr}^{2+} > \text{Ni}^{2+} > \text{Ca}^{2+} > \text{Zn}^{2+} > \text{Co}^{2+} > \text{Mn}^{2+} > \text{Mg}^{2+}$.^[164]

Alginate can be modified for tissue engineering purposes with certain ligands to improve cell adhesion and survival. Alsberg *et al.*^[165] have modified their alginate with RGD-peptide sequences in order to improve the cell viability, proliferation and attachment of osteoblasts. Alginate has further been used as a scaffold for Mesenchymal Stem Cells,^[166] nerve regeneration,^[167, 168] parathyroid glands,^[169] cartilage^[170] and skin.^[171]

Lim *et al.* were the first to use alginate as material to shield pancreatic islets from the immune system, in 1980.^[172] Ever since, scientist have tried to use alginate for the immunoprotection of pancreatic islets^[4] and they have found a wide array of alginate parameters that can influence the immunoprotective properties of these micro-encapsulations. The first being the cations chosen for gelation; alginate crosslinked with calcium is usually too porous and

mechanically weak to provide a good protection from the immune system,^[10] but barium cross linked alginate can provide that immunoprotection.^[173, 174] Furthermore, the average molecular weight of the alginate has an influence on its immunoprotective properties. Zimmermann *et al.*^[4, 175] have shown that alginate with a higher molecular weight provides immunoprotection at a lower concentration than alginates with lower molecular weights. This was attributed to the inter-penetration of the polymer networks. Another parameter that influences the immunoprotective properties is the ratio of G- to M-blocks. As stated before, a higher concentration of G-blocks results in a better immunoprotection, but too much could have a negative influence on the biocompatibility of the alginate hydrogel.^[163] The biocompatibility is another huge factor. Even if there is no specific inflammation reaction against the cells within the alginate, a non-specific foreign body reaction against the microcapsules with fibrotic overgrowth of the microcapsules can still result in the necrosis of the encapsulated islets.^[15] Furthermore, when larger islets are encapsulated, they can develop a necrotic core, which will release danger associated molecular pattern molecules,^[10] which in turn can activate the immune system. The same can happen to smaller islets if they do not receive adequate oxygen and nutrients in their transplantation area.^[176]

To circumvent the biocompatibility problem of alginate, some researchers have covered the alginate beads with another immunoprotective membrane. Most commonly used membranes are Poly-L-Lysine^[166, 177, 178] and Poly-L-Ornithine.^[179-181] The variable success of encapsulating pancreatic islets in alginate so far could be attributed to the purity of the alginate.^[182] Alginate is a material harvested from nature, and therefore can be contaminated with impurities like proteins, polyphenols and endotoxins.^[65] Even though the alginate hydrogel itself is biocompatible, these impurities can induce an inflammation reaction, which in turn can result in the necrosis of the encapsulated islets. De Vos *et al.*^[65] therefore hypothesize that the variability in success could be attributed to the different

amounts of contaminations in the alginates used by the researchers. Purified alginate results in better biocompatibility and long term survival of islets.^[182-185]

Alginate has proven to be very durable and biocompatible, even sustaining xenotransplanted porcine islets for 10 years within a human patient.^[186] However, for truly good biocompatibility, the alginate chosen should have a medium to high molecular weight and must be very pure, containing almost no proteins, polyphenols or endotoxins.^[61, 185, 187] Furthermore, it should be crosslinked using a suitable cation and the islets encapsulated shouldn't be too large. Finally, the encapsulation of the islets will be to no avail if the islets do not get enough nutrients and oxygen after transplantation, due to either a lack of vascularization nearby or to large of diffusion distance.

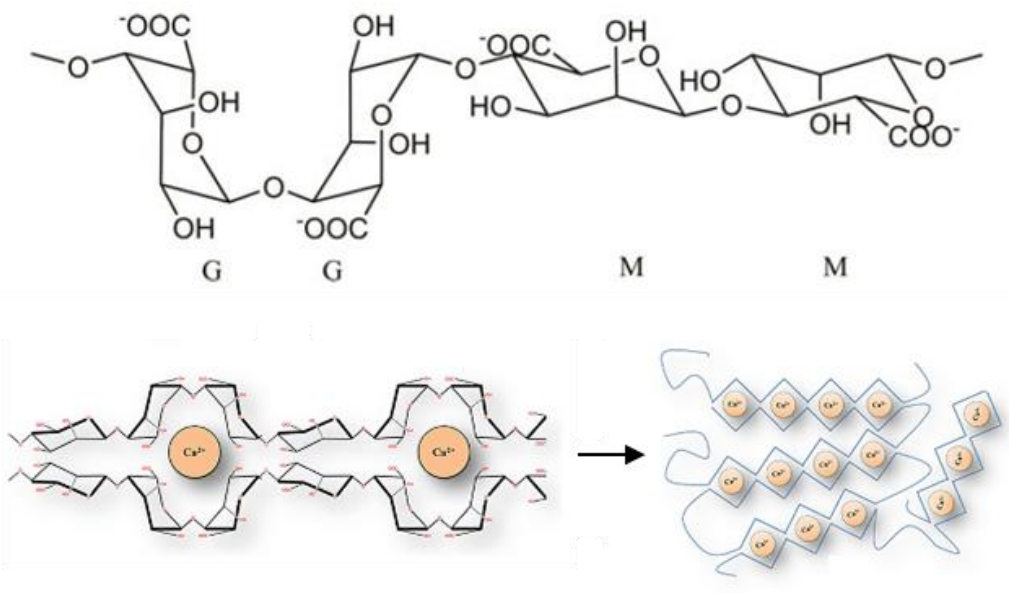


Figure 1.13: Alginate polymers consist out of β -D-mannuronic acid (M) and α -L-guluronic acid (G) monomers, ordered in GG-blocks, MM-blocks or MG-blocks. The GG-blocks are responsible for the selective capturing of cations, crosslinking through an "egg-box" pattern.^[12]

1.3. Summary, Aims and Objectives

This chapter presented a literature review about diabetes, cell encapsulation techniques, and materials used for cell encapsulation. In this thesis, the development and improvement of the encapsulation of pancreatic islets for better transplantation outcomes are investigated. Current islet transplantation has good short-term outcomes, but most patients become insulin dependent again within 5 years. The three main problems with the current transplantation method are the high demand of human donors (with multiple donors necessary to fully treat 1 patient), the fact that the person's own immune-system tries to destroy the islets and that the immunosuppressants administered to stop this from happening are cytotoxic to the islets. Encapsulation of the islets could deal with 2 out of 3 of these problems. Since the islets will not be vascularized (due to the encapsulation) and have to get all their nutrients through diffusion, the diffusion distance should be minimized and the transplantation site should be highly vascularized. Macro-encapsulation is a method that could transplant all the necessary islets in one device and allows for the retrieval of all the islets at a later timepoint, if necessary. However, due to their size the diffusion distance in these devices is large, which results in poor glucose-mediated insulin secretion, even when islets were kept alive with additional oxygen, or transplanted in a pre-vascularized area. Micro-encapsulation encapsulates all the islets separately, allowing for a much smaller diffusion distance, and therefore better results with survival and reaction time when blood glucose levels increase. For those reasons micro-encapsulation has our preference.

If possible, the transplantation site should be highly vascularized, to increase the diffusion of oxygen, nutrients and insulin between the non-vascularized islets and the blood flow. The deprivation of any direct vascularization can also result in the necrosis of larger encapsulated islets, so creating smaller islets for encapsulation would be preferable.

To encapsulate the islets, multiple options were investigated. Since the diffusion distance should preferably be minimized, using a droplet generator or the emulsion method do not meet our criteria, as they create larger encapsulations. This left electro-spraying and microfluidics as available options. The choice was made to use electro-spraying, as this does not involve any form of oils that might adhere to the encapsulations but still allows for the creation of reproduceable, mono-sized encapsulations. Furthermore, although it is a well-researched cell encapsulation method, it had not yet been for the encapsulation of human pancreatic islets.

The encapsulation material should be able to shield the islets from white blood cells and their secreted antibodies, while not invoking any sort of immune-reaction itself (Figure 1.14). For the encapsulation material, a choice had to be made between synthetic or natural biomaterials. Since synthetic biomaterials are either quite expensive or need intricate techniques to be fabricated, a choice was made for natural materials. The biomaterials from mammalian sources that were reviewed are useful for islet encapsulation, as they can support the islets with their function or increase the vascularization of the islets. However, they do not provide any immune-protection, which is the main reason for the encapsulation of the islets. Therefore, the plant-based materials were deemed more appropriate. Alginate was chosen, as alginate is a cheap, readily available material, which provides immunoprotection, and is easy to work with as it will stay liquid until cross-linked with cations. Furthermore, it is the only material already approved for clinical trials. The absence of gelation triggers based on temperature, pH or UV-light, usually found in synthetic hydrogels, make the use of alginate a very safe choice to use with cells. However, as it is a natural biomaterial, it will have some impurities. For alginate to be useful for immunoprotection, it will have to be very pure, so it will not set off a non-specific immune reaction.

To fulfil all the requirements necessary for a successful transplantation, this thesis has the following objectives:

- To develop the method of encapsulation; focusing on small, uniform encapsulations.
- To research the material used for encapsulation; specifically, its purity and its permeability for antibodies
- To encapsulate islets and research their viability and function
- To research the possibility of creating smaller functional islets.
- To research the possibility of a pancreatic islet patch for increased vascularization

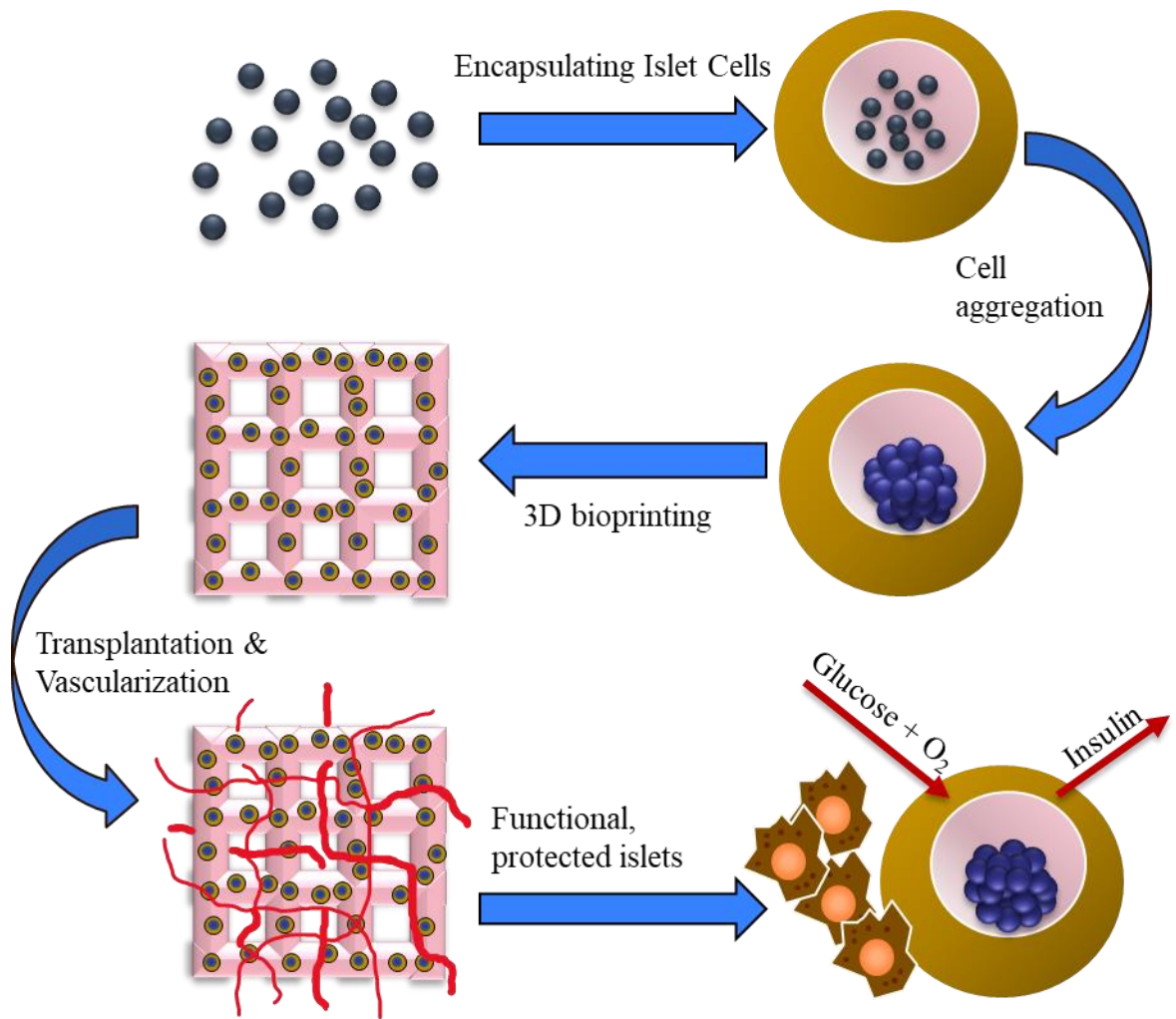


Figure 1.14: The main objective of this research is to develop and improve methods for the encapsulation of Islets of Langerhans for transplantation. The ideal outcome of this research would be to develop a method where dissociated islets are encapsulated, allowed to aggregate into smaller islet in situ to prevent necrosis of the core of the islets. The material used for the encapsulation should prevent the immune system from reaching the islets, while allowing oxygen and nutrients to pass, and the islet to function normally. As the encapsulated islets themselves cannot be vascularized, the encapsulated islets could be 3D bioprinted into a material that will enhance angiogenesis locally, creating the perfect, high vascularized environment for the islets to function.

1.4. Structure of the Thesis

Each chapter of this thesis will describe a different part of the research. Below a short overview can be seen for the structure of this thesis.

- Chapter 1: Introduction.

In this chapter the motivation and background for this thesis are given, as well as a short review of what is known in literature. Based on these findings, an overview of the aims and objectives of the project are given.

- Chapter 2: Methods and materials.

In this chapter the methodology and experimental details of the experiments are described.

- Chapter 3: Design, construction and optimisation of the micro-encapsulator.

In this chapter the design of the micro-encapsulator is described, as well as the testing of the parameters of the micro-encapsulator and the improvements and adjustments made to the machine.

- Chapter 4: Purified alginate for clinical cell encapsulation.

This chapter deals with the purification of alginate as a material for the encapsulation of pancreatic islets and also tests the permeability of the material using confocal microscopy.

- Chapter 5: One-step encapsulated organoid formation.

In this chapter the method of creating core-shell encapsulations is described, as well as design changes to the micro-encapsulator and testing new parameters. These encapsulations with a liquid core but a hydrogel shell allow encapsulated cells to migrate through the core freely and aggregate. This method was tested using HepaRG cells, monitoring their viability and function.

- Chapter 6: Islet encapsulation.

In the 6th chapter islet encapsulation is investigated, both the direct encapsulation as well as the core-shell encapsulation. The viability and function of the (encapsulated) islets is investigated.

- Chapter 7: Towards a pancreatic islet patch.

In this chapter the possibility and method of creating a pancreatic patch that will enhance vascularisation surrounding the encapsulated islets is investigated. Both alginate and collagen patches are created and tested for their vascularization properties by placing them on the Chorioallantoic membrane (CAM) of a chicken egg.

- Chapter 8: Summary and future works.

In this chapter the main findings of each chapter are summarized and recommendations for improvements and for future work is given.

1.5. References

- [1]. Federation ID, *Key Messages*, <http://www.diabetesatlas.org/key-messages.html>, March **2018**
- [2]. OpenStax, *The Endocrine Pancreas*, OpenStax CNX, <http://cnx.org/contents/93048ca2-ed02-4cf8-a310-8a8474fc1b21@3.>, 24-04-2019 **2019**
- [3]. de Vos P, Spasojevic M, Faas MM. Treatment of diabetes with encapsulated islets. *Therapeutic Applications of Cell Microencapsulation: Springer*; **2010**. p. 38-53.
- [4]. Zimmermann H, Shirley SG, Zimmermann U. Alginate-based encapsulation of cells: past, present, and future. *Current diabetes reports*. **2007**;7(4):314-20.
- [5]. Moghadam H, Samimi M, Samimi A, Khorram M. Study of parameters affecting size distribution of beads produced from electro-spray of high viscous liquids. *Iran J Chem Eng*. **2009**;6(3):83-98.
- [6]. Batorsky A, Liao J, Lund AW, Plopper GE, Stegemann JP. Encapsulation of adult human mesenchymal stem cells within collagen-agarose microenvironments. *Biotechnology and Bioengineering*. **2005**;92(4):492-500.
- [7]. Wiedemeier S, Ehrhart F, Mettler E, Gastrock G, Forst T, Weber MM, *et al*. Encapsulation of Langerhans' islets: Microtechnological developments for transplantation. *Engineering in Life Sciences*. **2011**;11(2):165-73.
- [8]. Zhu J. Bioactive modification of poly(ethylene glycol) hydrogels for tissue engineering. *Biomaterials*. **2010**;31(17):4639-56.
- [9]. Li C, Faulkner-Jones A, Dun AR, Jin J, Chen P, Xing Y, *et al*. Rapid Formation of a Supramolecular Polypeptide–DNA Hydrogel for In Situ Three-Dimensional Multilayer Bioprinting. *Angewandte Chemie International Edition*. **2015**;54(13):3957-61.
- [10]. de Vos P, Lazarjani HA, Poncelet D, Faas MM. Polymers in cell encapsulation from an enveloped cell perspective. *Advanced Drug Delivery Reviews*. **2014**;67–68(0):15-34.
- [11]. Diagnosis and Classification of Diabetes Mellitus. *Diabetes Care*. **2013**;36(Supplement 1):S67-S74.
- [12]. Paredes Juarez GA, Spasojevic M, Faas MM, de Vos P. Immunological and technical considerations in application of alginate-based microencapsulation systems. *Front Bioeng Biotechnol*. **2014**;2:26.
- [13]. Visser CW, Kamperman T, Karbaat LP, Lohse D, Karperien M. In-air microfluidics enables rapid fabrication of emulsions, suspensions, and 3D modular (bio)materials. *Science Advances*. **2018**;4(1).
- [14]. Hoesli CA, Raghuram K, Kiang RLJ, Mocinecová D, Hu X, Johnson JD, *et al*. Pancreatic cell immobilization in alginate beads produced by emulsion and internal gelation. *Biotechnology and Bioengineering*. **2011**;108(2):424-34.

- [15]. De Haan BJ, Faas MM, De Vos P. Factors influencing insulin secretion from encapsulated islets. *Cell Transplantation*. **2003**;12(6):617-25.
- [16]. Nathan DM. Long-term complications of diabetes mellitus. *New England Journal of Medicine*. **1993**;328(23):1676-85.
- [17]. You W-P, Henneberg M. Type 1 diabetes prevalence increasing globally and regionally: the role of natural selection and life expectancy at birth. *BMJ Open Diabetes Research & Care*. **2016**;4(1).
- [18]. Korsgren O, Lundgren T, Felldin M, Foss A, Isaksson B, Permert J, *et al*. Optimising islet engraftment is critical for successful clinical islet transplantation. *Diabetologia*. **2008**;51(2):227-32.
- [19]. Carlsson P-O, Espes D, Sedigh A, Rotem A, Zimmerman B, Grinberg H, *et al*. Transplantation of macroencapsulated human islets within the bioartificial pancreas β Air to patients with type 1 diabetes mellitus. *American Journal of Transplantation*. **2018**;18(7):1735-44.
- [20]. Shapiro AM, Ricordi C, Hering BJ, Auchincloss H, Lindblad R, Robertson RP, *et al*. International trial of the Edmonton protocol for islet transplantation. *New England Journal of Medicine*. **2006**;355(13):1318-30.
- [21]. Ryan EA, Paty BW, Senior PA, Bigam D, Alfadhli E, Kneteman NM, *et al*. Five-Year Follow-Up After Clinical Islet Transplantation. *Diabetes*. **2005**;54(7):2060-9.
- [22]. Keymeulen B, Gillard P, Mathieu C, Movahedi B, Maleux G, Delvaux G, *et al*. Correlation between beta cell mass and glycemic control in type 1 diabetic recipients of islet cell graft. *Proc Natl Acad Sci U S A*. **2006**;103(46):17444-9.
- [23]. Calafiore R, Basta G. Clinical application of microencapsulated islets: actual perspectives on progress and challenges. *Adv Drug Deliv Rev*. **2014**;67-68:84-92.
- [24]. Murua A, Portero A, Orive G, Hernandez RM, de Castro M, Pedraz JL. Cell microencapsulation technology: towards clinical application. *J Control Release*. **2008**;132(2):76-83.
- [25]. Yang HK, Yoon KH. Current status of encapsulated islet transplantation. *J Diabetes Complications*. **2015**;29(5):737-43.
- [26]. Basta G, Montanucci P, Luca G, Boselli C, Noya G, Barbaro B, *et al*. Long-term metabolic and immunological follow-up of nonimmunosuppressed patients with type 1 diabetes treated with microencapsulated islet allografts: four cases. *Diabetes Care*. **2011**;34(11):2406-9.
- [27]. Association AD. Type 2 Diabetes in Children and Adolescents. *Pediatrics*. **2000**;105(3):671-80.
- [28]. Kahn SE, Hull RL, Utzschneider KM. Mechanisms linking obesity to insulin resistance and type 2 diabetes. *Nature*. **2006**;444:840.

- [29]. Goodyear LJ, Kahn BB. Exercise, glucose transport, and insulin sensitivity. *Annual review of medicine*. **1998**;49(1):235-61.
- [30]. Vaxillaire M, Froguel P. The Genetics of Type 2 Diabetes: From Candidate Gene Biology to Genome - Wide Studies. *Textbook of Diabetes*. **2010**:191-214.
- [31]. Khunti K, Kumar S, Brodie J. Diabetes UK and South Asian Health Foundation recommendations on diabetes research priorities for British South Asians. *London: Diabetes UK*. **2009**.
- [32]. Malik VS, Popkin BM, Bray GA, Després J-P, Willett WC, Hu FB. Sugar sweetened beverages and risk of metabolic syndrome and type 2 diabetes: a meta-analysis. *Diabetes Care*. **2010**.
- [33]. White P. Diabetes mellitus in pregnancy. *Clinics in perinatology*. **1974**;1(2):331-48.
- [34]. DeFronzo RA. Glucose intolerance and aging: evidence for tissue insensitivity to insulin. *Diabetes*. **1979**;28(12):1095-101.
- [35]. Astrup A, Finer N. Redefining Type 2 diabetes: 'Diabesity' or 'Obesity Dependent Diabetes Mellitus'? *Obesity Reviews*. **2000**;1(2):57-9.
- [36]. Mohammad S, Ahmad J. Management of obesity in patients with type 2 diabetes mellitus in primary care. *Diabetes & Metabolic Syndrome: Clinical Research & Reviews*. **2016**;10(3):171-81.
- [37]. Bosco D, Armanet M, Morel P, Niclauss N, Sgroi A, Muller YD, *et al*. Unique Arrangement of α - and β -Cells in Human Islets of Langerhans. *Diabetes*. **2010**;59(5):1202-10.
- [38]. Knip M, Veijola R, Virtanen SM, Hyoty H, Vaarala O, Akerblom HK. Environmental triggers and determinants of type 1 diabetes. *Diabetes*. **2005**;54 Suppl 2:S125-36.
- [39]. Redondo MJ, Jeffrey J, Fain PR, Eisenbarth GS, Orban T. Concordance for Islet Autoimmunity among Monozygotic Twins. *New England Journal of Medicine*. **2008**;359(26):2849-50.
- [40]. Pociot F, Akolkar B, Concannon P, Erlich HA, Julier C, Morahan G, *et al*. Genetics of type 1 diabetes: what's next? *Diabetes*. **2010**;59(7):1561-71.
- [41]. Eringsmark Regnéll S, Lernmark Å. The environment and the origins of islet autoimmunity and Type 1 diabetes. *Diabetic Medicine*. **2013**;30(2):155-60.
- [42]. Ben-Ami H, Nagachandran P, Mendelson A, Edoute Y. Drug-Induced Hypoglycemic Coma in 102 Diabetic Patients. *Archives of Internal Medicine*. **1999**;159(3):281-4.
- [43]. Alsahli M, Gerich JE. Hypoglycemia in Patients with Diabetes and Renal Disease. *Journal of clinical medicine*. **2015**;4(5):948-64.
- [44]. Brazeau A-S, Rabasa-Lhoret R, Strychar I, Mircescu H. Barriers to Physical Activity Among Patients With Type 1 Diabetes. *Diabetes Care*. **2008**;31(11):2108-9.

- [45]. Niclauss N, Morel P, Berney T. Has the gap between pancreas and islet transplantation closed? *Transplantation*. **2014**;98(6):593-9.
- [46]. Berney T, Johnson PRV. Donor Pancreata: Evolving Approaches to Organ Allocation for Whole Pancreas Versus Islet Transplantation. *Transplantation*. **2010**;90(3):238-43.
- [47]. Davies C. No more daily jabs or endless blood tests... The 30-minute op to give diabetics their lives back. Daily Mail. 2010 23-03-2010.
- [48]. Schive SW, Foss A, Sahraoui A, Kloster-Jensen K, Hafsahl G, Kvalheim G, *et al*. Cost and clinical outcome of islet transplantation in Norway 2010-2015. *Clinical Transplantation*. **2017**;31(1):e12871.
- [49]. Keymeulen B, Gillard P, Mathieu C, Movahedi B, Maleux G, Delvaux G, *et al*. Correlation between β cell mass and glycemic control in type 1 diabetic recipients of islet cell graft. *Proceedings of the National Academy of Sciences*. **2006**;103(46):17444-9.
- [50]. Calafiore R, Basta G. Clinical application of microencapsulated islets: Actual prospectives on progress and challenges. *Advanced Drug Delivery Reviews*. **2014**;67:84-92.
- [51]. Rezzesi FD. Eine Methode zur Züchtung der Gewebe in vivo: G. Fischer; **1932**.
- [52]. Algire GH, Weaver JM, Prehn RT. STUDIES ON TISSUE HOMOTRANSPLANTATION IN MICE, USING DIFFUSION-CHAMBER METHODS. *Ann N Y Acad Sci*. **1957**;64(5):1009-13.
- [53]. Algire GH, Legallais FY. Recent Developments in the Transparent-Chamber Technique as Adapted to the Mouse. *Journal of the National Cancer Institute*. **1949**;10(2):225-53.
- [54]. Uludag H, De Vos P, Tresco PA. Technology of mammalian cell encapsulation. *Advanced Drug Delivery Reviews*. **2000**;42(1-2):29-64.
- [55]. Kukreja A, Cost G, Marker J, Zhang C, Sun Z, Lin-Su K, *et al*. Multiple immunoregulatory defects in type-1 diabetes. *The Journal of Clinical Investigation*. **2002**;109(1):131-40.
- [56]. Janeway Jr CA, Travers P, Walport M, Shlomchik MJ. The structure of a typical antibody molecule. *Immunobiology: The immune system in Health and Disease 5th edition***2001**.
- [57]. Wheater PR, Burkitt HG, Daniels VG. Functional histology. A text and colour atlas**1979**.
- [58]. Beck J, Angus R, Madsen B, Britt D, Vernon B, Nguyen KT. Islet encapsulation: strategies to enhance islet cell functions. *Tissue Engineering*. **2007**;13(3):589-99.
- [59]. Information. NCfB, *PubChem Compound Database*; CID=16131099, <https://pubchem.ncbi.nlm.nih.gov/compound/16131099>, March **2018**
- [60]. Information. NCfB, *PubChem Compound Database*; CID=79025,, <https://pubchem.ncbi.nlm.nih.gov/compound/79025> March **2018**

- [61]. Vos PD, Haan BJD, Wolters GHJ, Strubbe JH, Schilfgaarde RV. Improved biocompatibility but limited graft survival after purification of alginate for microencapsulation of pancreatic islets. *Diabetologia*. **1997**;40(3):262-70.
- [62]. Fritschy W, de Vos P, Groen H, Klatter F, Pasma A, Wolters GJ, *et al.* The capsular overgrowth on microencapsulated pancreatic islet grafts in streptozotocin and autoimmune diabetic rats. *Transplant International*. **1994**;7(4):264-71.
- [63]. Říhová B. Immunocompatibility and biocompatibility of cell delivery systems. *Advanced Drug Delivery Reviews*. **2000**;42(1-2):65-80.
- [64]. De Vos P, De Haan B, Van Schilfgaarde R. Effect of the alginate composition on the biocompatibility of alginate-polylysine microcapsules. *Biomaterials*. **1997**;18(3):273-8.
- [65]. Van Schilfgaarde R, De Vos P. Factors influencing the properties and performance of microcapsules for immunoprotection of pancreatic islets. *Journal of molecular medicine*. **1999**;77(1):199-205.
- [66]. De Vos P, Van Straaten JFM, Nieuwenhuizen AG, De Groot M, Ploeg RJ, De Haan BJ, *et al.* Why do microencapsulated islet grafts fail in the absence of fibrotic overgrowth? *Diabetes*. **1999**;48(7):1381-8.
- [67]. Veisoh O, Doloff JC, Ma M, Vegas AJ, Tam HH, Bader Andrew R, *et al.* Size- and shape-dependent foreign body immune response to materials implanted in rodents and non-human primates. *Nature Materials*. **2015**;14:643.
- [68]. Gunton JE, Kulkarni RN, Yim S, Okada T, Hawthorne WJ, Tseng Y-H, *et al.* Loss of ARNT/HIF1 β Mediates Altered Gene Expression and Pancreatic-Islet Dysfunction in Human Type 2 Diabetes. *Cell*. **2005**;122(3):337-49.
- [69]. Sato Y, Endo H, Okuyama H, Takeda T, Iwahashi H, Imagawa A, *et al.* Cellular Hypoxia of Pancreatic β -Cells Due to High Levels of Oxygen Consumption for Insulin Secretion in Vitro. *Journal of Biological Chemistry*. **2011**;286(14):12524-32.
- [70]. Cantley J, Grey ST, Maxwell PH, Withers DJ. The hypoxia response pathway and β -cell function. *Diabetes, Obesity and Metabolism*. **2010**;12:159-67.
- [71]. Pedraza E, Coronel MM, Fraker CA, Ricordi C, Stabler CL. Preventing hypoxia-induced cell death in beta cells and islets via hydrolytically activated, oxygen-generating biomaterials. *Proceedings of the National Academy of Sciences*. **2012**;109(11):4245-50.
- [72]. de Groot M, Schuurs TA, van Schilfgaarde R. Causes of limited survival of microencapsulated pancreatic islet grafts. *Journal of Surgical Research*. **2004**;121(1):141-50.
- [73]. Lovett M, Lee K, Edwards A, Kaplan DL. Vascularization strategies for tissue engineering. *Tissue Eng Part B Rev*. **2009**;15(3):353-70.
- [74]. Olsson R, Carlsson P-O. Better vascular engraftment and function in pancreatic islets transplanted without prior culture. *Diabetologia*. **2005**;48(3):469-76.

- [75]. O'Sullivan ES, Johnson AS, Omer A, Hollister-Lock J, Bonner-Weir S, Colton CK, *et al.* Rat islet cell aggregates are superior to islets for transplantation in microcapsules. *Diabetologia*. **2010**;53(5):937-45.
- [76]. Buitinga M, Truckenmüller R, Engelse MA, Moroni L, Ten Hoopen HWM, van Blitterswijk CA, *et al.* Microwell Scaffolds for the Extrahepatic Transplantation of Islets of Langerhans. *PLoS One*. **2013**;8(5):e64772.
- [77]. Vériter S, Gianello P, Dufrane D. Bioengineered sites for islet cell transplantation. *Current Diabetes Reports*. **2013**;13(5):745-55.
- [78]. Sakata N, Aoki T, Yoshimatsu G, Tsuchiya H, Hata T, Katayose Y, *et al.* Strategy for clinical setting in intramuscular and subcutaneous islet transplantation. *Diabetes Metab Res Rev*. **2014**;30(1):1-10.
- [79]. de Vos P, Lazarjani HA, Poncelet D, Faas MM. Polymers in cell encapsulation from an enveloped cell perspective. *Adv Drug Deliv Rev*. **2014**;67-68:15-34.
- [80]. Yang HK, Yoon K-H. Current status of encapsulated islet transplantation. *Journal of Diabetes and its Complications*. (0).
- [81]. Scharp DW, Marchetti P. Encapsulated islets for diabetes therapy: History, current progress, and critical issues requiring solution. *Advanced Drug Delivery Reviews*. **2014**;67–68(0):35-73.
- [82]. Lanza RP, Chick WL. Transplantation of encapsulated cells and tissues. *Surgery*. **1997**;121(1):1-9.
- [83]. de Vos P, Spasojevic M, Faas M. Treatment of Diabetes with Encapsulated Islets. In: Pedraz J, Orive G, editors. *Therapeutic Applications of Cell Microencapsulation*. Advances in Experimental Medicine and Biology. 670: Springer New York; **2010**. p. 38-53.
- [84]. Gazda LS, Vinerean HV, Laramore MA, Diehl CH, Hall RD, Rubin AL, *et al.* Encapsulation of porcine islets permits extended culture time and insulin independence in spontaneously diabetic BB rats. *Cell Transplantation*. **2007**;16(6):609-20.
- [85]. Ludwig B, Reichel A, Steffen A, Zimmerman B, Schally AV, Block NL, *et al.* Transplantation of human islets without immunosuppression. *Proceedings of the National Academy of Sciences*. **2013**;110(47):19054-8.
- [86]. Barkai U, Weir GC, Colton CK, Ludwig B, Bornstein SR, Brendel MD, *et al.* Enhanced oxygen supply improves islet viability in a new bioartificial pancreas. *Cell Transplantation*. **2013**;22(8):1463-76.
- [87]. Duvivier-Kali VF, Omer A, Lopez-Avalos MD, O'Neil JJ, Weir GC. Survival of Microencapsulated Adult Pig Islets in Mice In Spite of an Antibody Response. *American Journal of Transplantation*. **2004**;4(12):1991-2000.
- [88]. Zimmermann H, Zimmermann D, Reuss R, Feilen PJ, Manz B, Katsen A, *et al.* Towards a medically approved technology for alginate-based microcapsules allowing long-term immunoisolated transplantation. *Journal of Materials Science: Materials in Medicine*. **2005**;16(6):491-501.

- [89]. Colton CK. Chapter 28 - Challenges in the Development of Immunoisolation Devices. In: Vacanti RLL, editor. *Principles of Tissue Engineering (Fourth Edition)*. Boston: *Academic Press*; **2014**. p. 543-62.
- [90]. Zimmermann H, Shirley S, Zimmermann U. Alginate-based encapsulation of cells: Past, present, and future. *Current Diabetes Reports*. **2007**;7(4):314-20.
- [91]. Zimmermann H, Ehrhart F, Zimmermann D, Müller K, Katsen-Globa A, Behringer M, *et al.* Hydrogel-based encapsulation of biological, functional tissue: fundamentals, technologies and applications. *Applied Physics A*. **2007**;89(4):909-22.
- [92]. Hoesli CA, Kiang RLJ, Mocinecová D, Speck M, Mošková DJ, Donald-Hague C, *et al.* Reversal of diabetes by β TC3 cells encapsulated in alginate beads generated by emulsion and internal gelation. *Journal of Biomedical Materials Research Part B: Applied Biomaterials*. **2012**;100B(4):1017-28.
- [93]. Selimović Š, Oh J, Bae H, Dokmeci M, Khademhosseini A. Microscale strategies for generating cell-encapsulating hydrogels. *Polymers*. **2012**;4(3):1554-79.
- [94]. Kang A, Park J, Ju J, Jeong GS, Lee S-H. Cell encapsulation via microtechnologies. *Biomaterials*. **2014**;35(9):2651-63.
- [95]. Moghadam H, Samimi M, Samimi A, Khorram M. Electro-spray of high viscous liquids for producing mono-sized spherical alginate beads. *Particuology*. **2008**;6(4):271-5.
- [96]. Moghadam H, Samimi M, Samimi A, Khorram M. Electrospray modeling of highly viscous and non-Newtonian liquids. *Journal of applied polymer science*. **2010**;118(3):1288-96.
- [97]. Fu H, Hoerr RA, Ryan PJ, editors. A high-throughput electrospray nozzle for nanoparticle production. Technical Proceedings of the 2014 NSTI Nanotechnology Conference and Expo, NSTI-Nanotech 2014; 2014.
- [98]. Ma M, Chiu A, Sahay G, Doloff JC, Dholakia N, Thakrar R, *et al.* Core-shell hydrogel microcapsules for improved islets encapsulation. *Advanced Healthcare Materials*. **2013**;2(5):667-72.
- [99]. Gasperini L, Maniglio D, Migliaresi C. Microencapsulation of cells in alginate through an electrohydrodynamic process. *Journal of Bioactive and Compatible Polymers*. **2013**;28(5):413-25.
- [100]. Ng KE, Joly P, Jayasinghe SN, Vernay B, Knight R, Barry SP, *et al.* Bio-electrospraying primary cardiac cells: In vitro tissue creation and functional study. *Biotechnology Journal*. **2011**;6(1):86-95.
- [101]. Xie J, Wang C-H. Electrospray in the dripping mode for cell microencapsulation. *Journal of Colloid and Interface Science*. **2007**;312(2):247-55.
- [102]. Zhang W, He X. Encapsulation of living cells in small ($\sim 100 \mu\text{m}$) alginate microcapsules by electrostatic spraying: a parametric study. *Journal of Biomechanical Engineering*. **2009**;131(7):074515.

- [103]. Barron C, He J-Q. Alginate-based microcapsules generated with the coaxial electro spray method for clinical application. *Journal of Biomaterials Science, Polymer Edition*. **2017**;28(13):1245-55.
- [104]. Zhao S, Agarwal P, Rao W, Huang H, Zhang R, Liu Z, *et al*. Coaxial electro spray of liquid core-hydrogel shell microcapsules for encapsulation and miniaturized 3D culture of pluripotent stem cells. *Integr Biol (Camb)*. **2014**;6(9):874-84.
- [105]. Lu Y-C, Song W, An D, Kim BJ, Schwartz R, Wu M, *et al*. Designing compartmentalized hydrogel microparticles for cell encapsulation and scalable 3D cell culture. *J Mater Chem B*. **2015**;3(3):353-60.
- [106]. Edalat F, Sheu I, Manoucheri S, Khademhosseini A. Material strategies for creating artificial cell-instructive niches. *Curr Opin Biotechnol*. **2012**;23(5):820-5.
- [107]. Bajaj P, Schweller RM, Khademhosseini A, West JL, Bashir R. 3D Biofabrication Strategies for Tissue Engineering and Regenerative Medicine. *Annual review of biomedical engineering*. **2014**;16(1):247-76.
- [108]. Chiono V, Nardo T, Ciardelli G. Chapter 9 - Bioartificial Biomaterials for Regenerative Medicine Applications. In: Stratta GOLSJ, editor. *Regenerative Medicine Applications in Organ Transplantation*. Boston: *Academic Press*; **2014**. p. 113-36.
- [109]. Mann BK, Gobin AS, Tsai AT, Schmedlen RH, West JL. Smooth muscle cell growth in photopolymerized hydrogels with cell adhesive and proteolytically degradable domains: synthetic ECM analogs for tissue engineering. *Biomaterials*. **2001**;22(22):3045-51.
- [110]. Hoffman MD, Van Hove AH, Benoit DSW. Degradable hydrogels for spatiotemporal control of mesenchymal stem cells localized at decellularized bone allografts. *Acta Biomater*. **2014**;10(8):3431-41.
- [111]. Goraltchouk A, Freier T, Shoichet MS. Synthesis of degradable poly(l-lactide-co-ethylene glycol) porous tubes by liquid-liquid centrifugal casting for use as nerve guidance channels. *Biomaterials*. **2005**;26(36):7555-63.
- [112]. Gong C, Shi S, Dong P, Kan B, Gou M, Wang X, *et al*. Synthesis and characterization of PEG-PCL-PEG thermosensitive hydrogel. *International Journal of Pharmaceutics*. **2009**;365(1-2):89-99.
- [113]. Krishna L, Jayabalan M. Synthesis and characterization of biodegradable poly (ethylene glycol) and poly (caprolactone diol) end capped poly (propylene fumarate) cross linked amphiphilic hydrogel as tissue engineering scaffold material. *Journal of Materials Science: Materials in Medicine*. **2009**;20(1):115-22.
- [114]. Lutolf MP, Lauer-Fields JL, Schmoekel HG, Metters AT, Weber FE, Fields GB, *et al*. Synthetic matrix metalloproteinase-sensitive hydrogels for the conduction of tissue regeneration: Engineering cell-invasion characteristics. *Proceedings of the National Academy of Sciences*. **2003**;100(9):5413-8.

- [115]. Su J, Hu B-H, Lowe Jr WL, Kaufman DB, Messersmith PB. Anti-inflammatory peptide-functionalized hydrogels for insulin-secreting cell encapsulation. *Biomaterials*. **2010**;31(2):308-14.
- [116]. Cheung CY, Anseth KS. Synthesis of Immunoisolation Barriers That Provide Localized Immunosuppression for Encapsulated Pancreatic Islets. *Bioconjugate Chemistry*. **2006**;17(4):1036-42.
- [117]. Nuttelman CR, Tripodi MC, Anseth KS. Synthetic hydrogel niches that promote hMSC viability. *Matrix Biology*. **2005**;24(3):208-18.
- [118]. Liu SQ, Tay R, Khan M, Rachel Ee PL, Hedrick JL, Yang YY. Synthetic hydrogels for controlled stem cell differentiation. *Soft Matter*. **2010**;6(1):67-81.
- [119]. Mason MN, Mahoney MJ. Selective β -Cell Differentiation of Dissociated Embryonic Pancreatic Precursor Cells Cultured in Synthetic Polyethylene Glycol Hydrogels. *Tissue Engineering Part A*. **2008**;15(6):1343-52.
- [120]. Holland TA, Tabata Y, Mikos AG. Dual growth factor delivery from degradable oligo(poly(ethylene glycol) fumarate) hydrogel scaffolds for cartilage tissue engineering. *Journal of controlled release*. **2005**;101(1-3 SPEC. ISS.):111-25.
- [121]. Zhang C, Sangaj N, Hwang Y, Phadke A, Chang CW, Varghese S. Oligo(trimethylene carbonate)-poly(ethylene glycol)-oligo(trimethylene carbonate) triblock-based hydrogels for cartilage tissue engineering. *Acta Biomater*. **2011**;7(9):3362-9.
- [122]. Weber LM, He J, Bradley B, Haskins K, Anseth KS. PEG-based hydrogels as an in vitro encapsulation platform for testing controlled β -cell microenvironments. *Acta Biomater*. **2006**;2(1):1-8.
- [123]. Cruise GM, Hegre OD, Lamberti FV, Hager SR, Hill R, Scharp DS, *et al*. In vitro and in vivo performance of porcine islets encapsulated in interfacially photopolymerized poly(ethylene glycol) diacrylate membranes. *Cell Transplantation*. **1999**;8(3):293-306.
- [124]. Kizilel S, Scavone A, Liu X, Nothias JM, Ostrega D, Witkowski P, *et al*. Encapsulation of pancreatic islets within nano-thin functional polyethylene glycol coatings for enhanced insulin secretion. *Tissue Engineering - Part A*. **2010**;16(7):2217-28.
- [125]. Kopesky PW, Vanderploeg EJ, Sandy JS, Kurz B, Grodzinsky AJ. Self-Assembling Peptide Hydrogels Modulate In Vitro Chondrogenesis of Bovine Bone Marrow Stromal Cells. *Tissue Engineering Part A*. **2009**;16(2):465-77.
- [126]. Holmes TC. Novel peptide-based biomaterial scaffolds for tissue engineering. *Trends Biotechnol*. **2002**;20(1):16-21.
- [127]. Liao SW, Rawson J, Omori K, Ishiyama K, Mozhdehi D, Oancea AR, *et al*. Maintaining functional islets through encapsulation in an injectable saccharide-peptide hydrogel. *Biomaterials*. **2013**;34(16):3984-91.
- [128]. Chawla K, Yu TB, Liao SW, Guan Z. Biodegradable and Biocompatible Synthetic Saccharide-Peptide Hydrogels for Three-Dimensional Stem Cell Culture. *Biomacromolecules*. **2011**;12(3):560-7.

- [129]. Haines-Butterick L, Rajagopal K, Branco M, Salick D, Rughani R, Pilarz M, *et al.* Controlling hydrogelation kinetics by peptide design for three-dimensional encapsulation and injectable delivery of cells. *Proceedings of the National Academy of Sciences*. **2007**;104(19):7791-6.
- [130]. Rajangam K, Behanna HA, Hui MJ, Han X, Hulvat JF, Lomasney JW, *et al.* Heparin Binding Nanostructures to Promote Growth of Blood Vessels. *Nano Letters*. **2006**;6(9):2086-90.
- [131]. Hunt N, Grover L. Cell encapsulation using biopolymer gels for regenerative medicine. *Biotechnology Letters*. **2010**;32(6):733-42.
- [132]. Janmey PA, Winer JP, Weisel JW. Fibrin gels and their clinical and bioengineering applications. *Journal of The Royal Society Interface*. **2009**;6(30):1-10.
- [133]. Ye KY, Sullivan KE, Black LD. Encapsulation of cardiomyocytes in a fibrin hydrogel for cardiac tissue engineering. *Journal of visualized experiments: JoVE*. **2011**(55).
- [134]. Rajangam T, An SSA. Fibrinogen and fibrin based micro and nano scaffolds incorporated with drugs, proteins, cells and genes for therapeutic biomedical applications. *International Journal of Nanomedicine*. **2013**;8:3641-62.
- [135]. Park KH, Kim H, Moon S, Na K. Bone morphogenic protein-2 (BMP-2) loaded nanoparticles mixed with human mesenchymal stem cell in fibrin hydrogel for bone tissue engineering. *Journal of Bioscience and Bioengineering*. **2009**;108(6):530-7.
- [136]. Ahmed TAE, Dare EV, Hincke M. Fibrin: A Versatile Scaffold for Tissue Engineering Applications. *Tissue Engineering Part B: Reviews*. **2008**;14(2):199-215.
- [137]. Lind M, Larsen A, Clausen C, Osther K, Everland H. Cartilage repair with chondrocytes in fibrin hydrogel and MPEG polylactide scaffold: An in vivo study in goats. *Knee Surgery, Sports Traumatology, Arthroscopy*. **2008**;16(7):690-8.
- [138]. Yuan Ye K, Sullivan KE, Black LD. Encapsulation of cardiomyocytes in a fibrin hydrogel for cardiac tissue engineering. *Journal of visualized experiments : JoVE*. **2011**(55).
- [139]. Yao L, Liu J, Andreadis ST. Composite fibrin scaffolds increase mechanical strength and preserve contractility of tissue engineered blood vessels. *Pharmaceutical Research*. **2008**;25(5):1212-21.
- [140]. Klar AS, Güven S, Biedermann T, Luginbühl J, Böttcher-Haberzeth S, Meuli-Simmen C, *et al.* Tissue-engineered dermo-epidermal skin grafts prevascularized with adipose-derived cells. *Biomaterials*. **2014**;35(19):5065-78.
- [141]. Kim JS, Lim JH, Nam HY, Lim HJ, Shin JS, Shin JY, *et al.* In situ application of hydrogel-type fibrin-islet composite optimized for rapid glycemic control by subcutaneous xenogeneic porcine islet transplantation. *Journal of controlled release*. **2012**;162(2):382-90.
- [142]. Brady A-C, Martino MM, Pedraza E, Sukert S, Pileggi A, Ricordi C, *et al.* Proangiogenic Hydrogels Within Macroporous Scaffolds Enhance Islet Engraftment in an Extrahepatic Site. *Tissue Engineering Part A*. **2013**;19(23-24):2544-52.

- [143]. Lee CH, Singla A, Lee Y. Biomedical applications of collagen. *International Journal of Pharmaceutics*. **2001**;221(1–2):1-22.
- [144]. Johnson TD, Christman KL. Injectable hydrogel therapies and their delivery strategies for treating myocardial infarction. *Expert Opinion on Drug Delivery*. **2013**;10(1):59-72.
- [145]. Parenteau-Bareil R, Gauvin R, Cliche S, Gariépy C, Germain L, Berthod F. Comparative study of bovine, porcine and avian collagens for the production of a tissue engineered dermis. *Acta Biomater*. **2011**;7(10):3757-65.
- [146]. Rubert Pérez CM, Panitch A, Chmielewski J. A collagen peptide-based physical hydrogel for cell encapsulation. *Macromol Biosci*. **2011**;11(10):1426-31.
- [147]. Weber LM, Anseth KS. Hydrogel encapsulation environments functionalized with extracellular matrix interactions increase islet insulin secretion. *Matrix Biology*. **2008**;27(8):667-73.
- [148]. Weber LM, Hayda KN, Anseth KS. Cell–Matrix Interactions Improve β -Cell Survival and Insulin Secretion in Three-Dimensional Culture. *Tissue Engineering Part A*. **2008**;14(12):1959-68.
- [149]. Lee KY, Mooney DJ. Hydrogels for Tissue Engineering. *Chemical Reviews*. **2001**;101(7):1869-80.
- [150]. Kobayashi T, Aomatsu Y, Iwata H, Kin T, Kanehiro H, Hisanaga M, *et al*. Indefinite islet protection from autoimmune destruction in nonobese diabetic mice by agarose microencapsulation without immunosuppression. *Transplantation*. **2003**;75(5):619-25.
- [151]. Gazda LS, Vinerean HV, Laramore MA, Hall RD, Carraway JW, Smith BH. No Evidence of Viral Transmission following Long-Term Implantation of Agarose Encapsulated Porcine Islets in Diabetic Dogs. *Journal of Diabetes Research*. **2014**;2014:11.
- [152]. Iwata H, Kobayashi K, Takagi T, Oka T, Yang H, Amemiya H, *et al*. Feasibility of agarose microbeads with xenogeneic islets as a bioartificial pancreas. *Journal of Biomedical Materials Research*. **1994**;28(9):1003-11.
- [153]. Yang H, Iwata H, Shimizu H, Takagi T, Tsuji T, Ito F. Comparative studies of in vitro and in vivo function of three different shaped bioartificial pancreases made of agarose hydrogel. *Biomaterials*. **1994**;15(2):113-20.
- [154]. Holdcraft RW, Gazda LS, Circle L, Adkins H, Harbeck SG, Meyer ED, *et al*. Enhancement of In Vitro and In Vivo Function of Agarose-Encapsulated Porcine Islets by Changes in the Islet Microenvironment. *Cell Transplantation*. **2014**;23(8):929-44.
- [155]. Miyoshi Y, Date I, Ohmoto T, Iwata H. Histological analysis of microencapsulated dopamine-secreting cells in agarose/poly(styrene sulfonic acid) mixed gel xenotransplanted into the brain. *Experimental Neurology*. **1996**;138(1):169-75.
- [156]. Sakai S, Hashimoto I, Kawakami K. Agarose-gelatin conjugate for adherent cell-enclosing capsules. *Biotechnology Letters*. **2007**;29(5):731-5.

- [157]. Mauck RL, Soltz MA, Wang CCB, Wong DD, Chao PHG, Valhmu WB, *et al.* Functional tissue engineering of articular cartilage through dynamic loading of chondrocyte-seeded agarose gels. *Journal of Biomechanical Engineering*. **2000**;122(3):252-60.
- [158]. Khanarian NT, Haney NM, Burga RA, Lu HH. A functional agarose-hydroxyapatite scaffold for osteochondral interface regeneration. *Biomaterials*. **2012**;33(21):5247-58.
- [159]. Gao M, Lu P, Bednark B, Lynam D, Conner JM, Sakamoto J, *et al.* Templated agarose scaffolds for the support of motor axon regeneration into sites of complete spinal cord transection. *Biomaterials*. **2013**;34(5):1529-36.
- [160]. Odawara A, Gotoh M, Suzuki I. Control of neural network patterning using collagen gel photothermal etching. *Lab on a Chip - Miniaturisation for Chemistry and Biology*. **2013**;13(11):2040-6.
- [161]. Mørch YA, Donati I, Strand BL. Effect of Ca²⁺, Ba²⁺, and Sr²⁺ on Alginate Microbeads. *Biomacromolecules*. **2006**;7(5):1471-80.
- [162]. Draget KI, Gåserød O, Aune I, Andersen PO, Storbakken B, Stokke BT, *et al.* Effects of molecular weight and elastic segment flexibility on syneresis in Ca-alginate gels. *Food Hydrocolloids*. **2001**;15(4-6):485-90.
- [163]. Kendall Jr W, Darrabie M, El-Shewy H, Opara E. Effect of alginate composition and purity on alginate microspheres. *Journal of microencapsulation*. **2004**;21(8):821-8.
- [164]. Haug A, Smidsrød O. The effect of divalent metals on the properties of alginate solutions. *Acta Chemica Scandinavica*. **1965**;19(2):341-51.
- [165]. Alsberg E, Anderson KW, Albeiruti A, Franceschi RT, Mooney DJ. Cell-interactive alginate hydrogels for bone tissue engineering. *Journal of Dental Research*. **2001**;80(11):2025-9.
- [166]. Trouche E, Girod Fullana S, Mias C, Ceccaldi C, Tortosa F, Seguelas MH, *et al.* Evaluation of Alginate Microspheres for Mesenchymal Stem Cell Engraftment on Solid Organ. *Cell Transplantation*. **2010**;19(12):1623-33.
- [167]. Prang P, Müller R, Eljaouhari A, Heckmann K, Kunz W, Weber T, *et al.* The promotion of oriented axonal regrowth in the injured spinal cord by alginate-based anisotropic capillary hydrogels. *Biomaterials*. **2006**;27(19):3560-9.
- [168]. Matyash M, Despang F, Ikonomidou C, Gelinsky M. Swelling and mechanical properties of alginate hydrogels with respect to promotion of neural growth. *Tissue Engineering - Part C: Methods*. **2014**;20(5):401-11.
- [169]. Lee CH, Wang YJ, Kuo SM, Chang SJ. Microencapsulation of parathyroid tissue with photosensitive poly(L-lysine) and short chain alginate-co-MPEG. *Artificial Organs*. **2004**;28(6):537-42.
- [170]. Tritz J, Rahouadj R, De Isla N, Charif N, Pinzano A, Mainard D, *et al.* Designing a three-dimensional alginate hydrogel by spraying method for cartilage tissue engineering. *Soft Matter*. **2010**;6(20):5165-74.

- [171]. Kim G, Ahn S, Kim Y, Cho Y, Chun W. Coaxial structured collagen-alginate scaffolds: Fabrication, physical properties, and biomedical application for skin tissue regeneration. *Journal of Materials Chemistry*. **2011**;21(17):6165-72.
- [172]. Lim F, Sun A. Microencapsulated islets as bioartificial endocrine pancreas. *Science*. **1980**;210(4472):908-10.
- [173]. Omer A, Duvivier-Kali VF, Trivedi N, Wilmot K, Bonner-Weir S, Weir GC. Survival and Maturation of Microencapsulated Porcine Neonatal Pancreatic Cell Clusters Transplanted into Immunocompetent Diabetic Mice. *Diabetes*. **2003**;52(1):69-75.
- [174]. Arifin DR, Manek S, Call E, Arepally A, Bulte JWM. Microcapsules with intrinsic barium radiopacity for immunoprotection and X-ray/CT imaging of pancreatic islet cells. *Biomaterials*. **2012**;33(18):4681-9.
- [175]. Storz H, Müller KJ, Ehrhart F, Gómez I, Shirley SG, Gessner P, *et al*. Physicochemical features of ultra-high viscosity alginates. *Carbohydrate research*. **2009**;344(8):985-95.
- [176]. De Vos P, Van Straaten J, Nieuwenhuizen AG, de Groot M, Ploeg RJ, De Haan BJ, *et al*. Why do microencapsulated islet grafts fail in the absence of fibrotic overgrowth? *Diabetes*. **1999**;48(7):1381-8.
- [177]. Liu XY, Nothias JM, Scavone A, Garfinkel M, Millis JM. Biocompatibility investigation of polyethylene glycol and alginate-poly-L-lysine for islet encapsulation. *ASAIO Journal*. **2010**;56(3):241-5.
- [178]. Gugerli R, Cantana E, Heinzen C, Stockar Uv, Marison IW. Quantitative study of the production and properties of alginate/poly-L-lysine microcapsules. *Journal of Microencapsulation*. **2002**;19(5):571-90.
- [179]. Darrabie MD, Kendall Jr WF, Opara EC. Characteristics of Poly-L-Ornithine-coated alginate microcapsules. *Biomaterials*. **2005**;26(34):6846-52.
- [180]. Pareta R, McQuilling JP, Sittadjody S, Jenkins R, Bowden S, Orlando G, *et al*. Long-term function of islets encapsulated in a redesigned alginate microcapsule construct in omentum pouches of immune-competent diabetic rats. *Pancreas*. **2014**;43(4):605-13.
- [181]. Opara EC, Mirmalek-Sani SH, Khanna O, Moya ML, Brey EM. Design of a bioartificial pancreas. *Journal of Investigative Medicine*. **2010**;58(7):831-7.
- [182]. Langlois G, Dusseault J, Bilodeau S, Tam SK, Magassouba D, Halle JP. Direct effect of alginate purification on the survival of islets immobilized in alginate-based microcapsules. *Acta Biomater*. **2009**;5(9):3433-40.
- [183]. Mallett AG, Korbitt GS. Alginate modification improves long-term survival and function of transplanted encapsulated islets. *Tissue Engineering Part A*. **2009**;15(6):1301-9.
- [184]. De Vos P, De Haan B, Wolters G, Strubbe J, Van Schilfgaarde R. Improved biocompatibility but limited graft survival after purification of alginate for microencapsulation of pancreatic islets. *Diabetologia*. **1997**;40(3):262-70.

- [185]. Klöck G, Frank H, Houben R, Zekorn T, Horcher A, Siebers U, *et al.* Production of purified alginates suitable for use in immunisolated transplantation. *Applied Microbiology and Biotechnology*. **1994**;40(5):638-43.
- [186]. Elliott RB, Escobar L, Tan PLJ, Muzina M, Zwain S, Buchanan C. Live encapsulated porcine islets from a type 1 diabetic patient 9.5 yr after xenotransplantation. *Xenotransplantation*. **2007**;14(2):157-61.
- [187]. Dusseault J, Tam SK, Ménard M, Polizu S, Jourdan G, Yahia LH, *et al.* Evaluation of alginate purification methods: Effect on polyphenol, endotoxin, and protein contamination. *Journal of Biomedical Materials Research Part A*. **2006**;76A(2):243-51.

Chapter 2

Materials and Methods

2.1. Designing and Production of the Micro-encapsulator

A prototype of the micro-encapsulator was developed using rapid manufacturing methods like laser cutting and 3D printing.

2.1.1. Frame

The frame of the micro-encapsulator was very simply designed as a box, made with the Openbeam aluminium beams (Makerbeam), and connected using the Openbeam brackets, bolts and nuts (Makerbeam). Dimensions of the box were 225 mm by 255mm by 330mm (length, width, height).

2.1.2. Laser Cutting

Panels for the box of the micro-encapsulator were designed using Coral draw graphics suite X3. The box was designed in such a way that there would be no direct path possible between the electrodes needed for electrospaying and the aluminium frame of the machine. Designs were exported as DXF files and loaded into the Trotec Speedy 300 Laser cutting machine (Figure 2.1) and cut out of 5 mm thick acrylic.



Figure 2.1: The Trotec Speedy 300 laser cutting machine was used to cut out the acrylic panels for the micro-encapsulator.

2.1.3. 3D Printing

Custom parts for the housing of the micro-encapsulator and the custom syringe pump that could not be fabricated by laser cutting were 3D printed using fused filament fabrication (FFF), also known as fused deposition modelling (FDM). Parts were designed using the free for students Inventor software (Autodesk). 3D models were exported as STL files and printed using Acrylonitrile Butadiene Styrene (ABS) filament on either the Makerbot's Replicator 2X (micro-encapsulator parts, Figure 2.2) or the Fortus 400MC (custom syringe pump parts).

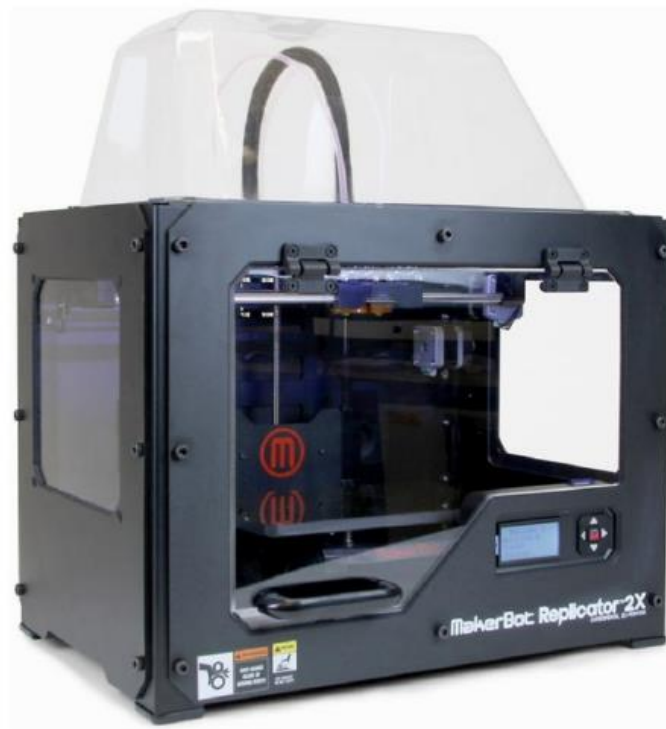


Figure 2.2: Makerbot's Replicator 2X was used to 3D print parts for the micro-encapsulator.

2.2. Solutions

2.2.1. Alginate

Crude alginate solutions were made by slowly sprinkling alginate powder in MilliQ filtered water (dH₂O) in a small beaker while stirring using a magnetic stirrer. For instance, for a 1.0% (w/v) alginate solution, 0.25 gram alginate powder was sprinkled in 25 ml water. Crude alginate solutions were sterile filtered through a 0.20 µm syringe filter (Surfactant free cellulose acetate, Sartorius Minisart, Fisher Scientific) before being used for 3D bioprinting or encapsulating. Two types of alginate were used: M-block rich, low molecular weight, Low Viscosity alginate (A1112, Sigma Aldrich) or G-block rich, high molecular weight Protanal (10/60FT, FMC Biopolymers).

For purified alginate solutions, an empty sterile centrifuge tube (15 ml, Fisherbrand, Fisher Scientific) was weighed on an analytical balance (Fisherbrand, Fisher Scientific), before adding the dried purified alginate in sterile conditions in a laminar air flow hood (LAF-hood) and weighing again. Based on the weight of the alginate, embryo transfer water (W1503, BioXtra, Sigma Aldrich) was added to the alginate flakes inside a LAF-Hood. The tube was shaken and kept in an upright position on room temperature until all the flakes were dissolved. The solution was then mixed using a vortex (Fisherbrand) and left to settle until there were no more bubbles in the solution before being used for cell encapsulation or 3D bioprinting.

2.2.2. Crosslinking Solutions

Gelling baths consisting of cationic solutions, were made with either BaCl₂ dihydrate (B0750, Sigma Aldrich), CaCl₂ dihydrate (C8106, Sigma Aldrich) or SrCl₂ hexahydrate (194122500, Acros Organics, Fisher Scientific). In this research two types of gelling baths were used:

ordinary gelling baths, and isotonic gelling baths. The CaCl₂ crosslinking solutions were also used to pre-crosslink alginate for 3D bioprinting.

For ordinary baths, the cationic salts were dissolved in MilliQ filtered water in a beaker on a magnetic stirrer. Gelling baths were sterile filtered using a 0.20 µm syringe filter before being used for 3D bioprinting or encapsulating procedures. For the amounts used, see Table 3.1.

For isotonic gelling baths, cationic salts were dissolved in 80% of the total volume of MilliQ water in a beaker on a magnetic stirrer, together with 4-(2-hydroxyethyl)-1-piperazineethanesulfonic acid-powder (HEPES-powder) (H3375, Sigma Aldrich) to create a 10 mM HEPES solution, and NaCl (S7653, Sigma Aldrich) to get a final osmotic concentration of 300 mOsm/L, which is close to the osmotic concentration of the human serum^[1]. After all the powders had dissolved, the pH of the solution was set to ~7.4 by dropwise adding 1 M NaOH (Fisher Chemical) while measuring the pH using a pH meter (Accumet AB150). Once the pH was stable, MilliQ was added to the final volume as stated in Table 2.1.

Table 2.1: Cationic Solutions for alginate crosslinking

100mM CaCl₂	500ml dH ₂ O, 7.35gr CaCl ₂ dihydrate
100mM SrCl₂	500ml dH ₂ O, 13.33gr SrCl ₂ hexahydrate
100mM BaCl₂	500ml dH ₂ O, 12.21gr BaCl ₂ dihydrate
25mM BaCl₂	500ml dH ₂ O, 3.05gr BaCl ₂ dihydrate
100mM CaCl₂, Isotonic	500ml dH ₂ O, 7.35gr CaCl ₂ dihydrate, 1.19gr HEPES
25mM BaCl₂, isotonic	500ml dH ₂ O, 3.05gr BaCl ₂ dihydrate, 3.29gr NaCl, 1.19gr HEPES
55mM BaCl₂, isotonic	500ml dH ₂ O, 6.71gr BaCl ₂ dihydrate, 1.97gr NaCl, 1.19gr HEPES

2.2.3. Pluronic Hydrogel

Pluronic hydrogel with calcium chloride was used as a sacrificial moulding material. The hydrogel was created by dissolving Pluronic F127 (P2443, Sigma Aldrich) together with CaCl₂

in MilliQ filtered water on a magnetic stirrer. For 30% Pluronic with 100mM CaCl₂, 1.47 gram CaCl₂ was dissolved in 100ml MilliQ filtered water. The magnetic stirrer was set to a speed where a small vortex would form in the solution, but the air wouldn't reach the magnet on the bottom. Once the salt was completely dissolved, 30 g Pluronic powder was slowly sprinkled in the vortex of the solution to prevent clumping of the Pluronic. Once completely dissolved, the solution was autoclaved to sterilise it before use. The solution was kept in the fridge for up to one month before usage.

2.2.4. Collagen Hydrogel

Collagen hydrogels were used to create 3D moulded collagen structures. Collagen solutions were prepared in sterile conditions, in a LAF-hood. A stock solution of Dulbecco's Modified Eagle Medium (DMEM) - NaOH was made by mixing two parts 10x DMEM (D2429, Sigma Aldrich) with one part 0.4 mM NaOH (Fisher Scientific). A stock solution of 1/1000 acidic acid was created by diluting 10 µl Glacial Acetic Acid (Fisher Scientific) in 10 ml endotoxin free water (HyClone, Fisher Scientific). A stock solution of 100 mM HEPES was made by dissolving 0.238 gr of HEPES in 10 ml of endotoxin free water. All stock solutions and a mixing beaker were kept on ice until used. In the cold, sterile beaker, 4ml of acid soluble rat tail collagen (6.5 mg/ml; created and kindly donated by Katie Henderson) was mixed with 400 µl 1/1000 acidic acid. 650 µl of stock HEPES solution was added, followed by 650 µl DMEM/NaOH solution. The DMEM turned yellow due to the acidity of the solution. 0.1 mM NaOH was then added dropwise (about 800 µl), while swirling the solution, until the solution turned pink. The final collagen solution (4 mg/ml) was kept on ice until used, usually within 10 minutes.

2.3. Alginate Purification

2.3.1. Purification Protocol

For the purification of alginate, the original protocol by Klöck et al^[2] was modified. 4,5 grams of alginate (either Low Viscosity alginate (A1112, Sigma Aldrich) or Protanal (10/60FT, FMC Biopolymers) was added to 250 ml of chloroform (Fisher Scientific) and stirred on a magnetic stir plate for 30 minutes. The alginate was then separated from the chloroform by vacuum filtration through no. 4 Whatman filter paper. This process was repeated twice. After the last filtration, all chloroform was allowed to evaporate, before the alginate was dissolved in 300 ml of MilliQ filtered water. 4,5 grams of acetic washed activated charcoal (C4386, Sigma Aldrich) was added and the solution was stirred for 4 hours. The charcoal was filtered out of the solution using a .22 µm vacuum filter (Corning), and replaced with neutral activated charcoal (C9157, Sigma Aldrich), before stirring for another 4 hours. The charcoal was removed through filtration through a .22 µm vacuum filter and 0.18 grams of NaCl was added to get a final concentration of 10mm NaCl. The alginate was then precipitated out of the solution with ethanol and dried overnight in a LAF-hood before weighing to measure recovery.

2.3.2. Measuring Impurities

To measure any protein impurities, the Pierce™ Bicinchoninic acid (BCA) Protein Assay Kit (Thermo Scientific) was used, as instructed by the supplier. Any endotoxin impurities were detected using the Pierce Limulus Amebocyte Lysate (LAL) Chromogenic Endotoxin Quantitation Kit (Thermo scientific). The presence of Polyphenol-like compounds was detected using a spectrofluorimeter (FlexStation 3, Molecular Devices). An emission wavelength of 445nm and an excitation wavelength of 365nm were used. The appearance of a characteristic absorbance peak at 445 nm was used to measure the relative amounts of

polyphenols in terms of arbitrary fluorescence units (AFU). All assays were performed on 1%(w/v) alginate solutions.

The purification method was performed 3 times for each alginate type, and all impurity tests were performed on each batch of purified alginate in triplicate.

2.3.3. Measuring Viscosity

Viscosity of solutions was measured using a viscosity cup (ISO 2431, Fungilab). The cup would be filled to the brim with the solution, while keeping the bottom hole plugged. The meniscus formed on top would be flattened quickly by wiping away the excess using a glass plate. The hole in the bottom would then be opened up and the solution was allowed to flow out of the cup. A stopwatch was used to measure the time between unplugging the hole and the first moment the flow from the hole broke. This would be done in triplicate for each solution. The time would be entered into the software provided by the manufacturer of the cup to calculate the viscosity.

2.4. Micro-encapsulation and Bead Fabrication

2.4.1. Single Nozzle Bead Fabrication and Micro-encapsulation

Alginate microbeads were created using the custom build electro-spray machine as illustrated in Figure 2.3. In short, alginate solutions of different concentrations were dispensed through a dispensing needle into a gelling bath. A high voltage generator was used to charge the nozzle to a high DC (direct current) voltage, while the earthed counter electrode was dipped into the gelling bath. The electric field created between these two electrodes would separate the viscous alginate solution in small beads at the tip of the dispensing needle (electro-spraying). Parameters differed per experiment and will be described as such for each different experiment. Parameters that could differ are described in Table 2.2.

For experiments where the bead-size was measured, samples of beads were imaged under a brightfield microscope using a 4x objective. ImageJ would then be used to measure the size of the beads by hand, using the line tool and the measurement option. At least 50 beads were measured for each experiment.

For experiments where cells or aggregates (including islets) were encapsulated in these single nozzle beads (micro-encapsulation), cells or aggregates would be counted and spun down in a 15 ml centrifuge tube at 500 rounds per minute (rpm) (aggregates) or 1000 rpm (cells) in a centrifuge (Heraeus Multifuge 3SR) before removing the supernatant. They would then be resuspended in an alginate solution at a concentration specified per experiment, and micro-encapsulated as stated above. All experiments using live cells were performed in sterile conditions in a LAF-hood and electro-sprayed in isotonic gelling baths.

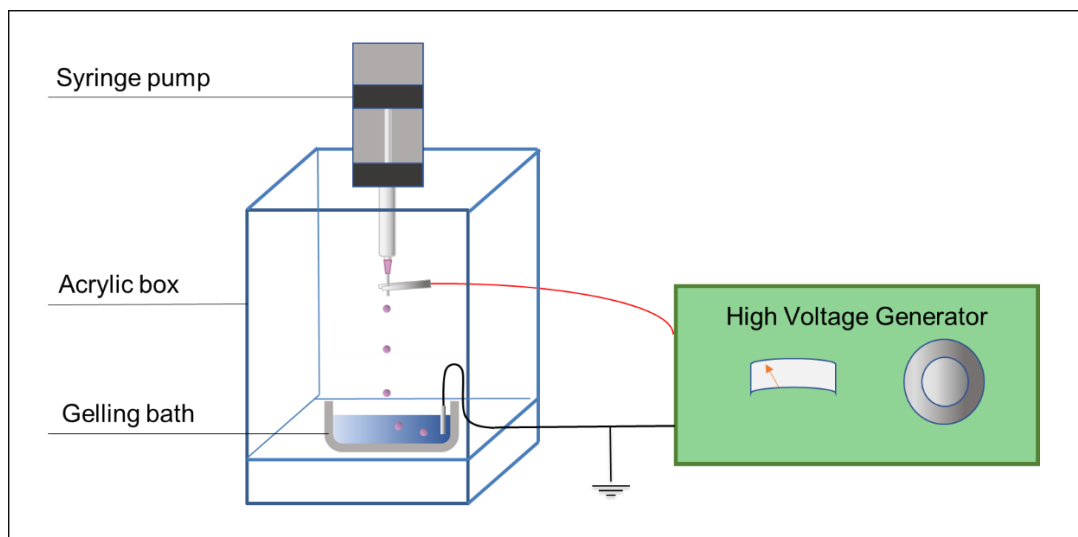


Figure 2.3: Schematic overview of the micro-encapsulation set up for single nozzle solid bead fabrication.

Table 2.2: Parameters defined when electro-spraying alginate beads, with examples of used settings.

PARAMETER	COMMON USED SETTINGS
DISPENSING NEEDLE GAUGE	25G, 27G, 30G
EXTRUSION FLOW RATE	0.5 ml/h, 1.0 ml/h, 2.0 ml/h, 5.0ml/h
HIGH VOLTAGE FIELD	5.0kV, 6.0kV, 6.5kV, 7.0kV
DISTANCE BETWEEN NEEDLE AND GELLING BATH	0.5cm, 1.0cm
TYPE OF ALGINATE	Low viscosity alginate, Protanal, Purified Protanal
CONCENTRATION OF ALGINATE (W/V)	0.5%, 1.0%, 1.2%, 1.5%, 2.0%
GELLING BATH	100mM CaCl ₂ , 100mM BaCl ₂ , 55mM BaCl ₂ , 25mM BaCl ₂ , 100mM SrCl ₂

2.4.2. Coaxial Core-Shell Bead Fabrication and Micro-encapsulation

A coaxial core-shell bead fabrication system was created to produce beads which would have a liquid core and a hydrogel shell. The coaxial electro-spray system and a cross-sectional view of the coaxial needle are illustrated in Figure 2.4. The system consists of two syringe pumps for pushing the core fluid and shell fluid of alginate through the concentric inner (28G or 26G) and outer needles (21G, 20G or 19G) (Raméhart). A high voltage generator creates an electric field between the coaxial needle and the gelling bath, breaking the fluids into concentric micro-drops and spraying them into a gelling bath. The core fluid usually consists out of 1, 1.2 or 1.5% carboxymethylcellulose (CMC, C4888, Sigma Aldrich) dissolved in embryo transfer water, or cell medium. The outer fluid usually consists out of 1 or 1.5% alginate (Protanal, FMC Biopolymers). Exact parameters are given per experiment.

Experiments that include living cells in the inner solution were performed in sterile conditions in a LAF-hood and sprayed into isotonic gelling baths.

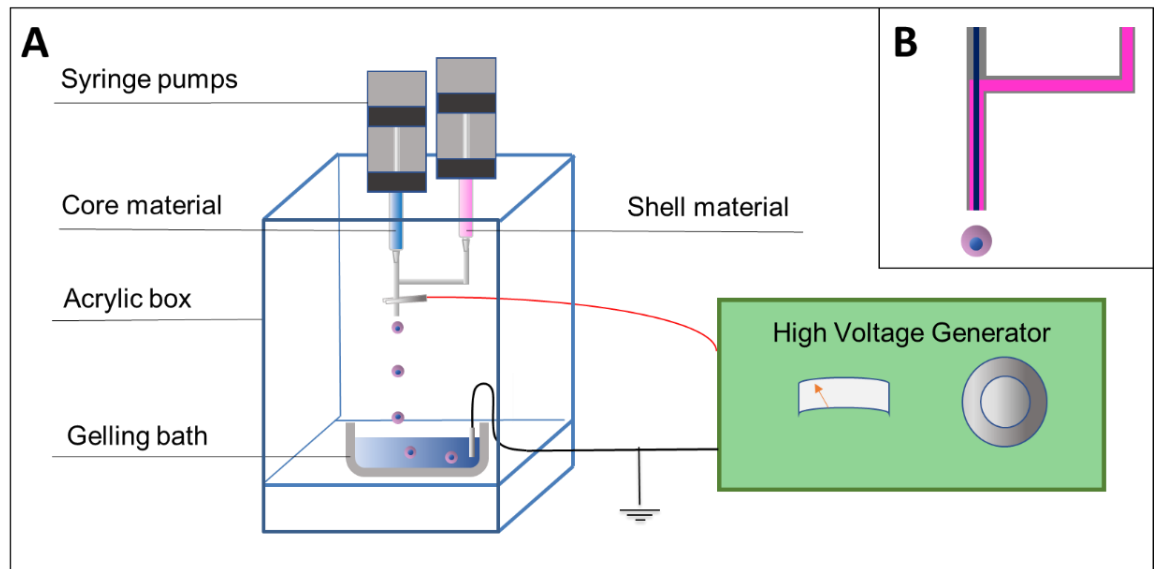


Figure 2.4: A) schematic overview of the electro spray printer. B) Schematic overview of the coaxial needle

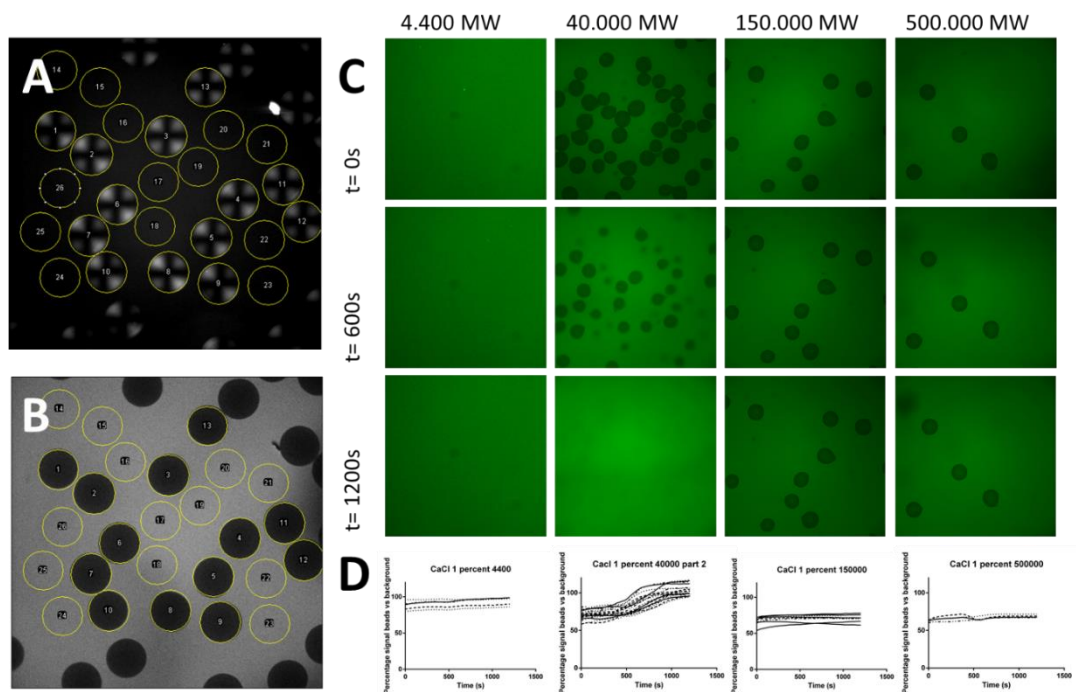
2.4.3. Determining Alginate Permeability Using Confocal Microscopy

The permeability of the microbeads was tested by immersing the beads in solutions containing fluorescently labelled dextran and using confocal microscopy to see whether or not the molecules could enter the beads.^[3]

Alginate beads (as stated above) were created not more than 24 hours before each experiment and kept in Phosphate buffered saline (PBS, Gibco). The beads in PBS solution were mixed 1:1 with a solution containing 200 $\mu\text{g}/\text{ml}$ of fluorescent labelled (Fluorescein isothiocyanate; FITC) dextran of different average sizes (4,400, 40,000, 150,000 or 500,000 Molecular Weight (MW); Sigma Aldrich). The final solution containing 100 $\mu\text{g}/\text{ml}$ dextran and the alginate beads was then imaged every 30 seconds over a time period of 20 minutes using a confocal microscope (Leica SP5). Both differential interference contrast (DIC) and confocal fluorescence microscopy were used to image the beads. Images were analysed using ImageJ software. Regions of interest (ROI) were created based on the beads location in the DIC images, both on the beads and on the background (Figure 2.5 A). The DIC images were used

as in some fluorescent images the beads were not visible. In the fluorescent images, the average grey value of the set ROIs were measured for each frame (Figure 2.5 B/C). The average grey value of the bead-areas was converted to a percentage of the average grey value of the background areas for each frame and plotted in a graph as normalized average grey value over time (Figure 2.5 D). These values would then be averaged again to create the final graphs.

Figure 2.5: Fluorescence detection of pore size in alginate beads. Alginate beads crosslinked with different cationic



solutions were added with a solution containing fluorescein coupled dextran molecules of different sizes, and then imaged using a confocal microscope over a period of 20 minutes in fluorescent and DIC mode. A: DIC microscope images were used to find alginate beads, as these were not always visible in the fluorescent images when fluorescent dye would diffuse into the beads, and regions of interest (ROI) were drawn over the beads. The same amount of ROI containing only background were also created. B: The ROI defined by the DIC images were then used to measure the average signal in the fluorescent images, which was then normalized as a percentage of the background signal. C: Examples of fluorescent images of the diffusion of fluorescent molecules into 1% alginate beads crosslinked with 100mM CaCl₂. D: Examples of the measured values, with each line depicting a separate bead.

2.5. Cell Culture

2.5.1. Adipose Derived Stem Cells and HepaRG cells

Adipose Derived Stem Cells (ADSC) were generously donated by Dr. Mathis Riele from Glasgow University. They were cultured in Minimum Essential Medium (MEM) Alpha (Gibco), supplemented with 10% Fetal Bovine Serum (FBS, Gibco) and 1% Penicilin/Streptomycin (Gibco). . Both cell lines were passaged once 80-90% confluence was observed under the microscope. Cells were washed with PBS once and then incubated with enough TrypLE (Gibco) to cover the bottom of the flask. Once detachment of the cells was observed the cell suspension was neutralized with complete media, five times the volume of TrypLE used. The cell suspension was centrifuged at 1000 rpm for 3 minutes before seeding in a new flask at the appropriate split ratio.

2.5.2. Aggregate Creation

Aggregates of ADSC's or HepaRG's were created using the method described by Dahlmann et al.^[4] Briefly, silicone moulds were created by pouring liquid hydrophilic silicone (Hydrosil; Siladent) onto the bottom patterned surface of Aggrewell™ plates (Stemcell Technologies) and centrifuged at 1500 rpm for 1 minute, to remove any trapped air bubbles. Once solidified, these silicone moulds were peeled off and further sterilised in the autoclave. 3% agarose solution was created by mixing 3 grams of agarose NEEO ultra Quality (Carl Roth, Fisher Scientific) in 100 ml of PBS and dissolving it in an autoclave. In a LAF-hood, 3 ml of the still hot agarose solution was pipetted in each well of a 6 well plate. The silicone moulds were then placed in the agarose, pushing on the silicone to remove any trapped air bubbles. The 6 well plates were then placed on ice until the agarose had solidified, before gently removing the silicone moulds (Figure 2.6 A). Microwell chips were kept at 4°C under corresponding medium overnight, before being seeded with 100 cells per microwell. For imaging purposes, in some cases cells would be fluorescently marked using fluorescent cell-tracker CM-Dil

(Fisher scientific) as instructed by the supplier. After allowing the cells to aggregate for 48 hours (Figure 2.6 B), the aggregates were harvested by inverting the microwell chips in the plate and centrifuging at 1500 rpm.

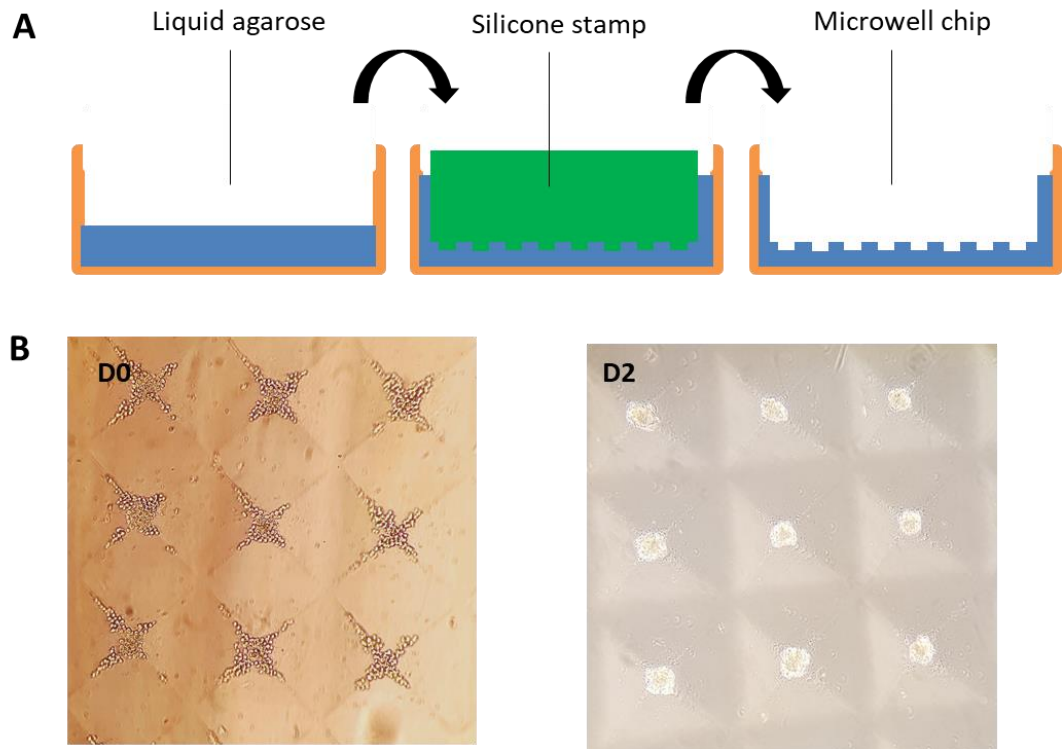


Figure 2.6: Creating aggregates. A: A microwell chip was created by pressing a silicone mould into warm agarose. Once the agarose had cooled down, the silicone mould could be removed, leaving the microwell chip. B: ADSC's were seeded in the microwell chips at 100 cells/microwell. After 2 days in culture they had formed aggregates.

2.5.3. Donated Human Pancreatic Islets

Donated human islets of Langerhans could be used in these studies if they were not suitable for clinical transplantation and if signed research consent was available, according to national laws. Islets were obtained from the Scottish National Blood Transfusion Services Islet Isolation Laboratory (SNBTS) and cultured in islet culture medium (CMRL-1066; Corning), supplemented with 10% FBS and 1% Penicillin/Streptomycin. They were maintained in an incubator at 37°C, in a humidified environment with 5% CO₂. As soon as the islets arrived in the lab the medium from the stock flask was replaced by centrifuging the islet suspension for 3 minutes at 500 rpm and replacing 3/4th of the supernatant. Islets were handpicked from the stock flask within 3 days of arrival. 15-20 ml of islet suspension was transferred into a petri dish. Islets were picked out of the pancreatic slurry underneath a microscope within a LAF-flow hood and counted. Handpicked islets were placed in 6 well plates made from Ultra-Low Adhesion (ULA) plastic (Corning), at a concentration of 1000 islets per well. To ensure only islets were handpicked, every so often a small sample would be placed in a 24 well plate and stained using a few drops of a dithizone (DTZ) solution (6 µg/ml in Dimethyl sulfoxide (DMSO), Sigma Aldrich). Samples were then observed under a microscope: islets turn bright red using this staining, while pancreatic endocrine tissue will not (Figure 2.7). Medium was replaced every 2/3 days with a micropipette under the microscope, to ensure no islets were accidentally removed during aspiration.

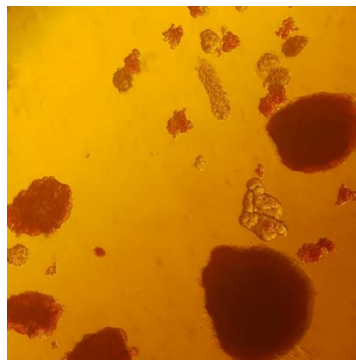


Figure 2.7: Islets stained with Dithizone

2.5.4. Islet Dissociation

For some experiments islets would be dissociated into islet cells. For single cell purposes, islets were handpicked out of the pancreatic slurry using a 200 µl pipette and a microscope in a LAF-hood as described before. 50 islets per group (n=3, 6 groups) were placed in a 24 well plate. Under a microscope, the medium was aspirated and islets were washed thrice with PBS. 0,4 ml of trypsin (0,25%), trypsin (0,05%)+ Ethylenediaminetetraacetic acid (EDTA; 0,02%) or PBS were added to the islets. The 24 well plate was placed in the incubator (37 °C, 5% CO₂) and after 2minutes, the islets were checked every 2 minutes under the microscope to check for dissociation. For each dissociation solution, two groups were created. One group received mechanical stimulation for the dissociation using a micropipette every time they were checked upon, while the other group received only the chemical dissociation. Once islets appeared to be dissociated, or after 15 minutes, a live/dead staining was performed as described in 2.9.1.

2.5.5. 3D Culture

Cells kept in 3D culture (either encapsulated in beads or 3D printed in alginate) were kept in 6 well cell culture plates with 2 ml of cell specific medium. For 3D printed structures the medium was replaced 3 times a week by gently removing it using a micropipette and replacing it. For beads, medium was removed through a cell strainer (40 µm, Corning) using a micropipette before replacing it.

2.6. Cell Function Assays

2.6.1. Islet Function

To assess islet function, a glucose induced insulin secretion test was performed 14 days after islet encapsulation on encapsulated and non-encapsulated islets. 30 islets per condition (in triplicate) were incubated for 90 minutes in a modified Krebs Ringer Bicarbonate (KRBH) buffer (115mM NaCl, 5mM KCl, 24mM NaHCO₃, 2.2mM CaCl₂, and 1mM MgCl₂, pH 7.4), supplemented with 20mM HEPES and 2 mg/mL human serum albumin (Octapharma), with 1.7mM D-glucose. Islets were then successively incubated for 1 h in KRBH buffer with 1.7mM, 16.7mM and again 1.7mM D-glucose at 37°C. Insulin concentration was determined in the supernatants by a human insulin enzyme-linked immunosorbent assay (ELISA) kit (Merckodia). This assay was repeated for the encapsulated islets at day 96 after encapsulation, but not on the non-encapsulated islets as they were no longer viable.

2.6.2. HepaRG Function

To assess the Cytochrome P450 3A4 (CYP3A4) activity of the HepaRG organoids, a commercial CYP3A4 activity kit was used (P450-Glo CYP3A4 Luciferin-PFBE cell-based/biochemical assay, V8902, Promega). Encapsulated HepaRG organoids were handpicked out of their culture plates after 60 days in culture and placed in the wells of 24 well plate (100 encapsulations per well, 3 wells per group). The encapsulated HepaRG organoids were cultured in the 24 well plate for 24 hours in either normal HepaRG medium, or HepaRG medium with 10 µM Rifampicin. Activity per well was assessed using the P450-Glo luminescence assay, following the manufacturer's instructions. Bioluminescent signals were detected after 3 hours using a spectrofluorimeter.

For the 2D experiment, 6 wells were seeded with 150,000 cells per well of a 24 well plate. They were allowed to attach and proliferate under normal culturing conditions for 5 days.

Half of the 2D culture wells was then cultured using HepaRG medium with 1% DMSO, while the other half received normal culture medium. After 14 days of culture, the activity per well was assed using the P450-Glo luminescence assay, following the manufacturer's instructions. Bioluminescent signals were detected after 3 hours using a spectrofluorimeter.

After measuring the CYP3A4 activity, cells were lysed using RIPA Buffer (Sigma Aldrich), and total protein content was measured using the Pierce™ BCA Protein Assay Kit, as per manufacturer's instructions. All CYP3A4 activity was normalized to the amount of protein per well, to adjust for the difference of the number of cells per well.

2.7. 3D Bioprinting

3D bioprinting was done using the custom built extrusion-based 3D bioprinter, the Mark V, made by Dr. Alan Faulkner-Jones (Figure 2.8). In short, a syringe pump on a X/Y axes slowly extrudes bioink from a syringe, with the baseplate moving down for every step in the Z direction. All bioprinting with living cells in the experiment were performed under sterile conditions in a LAF-hood. The Mark V would be cleaned with 0.1% Distel and 70% ethanol before placing it in the hood and printing. The Mark V can create prints based on 3D designs

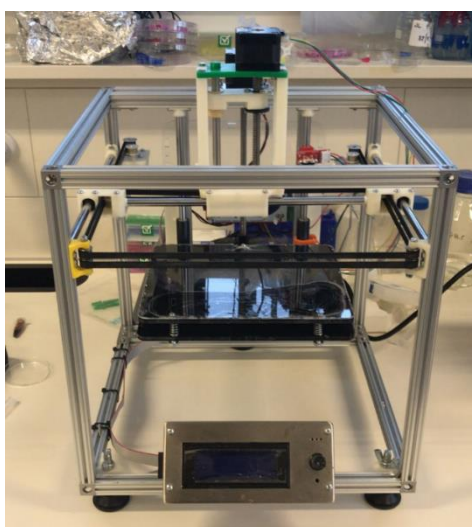


Figure 2.8: The Mark V was the 3D Bioprinter used in this research.

created using the Inventor software, which are transformed into G-code files using the free Slic3r software.

2.7.1. 3D Bioprinting Cells and Beads

For cell printing, a sterile 2% purified Protanal solution would be mixed 1:1 with 20mM CaCl₂ in a 15 ml falcon tube by shaking vigorously, creating a pre-crosslinked bio-ink, with a final concentration of 1% alginate and 10 mM CaCl₂. The pre-crosslinked bio-ink was centrifuged for 5 minutes at 1500 RPM to remove any air bubbles stuck in it. At this point, cells or alginate beads could be added. Alginate beads were created as stated before in section 2.4, washed with PBS and then spun down. The pre-crosslinked bio-ink was added to the beads, and slowly pipetted up and down to create a solution with 20.000 beads/ml. To add cells, the cells would be dissociated from their cell culture plate and counted, before spinning down in a 15 ml falcon tube for 3 minutes at 1000 RPM and gently removing the supernatant using a micropipette. The cell pallet would then be resuspended carefully in the pre-crosslinked bio-ink at a concentration of $2 \cdot 10^6$ cells/ml, without forming any air bubbles in the bio-ink. The bio-ink loaded with cells was then transferred into a 5ml syringe (BD), and the syringe was loaded into the Mark V, and fitted with a ¼ inch 25G blunt dispensing needle. The bio-ink would then be deposited layer by layer in the desired design as instructed by the G-code. Printing was performed at 10 mm/s, with an extrusion multiplier of 1.2 and a layer height of 0.2 mm. After every 2 layers, the construct would be sprayed with a mist of 100 mM CaCl₂, to further crosslink the alginate and increase mechanical stability of the construct. Once finished, the construct would be submerged in isotonic 100 mM CaCl₂ to fully crosslink the alginate. Constructs were then placed in medium and cultured as stated above.

2.7.2. 3D Biofabrication Using Pluronic Moulds

Pluronic is a material that is gel-like at room temperature but turns liquid when it's cooled down^[5]. It therefore makes a perfect sacrificial material for moulds, as it will hold its shape until the biomaterial used for the structure has fully crosslinked and can then be easily removed. The pluronic-CaCl₂ solution would be taken from the fridge and transferred into a 5ml syringe in a LAF-hood under sterile conditions. The solution was allowed to fully gel by letting it come to room temperature over a period of an hour before printing commenced. The syringe would then be loaded into the Mark V with 22G dispensing needle, and Pluronic moulds would be printed in plastic petri dishes. Prints with pluronic were done at 15 mm/s, with an extrusion multiplier of 1.35 and a layer height of .17mm. Printed structures were stored in an incubator at 37°C.

Pluronic moulds would be used to create both alginate and collagen structures. Alginate or collagen solutions would be prepared as stated before and pipetted into the moulds using a micropipette. The solutions were allowed to gel for 30 minutes in the incubator before adding either 30 ml PBS (4°C; for collagen structures) or 30 ml 100mM isotonic CaCl₂ (4°C; for alginate structures) to the petri dishes and washing away the Pluronic by gently swirling the cold liquids around in the petri dishes. Once the structures started floating around in the liquid and were no longer attached to the moulds, they were scooped out of the solution using a piece of Parafilm and placed in cell culture medium. Constructs were kept in the incubator at 37°C and 5% CO₂.

2.8. Chorioallantoic Membrane Assay

The chorioallantoic membrane (CAM) assay uses the highly vascularized CAM of a chicken egg to research (anti)angiogenic activity of compounds and vascularization. In this research the CAM-Assay was used to see if blood vessels would grow into our biofabricated structures.

Per batch, 30 fresh (refrigerated for less than 3 weeks) chicken eggs (Dekalb White, Henry Stewart & Co.Ltd) were cleaned with 70% ethanol and numbered with pencil. The eggs were then placed with the blunt end upwards in a special egg incubator (Figure 2.9 A) that continuously tilts the eggs back and forth at a temperature of 38°C and a relative humidity of 60-75% (D0). After 3 days, eggs were taken to the LAF-hood and a small hole was made on the side of the egg, near the pointy end using an egg piercer. A 22G needle was then inserted into the egg under an angle, as close to the shell as possible, to remove 3-4 ml of albumin, without piercing the yoke. The hole was then sealed with a piece of scotch tape and a small square (2x2 cm) was sawed at the blunt end using a hacksaw blade and removed with a pair of tweezers (Figure 2.9 B). Any white membrane was removed using the tweezers before closing the square with scotch tape and returning the egg to the now stationary egg incubator.

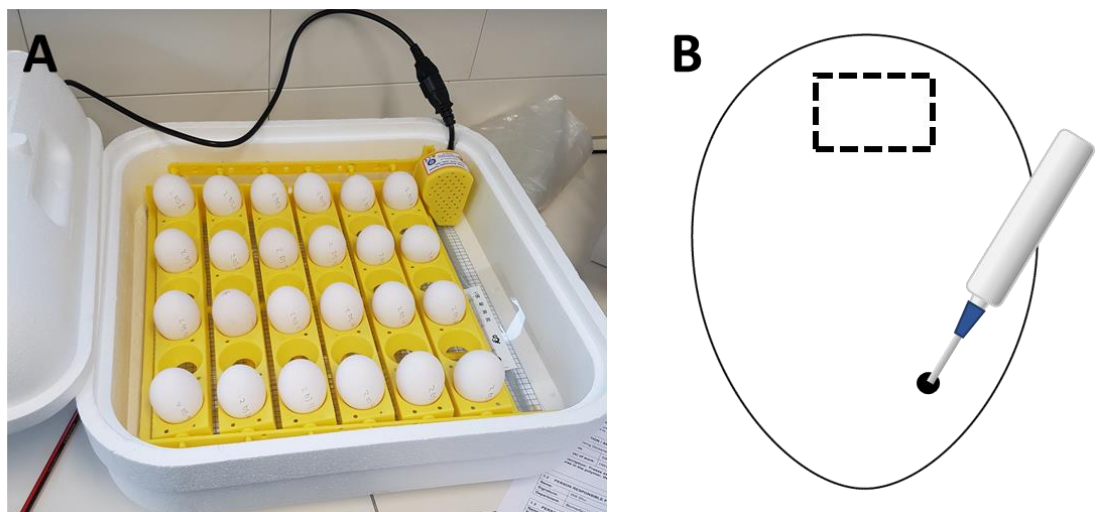


Figure 2.9: Preparing islets for CAM Assay. A: islets were incubated in a special egg incubator, that continuously tilts the eggs back and forth for the first three days. B: using a syringe, a small amount of albumin was removed from the egg, before sawing open a square window at the blunt end.

On day 10 of the egg incubation, eggs were taken to the incubator and the patches were placed on the CAM. If more space was needed to place the patches, the hole would be increased by breaking a way small pieces of shell using tweezers. After placing the patches, eggs would be closed using scotch tape and returned to the incubator. At day 13, eggs were taken from the incubator and 200 μ l of 1 mg/ml FITC-Dextran (2,000,000 MW, Sigma Aldrich, 52471) dissolved in PBS was injected directly into a vein, to stain all the blood vessels as described by Miller et al.^[6] before returning the eggs to the incubator. After roughly 20-30 minutes 200 μ l of 0.2 mg/ml sodium pentobarbitone solution was injected into a vein on the CAM to humanely euthanize the developing chick.^[7] After 15 minutes, the patch was cut from the cam with scissors, with at least 1 cm of CAM on all sides, and placed in 10% formalin. After 2 hours, the CAM was placed in PBS and kept in the dark at room temperature until microscopy.

2.9. Imaging

2.9.1. Live / Dead Assay

Viability of cells and islets was tested by using a fluorescent live / dead assay. A small number of beads / islets or a small piece of a 3D printed construct were removed from culture and transferred into a 24 well plate. 1 ml of PBS was added to the well, containing 2 μ l of Propidium Iodide (PI; Sigma Aldrich) stock solution (2mg/ml) before incubating the plate in the incubator. After half an hour, 1 μ l of Fluorescein Diacetate (FDA; Sigma Aldrich, 5mg/ml, dissolved in acetone) was added and cells were imaged.

2.9.2. Immunohistochemistry

Encapsulated HepaRG organoids were fluorescently stained to see their morphology and to get a better idea of what type of cells are in the organoids.

A special fixing solution of 25 mM BaCl₂ in 10% formalin was created by dissolving 1.22 grams of BaCl₂ dihydrate in 200 ml of 10% formalin. This fixing solution was used to prevent the alginate from disintegrating while fixing. On day 60 of culture, the medium was removed from the encapsulations and they were washed with PBS. HepaRG cells were then fixed with the fixing solution for 25 minutes, before washing three times with PBS. The encapsulations were kept in PBS until stained.

To see the morphology of the organoids, encapsulated HepaRG organoids were stained with Phalloidin iFluor-555 (Abcam) and DRAQ5 (Abcam). The Phalloidin staining solution was made by dissolving 10 µg of Bovine Serum Albumin (BSA, A9418, Sigma Aldrich) in 999 µl PBS, and adding 1 µl of the phalloidin stock solution. The DRAQ5 staining solution was created by adding 1 µl of DRAQ5 to 999 µl of PBS. Fixed HepaRG beads were stained with the Phalloidin staining solution for 1 hour at room temperature before washing three times with PBS for 10 minutes. They were then stained with the DRAQ 5 Solution for 1 hour before imaging.

For the specific protein staining, beads were washed for 20 minutes using PBST; PBS with 0,1% added Tween20 (P2287, Sigma Aldrich). Non-specific antibody attachment was prevented by blocking with 10% Normal Goat Serum (NGS, Invitrogen) in PBST for 3 hours at room temperature. It was then washed twice with antibody diluent buffer (ADB), consisting of 1% NGS in PBST. Beads were then incubated overnight at 4°C in primary antibodies (chicken anti-human serum albumin FITC [Abcam] 1:100 and either rabbit anti-Cytokeratin 19 (CK19) [Abcam] 1:200 or rabbit anti- Hepatocyte nuclear factor 4 alpha (HNF4α) [Abcam]), before washing thrice in ADB for 20 minutes at room temperature. Beads were then incubated overnight at 4°C in secondary antibodies (Goat Anti-rabbit Alexa-fluor594 [Abcam] 1:500), before washing thrice in ADB for 20 minutes at room temperature. They were then

incubated for 1 hour at room temperature in DRAQ5 solution, before washing once in PBST and imaging.

2.9.3. Microscopes

Imaging of cells stained with a Live/Dead assay was performed on an EVOS FLoid imaging station.

Imaging of fluorescently stained cells was done on a Confocal Scanning Laser Microscope (CSLM, Leica microsystems, SP 5). Fluorophores were visualised and recorded using the settings in Table 2.3. Stacks of approximately 150 μm in depth were acquired at 512x512 p or 1024x1024 p resolution, 400 Hz frequency. The stack steps were calculated automatically based on Nyquist criteria. All CLSM images were obtained using a dry 10x lens, a dry 20x lens or an oil 60x lens. Image processing and data analysis was done using the free ImageJ software in almost all cases.

Bright field microscopy of non-fluorescent samples was performed using a Brunel SP400 microscope or a SP50D Digital microscope.

Table 2.3: Imaged fluorophores and their excitation and emission maximum^[8-10]

FLUORPHORE	EXCITATION	EMISSION
FITC	493	517
FDA	495	517
PI	538	617
DRAQ5	547	681
DII	551	565
IFLUOR-555	556	559
ALEXA FLUOR-594	590	619

2.10. Statistical analysis

Statistical analysis was done using GraphPad Prism 6. Data represented as mean \pm standard deviation (SD). Number of replicates (N) for every experiment was 3 unless stated otherwise. ANOVA and t-test were used for comparison analysis. Every experiment was repeated three times unless otherwise specified. Differences were considered statistically significant using a p-value lower than 0.05.

2.11. References

- [1]. Hendry EB. Osmolarity of human serum and of chemical solutions of biologic importance. *Clinical chemistry*. **1961**;7(2):156-64.
- [2]. Klöck G, Frank H, Houben R, Zekorn T, Horcher A, Siebers U, *et al.* Production of purified alginates suitable for use in immunisolated transplantation. *Applied Microbiology and Biotechnology*. **1994**;40(5):638-43.
- [3]. Mørch YÁ, Donati I, Strand BL. Effect of Ca²⁺, Ba²⁺, and Sr²⁺ on Alginate Microbeads. *Biomacromolecules*. **2006**;7(5):1471-80.
- [4]. Dahlmann J, Kensah G, Kempf H, Skvorc D, Gawol A, Elliott DA, *et al.* The use of agarose microwells for scalable embryoid body formation and cardiac differentiation of human and murine pluripotent stem cells. *Biomaterials*. **2013**;34(10):2463-71.
- [5]. Malmsten M, Lindman B. Self-assembly in aqueous block copolymer solutions. *Macromolecules*. **1992**;25(20):5440-5.
- [6]. Miller WJ, Kayton ML, Patton A, O'Connor S, He M, Vu H, *et al.* A novel technique for quantifying changes in vascular density, endothelial cell proliferation and protein expression in response to modulators of angiogenesis using the chick chorioallantoic membrane (CAM) assay. *Journal of translational medicine*. **2004**;2(1):4-.
- [7]. Aleksandrowicz E, Herr I. Ethical euthanasia and short-term anesthesia of the chick embryo. *Altex*. **2015**;32(2):143-7.
- [8]. Carl Zeiss Microscopy G, *Fluorescence Dye and Filter Database*, <https://www.micro-shop.zeiss.com/index.php?s=15498299232a1c5&l=en&p=de&f=f&a=d>, August **2018**
- [9]. Bioquest A, *iFluor™ 555 succinimidyl ester*, <https://www.aatbio.com/products/ifluor-555-succinimidyl-ester>, August **2018**
- [10]. Scientific TF, *DRAQ5 Fluorescent Probe solution*, <https://www.thermofisher.com/order/catalog/product/62251>, August **2018**

Chapter 3

Design, Construction and Optimisation of the Micro-encapsulator

3.1. Introduction

Based on the findings in the literature review, electro-spraying was chosen as the preferred method for cell encapsulation (micro-encapsulation). It allows for the individual encapsulation of the islets, with the encapsulations having a smaller diameter than the air based droplet generators.^[1] Electro-spraying also allows for mono-sized encapsulations,^[2] in the same way as microfluidic encapsulation does,^[3] without the necessity of an oil based component. Furthermore, when this project started, there were no known attempts at using electro-spraying as a method for the encapsulation of human pancreatic islets.

The design and development of the micro-encapsulator are described in this chapter. In section 3.2 the original design will be described, with any changes to the design detailed in section 3.3. Finally, section 3.4 will describe the experiments completed to determine the parameters that influence the bead size and uniformity.

3.2. Design

The micro-encapsulator has been continuously developed to come to its final design that was used in most experiments in this thesis. When the original was designed, a few requirements were taken into account. Most importantly the electro-spraying should be done safely. Since the high voltage generator can generate voltage up to 40 kV, it was essential that the chance of electrocuting the user would be at a minimum. For this reason, the outer box was designed in such a way that no direct path would be possible between the electrodes needed for the electro-spraying and the aluminium frame. Therefore, the working area was designed to be surrounded from all sides with an insulating material, for which 5 mm thick acrylic was chosen.

The frame of the box was made using Makerbeam aluminium beams. Since these beams come in standard sizes, a decision was made to start with the frame and design the insulating panels to fit within that frame.

In the first design (Figure 3.1 A), the syringe pump was situated at the side and alginate would be lead to the micro-encapsulator through a silicone tube (Figure 3.1 B). The tube would lock into a dispensing needle, which in turn would be held in place by a specially designed 3D printed part (Figure 3.1 C). To ensure the dispensing needle could easily be changed, the high voltage generator was connected to the dispensing needle using a crocodile clip (Figure 3.1 D). In the side panel of the enclosure two high voltage coax-connectors were installed, to connect the internal wiring with the high voltage generator. This was done as another precaution to ensure no accidental electrocution would happen during setup without the crocodile clip being connected to the generator. In the original design, the bottom plate consisted of a double layer of acrylic, through which the ground wire ran that connected to a spring that protruded through the acrylic base plate (Figure 3.1 E). A stainless-steel petri dish could be placed on the spring to act as the negative electrode in the electro-spraying procedure. The bottom plate was attached to a Jiffy Jack, to allow the distance between the dispensing needle and the petri dish to be controlled.

The micro-encapsulator was not only designed to be safe, it was also designed so it could easily be adapted for use in good manufacturing practice (GMP). The dispensing needles, silicone tubing and the petri dish can be autoclaved, and the syringes and dispensing needles are disposable. Within the micro-encapsulator there are no ridges, allowing easy cleaning using 1% distel and 70% ethanol. Finally, the entire micro-encapsulator fits in a LAF-hood, allowing for sterile working conditions.

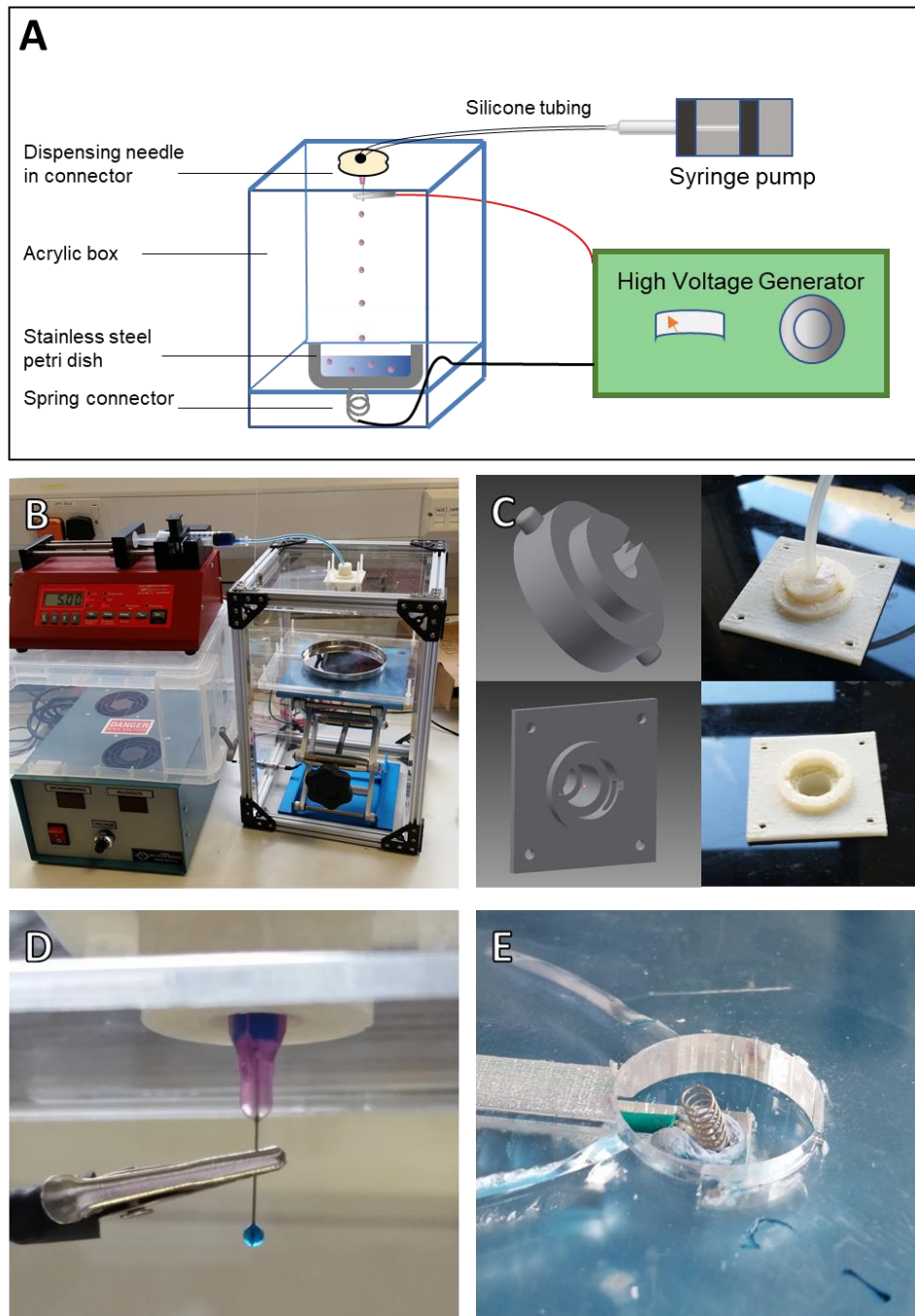


Figure 3.10: The encapsulator set up. A: A schematic overview of the original design. In the original design, a commercially available syringe pump stood to the side of the micro-encapsulator, with silicone tubing connecting the syringe to a dispensing needle in a specially designed connector. The stainless steel petri dish was connected to the ground wire by placing it on top of a spring. B: A photograph of the original set-up. C: The silicone tube and the dispensing needle are locked into place using a custom designed locking mechanism. D: The high voltage generator was connected to the dispensing needle with a crocodile clip. E: A spring protruding from the base plate was used as a connector to connect the sterile steel petri dish to the ground wire.

3.3. Optimisation of the System

Over time changes were made to the micro-encapsulator. These changes were usually done in order to improve the functionality of the micro-encapsulator, the reproducibility of the experiments, or to improve on the morphology of the created encapsulation. Finally, the micro-encapsulator had to be adjusted in order to allow coaxial printing (Chapter 5).

3.3.1. Syringe Pump

One of the first things that needed to be adjusted was the syringe pump, and the delivery of the alginate to the dispensing needle. Although the silicone tubing worked for larger amounts of alginate, the dead volume (the space between the syringe and the dispensing needle) of almost 0.5 ml was far too large for printing with cells or islets. For instance, when printing at a concentration of 10 million cells/ml of alginate, 5 million cells would not be printed, as they would still be in the silicone tubing when the syringe was already completely emptied by the syringe pump. An initial solution to this problem was found by switching the syringe with cells for one with just alginate once the syringe was completely empty. However, this meant that the micro-encapsulation had to be stopped and restarted for the last part, which was not ideal, and it is questionable whether switching the syringe midway the encapsulating process would be possible in a GMP setting. A second negative property of the silicone tube is its elasticity. It was found that the silicone tube would expand a little bit at the start of the encapsulating due to the increased pressure, and contracted when the syringe pump was turned off, continuing to press alginate out of the dispensing needle even when the micro-encapsulator was shut off. This variability in pressure resulted in beads with a bigger variability in size. To illustrate this, beads were created by spraying a 2% Protanal alginate solution using either the silicone tube connection or with a direct connection between the syringe and the dispensing needle by balancing the syringe pump on its side on top of the micro-encapsulator. For both experiments the alginate solution was sprayed at a speed of

1 ml/h through a 27G dispensing needle, with a distance of 0.5 cm to the gelling bath (100 mM CaCl₂) and an electric potential of 8 kV (Figure 3.2).

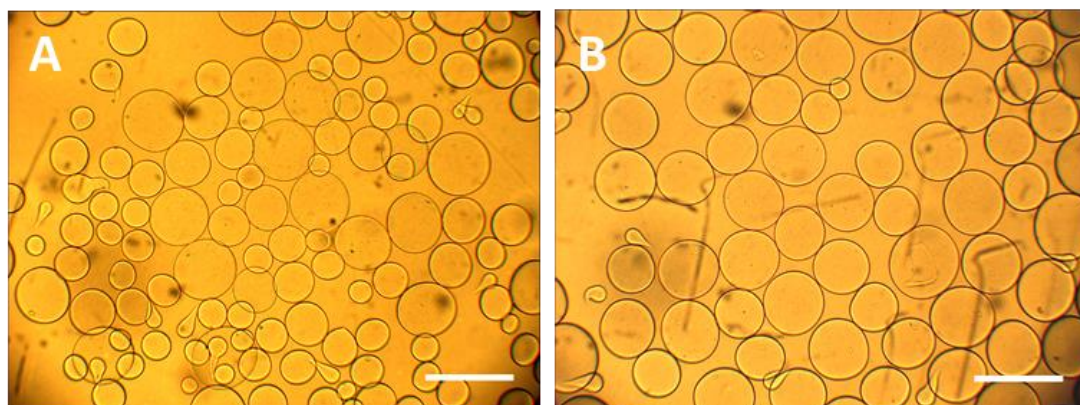


Figure 3.1: The silicone tubing between the syringe and the dispensing needle had an effect on the variability of the size of the alginate beads. A: alginate beads with a silicone connection tube used between the syringe and the dispensing needle. B: alginate beads with the dispensing needle connected directly on the syringe in the syringe pump. (Scalebar 500 μ m)

These results show that beads with less variability are created when the syringe was directly coupled to the dispensing nozzle. As the commercially available syringe pump was not stable on its side, a simple syringe pump that could be mounted on top of the encapsulator instead of next to it was designed.

A simple syringe pump for 1 ml syringes was designed in Autodesk Inventor. It was designed to only accommodate one size of syringe, as that would simplify the design. 1 ml was chosen as the desired syringe size, as most of the experiments done only needed small volumes. Later a second syringe pump for only 5ml syringes was simply adopted from the original design. The syringe pump was designed to be a simple stepper motor with a lead screw, that can push or pull a block that in turn will push or pull the plunger of a syringe (Figure 3.3 A). All parts were 3D printed out of Acrylonitrile Butadiene Styrene (ABS), with the exception of the electronics, lead rods and the ball bearings (Figure 3.3 B). To operate the stepper motor,

an Arduino Micro was used (Figure 3.3 C). The Arduino Micro can be programmed by attaching it to a computer to make it run at a certain speed as soon as it is turned on. The speed can be changed by changing the number of steps per second (the code used can be found in Supplementary data S1). A housing was 3D printed to contain the electronics and the actual stepper motor. The housing was merged to the carriage of the stepper motor by melting it a bit using a soldering iron. An end-stop was incorporated in the design to stop the pump running once it completely emptied the syringe (Figure 3.3 C).

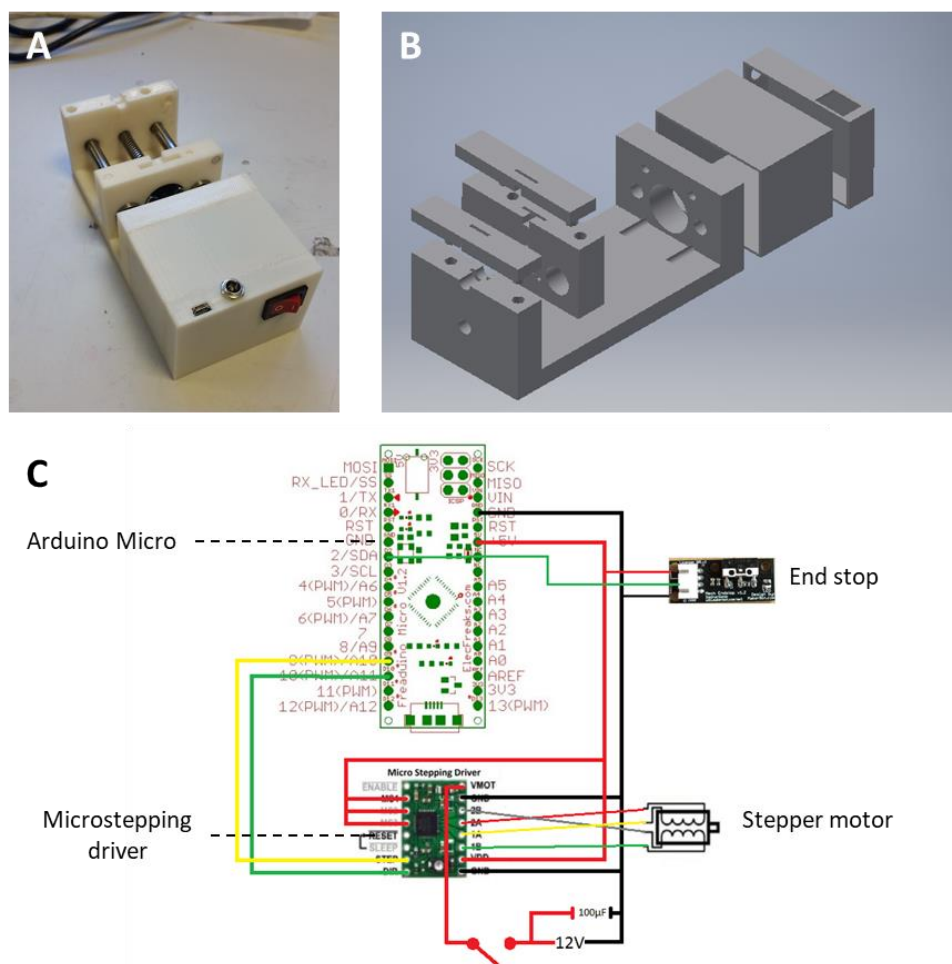


Figure 3.2: A syringe pump was designed that would be able to fit on top of the encapsulator, to allow the syringes to be directly inserted into the dispensing needle. A: The completed syringe pump was a simple design, where a stepper motor with a lead screw pushes or pulls a block that in turn will push or pull the plunger of a syringe. B: A schematic exploded view of the printed parts of the syringe pump. C: Wiring diagram for the electronics of the syringe pump.

After the syringe pump was created, it was tested by measuring the amount of distilled water it could dispense in 36 seconds at an extrusion speed of 10 ml/h, and how much water it could dispense in 450 seconds at 1 ml/h. This was done by dispensing the water directly on a petri dish placed inside of a balance. At exactly 36 or 450 seconds the syringe pump would be turned off and the dispensing needle got a gentle flick, to dislodge any droplets still attached to it. To compensate for any water evaporating during these experiments, the weight of the water was measured immediately after the syringe pumps were turned off, and again 36 or 450 seconds after it was turned off. The difference between these numbers was assumed to be the amount of water evaporated during the experiment, and the difference was added on top the first measurement. Both these experiments were repeated 5 times (n=6). Another experiment to test the syringe pump was by using it to create some beads. The results (Figure 3.4) show that the home-made syringe pumps actually perform better (more reproducible) than the commercial available syringe pump. When pumping for 36 seconds at 10 ml/h, 100 μ l of water should be dispensed. The home-made syringe pump dispensed 99.98 μ l of water on average, while the off-the-shelve syringe pump dispensed only 94.60 μ l of water (Figure 3.4 A). When pumping for 450 seconds (7.5 minutes) at 1 ml/h, roughly 125 μ l of water should be dispensed. The home-made syringe pump dispensed 124.6 μ l on average, while the off-the-shelve syringe pump dispensed 113.75 μ l of water, with a lot more variance (Figure 3.4 B).

The home-made syringe pump solved all the problems, being able to stand directly on the encapsulator, with no dead space between the syringe and the dispensing needle. Furthermore, it can easily be modified, has an end-stop and multiple syringes can be controlled from one interface.

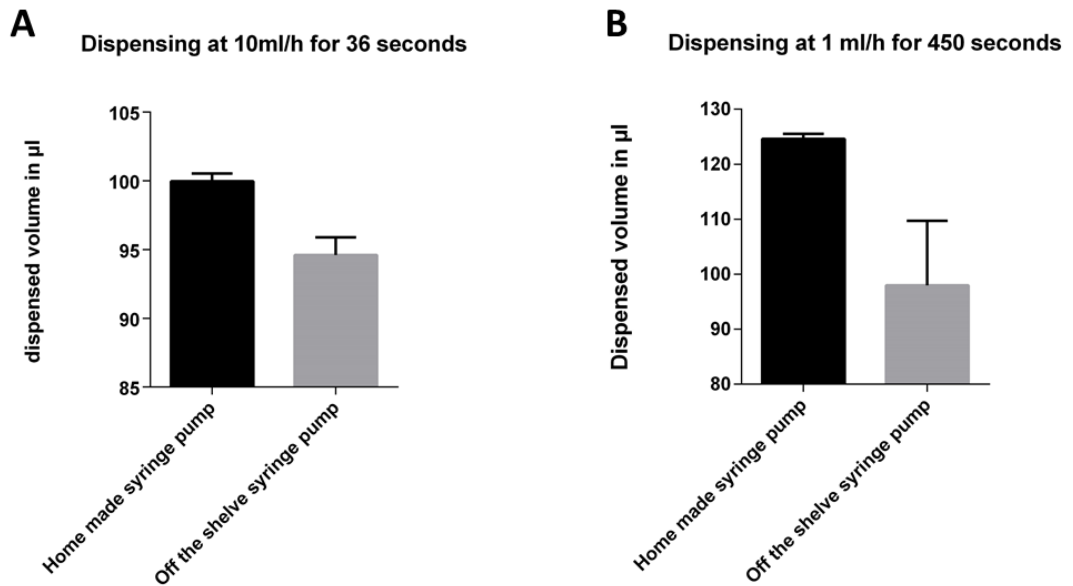


Figure 3.3 To test the home-made syringe pump versus the off-the-shelve syringe pump, they used to pump water at a certain speed for specified period. A: The amount of water measured in μl after pumping for 36 seconds at 10 ml/h. B: The amount of water measured in μl after pumping for 450 seconds at 1 ml/h.

3.3.2. Ground Electrode

The second element that needed changing was the ground electrode. Even though the original idea of using a complete stainless steel petri dish as the ground electrode worked, it was really hard to reproduce the results. Since the entire stainless-steel petri dish is completely grounded, it was found that the electrical field was not between the dispensing needle and the gelling bath, but mainly between the dispensing needle and the rim of the petri dish (Figure 3.5). This meant that if the petri dish was not in the exact same place every time, the field strength would fluctuate, resulting in slightly different beads every time.

For the first trial to change the ground electrode, a midway ring design (Figure 3.6 A) was chosen. This had an added beneficial quality that the distance between the ground electrode and the dispensing needle could remain the same while the distance to the gelling bath could be increased. The longer distance to the gelling bath should in theory create more circular

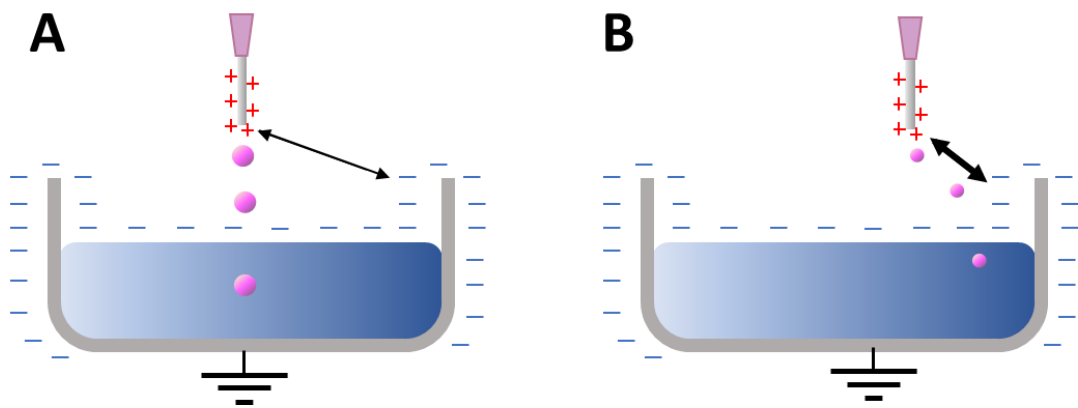


Figure 3.4 When using grounded stainless-steel petri dishes, the electrical field responsible for pulling the beads from the dispensing needle can be formed between needle and the rim of the petri dish. This could lead to a difference in field strength from when the dispensing needle is neatly in the middle (A) or slightly to the side (B)

beads.^[2] However, it was found that with the ring electrode, a lot of the material actually ended up on the electrode, or the trajectory of the beads was changed so much that the alginate ended up on the walls of the micro-encapsulator (Figure 3.6 B).

In the end, the “electrode in bath” design (Figure 3.6 C) was chosen, which is used by many other researchers.^[4-6] The positive characteristic of this set up is in its simplicity, the distance between the dispensing needle and the gelling bath is also the distance of the electric field. It also allows the use of disposable plastic petri dishes instead of the stainless-steel ones. The unfavourable quality of this technique is the fact that the same electrode is placed in the baths across experiments. This could be a potential source of contamination. To counteract this, the electrode was rinsed in 70% ethanol followed by sterile PBS before placing it in the gelling bath, between experiments.

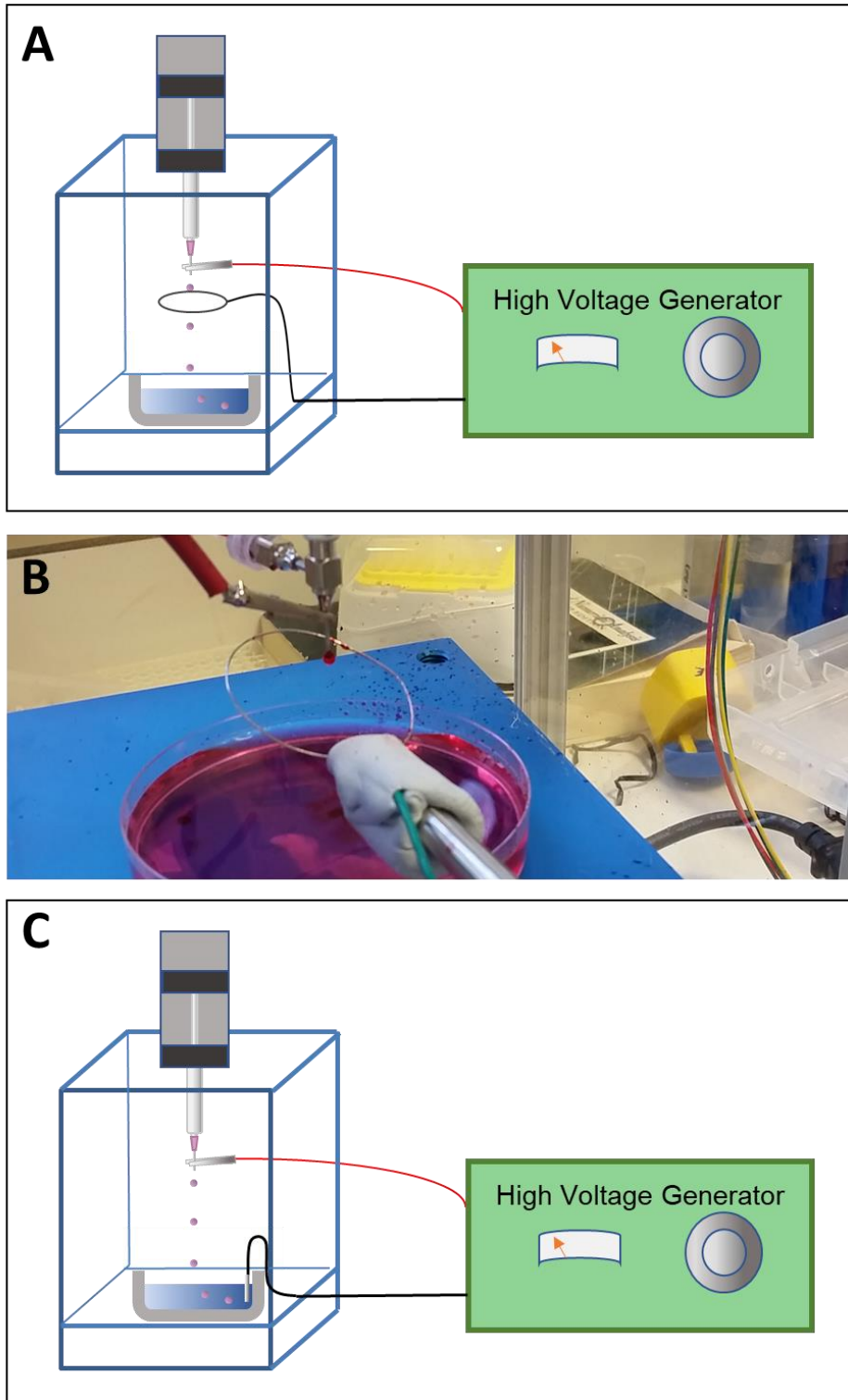


Figure 3.5: The first replacement of the grounded stainless-steel petri dishes was a midway round ground electrode (A). However, after a few tests it was found that a lot of alginate was brought out of trajectory and ended up on the electrode, or the walls of the encapsulator (B). In the end the “electrode in bath” method was used (C).

3.3.3. Top Panel

The final part of the encapsulator that needed minor changes was the top panel. With the new syringe pumps that can just sit on top, there was no more need for the part that locked the dispensing needle in place. On top of that, for the coaxial printing (Chapter 5) the top needed a second hole for the second syringe pump. Therefore the top was slightly changed (Figure 3.7), with a small hole in the middle to fit 1 ml syringes, and a bigger hole on the side, so that 5 ml syringes could be used for the outer material of the coaxial beads.

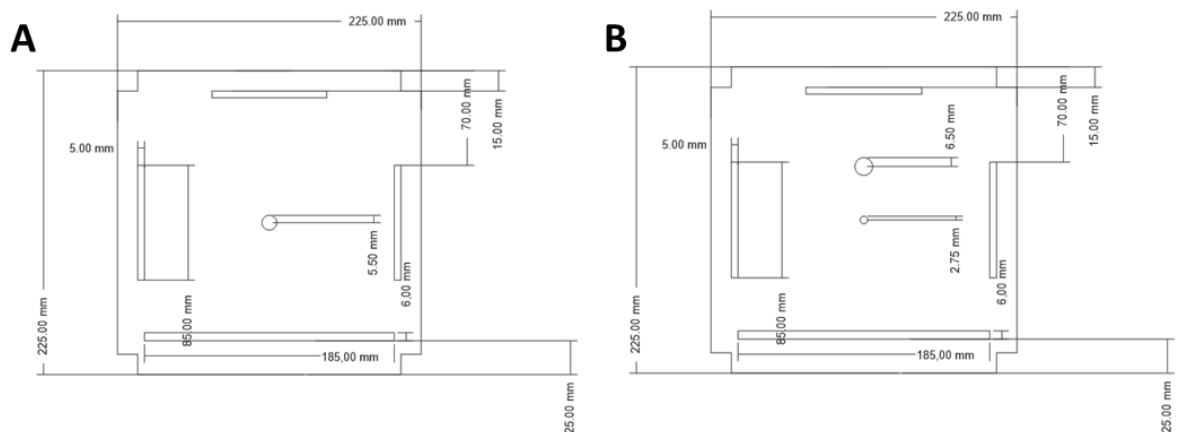


Figure 3.6 A minor change was made to the top panel, to allow coaxial printing with syringe pump placed directly on top of the encapsulator. A: original design. B: Revised design, with a smaller central hole to fit 1 ml syringes and a large hole to the side to accommodate 5 ml syringes.

3.4. Parameters Influencing the Bead Size and Morphology

After the micro-encapsulator was built, different parameters were tested to determine the influence on the printed droplets. The encapsulator was used to produce beads using different parameters. These beads were imaged underneath a microscope and their diameter was determined using imageJ software. At least 50 beads were measured for each set of parameters. Even though most of the parameters have already been studied before,^[2, 7, 8] there are so many parameters to take into account that results seem to be different from device to device. For that reason, this study was mainly done in order to find the parameters that would work for our applications.

The first thing that was investigated, was the influence of the electric potential on the shape and size of the alginate beads. After that, the influence of dispensing flow rate, distance to the gelling bath, alginate concentration, dispensing needle used and the gelling bath used were studied.

3.4.1. Voltage

The electric potential between the dispensing needle and the gelling bath is the driving force that pulls the viscous alginate solution into small beads from the tip of the dispensing needle. 1% Protanal alginate solution was dispensed at a speed of 5 ml/h through a 30G dispensing needle into a 100 mM CaCl₂ isotonic gelling bath. The distance between the gelling bath and the dispensing needle was kept constant at 5 cm. Electric potential was increased from 6 to 20 kV, in 2 kV increments.

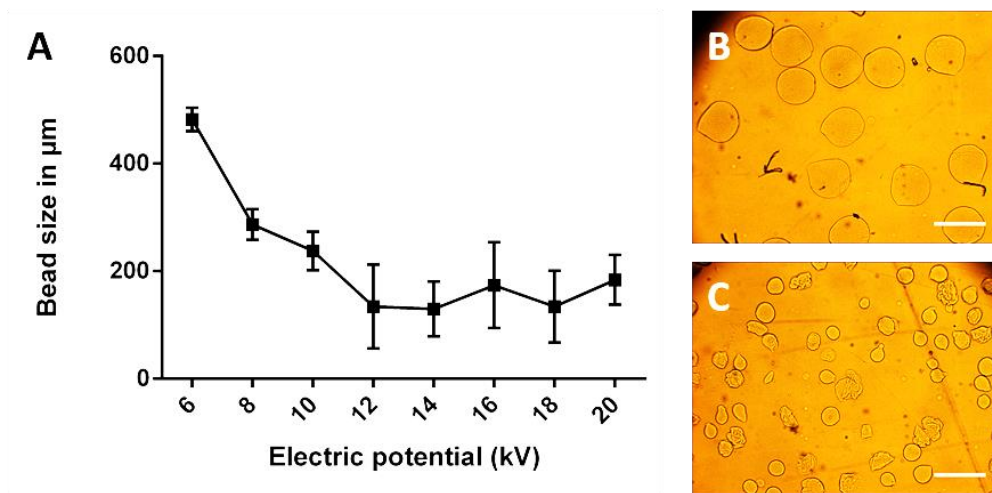


Figure 3.7: The size and shape of electro-sprayed beads are influenced by the electric potential used during the electro-spraying. A: The average bead size plotted against the electric potential used during their fabrication (\pm SD error bars). B: An example of relative monosized beads sprayed at 8 kV. C: An example of beads sprayed at 20 kV. (scale bar 50 μ m)

In the range from 6 to 12 kV a decrease in average bead size can be seen for an increased electric potential (Figure 3.8 A). However, this seems to plateau after the 12 kV point. A second observation that can be made is that where beads can be considered relatively

monosized for 6, 8 and 10 kV (Figure 3.8 B), the bead size has a higher variance at higher potentials. Finally, the shape of the beads become very irregular after 10 kV. The beads are no longer smooth spheres, but come in all kinds of weird shapes, often with wrinkly surfaces (Figure 3.8 C).

3.4.2. Dispensing Flow Rate

The second parameter that was investigated was the dispensing flow rate. The flow rate is the speed at which the alginate is moved through the nozzle. The size of alginate beads was measured after spraying a 1% alginate solution through a 30G dispensing needle at 5, 2.5 or 1 ml/h. The distance to the 100 mM Isotonic CaCl₂ gelling bath was 5 cm and the electric potential 10 kV. When dispensing at speeds lower than 1 ml/h the spray became discontinuous. At much higher speeds the alginate would just pour out of the dispensing needle in a strand and would not form beads.

As could be expected, larger beads are formed at higher flow rates (Figure 3.9). If only the flow rate increases, the amount of material at the end of the dispensing needle will increase,

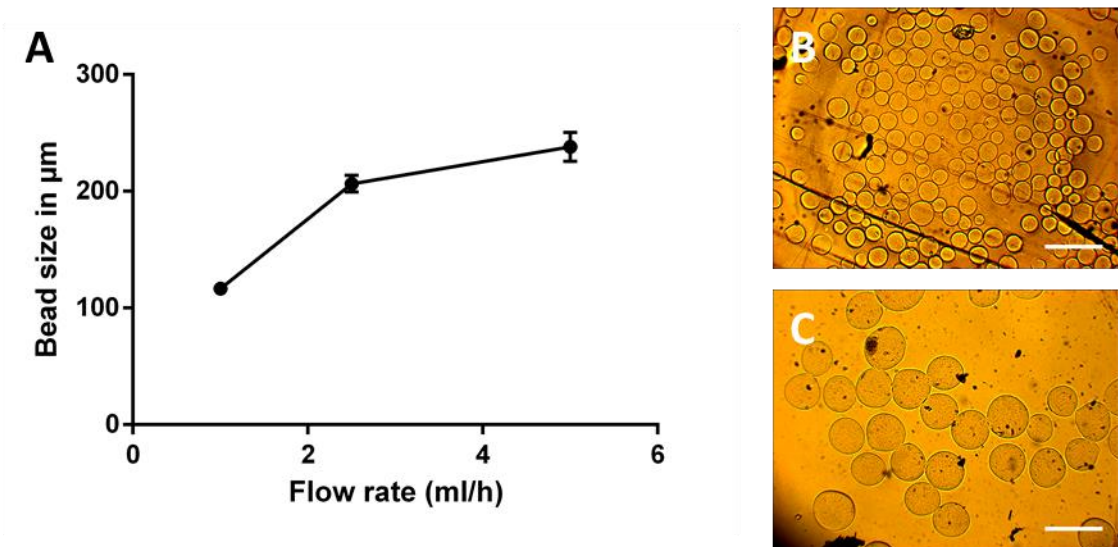


Figure 3.8: The size of electro-sprayed beads is influenced by the flow rate used during the electro-spraying. A: The average bead size plotted against the flow rate during their fabrication (\pm SD error bars). B: An example of beads sprayed with a flow rate set to 1 ml/h. C: An example of beads sprayed with a flow rate set to 5 ml/h. (Scalebar 500 μm)

which creates larger beads. There is a slight increase in size variation at higher flow rates, but they can still be considered mono-sized, when compared to other people's work,^[9] but especially when compared to other methods.^[10]

3.4.3. Distance Between Dispensing Needle and Bath

The distance between the dispensing needle and the bath has an influence on the strength of the electric field that is pulling on the alginate, with smaller distances creating stronger fields. The size of alginate beads was measured after spraying a 1% alginate solution through a 30G dispensing needle at 5 ml/h at either 3, 25, 50 or 100 mm into the 100mM CaCl₂ gelling bath. The electric potential was alternated at each location between 6, 8, 10, 15 and 20 kV. When dispensing at a distance of 100 mm there was no difference between spraying with the high voltage generator turned off or at 6 kV, therefore the beads made at 6kV were not measured. At a distance of 3 mm it was not possible to spray with an electric potential of 20 kV, as this resulted in an electrical discharge between the dispensing needle and the gelling bath.

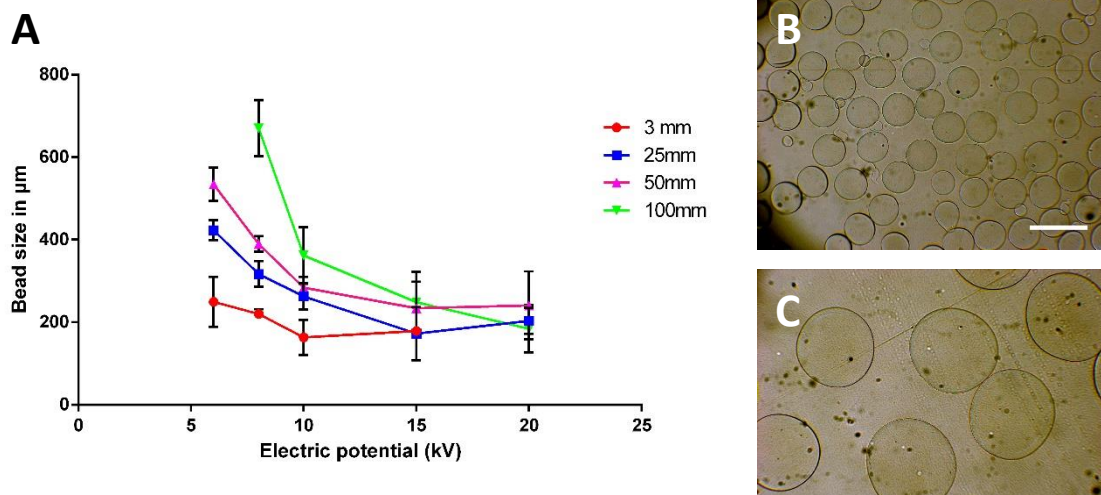


Figure 3.9 The size of electro-sprayed beads is influenced by the distance between the dispensing needle and the gelling bath, as this influences the strength of the electric field. A: The average bead size plotted against the electric potential for 4 different distances between the dispensing nozzle and the gelling bath (\pm SD error bars). B: An example of beads sprayed at a distance of 3 mm with an electric potential of 8kV. C: An example of beads sprayed at a distance of 100 mm with an electric potential of 8 kV. (Scalebar 500 μ m)

Up until 10 kV a clear difference can be seen in bead size, with beads decreasing in size with a decreased distance between the dispensing needle and the gelling bath (Figure 3.10). After the 10 kV point the sizes start to merge (Figure 3.10 A), which probably means that the electric field is so strong for all these distances that they are all reaching the same “plateau” that could be seen when only the electric potential was changed (Figure 3.8 A). The same plateau can be seen in other people’s work.^[7, 9]

3.4.4. Alginate Concentration

The alginate concentration also has an influence on the size and shape of the beads created. An increase of alginate increases the viscosity of the solution (Figure 3.11), as was measured using a viscosity cup. A higher viscosity makes it harder to break the material apart into separate droplets but does give the separate droplets more mechanical stability. The size of alginate beads was measured after spraying with different concentrations of Protanal alginate (0.5%, 1.0%, 1.5% or 2.0%), into a 100 mM CaCl₂ bath, at a distance of 2 cm through a 27G dispensing needle at a speed of 1 ml/h. The voltage was varied from 5 kV to 8 kV in 1 kV increments.

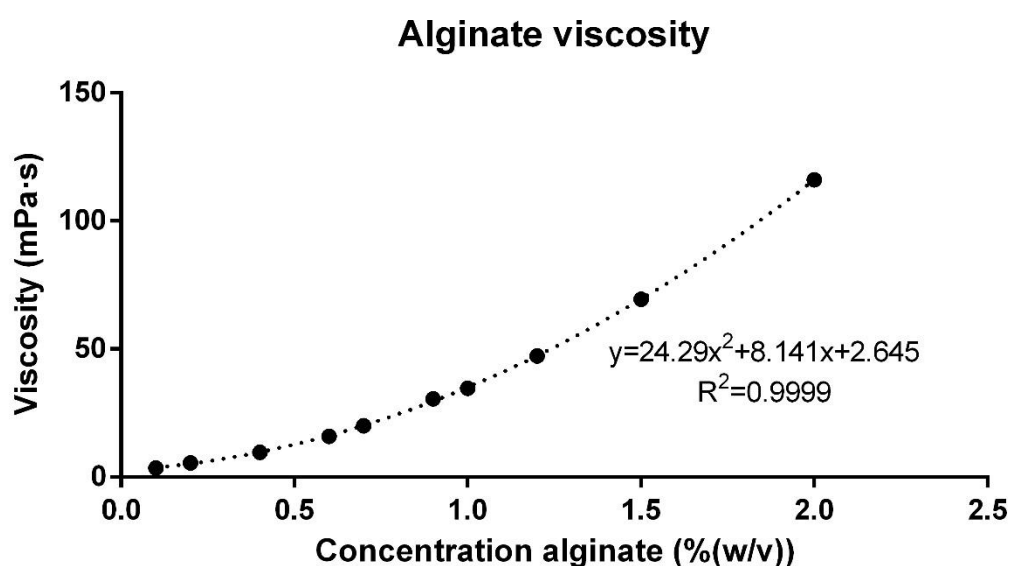


Figure 3.10: Viscosity of alginate plotted against the concentration. A trendline is plotted as a dotted line. At increasing concentrations of alginate, the viscosity increases exponentially.

Overall, an increase of bead size can be noticed for increased concentrations of alginate (Figure 3.11 A). Just as shown before, an increase of electric potential decreases the size of the alginate beads, for all concentrations. A slight increase in size variability could be seen for an increase of alginate concentration, but the most noticeable difference could be seen in the shape of the alginate beads. The 0.5% alginate solution did not form any nice, rounded beads, at whatever potential used (Figure 3.11 B). All the beads created with this concentration of alginate seemed to be misshapen after fully gelling. This could be due to the fact that their viscosity doesn't allow them to remain their shape when hitting the gelling bath, instead flattening out a bit before crosslinking. This flattening could also explain why, the 0.5% alginate beads sprayed with an electric potential of 5 kV created bigger structures than those printed with higher concentrations of alginate. When the beads flatten out their surface increases.

The beads created with 1% or 1.5% alginate solutions maintained their rounded morphology (Figure 3.11 C) up until the electric potential of 8 kV, where the created structures were basically shaped the same as those of the 0.5% alginate solution (Figure 3.11 D). This could imply that at higher electric potentials the velocity at which the alginate droplets hit the gelling bath is so high that also these beads cannot maintain their shape when hitting the bath. The beads created with 2% alginate solution were shaped nice and round for all conditions (Figure 3.11 E).

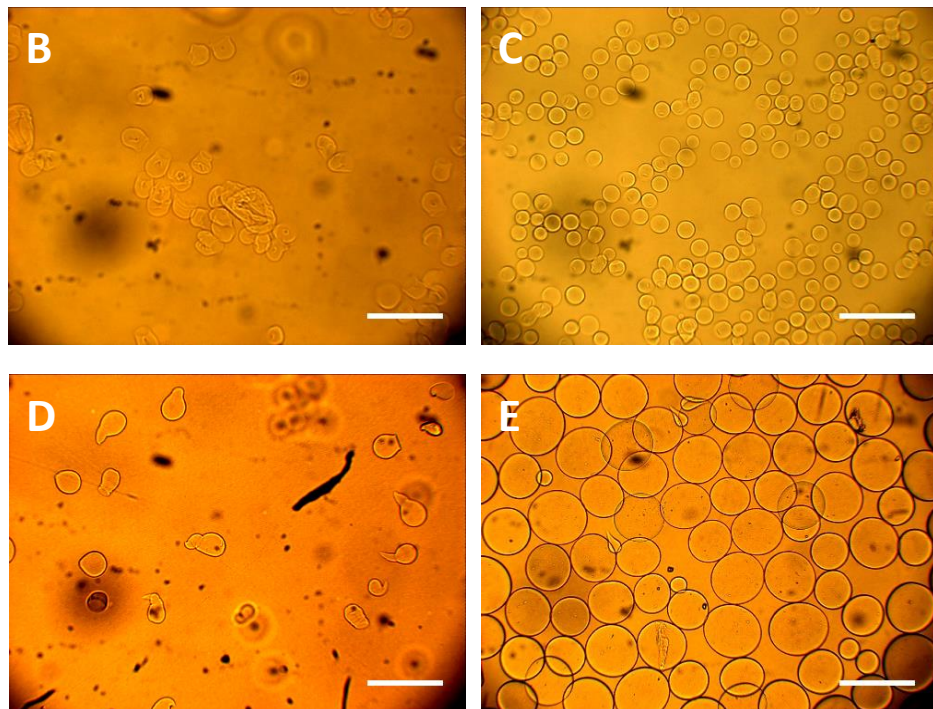
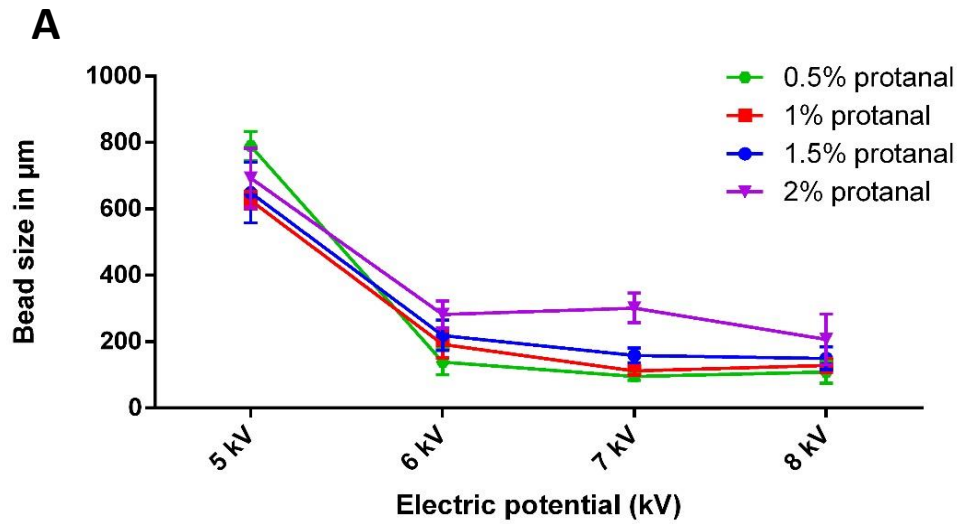


Figure 3.11: The size and shape of electro-sprayed beads are influenced by the concentration of alginate used. A: Average bead size of alginate beads plotted against the electric potential, for 0.5%, 1.0%, 1.5% and 2.0% alginate solutions (\pm SD error bars). B: 0.5% alginate beads sprayed at 6kV are misshapen and do not resemble spheres at all. C: 1% alginate beads sprayed at 7 kV form uniform, monosized beads. D: At 8 kV, 1.5% alginate beads do not maintain their neat spherical shape they have when sprayed at lower electric potential. E: 2% alginate maintained a nice rounded morphology, even at 8 kV. (Scalebar 500 μ m)

3.4.5. Dispensing Nozzle

The next parameter that was investigated was the influence of the dispensing nozzle on the electro-sprayed beads. Normal dispensing needles, comparable to blunt injection needles, were initially used for the encapsulator. Three different gauges were compared, 22G, 27G

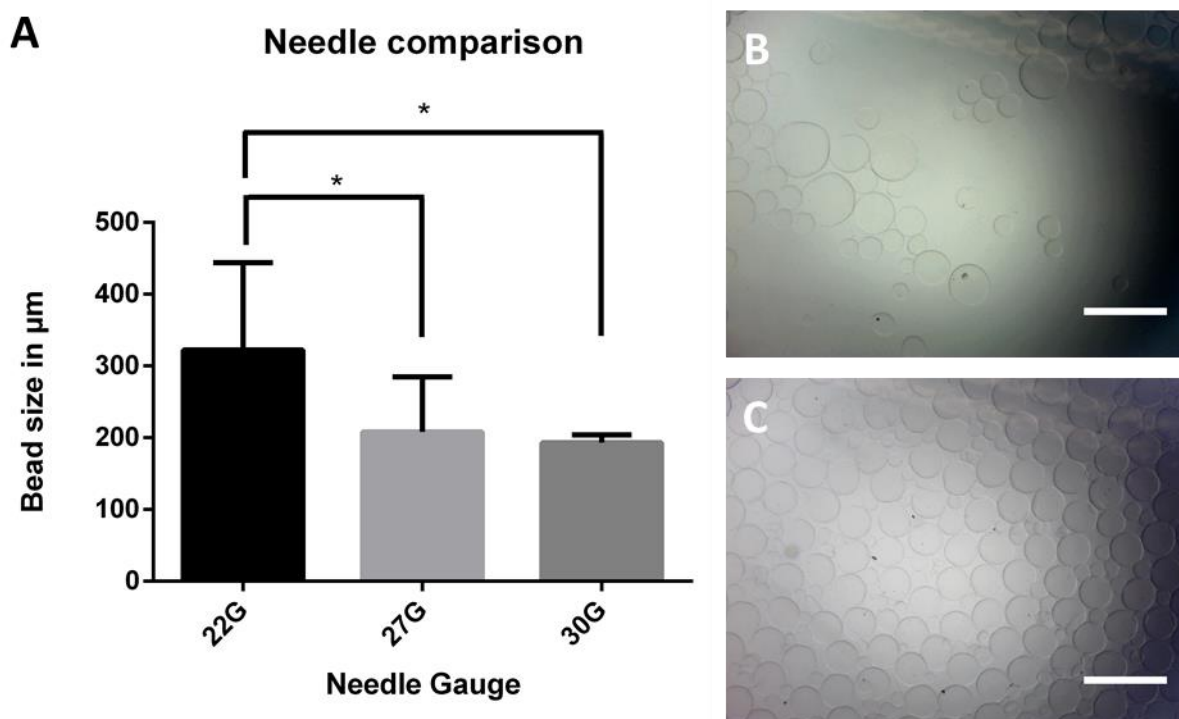


Figure 3.12: The size and uniformity of the beads is influenced by what gauge needle is used for the electro-spraying. (* $P < 0.0001$) A: The mean bead size per needle gauge (+SD error bars). B: Beads fabricated using a 27G needle. C: Beads fabricated using a 30G needle. (Scalebar 500 µm)

and 30G, which have an internal diameter of 413 µm, 210 µm and 159 µm respectively. A 1% Protanal alginate solution was electro-sprayed at a distance of 5 cm into a 100 mM BaCl₂ bath, at 5 ml/h with an electric potential of 10 kV through either of the different dispensing needles. With smaller gauge dispensing needles (larger internal diameter of the needles) an increase in bead size can be seen, as well as more variability in bead sizes (Figure 3.13 A). Even though there is no statistical difference in the mean size of the beads sprayed through 27G or 30G needles, a clear difference in uniformity can be seen (Figure 3.13 B and C).

3.4.6. Gelling Bath

The last parameter that was investigated was the gelling bath. The mechanical strength of the created alginate hydrogels can be influenced by the concentration of the gelling bath and the chosen cations.^[11] However, their influence on the fabrication of the alginate hydrogel beads is not known. A 1% Protanal alginate solution was electro-sprayed at a distance of 5 cm into a gelling bath, at 5 ml/h with an electric potential of 10 kV through a 30G dispensing needle. For the first experiment the influence of the cations was investigated. Beads were electro-sprayed in either a 100 mM CaCl₂, SrCl₂ or BaCl₂ gelling bath. There was no significant difference in size between the beads fabricated using either SrCl₂ or BaCl₂ but when printing in a CaCl₂ bath the beads were a little bit (10 μm) bigger (Figure 3.14 A). Furthermore, the beads created using CaCl₂ had a “wrinkly” surface compared to the other two (Figure 3.14 B and C). The second factor of the gelling baths that need to be investigated was the influence of the gelling bath concentration. For this experiment the beads were sprayed in gelling baths made of 100 mM, 50 mM, 25 mM or 12,5 mM BaCl₂. There was no significant difference in bead size or morphology between the 100 mM and 50 mM bath (Figure 3.14 D and E). However, for the 25 mM and 12.5 mM baths the beads started to lose their rounded morphology, and a fair number of beads with “tails” appeared (Figure 3.14 F). These beads are usually a bit narrower than the rounded ones, which explains the smaller size, but larger variability.

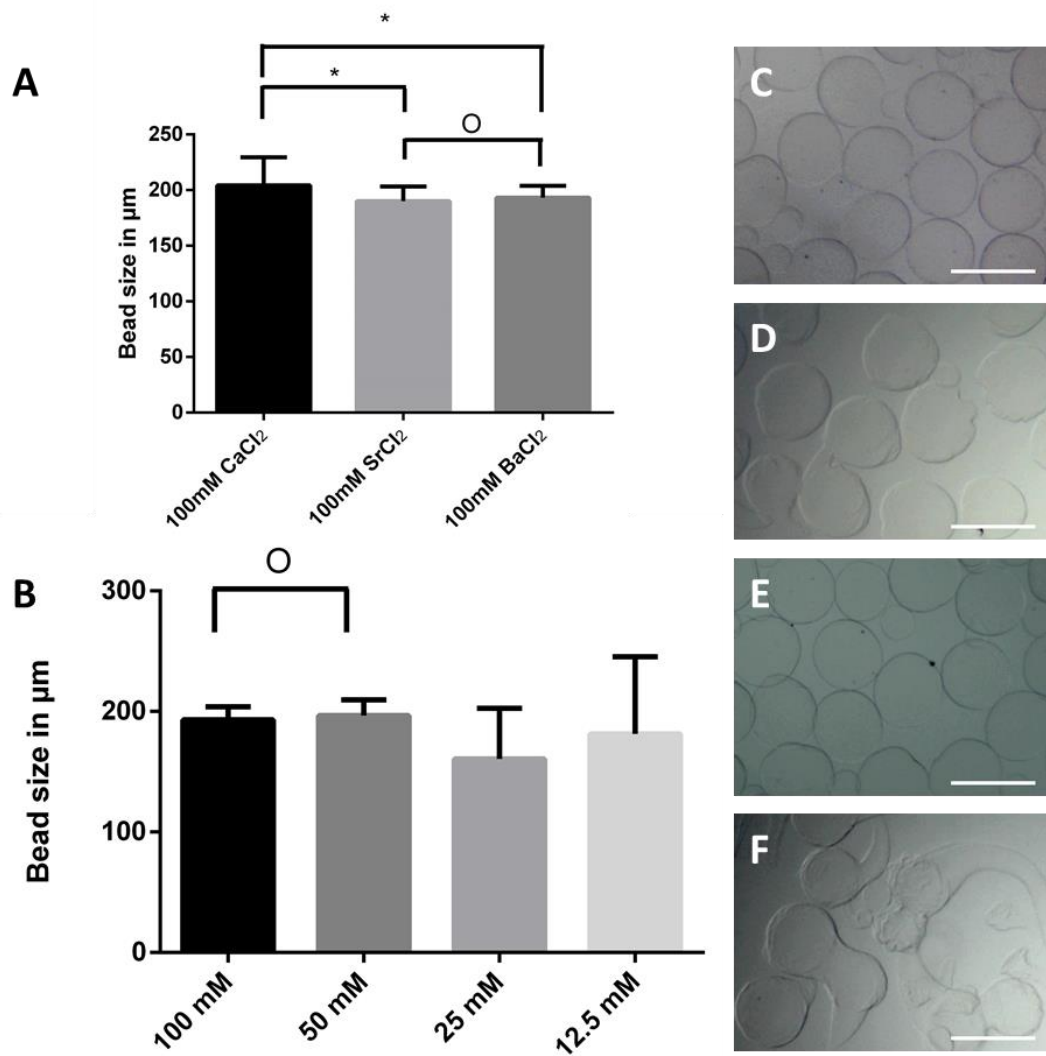


Figure 3.13: The size and shape of electro-sprayed beads are slightly influenced by the gelling bath used. A: Average bead size of alginate beads per gelling bath. B: Average bead size of alginate beads per concentration BaCl₂ in gelling bath. (+SD error bars; * $P < 0.0001$; O $P > 0.05$; rest $P < 0.01$) C: Beads electro-sprayed in 100 mM BaCl₂ are uniform and have a nice spherical morphology. D: Beads electro-sprayed in CaCl₂ are slightly bigger than those sprayed in other baths and have a more “wrinkly” morphology. E: Beads electro-sprayed in 50 mM do not differ from those electro-sprayed in 100 mM BaCl₂. F: Alginate beads sprayed in 12.5 mM BaCl₂ do not have a nice morphology, with a fair amount forming a tail. (Scalebar 250 µm).

3.5. Conclusion

In this chapter the creation of the micro-encapsulator was discussed, from the original design to the final adjustments, and the parameters that influence the function and efficiency of the micro-encapsulator.

The micro-encapsulator was designed as a method to quickly and safely encapsulate islets and cells in uniform capsules. A new, simple syringe pump was created to fit directly on top of the micro-encapsulator, to eliminate the use of a silicone connection tube. As an additional benefit, the new syringe-pump out-performed the off-the-shelf model that was used up until that point. The ground electrode was swapped from the original stainless-steel petri dish to an “electrode in bath” type, to increase reproducibility and uniformity of the created beads.

Six different parameters are defined that influence the shape, size and uniformity of the beads created by the encapsulator; electric potential, dispensing flow rate, distance to the gelling bath, concentration of the alginate, dispensing needle and the chosen gelling bath. In this chapter all these parameters were isolated to show their effect. However, there is a huge interplay between all these parameters. When the distance between the gelling bath and the dispensing needle is smaller, less voltage could be used, and gelling baths like 100 mM CaCl_2 could produce smooth, uniform beads. The same goes for the dispensing needles. In section 3.4.5 it looks as if smaller gauge needles can't produce uniform alginate beads. However, as can be seen in section 3.4.4, this is possible when adjusting the dispensing height, flow rate and electric potential.

3.6. References

- [1]. Zimmermann H, Shirley SG, Zimmermann U. Alginate-based encapsulation of cells: past, present, and future. *Current diabetes reports*. **2007**;7(4):314-20.
- [2]. Moghadam H, Samimi M, Samimi A, Khorram M. Electro-spray of high viscous liquids for producing mono-sized spherical alginate beads. *Particuology*. **2008**;6(4):271-5.
- [3]. Wiedemeier S, Ehrhart F, Mettler E, Gastrock G, Forst T, Weber MM, *et al.* Encapsulation of Langerhans' islets: Microtechnological developments for transplantation. *Engineering in Life Sciences*. **2011**;11(2):165-73.
- [4]. Zhang W, He X. Encapsulation of living cells in small (approximately 100 microm) alginate microcapsules by electrostatic spraying: a parametric study. *J Biomech Eng*. **2009**;131(7):074515.
- [5]. Park H, Kim P-H, Hwang T, Kwon O-J, Park T-J, Choi S-W, *et al.* Fabrication of cross-linked alginate beads using electrostatic spraying for adenovirus delivery. *International Journal of Pharmaceutics*. **2012**;427(2):417-25.
- [6]. Barron C, He J-Q. Alginate-based microcapsules generated with the coaxial electrostatic spray method for clinical application. *Journal of Biomaterials Science, Polymer Edition*. **2017**;28(13):1245-55.
- [7]. Moghadam H, Samimi M, Samimi A, Khorram M. Study of parameters affecting size distribution of beads produced from electro-spray of high viscous liquids. *Iran J Chem Eng*. **2009**;6(3):83-98.
- [8]. Xie J, Wang CH. Electrostatic spray in the dripping mode for cell microencapsulation. *J Colloid Interface Sci*. **2007**;312(2):247-55.
- [9]. Gasperini L, Maniglio D, Migliaresi C. Microencapsulation of cells in alginate through an electrohydrodynamic process. *Journal of Bioactive and Compatible Polymers*. **2013**;28(5):413-25.
- [10]. Paredes Juarez GA, Spasojevic M, Faas MM, de Vos P. Immunological and technical considerations in application of alginate-based microencapsulation systems. *Front Bioeng Biotechnol*. **2014**;2:26.
- [11]. Chan E-S, Lim T-K, Voo W-P, Pogaku R, Tey BT, Zhang Z. Effect of formulation of alginate beads on their mechanical behavior and stiffness. *Particuology*. **2011**;9(3):228-34.

Chapter 4

Purified Alginate for Clinical Cell Encapsulation

4.1. Introduction

Based on the literature review, it was decided that alginate was going to be the material of choice for the encapsulation of islets of Langerhans. Alginate is a cheap material,^[1] and easy to work with as it stays completely liquid until it is mixed with a solution containing divalent cations.^[4] Based on the chemical composition of the alginate, and the chosen crosslinking agent, it is a material that is biocompatible and can be immunoprotective.^[5-7] Alginates with a higher amount of G-blocks are mechanically stiffer and more immunoprotective, but can become less biocompatible if the amount of G-blocks get too high.^[6] As alginate is a biomaterial that is harvested from natural resources (brown algae), it does contain some impurities in the form of endotoxins, proteins and polyphenols.^[7, 8] It has already been shown that by removing these impurities islet survival after transplantation is improved.^[6, 7, 9] These known alginate purification protocols take up a lot of time to perform, sometimes as much as 10 days. However, ultrapure alginates that are commercially available can be extremely costly, with prices as high as \$199.00 for 250 mg (Pronova SLG20, Novamatrix). In this chapter the possibility of a shortened protocol while maintaining the low levels of impurity is investigated.

A pure and sterile alginate hydrogel is not sufficient to create a clinically relevant biomaterial that is immunoprotective. In type 1 diabetes, the immune system of the patient is the cause of the destruction of the original β -cells.^[10] Therefore, the materials chosen for encapsulation must prevent antibodies (150,000 MW)^[11] and white blood cells (7-30 μm),^[12] from reaching the transplanted cells.^[13] However, small molecules, like oxygen, insulin (5,734 MW)^[14] and glucose (180 MW),^[15] should still be able to diffuse through the barrier. There should be a fine balance of permeability to provide immunoprotection while also facilitating for the diffusion of nutrients for long term survival and function of the encapsulated tissue. It has been shown that although alginate crosslinked with barium or strontium can be immunoprotective,^[5, 16] alginate

crosslinked by calcium does not provide any immunoprotection.^[5] Since the porosity of hydrogels has been poorly characterized, fine-tuning the optimal porosity for specific applications, such as immunoprotection or stem cell survival, has been done on trial and error basis.^[16] In this chapter the development and usage of a method to investigate the permeability of alginate hydrogels in real time using fluorescent confocal microscopy will be discussed. This method was used to investigate the influence of alginate concentration and crosslinking baths on the permeability of the created alginate microbeads.

4.2. Purification of Alginate

4.2.1. Creating the Shortened Purification Protocol

As stated before, impurities in the alginate in the form of proteins, endotoxins and polyphenols have a negative influence on the survival rate of the encapsulated islets after transplantation. Since other protocols can take up to 10 days, one of the more common used protocols by Klöck *et al.*^[7] was investigated to see if any steps could be left out to create a shortened protocol. In the original protocol, alginate powder was dissolved in water to form a 1.5% solution, mixed with activated charcoal and stirred for 4 hours. Afterwards it was filtered to remove the charcoal, and the solution was jetted into a BaCl₂ solution to form alginate beads with a diameter of 1.5 mm, which are mechanically stable enough to survive washes with different chemicals to extract the impurities (see table 4.1 for all the steps). The beads were then dissolved using EDTA, the resulting solution dialysed to remove the Ba²⁺ ions and the purified alginate was then precipitated using ethanol. Dusseault *et al.*^[8] already modified this protocol slightly by adding an initial chloroform extraction step on the alginate when it is still in its powder form, and slightly modifying the chemical washes used to remove the contaminants.

Since the chemical washes and the final dialysis are the most time-consuming parts of this protocol, they were the most logical steps to eliminate. The initial chloroform wash extracts

some of the protein contaminants, the wash with charcoal removes endotoxins, and any polyphenols are removed by the charcoal or remain in the aqueous stage when precipitating the alginate. Therefore a protocol without the creation of hydrogel beads or the chemical extractions from those beads was created. All the steps to the purification protocol can be found in Table 4.1, and the materials and methods section of this thesis. In Table 4.1 there is also a sum of the minimum time needed to perform the protocol, based solely on the time periods that are actually specified (with “overnight” counted as 10 hours). Taking into account that steps such as filtering, washing and dissolving actually take time, the total time needed to perform the purification is even more. The shortened protocol for instance was performed over a time period of 2 days and 2 nights. It is theorized that the full Klöck protocol takes 10 days in total, which means that the shortened protocol provides a time gain of 80% over the original protocol.

Table 4.1: Overview of the original versus the shortened protocol

	Klöck et al	Shortened protocol
	Dissolve Alginate into a 1.5% solution	Three 30 minute washes with chloroform
	4 h treatment with activated charcoal	Dissolve alginate into a 1.5% solution
	Barium bead fabrication in 50 mM BaCl ₂	4 h treatment with acetic washed activated charcoal
	Three 14 h 1M acetic acid extractions (pH 2.3)	4 h treatment with neutral activated charcoal
	Three 8 h Sodium Citrate extractions (pH 8.0)	Filter through a 0.2 µm filter
	Two 16 h 50% ethanol extractions	Add 10 mM NaCl and precipitate by ethanol
	Two 16 h 70% ethanol extractions	Dry under sterile conditions overnight
	Wash with 20 mM BaCl and Distilled water	
	Dissolve beads overnight in 250mM EDTA (pH 10.0)	
	Filter through a 0.2 µm filter	
	20 h dialysis against demineralized water	
	Add 10 mM NaCl and precipitate by ethanol	
	Dry under sterile conditions overnight	
<i>total minimum time</i>	164 hours	19.5 hours

4.2.2. Measuring Impurities

The adapted purification protocol was tried on 2 different alginates; the Low Viscosity alginate from Sigma Aldrich, which has a low viscosity and high M-block content and the 10/60FT Protanal alginate from FMC biopolymers, which also has a low viscosity but a high G-block content. To assess the success of the purification protocol, alginates were checked for any impurities in the form of proteins, polyphenols or endotoxins. Results are compared to results of Klöck et al.^[7] and to the modified protocol by Dusseault et al.^[8]

For every 4,5 grams of crude alginate that went into the purification process, roughly 3,5 grams of purified alginate was obtained, roughly a 75% recovery. The alginate also changed in appearance after purification. It went from a brown powder to white/greyish flakes (Figure 4.1).

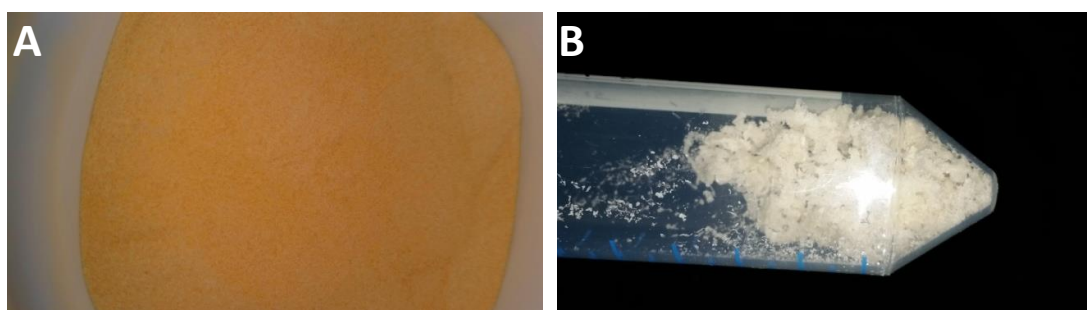


Figure 4.1: Low viscosity alginate before (A) and after (B) purification

4.2.2.1. Protein Contaminants

To measure the amount of protein contaminants, a Bicinchoninic acid (BCA) assay was performed. In a BCA assay the peptides found in protein reduce Cu^{2+} ions into Cu^+ ions under alkaline conditions. The amount of Cu^{2+} ions reduced is linearly proportional to the amount of protein in the solution. In the second step of this reaction every Cu^+ ion is chelated by 2 molecules of bicinchoninic acid, forming a complex that is purple in colour and exhibits a strong absorbance at 562 nm (Figure 4.2 A). An increase of absorbance at this wavelength is

therefore almost linearly proportional to an increase of proteins. A protein standard of known concentrations of BSA was made, ranging from a concentration of 0 to 2000 μg of BSA per ml. When measurements would result in an absorbance higher than that of the highest absorbance of the standard, the assay was repeated on a sample diluted 10x with endotoxin free water. An average protein content of 3.14 mg per gram of dried Purified Protanal alginate was found, versus the 8.6 mg per gram of crude Protanal alginate (Figure 4.2 B), or a reduction of $\sim 63\%$. For the Low Viscosity alginate, a protein content of 14.8 mg/gram of crude alginate was reduced to 4.8 mg/gram of purified alginate (Figure 4.2 B), or a reduction of $\sim 68\%$. This is comparable with the results shown by Dusseault *et al.*^[8]

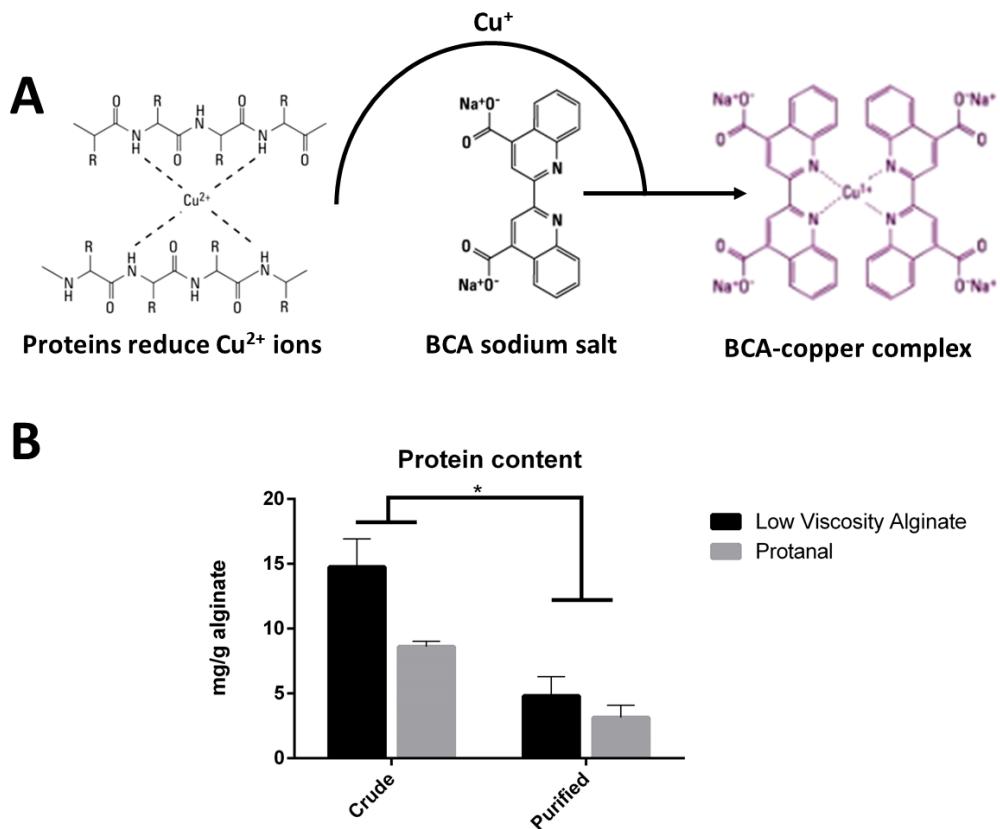


Figure 4.2: Alginate was tested for protein contaminants using a BCA assay. A: The BCA assay utilizes the reducing properties of proteins to transform Cu^{2+} into Cu^{+} , which then forms a purple complex with BCA, with a strong absorbance at 562 nm.^[2] B: Protein content of low viscosity alginate and Protanal were measured before and after purification. $*(p \leq 0.001; \text{Error bar indicates } +SD)$

4.2.2.2. Polyphenol Contaminants

Polyphenols are a structural class of mainly natural, organic chemicals. They are called polyphenols due to the fact that they contain large multiples of phenol structural units (Figure 4.3 A). Polyphenols have a characteristic emission peak at 445 nm when applying an excitation wavelength of 366 nm.^[17] Therefore, a spectrofluorimeter can be used to determine relative amounts of polyphenol content. Using the results from the spectrofluorimeter, it was shown that the polyphenol content was reduced in the Protanal alginate by an average of 91.4% and the polyphenol content of the Low Viscosity alginate by 85.6%. (Figure 4.3 B). This is comparable to the results of Klöck et al^[7] and Dusseault et al.^[8]

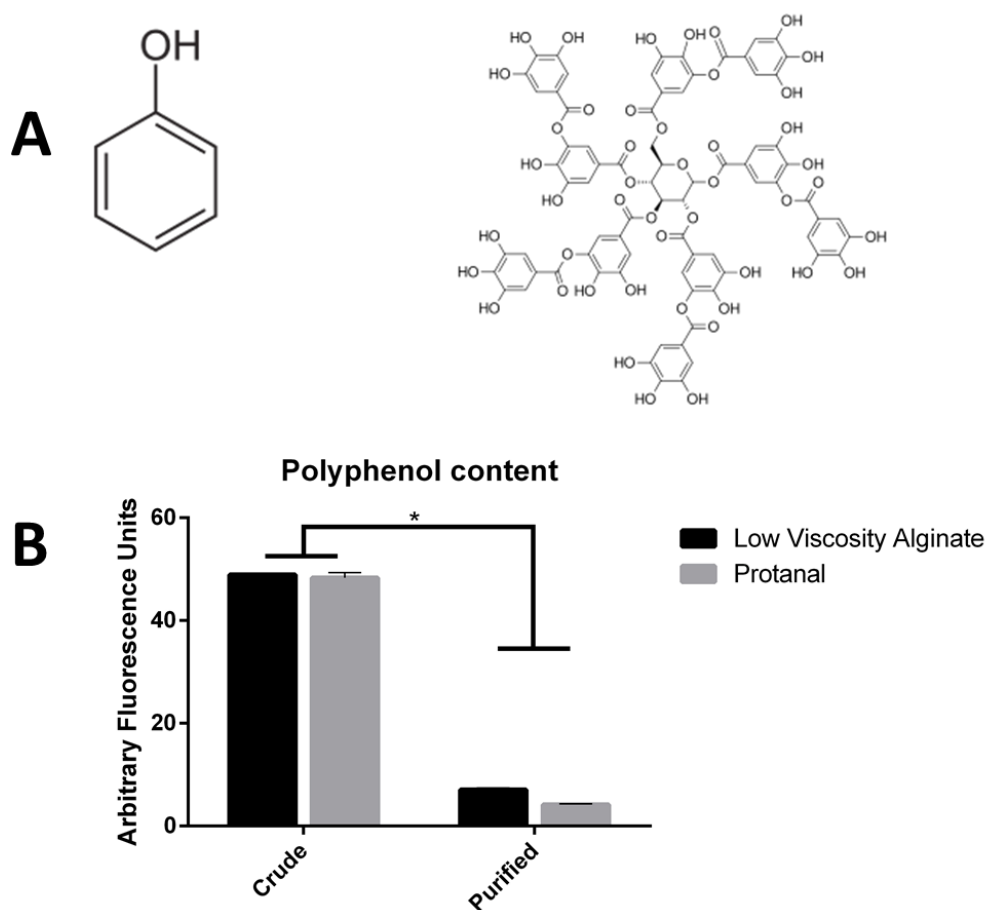


Figure 4.3: Alginate was tested for Polyphenol contaminants using a spectrofluorimeter. A: The chemical structures of a phenol and tannic acid, an example of a polyphenol. Phenols are the structural units that can be found in multitude in polyphenols. B: Proportional polyphenol contents of low viscosity alginate and Protanal alginate. *($p \leq 0.0001$; Error bar indicates +SD)

4.2.2.3. Endotoxin Contaminants

Endotoxins, also known as lipoglycans or lipopolysaccharides (Figure 4.4 A), are an integral part of the outer cell membrane of gram-negative bacteria.^[18] Their main structure consists of a hydrophobic domain known as lipid A, a nonrepeating “core” oligosaccharide and a distal polysaccharide (or O-antigen).^[3] Although endotoxins are only secreted in minute amounts during the normal life-cycle of a bacteria, they can be released in substantial amounts when the bacterial cell membrane is destroyed. Endotoxin contamination in biomaterials can have detrimental effects on the performance of the biomaterial, as even minute amounts of endotoxins can induce strong inflammatory reactions, which might overrule any biological effect of the biomaterial itself.^[19] The human immune system is capable of detecting endotoxins at a concentration less than 1 ng/ml.^[20] However, at larger amounts endotoxins can lead to septic shock, or even death by organ failure or intravascular coagulation.^[18]

The endotoxin content of the alginates was tested by using the *Limulus* Amebocyte Lysate (LAL) assay (Figure 4.4 B). For this assay a small amount of the alginate samples is mixed with a solution containing the proenzyme Factor C found in circulating amebocytes of the horseshoe crab *Limulus Polyphemus*. Endotoxins induce the proteolytic activities of the proenzyme. Endotoxin levels can then be measured by measuring the activity of protease of the enzyme on a synthetic peptide substrate that releases p-nitroaniline (pNA) after proteolysis. The yellow colour produced by pNA can be measured by reading the absorbance at 405 nm using a plate reader.^[21] This assay measures the endotoxins in endotoxin units (EU). As endotoxins can differ in their biological activity, using this standardized form gives us a better mode of comparison than when a unit based on weight would be used. Two endotoxins of the same weight can have very different pyrogenic activity, and two endotoxins of the same pyrogenic activity could differ widely in shape and weight.^[22, 23]

For the Protanal alginate an average of 974620 EU endotoxins per gram alginate was found before purification, which was reduced to 78.31 EU endotoxins after purification. An average of 68.60 EU endotoxins per gram purified Low Viscosity alginate was found, while this was 1139337 EU endotoxins per gram crude alginate. This is an endotoxin reduction of 99.99% (Figure 4.4 C), and comparable to the results of Klöck et al.^[7] However, Dusseault et al^[8] managed to create a final endotoxin content which is roughly a factor 10 less than what was measured in our purified alginate.

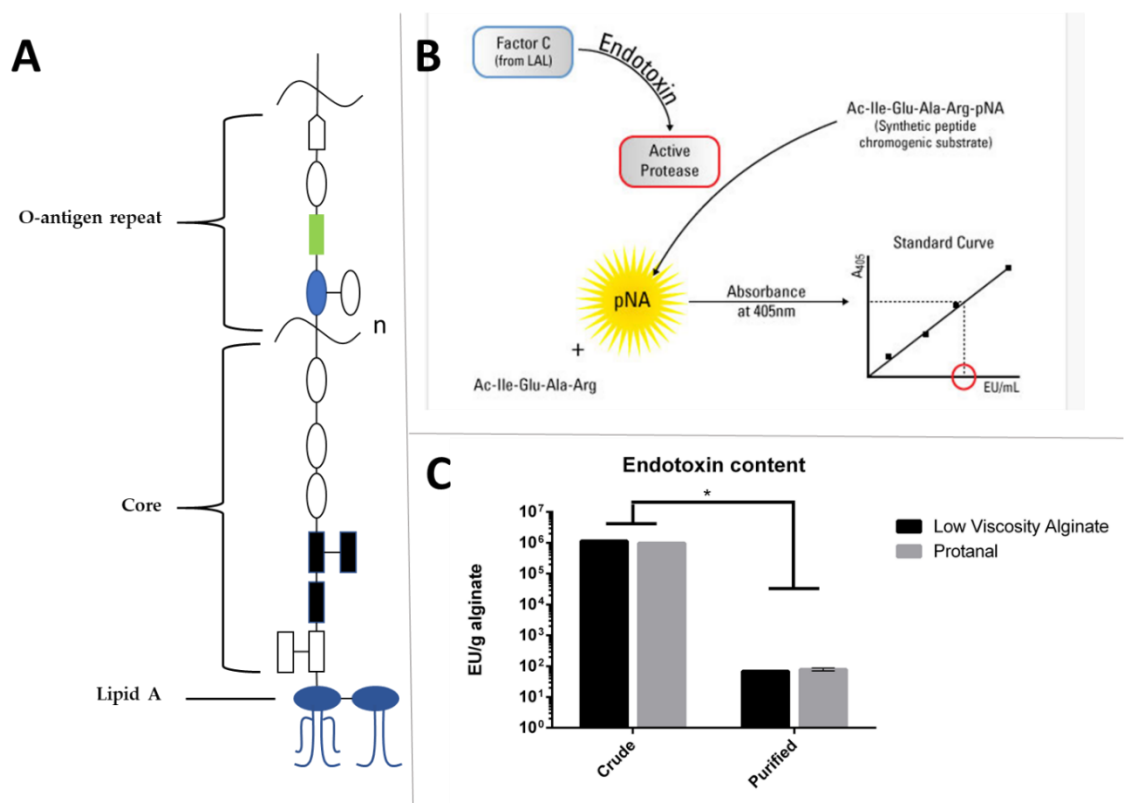


Figure 4.4: Alginate was tested for endotoxin contaminants using a LAL assay. A: A schematic representation of the structure of endotoxins, or lipopolysaccharides, modified from Raetz et al.^[3] B: The LAL assay utilizes the endotoxin mediated activation of the factor C enzyme, which then acts as a protease, cleaving a synthetic peptide to release pNA, which yellow colour can be measured using a plate reader. C: Endotoxin content of low viscosity alginate and Protanal alginate was measured before and after purification (logarithmic scale). *($p < 0.0001$; Error bar indicates +SD)

4.2.3. Viscosity

The viscosity of the alginate solutions was also measured pre- and post-purification using a viscosity cup. Viscosity has a role in the morphology and size of the encapsulation formed,^[24, 25] and the morphology and size are in turn parameters that have an influence on the development of immune reactions.^[26, 27]

In Table 4.2 it is shown that the viscosity of purified alginates is slightly increased due to the purification protocol. It is hypothesized that this could be due to the loss of smaller molecular weight strands of alginate, increasing the average molecular weight of the alginate and thereby increasing the viscosity.

Table 5.2: Viscosity of alginates (low viscosity alginate or Protanal) pre- and post-purification in millipascal seconds

	Pre-purification	Post-purification
Low viscosity alginate	8.5 ± 0.13 mPa·s	8.7 ± 0.35 mPa·s
Protanal	32.6 ± 0.12 mPa·s	33.2 ± 0.25 mPa·s

4.3. Measuring Permeability Using Confocal Microscopy

The purified alginate will be used to encapsulate islets of Langerhans and potentially protect them from the immune system. The encapsulation must prevent antibodies (150,000 MW)^[11] and white blood cells (7-30 µm)^[12] from reaching the transplanted cells.^[13] However, small molecules, like oxygen, insulin (5,734 MW)^[14] and glucose (180 MW),^[15] should still be able to diffuse through the barrier, to maintain the islets viability and function. To measure the permeability of the alginate beads, beads were incubated in solutions with different sized fluorescent coupled dextran molecules. Dextran molecules with an average molecular weight of 4,400, 40,000, 150,000 and 500,000 were chosen to cover the sizes of our molecules of interest.

The type of crosslinking cations, the concentration of the gelling bath, the concentration of alginate and whether or not the alginate was purified were parameters that were investigated to determine their influence on the permeability.

Over a period of 20 minutes the fluorescent signal from within the alginate beads was measured using a confocal microscope and normalized as a percentage of background fluorescence. This method allowed us to monitor diffusion of the different sized fluorescent molecules into the beads in real time (Figure 2.5). At the lowest dextran size (4,400 MW) it was very hard to distinguish the beads from the background (Figure 2.5 C). It is hypothesized that this is because during the (gentle) mixing process of the beads with the fluorescent dye, the dye has already penetrated the beads. By the time the beads are put under the microscope, there is almost no distinguishable difference. DIC microscope images were used to find the beads on the microscope (Figure 2.5 A), and to ensure that beads stayed in focus during the entire imaging process.

Dextran molecules with a molecular weight of 40,000 gave the most variability during measurements. They were able to penetrate 1% alginate beads crosslinked with CaCl_2 and SrCl_2 , and 2% alginate beads crosslinked with CaCl_2 , as can be seen by the increase of fluorescence over time (Figure 4.5). BaCl_2 crosslinked beads didn't allow penetration of the dye at either concentration. For the largest 2 molecules (150,000 MW and 500,000 MW) none of the beads were penetrated within the 20-minute time frame of measurement. These results show that both the concentration of the alginate, and the divalent cation used to crosslink it, have an influence on the porosity of the alginate beads.

After performing these experiments with crude alginate, the experiment was repeated with 1% alginate beads made from the purified alginate. Once again, the smallest dextran molecules were able to penetrate all the beads, however the 40,000 MW dextran molecules

could only penetrate the SrCl_2 crosslinked alginate beads (Figure 4.5 and Table 4.3). It is hypothesized that by removing the impurities during the purification, the alginate has a chance to crosslink in a tighter knit, as there are no impurities to prevent this from happening. Furthermore, if the average molecular weight is increased due to the purifications, as indicated by the increase in viscosity, this could also have an influence on the permeability.

Based on these results, a BaCl_2 solution seems to be the preferred crosslinking bath for the clinical encapsulation of islets of Langerhans, as it seems to have the lowest permeability, keeping out the immune system, while still allowing nutrients and insulin to pass the barrier. Furthermore, alginates crosslinked with BaCl_2 have better mechanical properties^[28, 29] and a longer survival rate after implantation.^[29] However, as BaCl_2 is toxic at high concentrations,^[30] the concentration used for the crosslinking bath needed to be as low as possible. 1% Protanal alginate beads were sprayed in to 25 mM BaCl_2 gelling baths, with or without 112.5 mM NaCl to make the bath isotonic. These beads were then tested for their porosity. It was found there was no difference in the porosity compared to the 100 mM BaCl_2 baths (Figure 4.5 and Table 4.3), and there was no noticeable difference between the gelling baths with or without the 112.5 mM NaCl, indicating that using an isotonic bath will not negatively influence the pore-size of the alginate.

This method of measuring gives us an approximation of the permeability of alginate hydrogels. Furthermore, this method allows for kinetic measurements, measuring the diffusion of the fluorescent markers over time and in spatial difference. To illustrate this, the fluorescent signal within a single bead was measured at three different locations; at the edge of the bead, a bit more to the centre and completely in the centre (Figure 4.6). The bead was created using 1% purified Protanal alginate, crosslinked with 100 mM CaCl_2 (Dextran size 40.000 MW). Not only can it be seen that the fluorescent signal goes up in different parts of

the bead at different time points, the speed at which the signal increases can also be measured per location. To do this, the slope at the parts where the fluorescence increases was calculated ($\text{slope} = \Delta Y / \Delta X$), and used to create the trendlines (Figure 4.6 B). Slopes of 0.102 (edge), 0.111 (middle) and 0.124 (centre) were found, indicating the fluorescent signal increased faster in the centre than it did at the edge. This implies that the diffusion speed of the fluorescent molecules is higher in the centre than it is at the edge. This is consistent with other research showing that alginate beads can be crosslinked non-uniformly, with a more crosslinked “shell” and a more fluid centre.^[31-33]

In this section the method of using fluorescent-labelled molecules to measure permeability has been used. This method allows for a kinetic, spatial measurement of the permeability of alginate beads, in physiological conditions. However, the fluorescent markers used in this research (dextran molecules) are linear in structure, whereas biomolecules are usually highly folded molecules with smaller dimensions. Therefore, molecules with the same molecular weight as the dextran molecules used, can have smaller dimensions and pass through the alginate, while the dextran could not. Better estimates could be made by using other fluorescent molecules, such as fluorescently tagged proteins, although that might be more expensive. In this research, it was found that larger molecules (>40,000 MW) can be kept out of the alginate beads when using the right crosslinking bath, but smaller molecules (<4,000 MW) can easily pass the barrier. This seems to imply that islets can be shielded from the immune system (cells and antibodies) without interfering with the uptake of nutrients or the secretion of insulin.

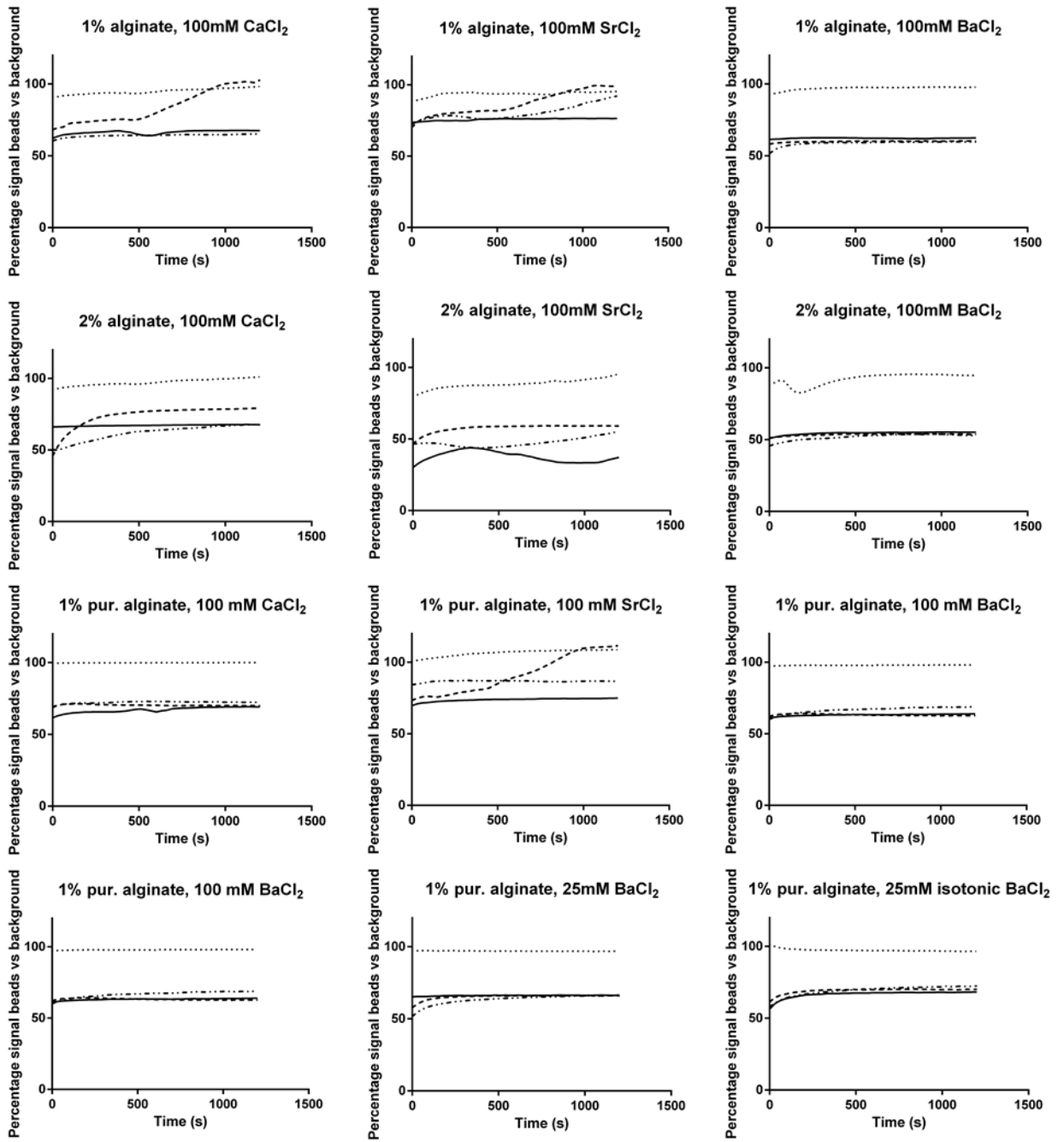



Figure 4 5: Percentage of average fluorescent signal within the area of beads versus the background signal.

Top row: difference between different crosslinking cations, for 1 percent alginate beads. 2nd row: difference between different crosslinking cations, for 2 percent alginate beads. 3rd row: difference between different crosslinking cations, for 1 percent purified alginate. Bottom row: difference between different concentrations of BaCl₂ crosslinking baths, for 1 percent purified alginate



	4,400 MW	40,000 MW	150,000 MW	500,000 MW
1% Alginate				
<i>CaCl₂</i>	++	++	-	-
<i>SrCl₂</i>	++	++	++	-
<i>BaCl₂</i>	++	-	-	-
2% Alginate				
<i>CaCl₂</i>	++	+	-	-
<i>SrCl₂</i>	++	-	-	-
<i>BaCl₂</i>	++	-	-	-
1% Purified Alginate				
<i>CaCl₂</i>	++	-	-	-
<i>SrCl₂</i>	++	++	-	-
<i>BaCl₂</i>	++	-	-	-
1% Purified Alginate				
100 mM <i>BaCl₂</i>	++	-	-	-
25 mM <i>BaCl₂</i>	++	-	-	-
25 mM Isotonic <i>BaCl₂</i>	++	-	-	-

Table 4.3: Overview table for the penetrations of different sized fluorescent dextran molecules into alginate beads within 20 minutes. ++: dye completely penetrated the bead within 20 minutes. +: Semi permeable. A definite difference in signal was noticeable, but beads didn't completely disappear within 20 minutes. - :No penetrations of the dye into the bead within 20 minutes.

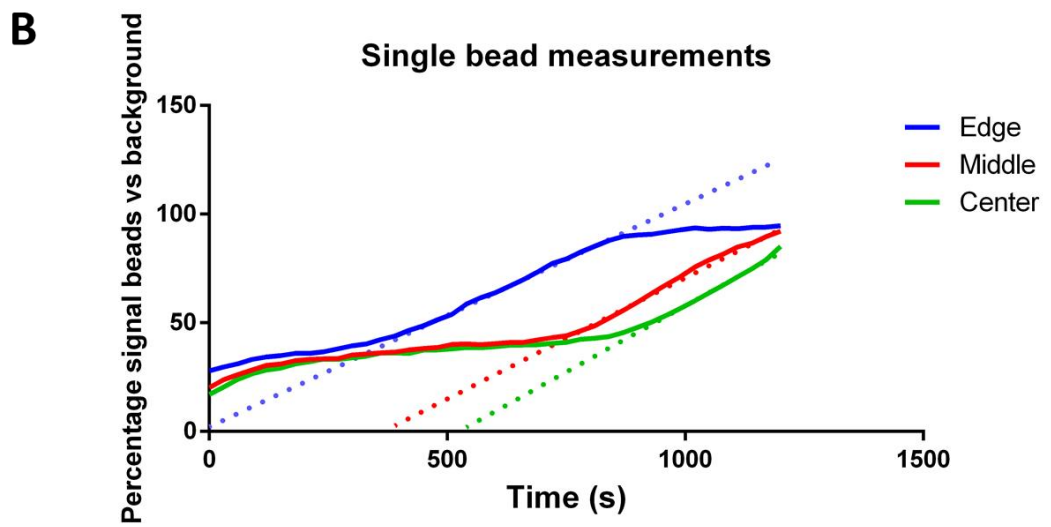
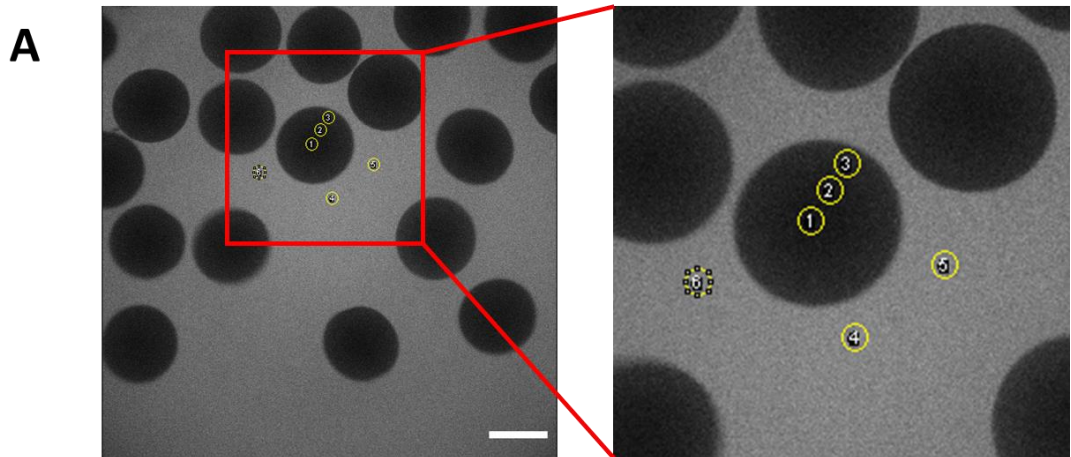


Figure 4.6: The fluorescent measurement technique allows for the kinetic analysis of the diffusion speed of fluorescent labelled molecules into an alginate bead. A: The fluorescent signal was measured at three places within one bead, the centre, the edge, and in between (middle). B: Percentage of fluorescent signal within the different areas of the bead versus the background signal. Dotted lines are indicating the slope at which the signal increases.

4.4. Antibody Resistance

Using the fluorescent dextran molecules gives a good indication for the permeability of the alginate hydrogels. However, knowing whether real antibodies can penetrate the alginate beads is of more interest. ADSC aggregates, fluorescently tagged with DII, were suspended in 1% Purified Protanal alginate and encapsulated by spraying the suspension in a 25mM isotonic BaCl₂ gelling bath at 5 ml/h through a 30G needle with a 7 kV voltage. Encapsulated ADSC aggregates were then incubated in medium containing 10 µg/ml Alexa-488 conjugated Rabbit Anti-Human IgM for 20 minutes, 2 hours, 24 hours or 7 days before washing them with PBS and checking for fluorescence using confocal microscopy. As a control, non-encapsulated aggregates cultured on ultra-low adhesion plates were used. Aggregates without any encapsulation started to aggregate even further, forming larger structures. Without the encapsulation, the antibodies could easily reach the aggregates, and stain them (Figure 4.7). However, the encapsulation managed to delay the antibody attachment in the majority of the beads, with green fluorescent signal on the aggregates not being apparent until after 7 days of incubation, but even then the green fluorescence of the antibodies was not as bright on the encapsulated aggregates as it was on the aggregates without encapsulation. This shows that even though the encapsulations are not a complete safe guard against antibodies, it does slow them down.

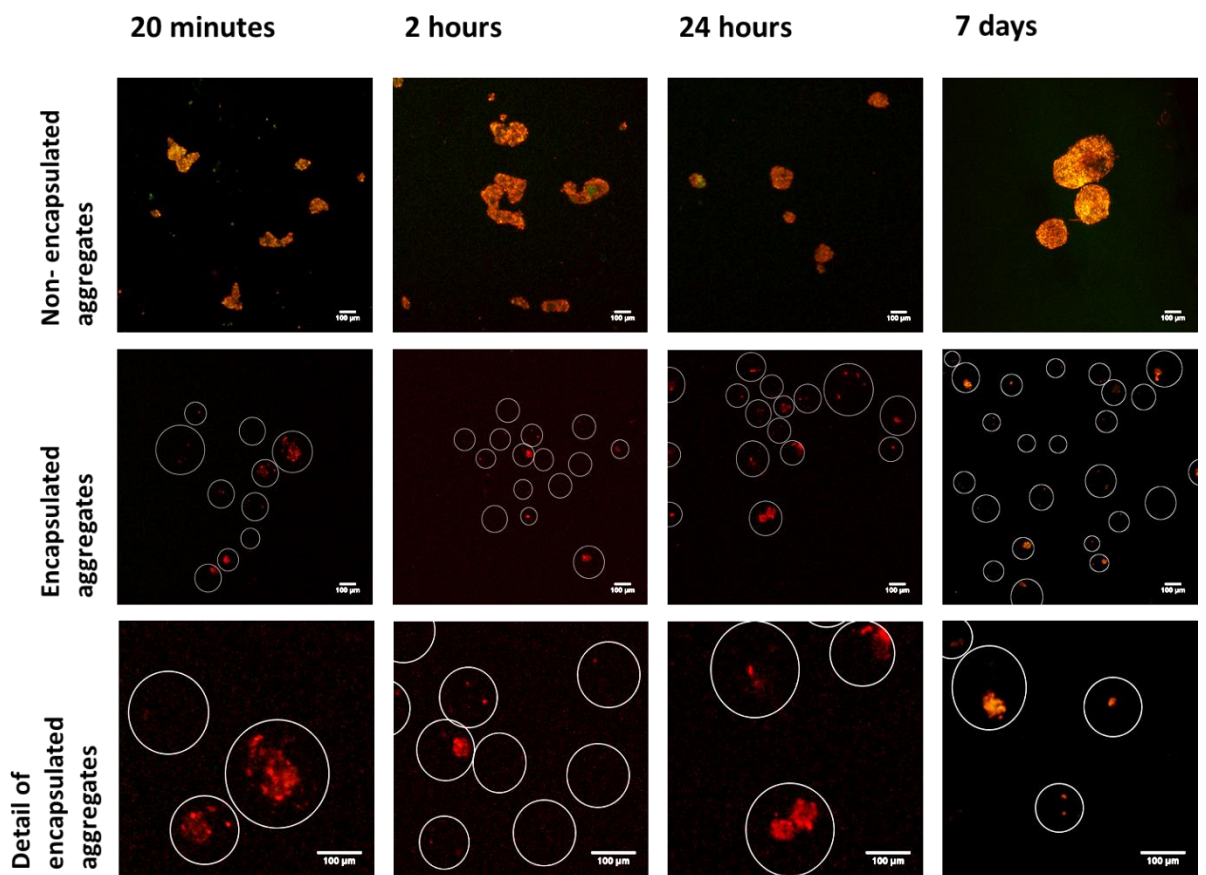


Figure 4.7: ADSC aggregates incubated with IGM antibodies (green) for 20 minutes, 2 hours, 24 hours or 7 days, with or without encapsulation. CellTracker CM-Dil (red) was used to make the ADSC aggregates red fluorescent. A clear overlap (yellow/orange) from the green IGM antibodies can be seen on the red ADSC's for all time points with non-encapsulated aggregates, implying that the antibodies can attach to the aggregates without any problem. However, for the encapsulated aggregates this overlap is not clear until 7 days of incubation.

4.5. Conclusion

In this chapter a novel, faster way to purify alginate is presented, based on the work of Klöck et al.^[7] It was shown that this purification method can remove up to 68% of the protein contaminants, 90% of the poly-phenol contaminants and 99.99% of the endotoxins, in only 20% of the time used by the original protocol. Furthermore, the permeability and immunoprotective properties of this alginate have been investigated. This chapter showed a systematic method of investigating the permeability of hydrogels, which is important for immunoprotection and for biofabrication purposes. The permeability of alginate hydrogels could be fine-tuned by focusing on the used crosslinking bath, the concentration of the alginate solution and the removal (or addition) of impurities. It was shown that BaCl₂ solutions provided the lowest permeability, although the concentration of the BaCl₂ solution did not make a huge difference. The alginate encapsulation managed to keep antibodies away from ADSC aggregates for at least short while. This research provides further promising results for the use of alginate as an immunoprotective material for clinical islet transplantation. Being able to fine tune the permeability of hydrogels is not only of importance for immunoprotection, but also for biofabrication and 3D cell cultures. If not all nutrients/hormones/growth factors can reach a cell culture within the hydrogel, the cells might not develop the way they were intended to. For instance, when trying to differentiate stem cells within alginate,^[34] it must be ensured that the chemical cues can reach the cells. The benefits of a higher permeability in hydrogels has already been shown by Armstrong *et al.*^[16] who used sacrificial Pluronic in their alginate hydrogels to create micron-sized pores. The method of measuring the permeability in this chapter can be a very useful tool for researchers investigating both biofabrication and immunoprotection, as it allows for a kinetic and spatial measurement of diffusion.

4.6. References

- [1]. Fadnavis NW, Sheelu G, Kumar BM, Bhalerao MU, Deshpande AA. Gelatin Blends with Alginate: Gels for Lipase Immobilization and Purification. *Biotechnology Progress*. **2003**;19(2):557-64.
- [2]. Scientific TF, *Chemistry of Protein Assays*, <https://www.thermofisher.com/uk/en/home/life-science/protein-biology/protein-biology-learning-center/protein-biology-resource-library/pierce-protein-methods/chemistry-protein-assays.html>,
- [3]. Raetz CRH, Whitfield C. Lipopolysaccharide Endotoxins. *Annual Review of Biochemistry*. **2002**;71(1):635-700.
- [4]. Mørch YA, Donati I, Strand BL. Effect of Ca²⁺, Ba²⁺, and Sr²⁺ on Alginate Microbeads. *Biomacromolecules*. **2006**;7(5):1471-80.
- [5]. Somo SI, Langert K, Yang C-Y, Vaicik MK, Ibarra V, Appel AA, *et al.* Synthesis and evaluation of dual crosslinked alginate microbeads. *Acta Biomaterialia*. **2018**;65:53-65.
- [6]. De Vos P, De Haan B, Wolters G, Strubbe J, Van Schilfgaarde R. Improved biocompatibility but limited graft survival after purification of alginate for microencapsulation of pancreatic islets. *Diabetologia*. **1997**;40(3):262-70.
- [7]. Klöck G, Frank H, Houben R, Zekorn T, Horcher A, Siebers U, *et al.* Production of purified alginates suitable for use in immunisolated transplantation. *Applied Microbiology and Biotechnology*. **1994**;40(5):638-43.
- [8]. Dusseault J, Tam SK, Menard M, Polizu S, Jourdan G, Yahia L, *et al.* Evaluation of alginate purification methods: effect on polyphenol, endotoxin, and protein contamination. *Journal of Biomedical Materials Research, Part A*. **2006**;76(2):243-51.
- [9]. Mallett AG, Korbitt GS. Alginate modification improves long-term survival and function of transplanted encapsulated islets. *Tissue Engineering Part A*. **2009**;15(6):1301-9.
- [10]. Kukreja A, Cost G, Marker J, Zhang C, Sun Z, Lin-Su K, *et al.* Multiple immunoregulatory defects in type-1 diabetes. *J Clin Invest*. **2002**;109(1):131-40.
- [11]. Janeway Jr CA, Travers P, Walport M, Shlomchik MJ. The structure of a typical antibody molecule. *Immunobiology: The immune system in Health and Disease* 5th edition **2001**.
- [12]. Wheater PR, Burkitt HG, Daniels VG. Functional histology. A text and colour atlas **1979**.
- [13]. Beck J, Angus R, Madsen B, Britt D, Vernon B, Nguyen KT. Islet encapsulation: strategies to enhance islet cell functions. *Tissue Engineering*. **2007**;13(3):589-99.
- [14]. Information. NCfB, *PubChem Compound Database*; CID=16131099, <https://pubchem.ncbi.nlm.nih.gov/compound/16131099>, March **2018**
- [15]. Information. NCfB, *PubChem Compound Database*; CID=79025,, <https://pubchem.ncbi.nlm.nih.gov/compound/79025> March **2018**

- [16]. Armstrong JPK, Burke M, Carter BM, Davis SA, Perriman AW. 3D Bioprinting Using a Templated Porous Bioink. *Advanced Healthcare Materials*. **2016**;5(14):1724-30.
- [17]. Skjåk-Bræk G, Murano E, Paoletti S. Alginate as immobilization material. II: Determination of polyphenol contaminants by fluorescence spectroscopy, and evaluation of methods for their removal. *Biotechnology and Bioengineering*. **1989**;33(1):90-4.
- [18]. Caroff M, Karibian D. Structure of bacterial lipopolysaccharides. *Carbohydrate research*. **2003**;338(23):2431-47.
- [19]. Lieder R, Petersen PH, Sigurjonsson OE. Endotoxins-the invisible companion in biomaterials research. *Tissue Eng Part B Rev*. **2013**;19(5):391-402.
- [20]. Miyake K. Endotoxin recognition molecules, Toll-like receptor 4-MD-2. *Seminars in Immunology*. **2004**;16(1):11-6.
- [21]. Scientific TF, *Pierce™ LAL Chromogenic Endotoxin Quantitation Kit*, https://www.thermofisher.com/order/catalog/product/88282?gclid=CjwKCAjw8uLcBRACEiwAaL6MSbtHADLOkN7QE9bBIRW8LnUMs0V3GBV4Pj4sU-CDAwPvS8R7n5XchxoCygAQAvD_BwE&s_kwcid=AL13652!3!284360268903!b!!g!!%2Bendotoxin%20%2Bkit&ef_id=WnYMMQAAHYLklHa:20180912113959:s,
- [22]. Poole S, Dawson P, Gaines Das RE. Second international standard for endotoxin: calibration in an international collaborative study. *Journal of Endotoxin Research*. **1997**;4(3):221-31.
- [23]. Michael E. Dawson PD. Harmonization of Endotoxin Standards and Units. 1997 December 1997.
- [24]. Hallé J-P, Leblond FA, Pariseau J-F, Jutras P, Brabant M-J, Lepage Y. Studies on Small (<300 µm) Microcapsules: II — Parameters Governing the Production of Alginate Beads by High Voltage Electrostatic Pulses. *Cell Transplantation*. **1994**;3(5):365-72.
- [25]. Shi P, He P, Teh TKH, Morsi YS, Goh JCH. Parametric analysis of shape changes of alginate beads. *Powder Technology*. **2011**;210(1):60-6.
- [26]. De Vos P, De Haan B, Pater J, Van Schilfgaarde R. Association between capsule diameter, adequacy of encapsulation, and survival of microencapsulated rat islet allografts. *Transplantation*. **1996**;62(7):893-9.
- [27]. Veisoh O, Doloff JC, Ma M, Vegas AJ, Tam HH, Bader Andrew R, *et al*. Size- and shape-dependent foreign body immune response to materials implanted in rodents and non-human primates. *Nature Materials*. **2015**;14:643.
- [28]. Haug A, Smidsrød O. The effect of divalent metals on the properties of alginate solutions. *Acta Chemica Scandinavica*. **1965**;19(2):341-51.
- [29]. Atabak Ghanizadeh T, Miguel AH, Nicholas RL, Wenmiao S. Three-dimensional bioprinting of complex cell laden alginate hydrogel structures. *Biofabrication*. **2015**;7(4):045012.

- [30]. Cano-Abad MaF, García AG, Sánchez-García P, López MG. Ba²⁺-induced chromaffin cell death: cytoprotection by Ca²⁺ channel antagonists. *European Journal of Pharmacology*. **2000**;402(1):19-29.
- [31]. Thu B, Gåserød O, Paus D, Mikkelsen A, Skjåk-Bræk G, Toffanin R, *et al.* Inhomogeneous alginate gel spheres: An assessment of the polymer gradients by synchrotron radiation-induced x-ray emission, magnetic resonance microimaging, and mathematical modeling. *Biopolymers*. **2000**;53(1):60-71.
- [32]. Zimmermann H, Wahlisch F, Baier C, Westhoff M, Reuss R, Zimmermann D, *et al.* Physical and biological properties of barium cross-linked alginate membranes. *Biomaterials*. **2007**;28(7):1327-45.
- [33]. Uludag H, De Vos P, Tresco PA. Technology of mammalian cell encapsulation. *Advanced Drug Delivery Reviews*. **2000**;42(1-2):29-64.
- [34]. Faulkner-Jones A, Fyfe C, Cornelissen DJ, Gardner J, King J, Courtney A, *et al.* Bioprinting of human pluripotent stem cells and their directed differentiation into hepatocyte-like cells for the generation of mini-livers in 3D. *Biofabrication*. **2015**;7(4):044102.

Chapter 5

One-step Encapsulated Organoid Formation

5.1. Introduction

One of the main problems of islet encapsulation is that the islets can't be vascularized after transplantation. This means that bigger islets get a necrotic core due to the lack of nutrition,^[1] which in turn can lead to the release of danger associated molecular pattern molecules which can set off the immune system. It is found that islets smaller than 150 μm do not suffer from that problem.^[2] However, if only smaller islets would be transplanted, a large portion of donated islets could not be used, as islets come in a large variety of sizes, ranging from 50 to 350 μm .^[3] Furthermore, it is known that smaller islets produce roughly the same amount of insulin per islet in reaction to an increase of glucose as larger islets.^[4] Therefore, when starting this research, the idea to break apart islets and re-aggregate them in smaller islets for encapsulation was conceived. As just breaking islets apart to re-aggregate them has been done before,^[5] a one-step process where the islets were allowed to re-aggregate after encapsulation was investigated, so there would be less time lost between taking the islets from the donor and transplanting them. The idea was to create a coaxial bead with a solid alginate hydrogel shell, which would act as the encapsulation, but a liquid core, which would allow cell aggregation (Figure 5.1). The coaxial beads would allow the cells to aggregate in-situ, for instance after transplantation. This would highly shorten the time needed between islet isolation and transplantation.

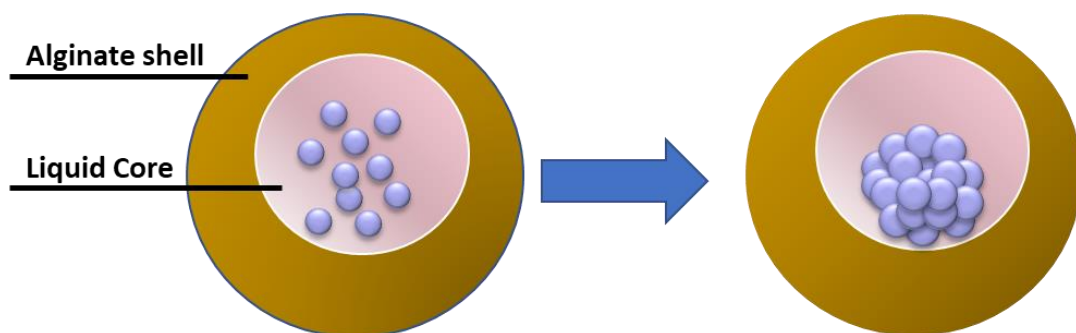


Figure 5.1 A schematic overview of the core-shell encapsulation idea. Cells will be in a liquid core, which will allow them to aggregate after encapsulation, while still being encapsulated in the alginate hydrogel.

In this chapter the one-step encapsulation and aggregation protocol is developed, which will be used on islets in chapter 6. HepaRG cells are used as a replacement for islet cells during the development phase, as islets were not readily available. HepaRG cells are known to aggregate readily^[6] and would therefore make a nice cell-line to develop the protocol. Furthermore, when this method would be used to create islet-like clusters from islet cells, up to 12.5% of hepatic cells could be added to increase the cell-volume, without influencing the function of the islet-like clusters.^[6] To test this, the HepaRG cells were already ordered and available for these experiments. Furthermore, HepaRG aggregates can be used for drug testing, as their function is close to physiological.^[7, 8] By creating encapsulated HepaRG aggregates the throughput of HepaRG-aggregate drug testing could be increased as they could be cultured in true 3D, instead of in a microwell system where there is still only a single layer of aggregates (Figure 5.2).

In this chapter the development of the coaxial encapsulation will be investigated, followed by the use of this system to create functional, encapsulated HepaRG aggregates that survive over a prolonged period of time.

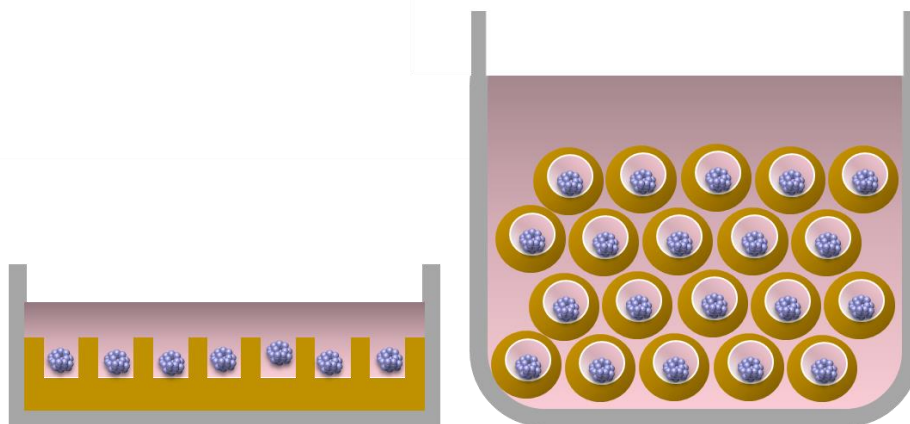


Figure 5.2 A schematic representation of the added value of encapsulating cells within the encapsulation (right) versus in a microwell system (left). When aggregates are formed within encapsulations, they can be cultured in true 3D, instead of a single layer of aggregates.

5.2. Coaxial Encapsulation

For the fabrication of coaxial encapsulations, a coaxial needle was used (Figure 5.3). This coaxial needle allows for dispensing two (different) materials through 2 different needles, aligned coaxially. In this case, the inner (core) material would be a material that would remain fluid while the outer (shell) material would be the alginate that will crosslink in the crosslinking bath to give the encapsulations its mechanical strength.

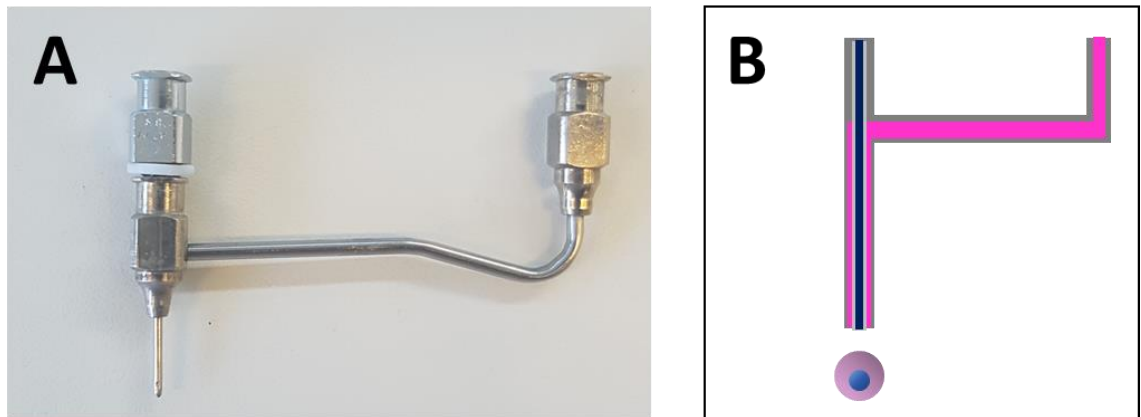


Figure 5.3 Coaxial needles were used to create coaxial encapsulations. A: An example of the coaxial needles used in this research. B: A schematic section of the coaxial needle.

5.2.1. Influence of Viscosity Difference on Bead Morphology

In the first few trials water was used as the core material and a 1.5% Protanal alginate solution as the shell material. Unfortunately, these turned out to create non spherical beads, that looked almost as if they had collapsed (Figure 5.4). To check if this was only due to the water as the core material, the experiment was repeated with using both 1.5% Protanal alginate as a core material, and 1.5% Protanal alginate as a shell material. The materials were extruded at speeds of 1 ml/h (core) and 5 ml/h (shell) through a 20-26G coaxial nozzle, at a distance of 1 cm to the 100 mM CaCl_2 bath, with an electric potential of 10 kV. This resulted in normal looking beads (Figure 5.4). To further investigate this, the inner material was increased from 0% to 2% Protanal alginate solutions, while maintaining the outer material at 1.5% (Figure 5.4). By comparing the morphology of the created beads, three different groups

can be determined. In the first group, where the concentration of the core material is much lower (0-0.6%) than that of the shell material, the beads look collapsed. The lower the concentration of the core material, the more collapsed the beads look. In the second group, where the beads core material concentration approximates the shell material (0.8-1.5%), nice beads are produced, with an increase in size when there is an increase of concentration of the core material. In the last group there are beads with a higher core concentration (1.6-2.0%) than that of the shell material. In this group, bigger beads have a higher variance in size.

From these results it was hypothesized that the interplay of viscosity between the core and shell material has an influence on the final morphology of the created beads. To further investigate this, it was decided to repeat the experiment on a smaller scale with a carboxymethyl cellulose (CMC) solution as the core material. CMC is a widely used material in the drug industry to increase viscosity, to stabilize emulsions or at higher concentrations even as a hydrogel base for applications and pastes.^[9] Since it does not crosslink in reaction to introduction of cations, it is perfect candidate to increase the viscosity of the core material while maintaining liquid after the alginate is crosslinked. Furthermore, after measuring the viscosity of CMC at different concentrations, it turned out that at lower concentrations (up to 1.5%) its viscosity profile is very similar to that of the Protanal alginate solutions (Figure 5.5). This made it easy to match the viscosity of the CMC core material to that of the Protanal alginate shell material by using the same concentration.

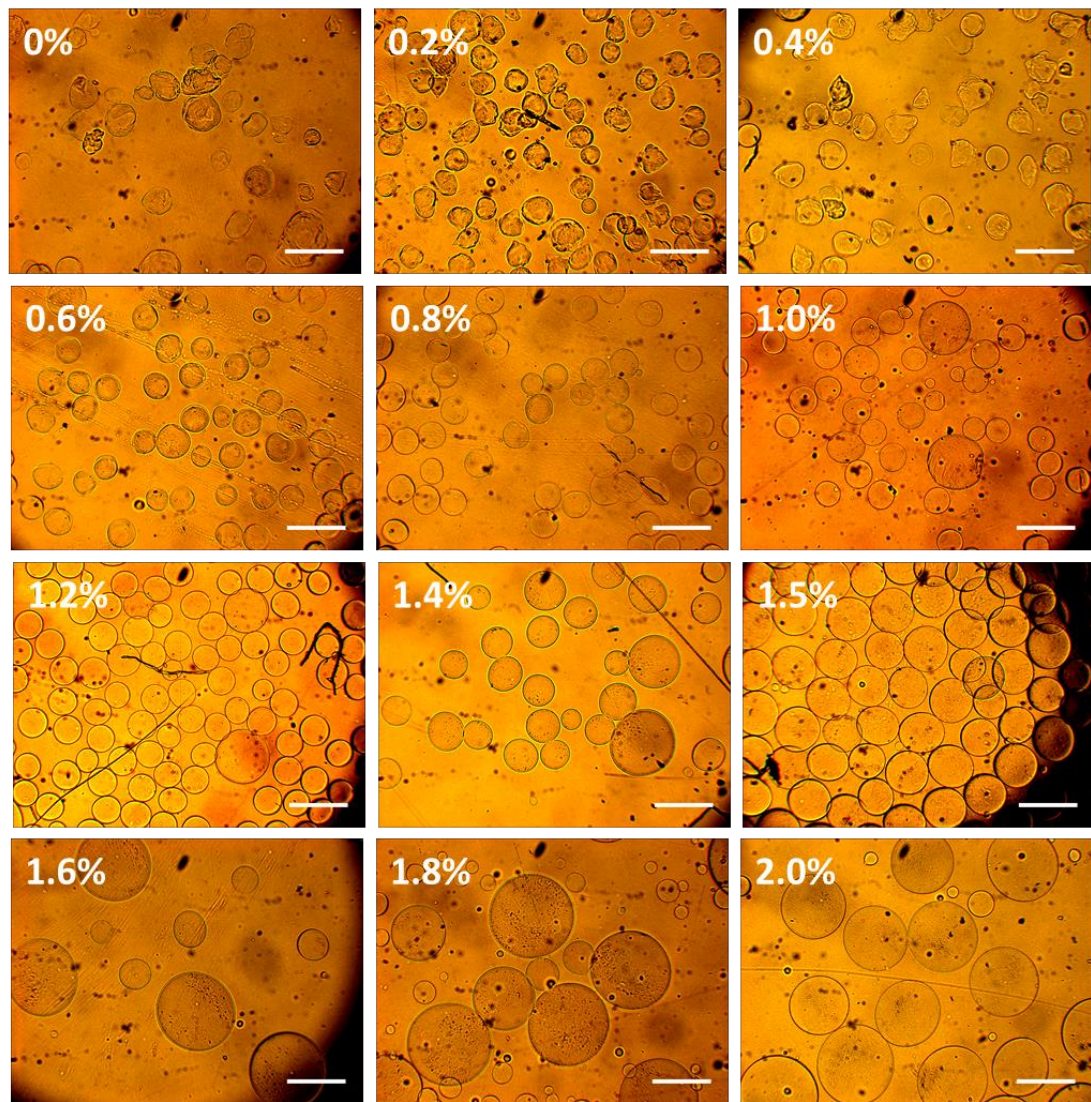


Figure 5.4: Microscopic pictures of beads created using the coaxial nozzle system. The shell material consisted out of 1,5% Protanal alginate, while the core material was altered from 0% Protanal alginate (water) to 2% alginate (annotated in the top left of each picture; Scalebar 500 μm)

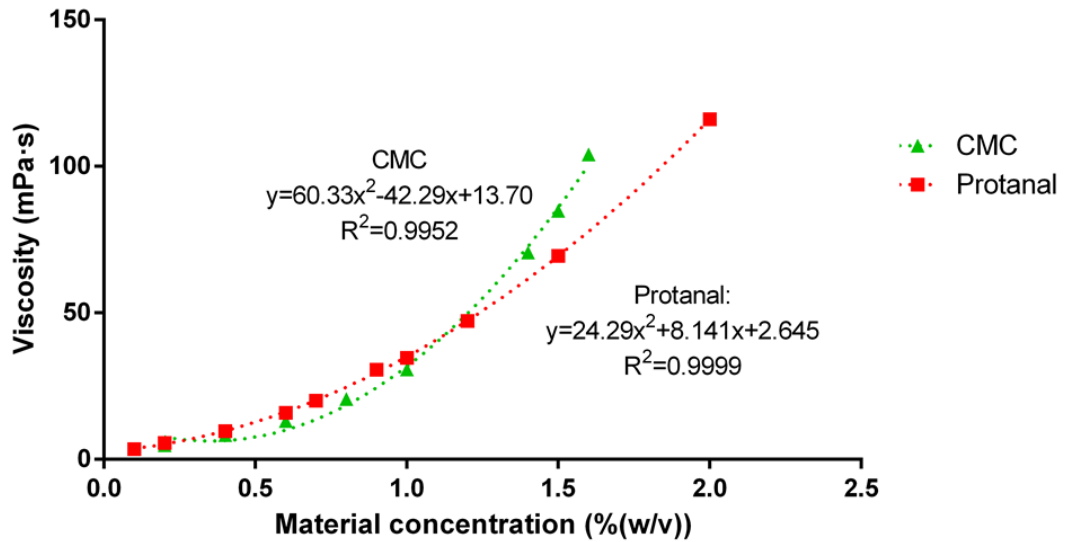


Figure 5.5: Viscosity of CMC and Protanal alginate plotted against the concentration. Trendlines are plotted in dotted lines. For both materials, viscosity increases exponentially with concentration.

The experiment with the different concentrations of core material was repeated on a smaller scale, with 0.5%, 1.5% or 2.5% CMC solutions as the core material and 1.5% Protanal alginate as the shell material, while maintaining the same printing parameters. The results are similar to those of the beads created with an alginate core and shell (Figure 5.6); a lower concentration in the core creates collapsed beads, a similar concentration creates relatively nice beads, and a higher concentration creates heterogeneous sized beads. Since there are 2 different materials used in this experiment, it is easier to determine the difference between the core and the shell. In Figure 5.6 C it can be seen that the smaller beads don't seem to have any core at all but appear to be fully made of alginate, which seems to indicate that at some points alginate beads dislodged from the dispensing needle without encapsulating any CMC material.

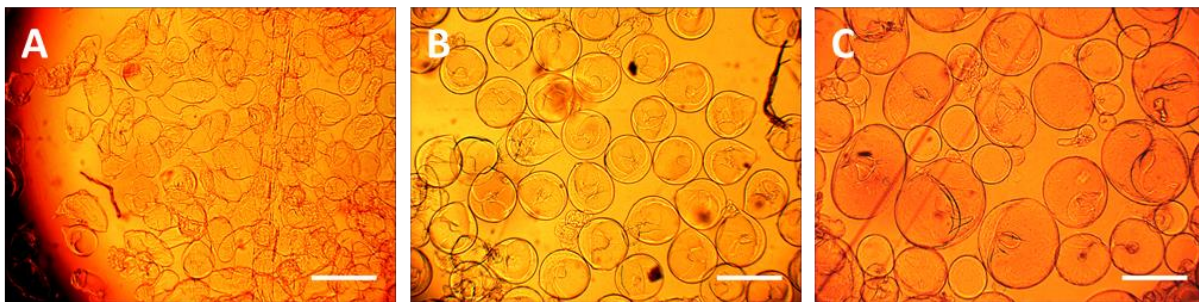


Figure 5.6: Microscopic pictures of CMC-Alginate core-shell beads. A: 0.5% CMC Core, 1.5% Protanal shell. B: 1.5% CMC Core, 1.5% Protanal shell. C: 2.5% CMC Core, 1.5% Protanal shell. (Scalebar 500 μm)

All the previous experiments were done with the same coaxial needle (20-26G needle), which produced bigger beads than what was aimed for. When trying out printing 1.5% CMC the same parameters with a smaller needle (21-28G coaxial needle) completely collapsed beads were formed (Figure 5.7 A). Even when lowering both the concentrations to 1%, where the viscosities match even better, the beads still didn't look spherical (Figure 5.7 B).

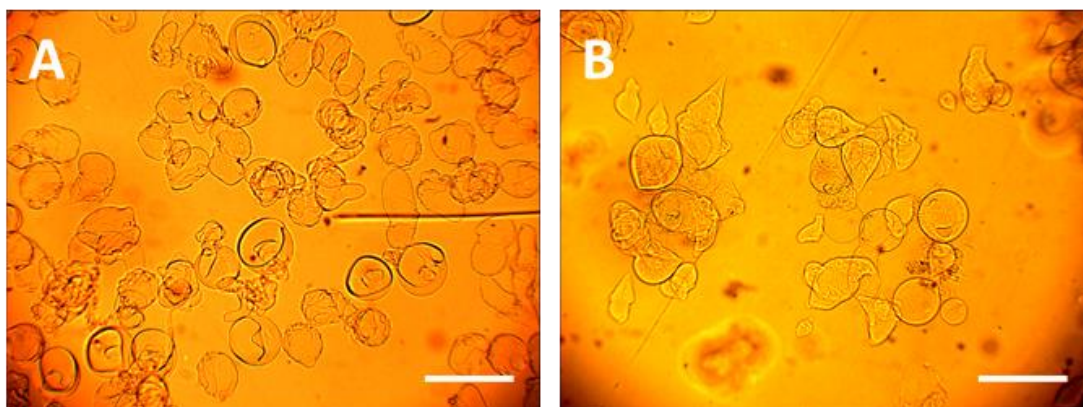


Figure 5.7 Coaxial beads fabricated through a 21-28G needle with the same parameters that worked for the 20-26G needle appeared very collapsed. A: 1.5% CMC core solution in 1.5% Protanal alginate shell solution. B: 1% CMC core solution in 1.5% Protanal shell solution. (Scalebar 500 μm)

By changing the needle size, the velocity at which the material comes out of the nozzle changed. So as an example, if a material is pushed at 1 ml/h out of a 26G needle (ID: 0.254 mm), it basically means that in an hour time, a cylinder with a volume of 1000 mm^3

and a diameter of 0.254 mm is produced. The speed is the same as the height of this cylinder per hour.

$$V = h \cdot \pi r^2 \qquad h = \frac{V}{\pi \cdot \left(\frac{1}{2}d\right)^2}$$

So for 1 ml/h through a 26g needle this would mean $1000/\pi(0.5 \cdot 0.254)^2 = 19735.25$ mm/h or 19.7 m/h.

To calculate the speed for the outer material, one additional step is needed to get the surface area of the needle. The surface that is taken in by the inner needle must be subtracted from the surface area from the outer needle. For the 20-26G needle, this would mean that the surface area (πr^2) from the inner 26G needle (OD: 0.457 mm, surface area 0.164 mm²) was subtracted from the surface area of the outer 20G needle (ID: 0.584 mm, surface area 0.268 mm²), to get an outer needle surface of 0.104 mm². At 5 ml/h, this would mean that the outer material comes out with a velocity of $5000/0.104 = 48153.26$ mm/h or 48.2 m/h, which is roughly 2.44 times as high as the inner material.

When the same calculations are done for a 21-28G needle, an inner speed of 40.2 m/h and an outer speed of 48.5 m/h are found. This means that with these speeds the outer material is only dispensed at 1.21 times the speed as the inner material, which might not be enough.

To further investigate the correlation between the speed differences and the morphology of the created beads, the 21-28G needle was used to create beads where the core material (1.5% CMC) was kept at 1 ml/h while the speed of the shell material (1.5% Protanal alginate) was increased from 5 ml/h to 15 ml/h and 25 ml/h. The distance to the 100 mM CaCl₂ gelling bath was kept at 1 cm, with an electric potential of 10 kV. While the beads with the 5 ml/h shell material once again created collapsed beads, the beads created with 15 ml/h and 25 ml/h shell material speed formed spherical beads (Figure 5.8). The beads created with

1-15 ml/h appeared to have a more spherical core compared to those created with 1-25 ml/h, where the core appeared to be more elongated. However, for some reason the 1-15 ml/h beads were bigger than the 1-25 ml/h beads. Another experiment with lower speeds for both the core and the shell material was performed with a maintained 1:15 ratio, printing at 0.33-5 ml/h (Figure 5.8 D). These were indeed smaller than before, which was to be expected with the results from chapter 3. Another way which was found in chapter 3 to make smaller beads is by decreasing the concentration of the materials used. Therefore another print was tried with 1% CMC and 1% Protanal alginate. For that print the extrusion rate for the shell was increased to 17 ml/h, in the hope that it would increase the wall size. (Figure 5.8 E). These beads turned out smaller, but with very nice cores and a visible shell.

When the speed ratio is looked at, the 1-17 ml/h for the 21-28G needle has a 4.10 speed ratio between the shell and core. To see if this higher speed ratio also works for other coaxial needles, the 19-26G needle was tried with 1-17 ml/h, which also gives it a 4.10 speed ratio. The resulting beads once again looked good, although a lot bigger than those of the 21-28G needle (Figure 5.8 F).

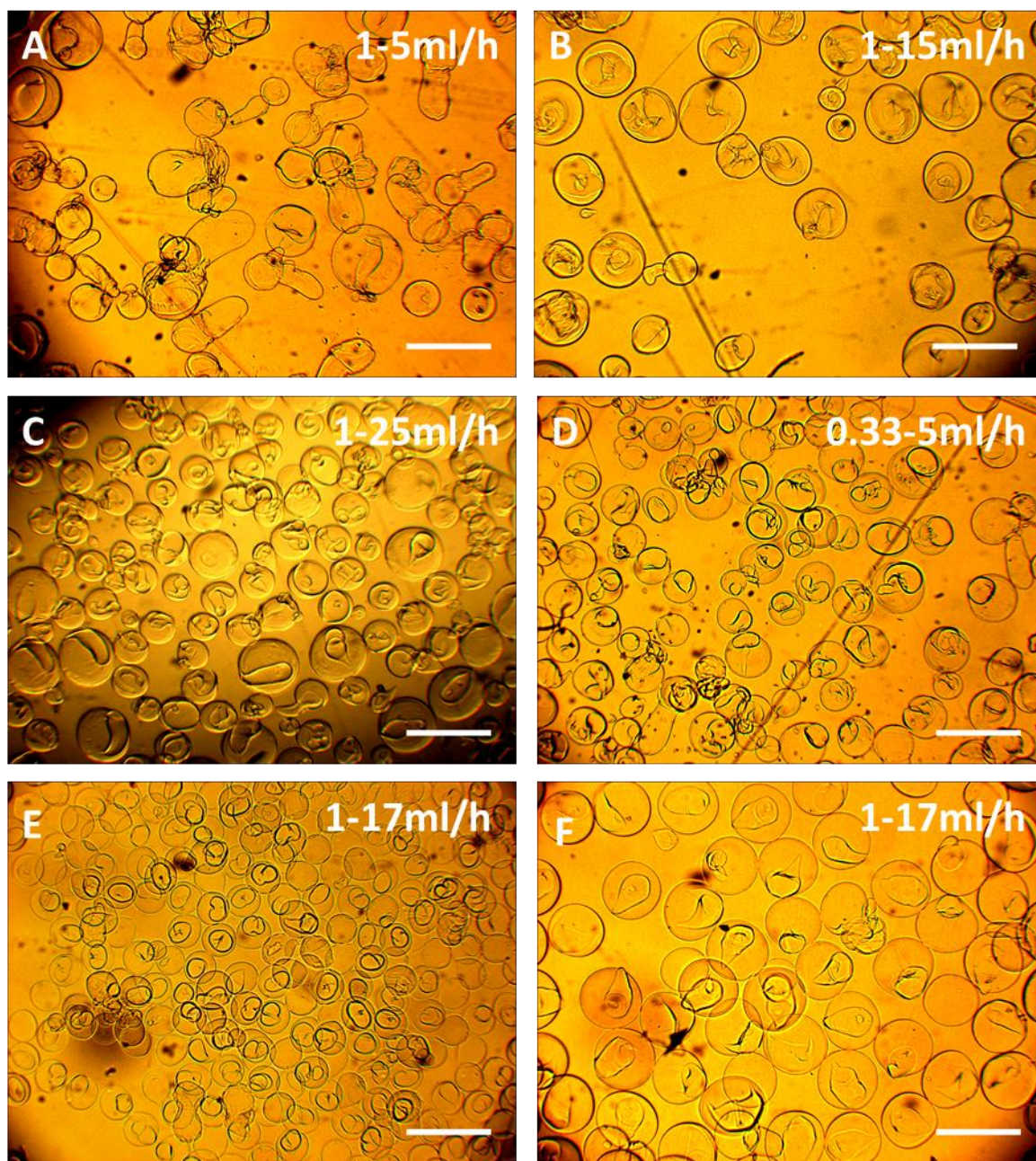


Figure 5.8 Microscopic pictures of coaxial printed beads. A-D and F: 1.5% CMC core solution in 1,5% Protanal alginate shell. E: 1.0% CMC solution in 1.0% Protanal alginate. A-E: Fabricated with a 21-28G needle. F: Fabricated with a 19-26G needle. Extrusion speeds (core speed-shell speed) are depicted in top right of each picture. (Scalebar 500 μm)

5.3. Coaxial Encapsulating HepaRG Cells

The idea of aggregating cells within the encapsulation was tested using HepaRG cells. In this section the details of the cell encapsulation, cell survival, morphology and function are described.

All cell printing was done in sterile conditions in a LAF-hood. The coaxial needle was sterilized by consecutively flushing it with 1% distel, 100% ethanol, 70% ethanol and twice with PBS, for 3 minutes each at a speed of 10 ml/h for both the core needle and the shell needle. HepaRG cells were printed at a concentration of $10 \cdot 10^6$ cells/ml in a 1.2% CMC solution (dissolved in embryo transfer water) as the core material. Purified Protanal alginate at a concentration of 1.2% (dissolved in embryo transfer water) was chosen as the shell material. The encapsulation of the HepaRG cells was done at a distance of 2 cm to the 25 mM isotonic BaCl_2 gelling bath, through the 19-26G coaxial needle with an electric potential of 10 kV. The core speed was set to 1 ml/h and the shell speed to 17 ml/h. All solutions were prewarmed in an incubator to 37° C before usage. Alginate was allowed to crosslink for roughly 10 minutes before removing the beads from the gelling bath using a 40 μm cell strainer and washing them 3x with PBS and dividing the beads over the wells of a 6 well plate and adding fresh, prewarmed HepaRG medium. The beads were very heterogenous in size, ranging from $\pm 300 \mu\text{m}$ to $\pm 800 \mu\text{m}$ in size. During the third repeat of this experiment, the bead size was more homogenous ($\pm 350\text{-}500 \mu\text{m}$; Figure 5.9), but there is no clear reason why. Beads were cultured in HepaRG medium, changing the medium 3 times a week.

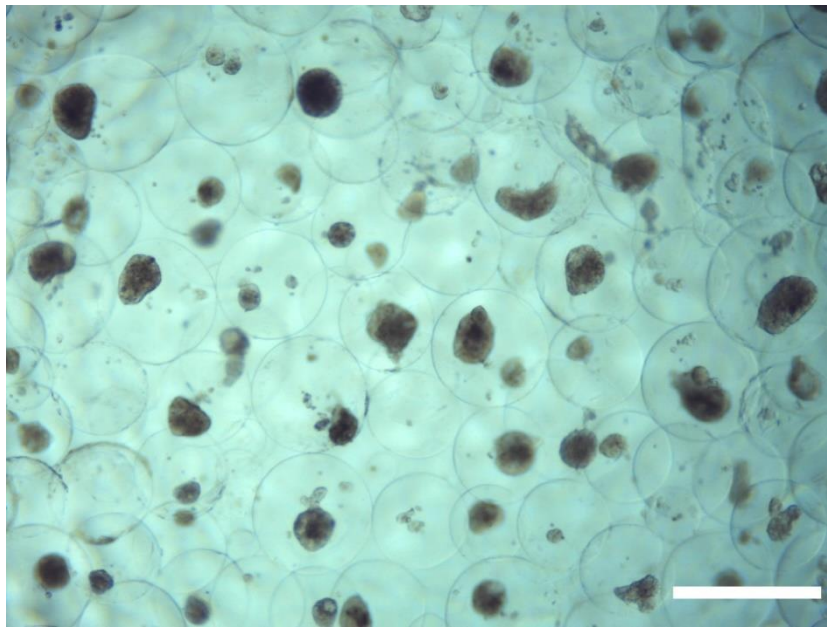


Figure 5.9: HepaRG organoids encapsulated in alginate beads on D60 after encapsulation (Scalebar 500 μ m).

5.3.1. HepaRG Viability

The viability and aggregation of the HepaRG cells within the encapsulation was the first thing to be investigated. Small samples of the encapsulated HepaRG cells would be taken from culture and a live / dead assay would be performed (Figure 5.10). Within 4 days the cells had aggregated into small cell clumps. In the first few days some of the cells had died in culture, but most of them were still alive. Over time the aggregates appear to grow, and any dead cells have disappeared. At D56, something unexpected happened: The aggregates appeared to sprout and started to expand quickly within the confined space of the encapsulation. It was concluded that the HepaRG cells had no problem surviving for prolonged periods of time, proliferating and aggregating within the encapsulation.

5.3.2. Histology

To further investigate the HepaRG aggregates, they were fluorescently stained to get a better idea of their morphology and function. To have a better idea of the structural morphology of the organoids that formed within the beads, part of the encapsulated HepaRG aggregates were fixed on day 77 using 10% formalin with 25 mM BaCl₂ before staining with Phalloidin-555 and DRAQ5. Phalloidin binds to the actin filaments, the cell components that give them mechanical strength and are the driving forces for movement.^[10]

Beads were imaged using a Leica confocal microscope (Figure 5.11). For bigger beads, intricate structures could be seen (Figure 5.11 D), which seem to indicate that the cells are rearranging themselves within the encapsulation to form these intricate structures, using the alginate encapsulation as a support. For smaller encapsulations the HepaRG cells seem to have filled the entire cavity of the bead, taking on the shape of the core (Figure 5.11 A). In some of these aggregates lumen could be found (Figure 5.11 B), which seems to indicate that even in these smaller beads, a form of self-organisation has taken place. Since HepaRG cells

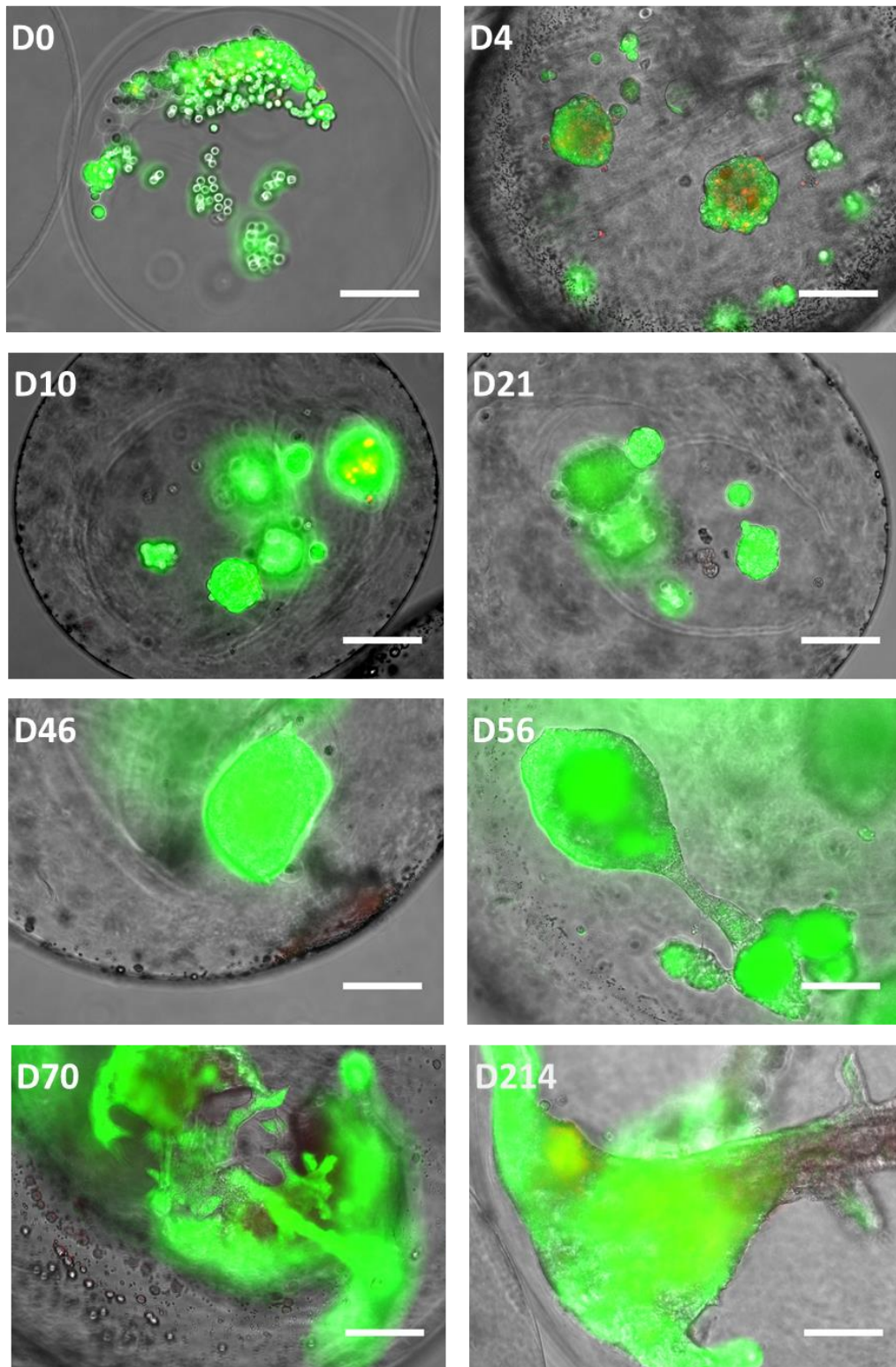


Figure 5.10 Live (green) / dead (red) staining of encapsulated HepaRG cells over time. After 4 days the cells are aggregated, but the cells keep proliferating. After almost 2 months in culture the aggregates start to sprout and form organized structures. When the cells are kept in culture, eventually they completely fill the entire core. (Scalebar 100 μm)

are progenitor cells to both hepatocytes and biliary duct endothelial cells,^[11] it is possible that they reorganize themselves once the cells are differentiated, which is known to happen spontaneously in 2D when the concentration of cells is high.^[11]

Another subset of encapsulated HepaRG aggregates was fluorescently stained for functional proteins. They were stained for HNF4 α , albumin and CK19. HNF4 α and albumin are hepatocyte markers, indicating that the HepaRG cells are going towards the hepatocyte lineage. HNF4 α is an early hepatocyte marker, which will stain positive early in the differentiating process,^[12] whereas albumin is expressed in mature hepatocytes.^[13] CK19 is a marker for the other type of cell the HepaRG cells can differentiate towards, the biliary duct cell.^[14]

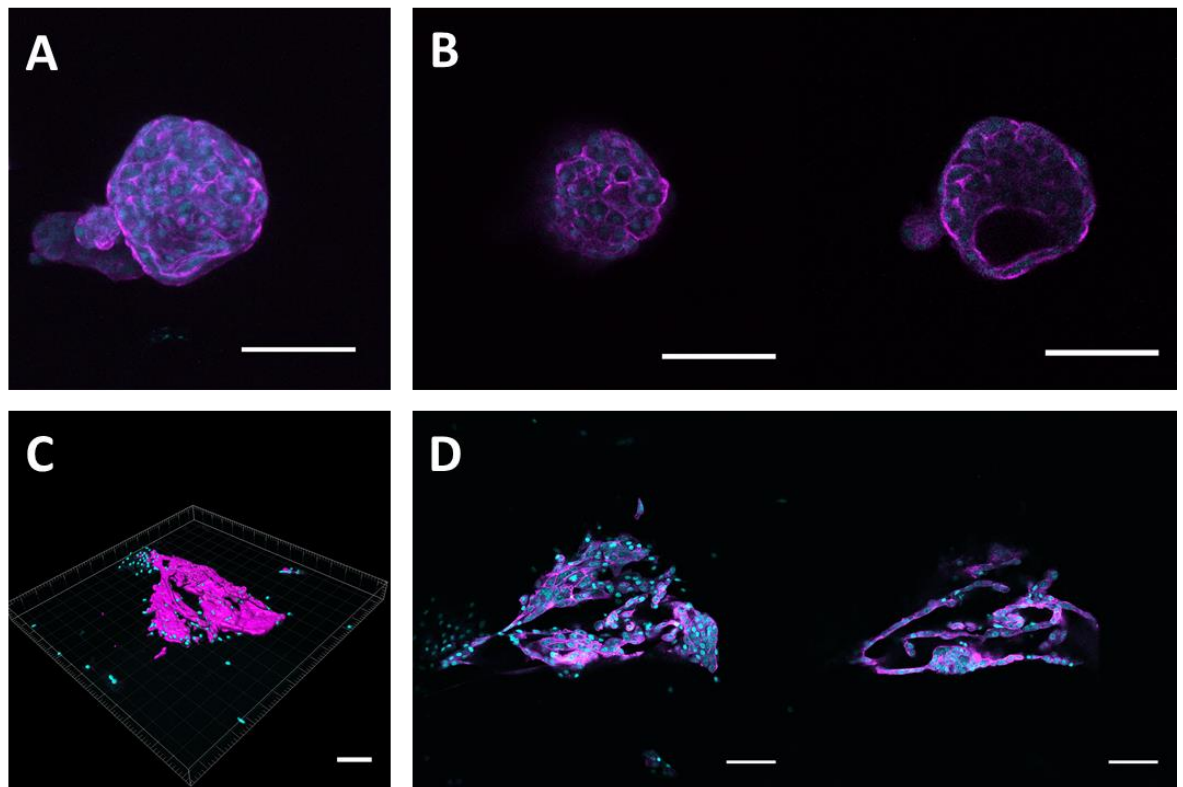


Figure 5.11: Confocal images of encapsulated HepaRG aggregates stained with Phalloidin (purple, actin filaments) and DRAQ5 (Blue, nucleus) A: A 3D representation of an aggregate in a small encapsulation. B: 2 slices taken at different heights within the smaller aggregate. C: A 3D representation of an aggregate in a larger encapsulation. (image rendered in Imaris) D: 2 slices taken at different heights within the larger aggregate. (Scalebar 100 μ m)

In Figure 5.12 it can be seen that there is no positive staining for HNF4 α , while there is a lot of positive staining for albumin, which indicates that at this point the HepaRG cells have differentiated into adult hepatocytes. Furthermore, the organoids test positive for albumin in certain areas and CK19 in different areas. This seems to indicate that the cells indeed have either selectively differentiated in either hepatocytes or biliary duct endothelial cells or have reorganized to form these patches after differentiation. The CK19 positive cells seem to have located mainly on the periphery of the aggregates, which is in line with the findings of Ramaiahgari et al.^[15]

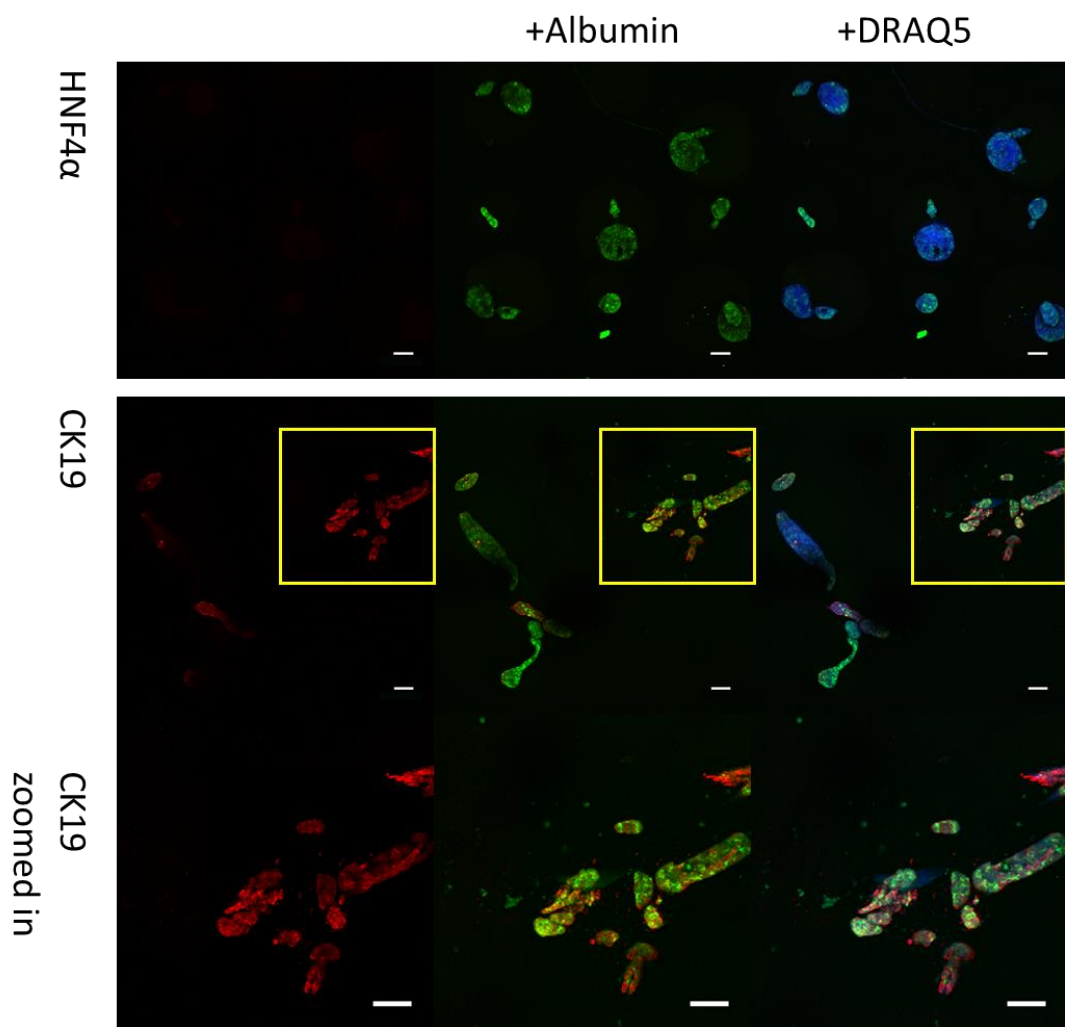


Figure 5.12: Fluorescent staining of HepaRG organoids. All beads were stained with DRAQ5 (Blue), albumin (Green) and either HNF4 α (red) or CK19(red). The yellow box indicates a smaller area to which is zoomed in on the bottom layer.

(Scalebar 100 μ m)

5.3.3. HepaRG Organoid Function

Since the fluorescent imaging implies the formation of mature hepatic organoids within the encapsulations, the metabolic functionality of the organoids was tested. CYP3A4 is the most abundant Cytochrome P450 (CYP450) isozyme. The CYP450 enzymes are essential for the metabolism of most medications, with the CYP3A4 isoenzyme being one of the 2 most significant isozymes, together with cytochrome P450 2D6 (CYP2D6).^[16, 17] For that reason, the CYP3A4 activity was chosen to determine the hepatic activity of the HepaRG organoids. A commercial CYP3A4 activity kit was used, to determine the activity. This kit uses a P450 substrate that is converted by CYP3A4 from a non-reactive derivative into luciferin, a substrate which reacts with luciferase to produce light that is directly proportional to the activity of CYP3A4. A known inducer of CYP3A4 activity is the drug rifampicin,^[8] an antibiotic used to treat tuberculosis, amongst others.^[18]

The live / dead data showed that cell rearrangement started happening around D60, which is why the commercial function test was performed at D60. To see whether these beads could be used as drug testing platform, and to further assess the hepatic activity of the organoids, some were cultured for 24h with 10 μ M rifampicin.

In this section the HepaRG cells were allowed to differentiate into organoids for 60 days before testing their activity, as this was the point where the cell started to rearrange themselves within the beads. This is a relatively long time to keep cells in culture, so a method to decrease this time was looked into. It was found that DMSO helps HepaRG cells to differentiate towards hepatocytes.^[11, 19, 20] So as a control, HepaRG cells were cultured in a 24 well plate for 5 days in normal medium, followed by 14 days in either normal medium (2D control) or medium with 1% DMSO. If this helps to increase the CYP3A4 activity in a 2D culture, it could also be used in 3D. The enzymatic activity was normalized to the amount of protein per well, to adjust for difference of the number of cells per well. The final results were

therefore expressed in Relative Light Units (RLU) per μg of protein per ml of Ripa-buffer. (2D data obtained by Gregor Skeldon)

CYP3A4 activity was found to be almost 4 times as high in the HepaRG organoids compared to the 2D control culture. When cultured for 24 hours with rifampicin, the CYP3A4 activity in the organoids more than doubled (Figure 5.13). This reaction to the drug shows that the encapsulated organoids have hepatic activity and could be used for drug testing. When cultured for 2 weeks with 1% DMSO, the enzymatic activity in the 2D cultured HepaRG cells became 6 times as high as that of the 2D control culture, even higher than that of the 60-day old organoid activity. This is a promising result that seems to indicate that the creation of functional encapsulated organoids could be done in a shorter time period.

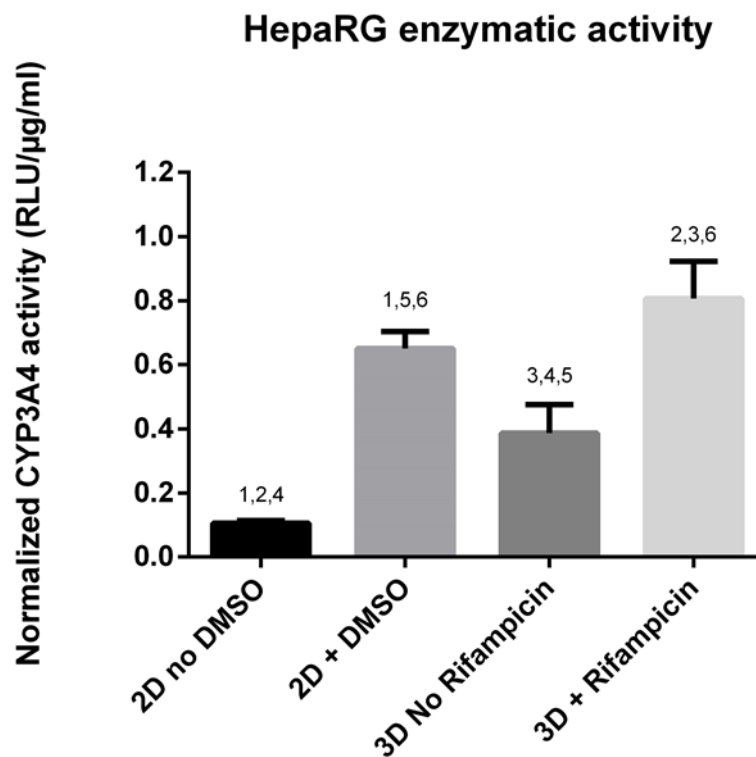


Figure 5.13: CYP3A4 activity for HepaRG cells cultured in 2D and HepaRG organoids normalized against their protein content. 2D cultures were cultured for 5 days in normal medium, followed by 2 weeks with or without DMSO. Organoids were cultured 60 days in normal medium followed by 24h with or without 10 μM Rifampicin. (Significant differences: 1, 2 and 3 $P < 0.01$; 4 and 5 $P < 0.001$; 6 no significant difference; Error bar indicates +SD)

5.3.4. Medium-core Encapsulations

A trial was performed where HepaRG cells would be encapsulated without the aid of CMC, using only medium as the core material. This experiment was only performed once. The micro-encapsulation was performed using the same parameters as for the CMC-core encapsulations, with the exception that cells were not resuspend in a CMC solution, but in medium, and that the flow rate of the Protanal alginate solution was set to 30 ml/h instead of 17 ml/h. This increase was chosen in the hope that a thicker alginate shell might support the medium-core better. Although the micro-encapsulation did not create spherical encapsulations (Figure 5.14 A), there appeared to be encapsulated cells. However, after only a week in culture, a confluent layer of HepaRG cells had formed on the bottom of the 6 well plates that were used to culture the medium-core HepaRG encapsulations (Figure 5.14 B). This could either be due to cells “escaping” from their encapsulations, or an indication that there were so many cells that were not encapsulated but ended up on the outside of the encapsulations that even washing multiple times with PBS was not enough to wash them all off. After placing the encapsulations over to a new plate, no more cells attached to the bottom, indicating that it was most likely the latter. In the same way as the CMC-core encapsulated HepaRG cells, the medium-core HepaRG cells started aggregating, and filling up the core over time. However, when staining the medium-core HepaRG cells after 77 days, a difference could be seen compared to the CMC-core organoids (Figure 5.15). The medium-core organoids showed less staining for albumin and had a visible staining for HNF4 α . This implies that even after 77 days, the HepaRG cells were not fully differentiated into hepatocytes. The CK19 staining was comparable to that of the CMC-core organoids. When tested for their CYP-activity at day 60, it was about 3 times as low as the activity of the CMC-core organoids, and only a little bit higher than the activity of the 2D control culture (Figure 5.16). There was no significant difference between the beads with added rifampicin and

those without, which also implies that these organoids are not fully functional as hepatocytes. The difference between the two organoid groups could be due to a beneficial effect of the CMC, but it is more likely that it is due to the concentration of cells within the encapsulation. It is known that on 2D HepaRG cells start to differentiate once they become confluent, so at a high concentration.^[11] The fact that for the medium-core encapsulations a lot of cells did not end up in the beads, but on the outside of the beads, could mean that the starting concentration of cells within the beads was lower than that of the CMC-core encapsulations. This could have led to the slower differentiation of the cells.

The medium-only core-shell encapsulation process resulted in non-spherical encapsulations, non-functional HepaRG organoids, and a loss of cells during the encapsulation process. For quickly dividing cells like HepaRG the cell-loss is not a big problem, but for the cells of donated islets (which almost do not divide at all) this loss of cell mass would not be acceptable.

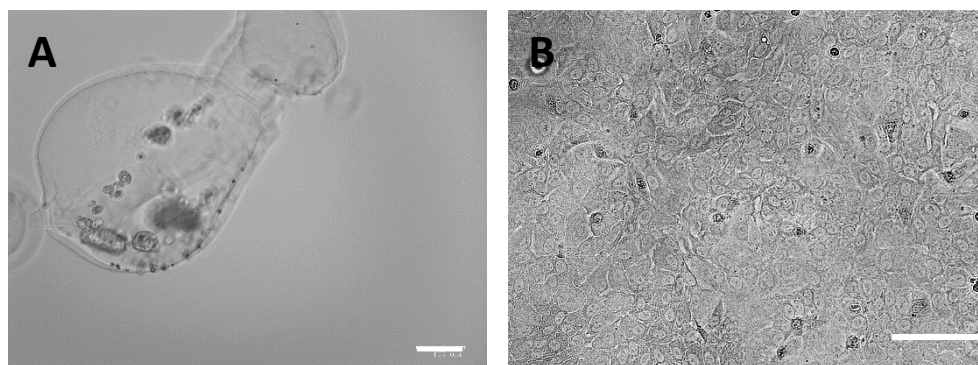


Figure 5.14: Encapsulating HepaRG cells using only medium as the core liquid did not deliver great results. A: A medium-core encapsulation 1 day after fabrication. The encapsulation is not spherical, and only a few cells can be seen in the core. B: The bottom of the plate used to culture the medium-core HepaRG encapsulations had a confluent layer of HepaRG cells after 1 week of culture. (Scalebar 100 µm)

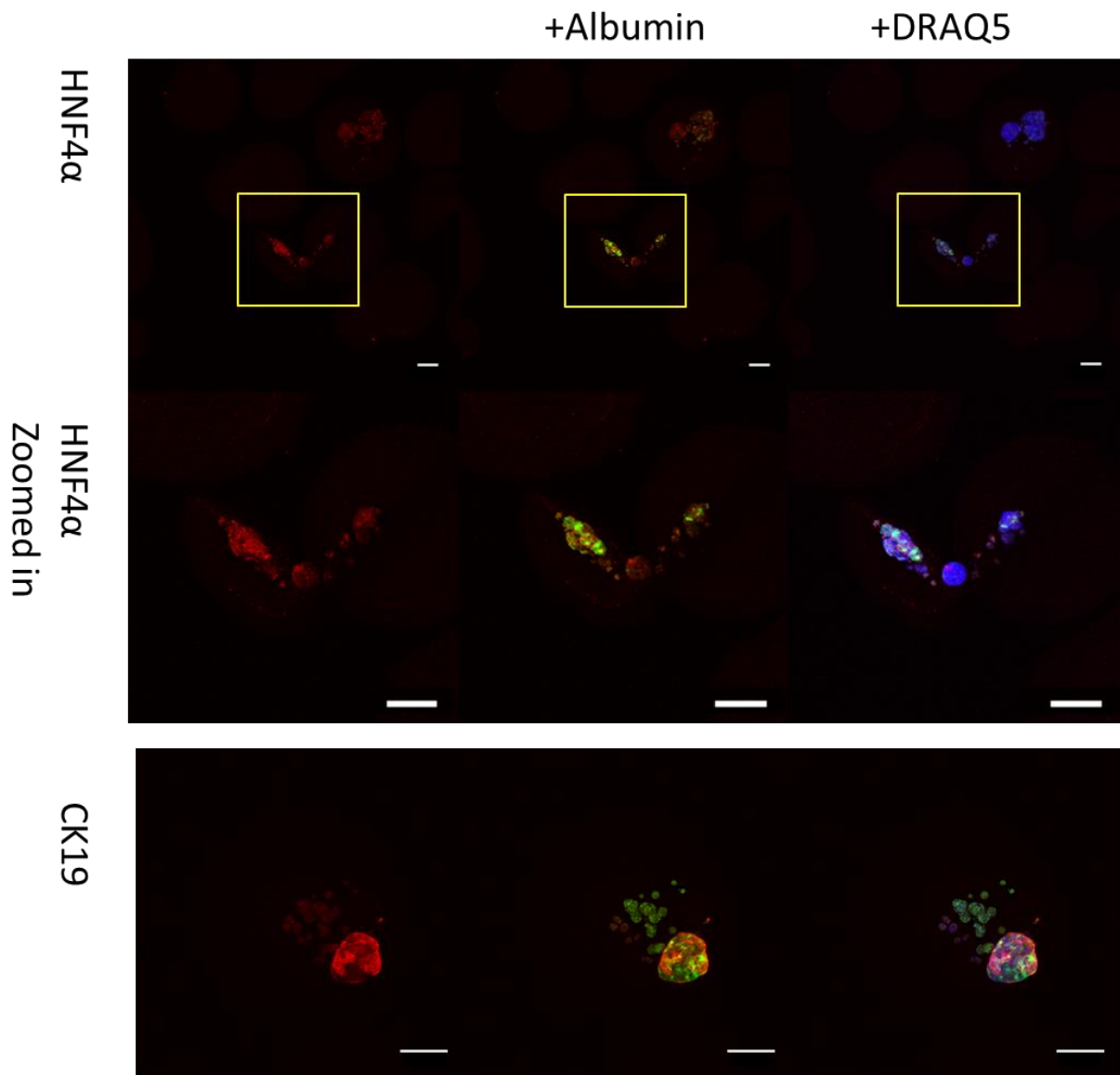


Figure 5.15: Fluorescent staining of HepaRG organoids. All beads were stained with DRAQ5 (Blue), albumin (Green) and either HNF4α (red) or CK19(red). The yellow box indicates a smaller area to which is zoomed in on the middle layer. (Scalebar 100 μm)

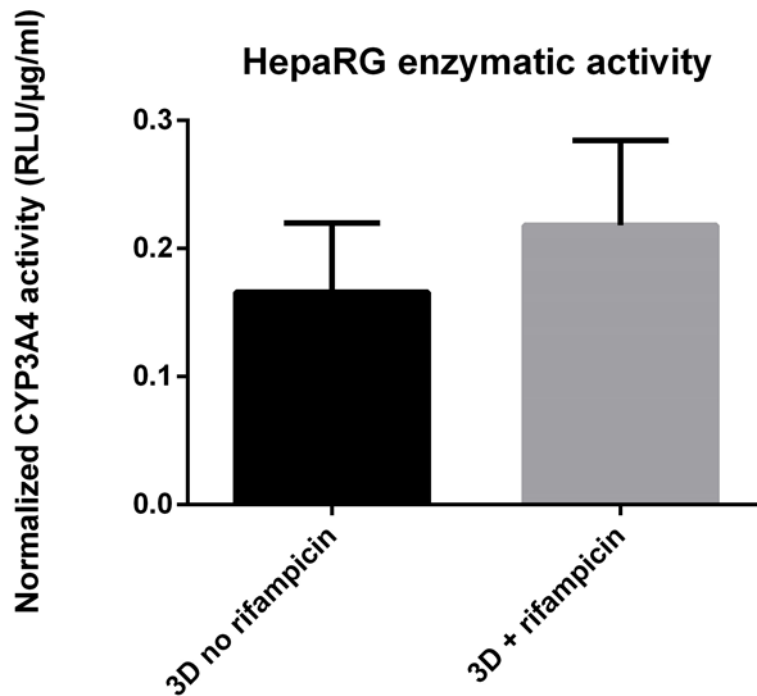


Figure 5.16: The CYP3A4 activity of the medium-core encapsulated HepaRG organoids normalised to their protein content. No significant difference was found between organoids cultured with rifampicin, and those cultured without. ($p > 0.05$; Error bar indicates +SD)

5.4. Conclusion

In this chapter the use of a coaxial needle in combination with the electrospray technology has been explored. It was found that a matching viscosity of both the core and the shell material fabricates beads with the most spherical morphology, that don't collapse on themselves and are relatively uniform in size. The ratio of extrusion velocity at the tip, and not the ratio of volume flow rate at which the core and shell material are dispensed turned out to be a key factor in the creation of spherical beads. Using these core-shell micro-encapsulation, it was possible to fabricate encapsulations with a single cell suspension of HepaRG cells in the core while having a mechanically strong alginate wall. Over time, the cells within the beads managed to aggregate, proliferate and differentiate, to form mature and

functional hepatic organoids, which could be used for drug testing. The size of the drugs tested should be taken into consideration, as the alginate's permeability might hinder the diffusion of the drug as explained in chapter 4.

One point for future research could be the long time it takes to develop these organoids. For all the experiments done in this thesis the functionality was not tested until day 60 and the histology was not done until day 77. It would be interesting to see whether the functionality of the hepatic organoids is already there on an earlier time point. Furthermore, normal HepaRG culture medium was used to culture these organoids. It would be interesting to see if the HepaRG differentiation medium (normal medium with 1% DMSO) can speed up the process of maturing the HepaRG cells into hepatic organoids, in the same way as it does in 2D.

As a test, HepaRG organoids were also encapsulated using a medium-only core. The encapsulations were not to the same standard as those that were encapsulated with a CMC-core, there was a lot of cell loss during the encapsulation process and the resulting organoids were unfortunately not functional.

An additional benefit of culturing encapsulated HepaRG aggregates, is that they can be cultured in true 3D, with multiple layers of beads on top of each other, and that medium can easily be replaced with the use of a cell strainer, without having to fear damaging or losing any of the aggregates.

5.5. References

- [1]. de Vos P, van Hoogmoed CG, van Zanten J, Netter S, Strubbe JH, Busscher HJ. Long-term biocompatibility, chemistry, and function of microencapsulated pancreatic islets. *Biomaterials*. **2003**;24(2):305-12.
- [2]. de Vos P, Lazarjani HA, Poncelet D, Faas MM. Polymers in cell encapsulation from an enveloped cell perspective. *Adv Drug Deliv Rev*. **2014**;67-68:15-34.
- [3]. Kilimnik G, Jo J, Periwal V, Zielinski MC, Hara M. Quantification of islet size and architecture. *Islets*. **2012**;4(2):167-72.
- [4]. De Haan BJ, Faas MM, De Vos P. Factors influencing insulin secretion from encapsulated islets. *Cell Transplantation*. **2003**;12(6):617-25.
- [5]. Lee DY, Park SJ, Nam JH, Byun Y. Optimal aggregation of dissociated islet cells for functional islet-like cluster. *Journal of Biomaterials Science, Polymer Edition*. **2008**;19(4):441-52.
- [6]. Ramaiahgari SC, Waidyanatha S, Dixon D, DeVito MJ, Paules RS, Ferguson SS. From the Cover: three-dimensional (3D) HepaRG spheroid model with physiologically relevant xenobiotic metabolism competence and hepatocyte functionality for liver toxicity screening. *Toxicological Sciences*. **2017**;159(1):124-36.
- [7]. Gunness P, Mueller D, Shevchenko V, Heinzle E, Ingelman-Sundberg M, Noor F. 3D organotypic cultures of human HepaRG cells: a tool for in vitro toxicity studies. *Toxicological Sciences*. **2013**;133(1):67-78.
- [8]. Nelson LJ, Morgan K, Treskes P, Samuel K, Henderson CJ, LeBled C, *et al*. Human Hepatic Hepa RG Cells Maintain an Organotypic Phenotype with High Intrinsic CYP 450 Activity/Metabolism and Significantly Outperform Standard HepG2/C3A Cells for Pharmaceutical and Therapeutic Applications. *Basic & clinical pharmacology & toxicology*. **2017**;120(1):30-7.
- [9]. Rowe RC, Sheskey PJ, Quinn ME. Handbook of pharmaceutical excipients. 6th ed **2009**.
- [10]. Pollard TD, Cooper JA. Actin, a Central Player in Cell Shape and Movement. *Science*. **2009**;326(5957):1208-12.
- [11]. Gripon P, Rumin S, Urban S, Le Seyec J, Glaise D, Canine I, *et al*. Infection of a human hepatoma cell line by hepatitis B virus. *Proc Natl Acad Sci U S A*. **2002**;99(24):15655-60.
- [12]. Faulkner-Jones A, Fyfe C, Cornelissen DJ, Gardner J, King J, Courtney A, *et al*. Bioprinting of human pluripotent stem cells and their directed differentiation into hepatocyte-like cells for the generation of mini-livers in 3D. *Biofabrication*. **2015**;7(4):044102.

- [13]. Hay DC, Zhao D, Fletcher J, Hewitt ZA, McLean D, Urruticoechea-Uriguen A, *et al.* Efficient differentiation of hepatocytes from human embryonic stem cells exhibiting markers recapitulating liver development in vivo. *Stem Cells*. **2008**;26(4):894-902.
- [14]. Zhou H, Rogler LE, Teperman L, Morgan G, Rogler CE. Identification of hepatocytic and bile ductular cell lineages and candidate stem cells in bipolar ductular reactions in cirrhotic human liver. *Hepatology*. **2007**;45(3):716-24.
- [15]. Ramaiahgari SC, Waidyanatha S, Dixon D, DeVito MJ, Paules RS, Ferguson SS. Three-Dimensional (3D) HepaRG Spheroid Model With Physiologically Relevant Xenobiotic Metabolism Competence and Hepatocyte Functionality for Liver Toxicity Screening. *Toxicol Sci*. **2017**;160(1):189-90.
- [16]. Lynch T, Price A. The effect of cytochrome P450 metabolism on drug response, interactions, and adverse effects. *Am Fam Physician*. **2007**;76(3):391-6.
- [17]. Roby CA, Anderson GD, Kantor E, Dryer DA, Burstein AH. St John's Wort: Effect on CYP3A4 activity. *Clinical Pharmacology & Therapeutics*. **2000**;67(5):451-7.
- [18]. Drugs.com, *Rifampin*, <https://www.drugs.com/monograph/rifampin.html>, October **2018**
- [19]. Guillouzo A, Corlu A, Aninat C, Glaise D, Morel F, Guguen-Guillouzo C. The human hepatoma HepaRG cells: a highly differentiated model for studies of liver metabolism and toxicity of xenobiotics. *Chem Biol Interact*. **2007**;168(1):66-73.
- [20]. Gerets H, Tilmant K, Gerin B, Chanteux H, Depelchin B, Dhalluin S, *et al.* Characterization of primary human hepatocytes, HepG2 cells, and HepaRG cells at the mRNA level and CYP activity in response to inducers and their predictivity for the detection of human hepatotoxins. *Cell biology and toxicology*. **2012**;28(2):69-87.

Chapter 6

Islet Encapsulation

6.1. Introduction

The main focus of this thesis is the encapsulation of pancreatic islets to shield them from the immune system to improve outcomes after transplantation. In chapter 3 the electro-spray method was optimised for the micro-encapsulation of pancreatic islets, while in chapter 4 a purified Protanal alginate was created and tested to enhance the biocompatibility and immunoprotective properties. In Chapter 5 a one-step method for the encapsulation and aggregation of cells was used to create encapsulated HepaRG organoids with the potential to be used for drug testing.

In this chapter all previous techniques are used and combined to encapsulate pancreatic islets and try to create smaller, functional islets out of dissociated larger islets. Different methods to dissociate pancreatic islets are investigated. The biocompatibility of the islets with the purified Protanal Alginate and the encapsulation method is investigated by looking at the islet viability over time and glucose induced insulin secretion. In the last section the core/shell bead system is used in combination with dissociated pancreatic islets in the hope of creating smaller functional islets.

6.2. Islet dissociation

To create smaller islets out of larger ones, the islets must first be dissociated to create a single cell suspension. The gentlest way to do this was researched by comparing 2 dissociation agents (0.25% Trypsin and 0.05% Trypsin+ 0.02% EDTA), with or without mechanical stimulation using a micropipette. As a control, islets in PBS with or without mechanical stimulation were used. After dissociation (or 15 minutes) a live / dead assay was performed (Figure 6.1). Unsurprisingly, mechanical stimulation helped the islets to dissociate faster, within 4 minutes after adding the dissociation reagents, whereas after 15 minutes the non-mechanical groups appeared to start to fall apart, but still had large clumps of cells. The control remained almost completely intact, with or without mechanical stimulation.

Viability of the islet cells was calculated for the single cell suspensions (Trypsin with mechanical stimulation, and Trypsin+EDTA with mechanical stimulation) from the microscopy pictures (Figure 6.2). Unfortunately, since it was impossible to determine the number of cells in the intact islets/ cell clumps, this could not be done for the other groups. Although there was no significant difference between the viability of the 2 different dissociation agents, the viability for the Trypsin+EDTA group was slightly higher, and the islets in this group that received no stimulation also appeared to be more dissociated than the ones in the Trypsin group. It was decided to continue using the Trypsin+EDTA dissociation method for further experiments where a single islet cell suspension was necessary.

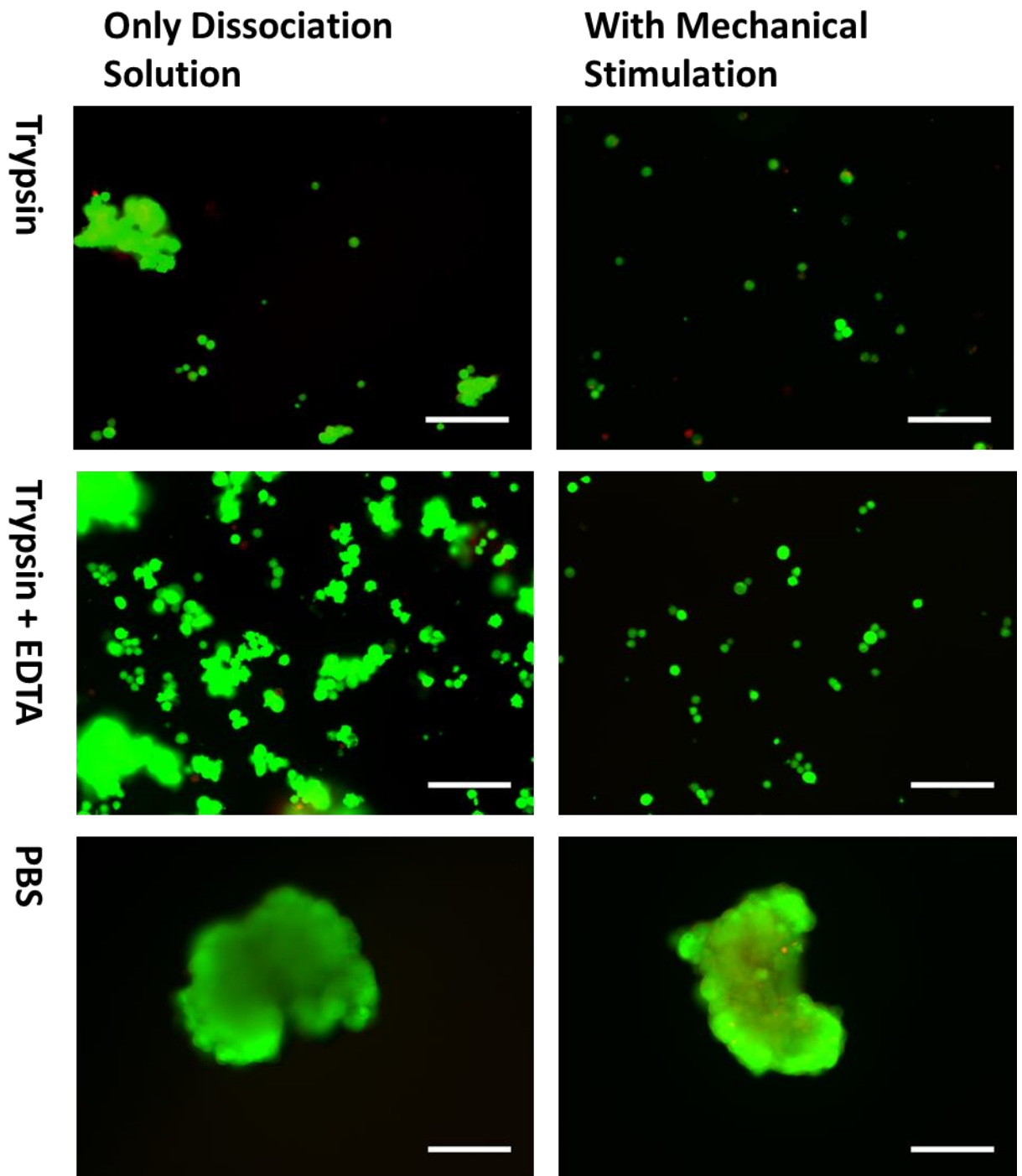


Figure 6.1: Live (green) / dead (red) staining on islets dissociated with either Trypsin(0.25%) or Trypsin(0.05%) + EDTA(0.02%), with or without mechanical stimulation. Islets in PBS were used as a control. (Scalebar 100 μm)

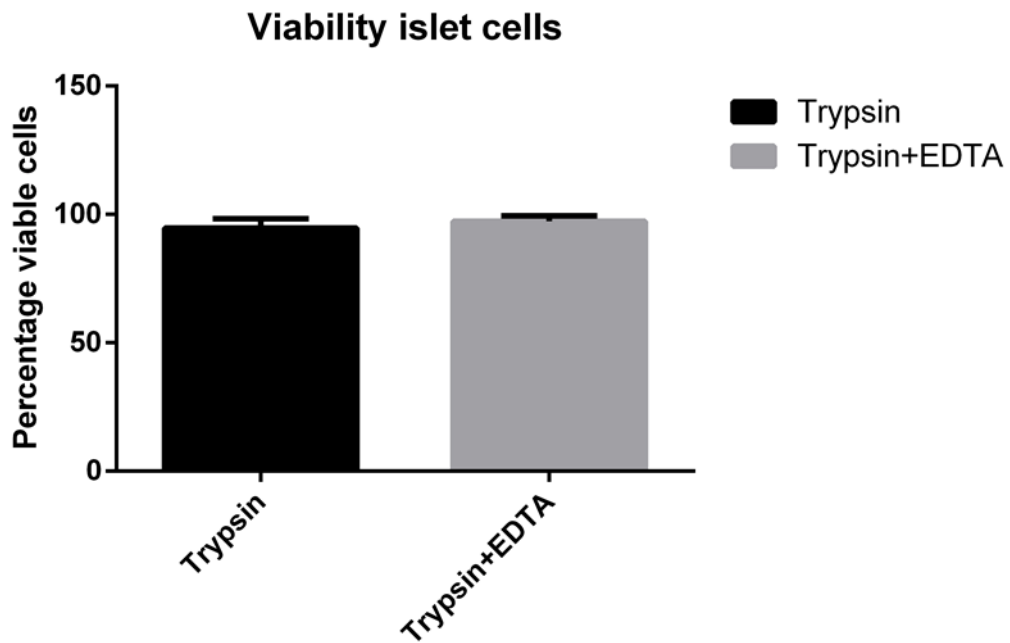


Figure 6.2 Islet cell viability of single cell suspensions. Stained cells were counted in ImageJ and used to calculate the viability. No statistical difference could be found between the two groups ($P>0.05$; Error bar indicates +SD)

6.3. Encapsulating in Alginate Hydrogel

As stated before, when this project was started there were no articles available of other researchers using the electrospray method to encapsulate human pancreatic islets. Therefore the impact of the encapsulation method and the purification method were tested by encapsulating islets of Langerhans in the purified Protanal and seeing if they were still viable and functional. Furthermore, it was investigated if dissociated islets would survive and stay functional within encapsulation.

Islets were handpicked from the pancreatic slurry (Figure 6.3 A) and divided into three groups. The first group was dissociated as stated above (4 minutes incubation in Trypsin+EDTA, breaking up the islets using a micropipette after 2 and 4 minutes), and cells were counted using a haemocytometer. The cells were spun down and resuspended at a concentration of 10×10^6 cells/ml in a 1.2% purified Protanal alginate solution. The islets in the second group

were spun down and resuspended at a concentration of 10,000 islets/ml in a 1.2% purified Protanal alginate solution. Both the cells and the whole islets were then encapsulated using the micro-encapsulator at a speed of 1 ml/h through a 30G needle, at a distance of 1 cm to the 25 mM Isotonic BaCl₂ gelling bath, with an electric potential of 7 kV. After encapsulation (Figure 6.3 B), beads were sieved out of the gelling bath using a cell-strainer, and washed 3 times with PBS, before distributing over the wells of an ultra-low adhesion 6 well plate with 2 ml islet culture medium per well. The encapsulated cell beads were slightly smaller ($291 \pm 20 \mu\text{m}$) than the encapsulated islets ($341 \pm 61 \mu\text{m}$; Figure 6.3 C) and it is hypothesized that this is due to the residual medium diluting the alginate, creating a slightly less viscous material. The control islets (3rd group) were distributed over 2 different 6 well plates; one normal tissue culture plastic (TCP) plate, and an ultra-low adhesion (ULA) plate. All groups were tested for viability at different time points (Figure 6.4 to Figure 6.7) by doing a fluorescent live / dead assay.

Islets cultured on the TCP-plate remained viable, but were completely flattened out and attached to the bottom of the TCP-plate within 3 weeks (Figure 6.4). Islets kept on the ULA-plate slowly aggregated into larger islets, and then degraded over time, losing cells and dying off within roughly 2 months (Figure 6.5). Encapsulated cells remained viable for a short period but all died eventually. This was very batch dependent, with the longest viable cells ($\pm 6-8$ weeks) shown in Figure 6.6. Single cell encapsulations of other batches died within roughly 4 weeks. In contrast, encapsulated islets remained viable and kept their morphology for more than 3 months (Figure 6.7). Extremely large islets (Supplementary Data S2) did not survive for so long in their encapsulation. They died within 2 weeks of encapsulation and were removed from the culture plate.

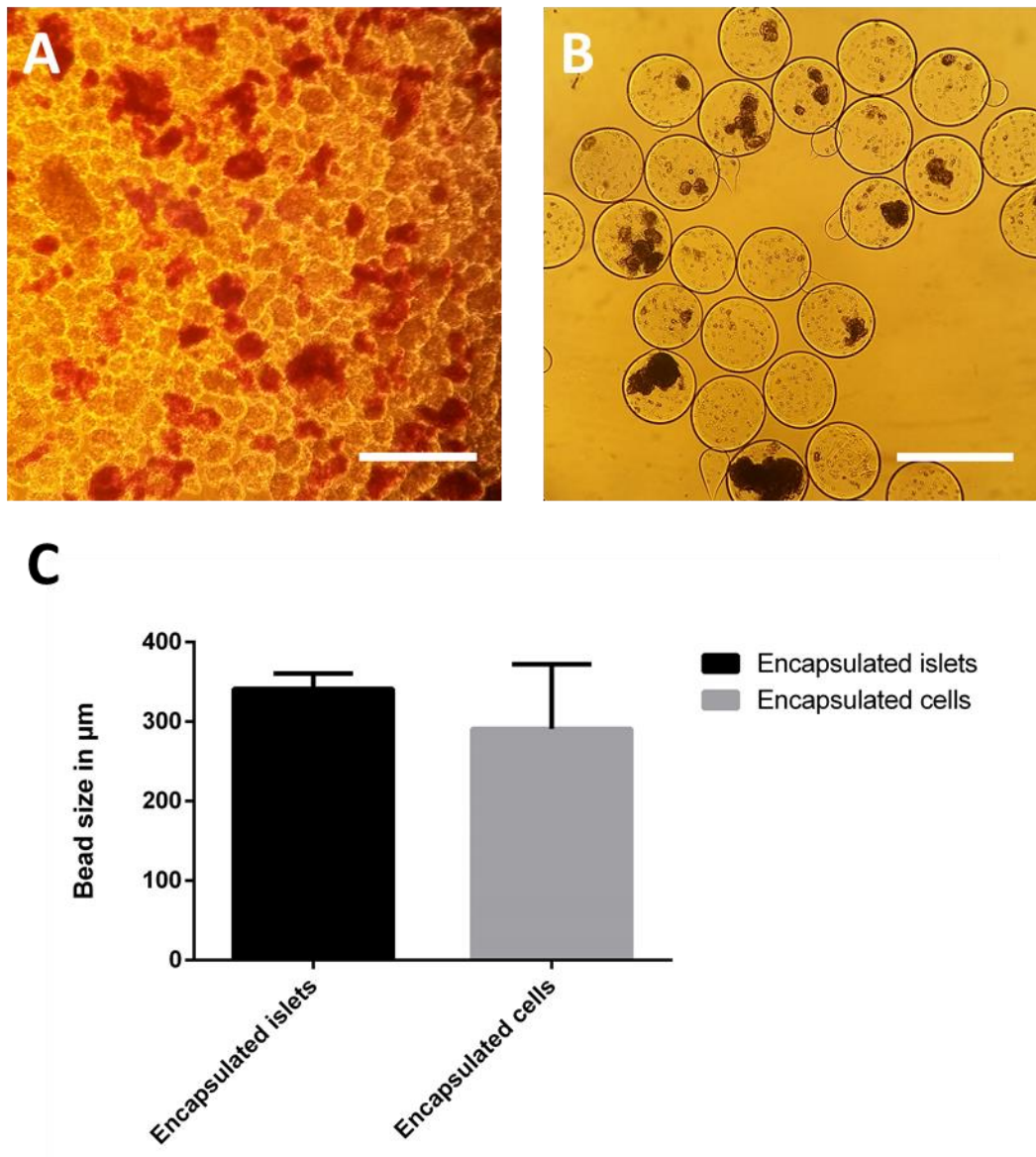


Figure 6.3: Pancreatic islets were handpicked from the pancreatic slurry and encapsulated in purified Protanal alginate using the micro-encapsulator. A: A sample of the pancreatic slurry stained with DTZ. Islets turn bright red once stained with DTZ. B: Islets encapsulated in Purified Protanal alginate. C: Mean bead size of encapsulated islets and islet cells. (error bar indicates +SD, Scalebar 500 μm)

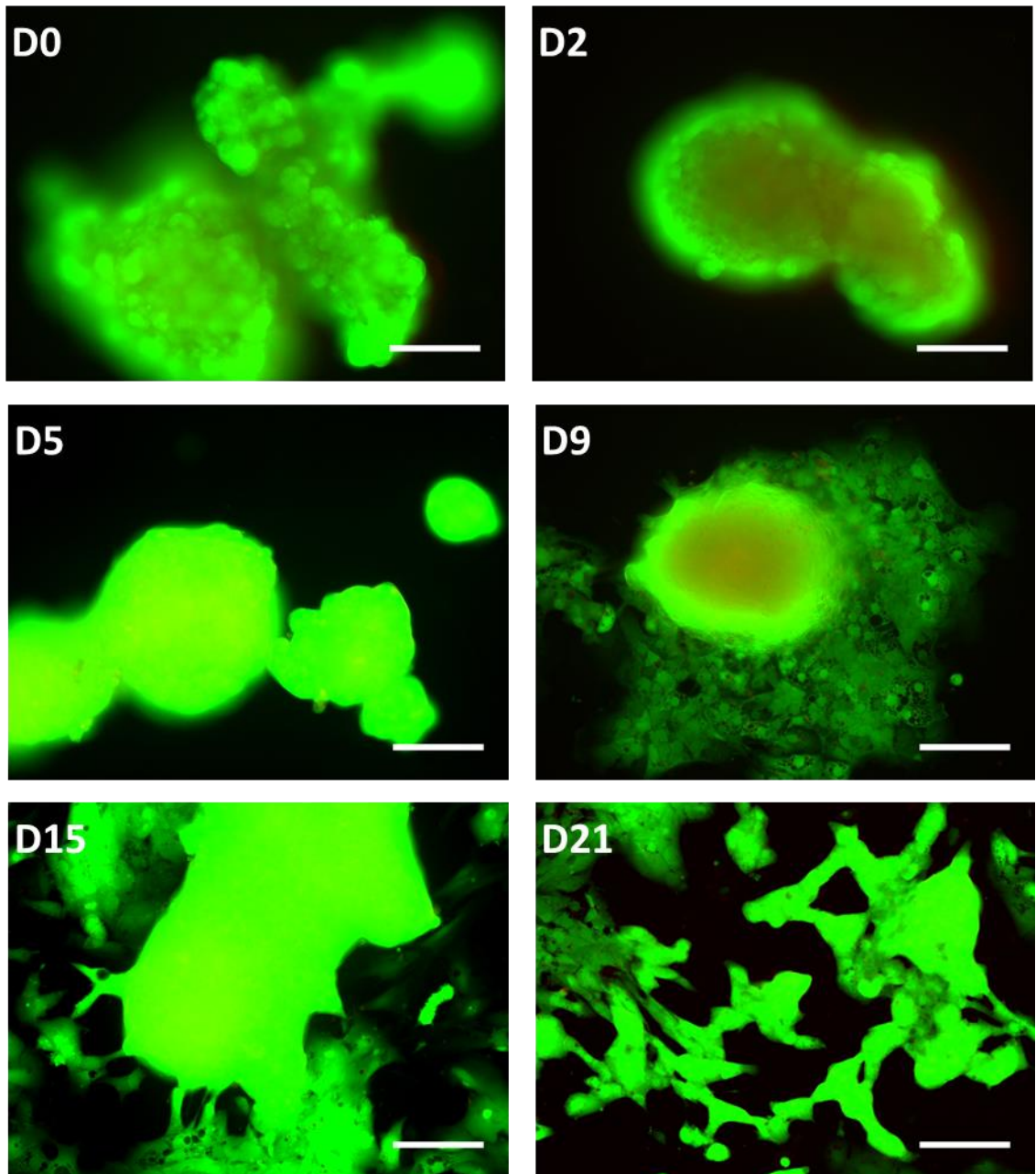


Figure 6.4: Live (green) / dead (red) staining over time on islets cultured on tissue culture plastic. Islets attach to the plastic and start spreading out over it over time. (Scalebar 100 μm)

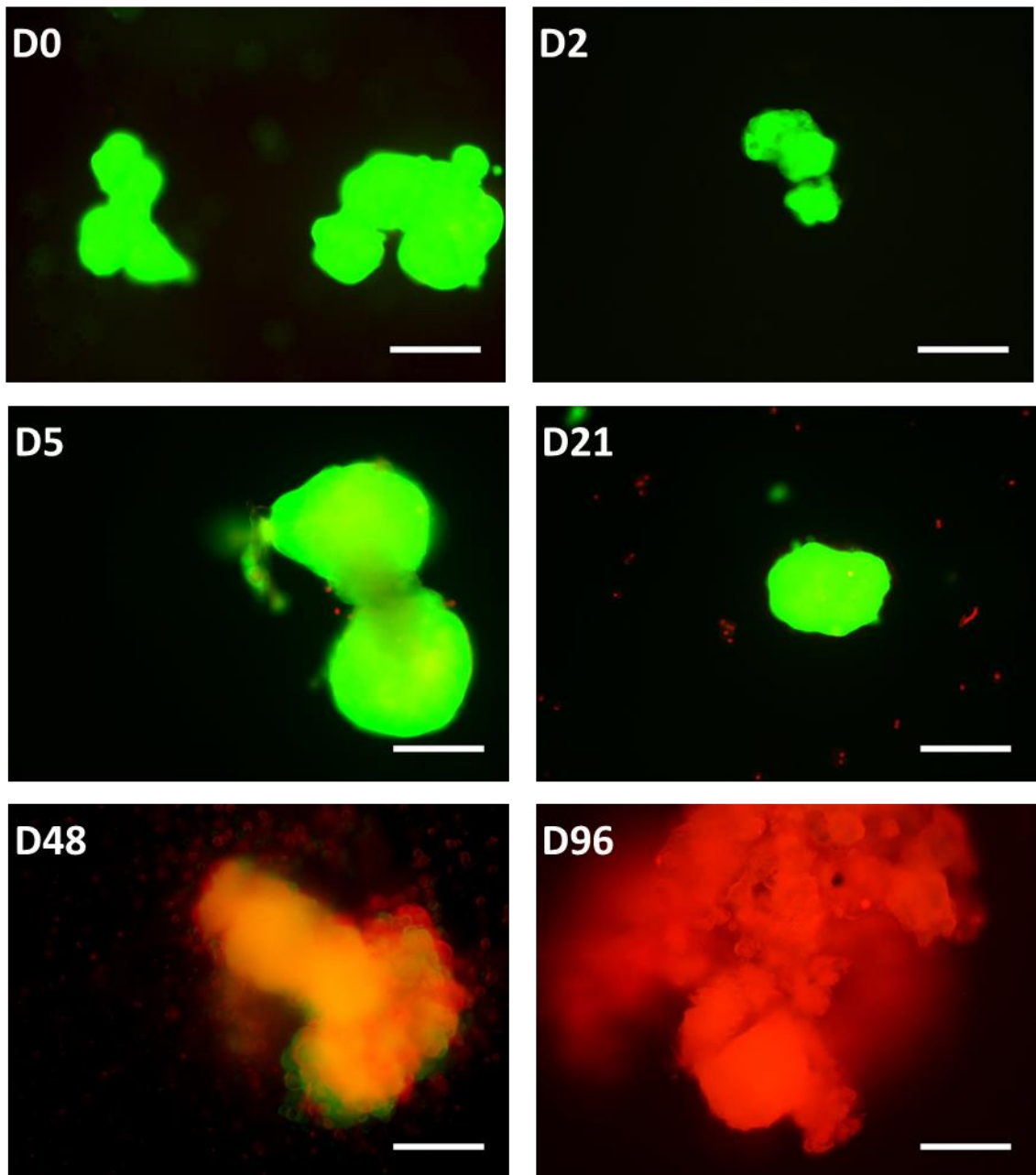


Figure 6.5: Live (green) / dead (red) staining over time on islets cultured on ultra-low adhesion plates. Islets don't attach to the plastic but aggregate together to form larger aggregates. Over time these islets start to fall apart and die. (Scalebar 100 μ m)

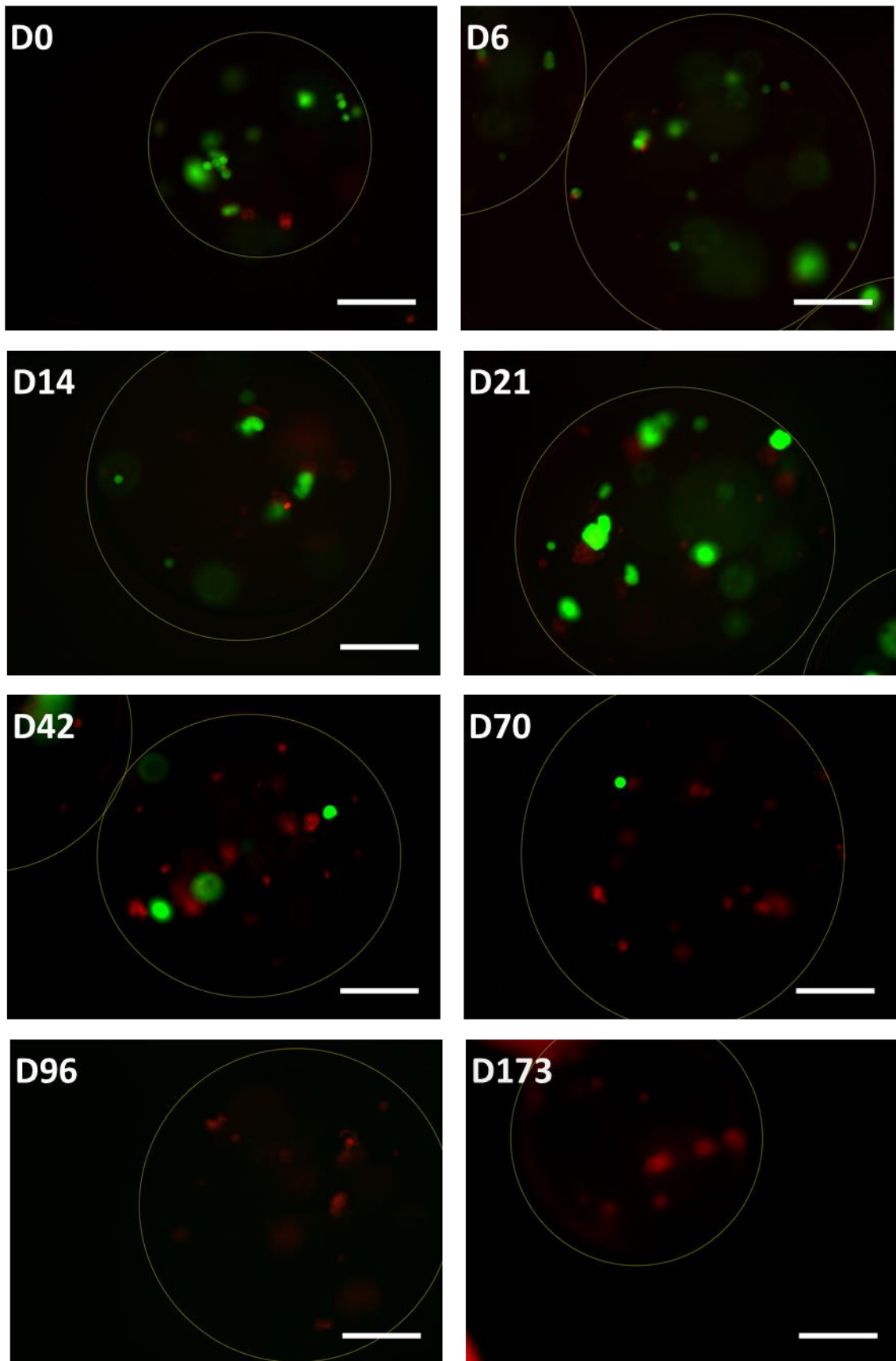


Figure 6.6: Live (green) / dead (red) staining over time on encapsulated islet cells. Cells remain viable for a few weeks, but then start deteriorating and eventually all die within the encapsulation. (Scalebar 100 μm)

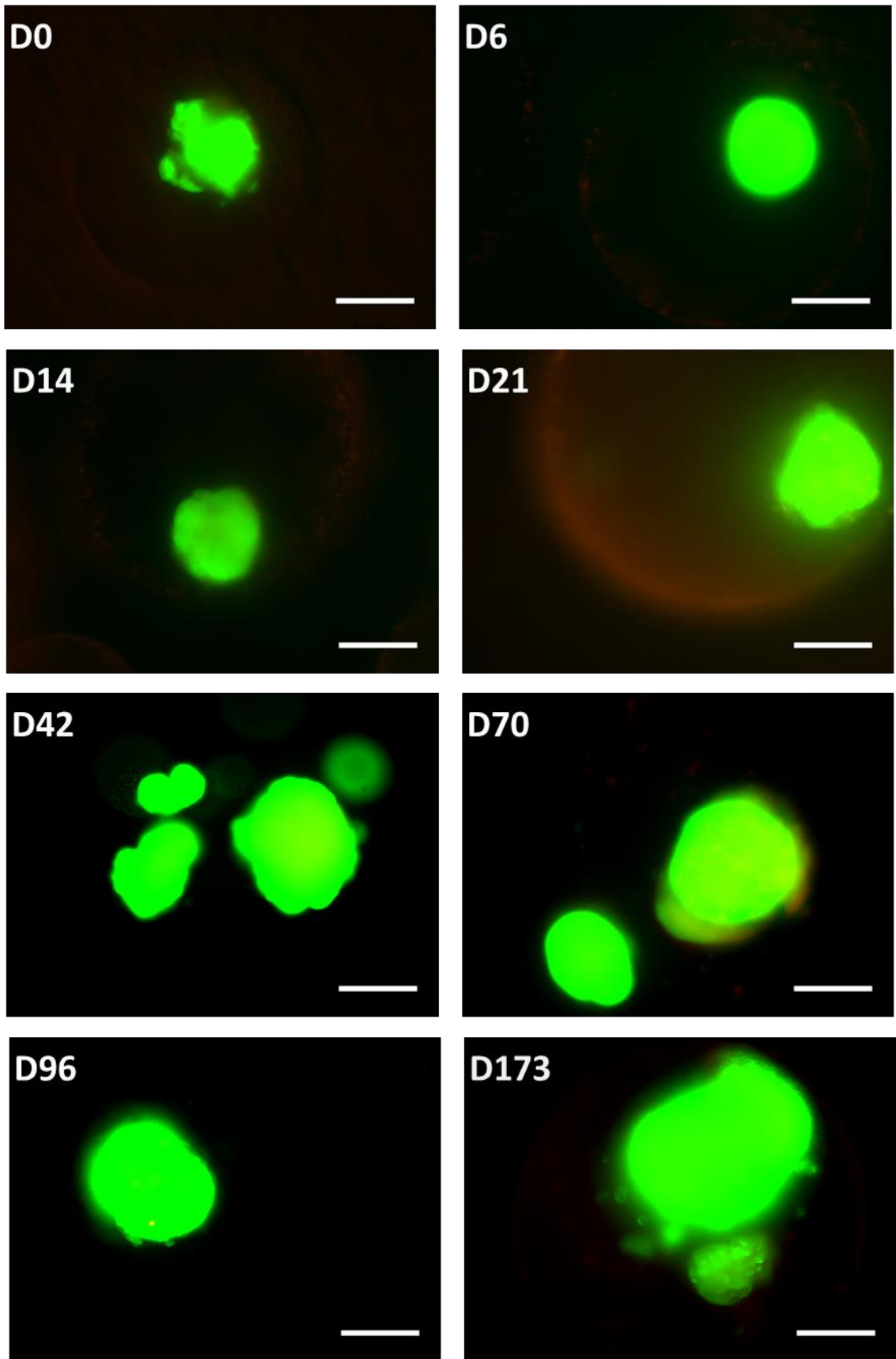


Figure 6.7: Live (green) / dead (red) staining over time on encapsulated islets. Encapsulated islets can be cultured for a long period of time without losing their morphology or viability (Scalebar 100 μm)

A glucose induced insulin secretion test was performed after 2 weeks on the encapsulated islets, encapsulated islet cells and the islets cultured on ULA-plates. The islets cultured on TCP-plates were not tested as the islets were already attached to the plate. Islets are deemed functional if they secrete at least twice as much insulin when in a high glucose environment, compared to the insulin they secrete in a low glucose environment.^[1] Therefore, all insulin secreted by the islets was normalized to the insulin secretion in their first low glucose buffer. There was no significant difference found between the encapsulated islets and the control, but the encapsulated islet cells were not functional. Since it is known that cell-cell contact between β -cells suppresses basal insulin secretion and enhances glucose-stimulated insulin secretion,^[2, 3] this result was to be expected. After 3 months the glucose induced insulin secretion test was performed again on only the encapsulated islets, as there were no more viable encapsulated islet cells or islets cultured on ULA-plates to perform the control test. Even after 3 months, the islets could still be deemed functional (Figure 6.8). It was found that encapsulated islets actually survive longer than their non-encapsulated counterparts *in vitro*, without losing their morphology, which is important for maintaining their functionality.^[4] It is hypothesized that the encapsulation does not only provide the islets with a barrier for the immune system, but also provide some mechanical stability to the islets, which aids in their survival. Islet cells that are encapsulated isolated from other cells do not survive within the alginate beads and were not functional. This further supports the theory that the cells within pancreatic islets need other cells and the extracellular matrix to survive and function.^[5]

In this section it was shown that the purified Protanal alginate is not harmful to the islets. Furthermore, the encapsulated islets remained viable and function *in vitro* longer than the non-encapsulated control group.

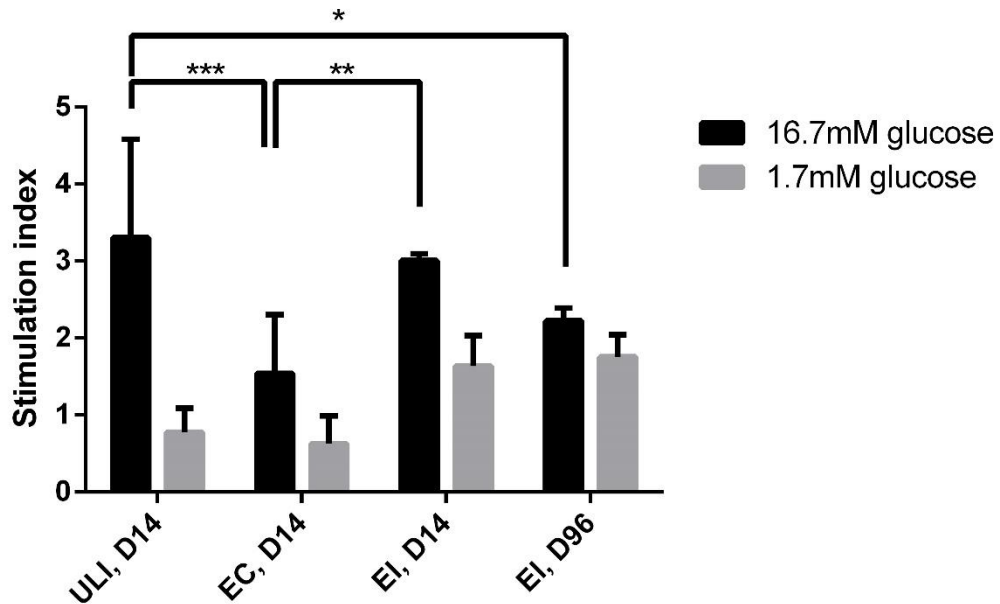


Figure 6.8 Stimulation index of high glucose (16.7 mM) and subsequently low glucose (1.7 mM) normalized to basal insulin secretion levels at 1.7 mM glucose for control islets cultured on ULA-plates (ULI), encapsulated islet cells (EC) and encapsulated islets (EI) on day 14 after encapsulation, and for the encapsulated islets on day 96 after encapsulation. (stars indicate statistical significant difference between the stimulation index for high glucose only; *($P < 0.05$), **($P < 0.001$), ***($P < 0.0001$); error bar indicates +SD)

6.4. Coaxial Encapsulation of Islets

After determining that the purified Protanal alginate encapsulations are not harmful to the pancreatic islets and that the encapsulated islets remain viable and functional for a long period of time, the next step was to investigate if it would be possible to use the coaxial encapsulation method to create smaller functional islets to prevent necrosis after encapsulation (Figure 6.8). If this is successful, other cells could be added to the islet cells, to further optimize this platform. For instance, up to 12.5% hepatic cells could be added to the cell suspension to increase the volume of cells without diminishing the function,^[6] Sertoli cells could be added to increase islet survival due to their anti-apoptotic properties and their

immunomodulatory properties,^[7, 8] or Mesenchymal stem cells could be added to reduce fibrotic overgrowth.^[9]

Just as before, islets were handpicked from the pancreatic slurry and divided in the three groups; The first group was dissociated as stated above to form the single cell suspension, the second group was used to encapsulated as whole islets and the third group was used as controls and cultured on ULA-plates. 3000 islets were handpicked for this experiment, which was only performed once.

For the coaxial printing of the pancreatic islets, 1000 islets were resuspended in 200 μ l of a 1.2% CMC in PBS solution. Pancreatic islet cells were resuspended at a concentration of $10 \cdot 10^6$ cells/ml in 1.2% CMC in PBS solution. These solutions were used as the core solution for the core-shell beads, with 1.2% purified Protanal alginate dissolved in embryo transfer water as the shell material. Coaxial printing was done using a 19-26G needle, at a distance of 2 cm to the 25 mM isotonic BaCl_2 gelling bath, with an electric potential of 8 kV. The core material was dispensed at 5 ml/h, while the shell material was dispensed at 85 ml/h. These higher speeds were chosen to ensure there would be enough material dispensed per bead to fully encapsulate the non-dissociated islets, and to minimize the time necessary for encapsulation. After encapsulation, beads were sieved out of the gelling bath using a cell-strainer, and washed 3 times with PBS before distributing over the wells of a ULA-plate with 2 ml islet culture medium per well.

All groups were tested for viability at different time points by doing a fluorescent live / dead assay. The results of the control islets are not shown, as they were similar to those shown before (Figure 6.5). For these beads the fluorescent images were combined with the brightfield images, to show the cores of the beads.

Both the cells (Figure 6.9) and the islets (Figure 6.10) had a high viability directly after printing, but unfortunately the viability did not remain high. The encapsulated islet cells died very quickly, with most cells dead after 3 days in encapsulation, and all cells dead within 2 weeks. This is in sharp contrast with islet cells that were encapsulated solely in purified Protanal alginate, that (for one batch) still had some living cells even after 10 weeks in culture (Figure 6.6). The encapsulated whole islets fared only slightly better, with islets looking mostly normal and viable for the first week. However, after 14 days in culture some islets started to show dead cells at their periphery. The dead portion of the islets increased over time, until all islets were completely dead after roughly 3 months. First of all, this looks very similar to the timeframe of the control islets losing viability, with the difference that any dead cells shed by the control islet would be removed during medium changes, whereas any dead cells from the encapsulated islets remain within the encapsulation. This could make it look like they are losing viability sooner, as their dead cells can actually be seen. However, this does not explain the high mortality of the pancreatic islet cells that were encapsulated as a single cell suspension. They lost their viability at a much higher rate than the cells encapsulated in crosslinked alginate. Therefore it is hypothesized that the CMC as viscosity enhancer might have had a toxic effect on the pancreatic islets.

Even though the encapsulated islet cells appeared to be dead and there were some whole islets that were already losing viability, a glucose induced insulin secretion test was performed after 2 weeks, to compare them to the islets and cells encapsulated in only Protanal. As before, all insulin secreted by the islets was normalized to the insulin secretion in their first low glucose buffer. The results from this insulin secretion test were very unexpected (Figure 6.11), as both the islets and the encapsulated islet cells seem to produce less insulin in the high glucose buffer compared to the low glucose buffers. With the

stimulation index going down to 0.17 for the high buffer insulin secretion of the encapsulated islets and 0.13 for the encapsulated islet cells, this encapsulation method was not a success.

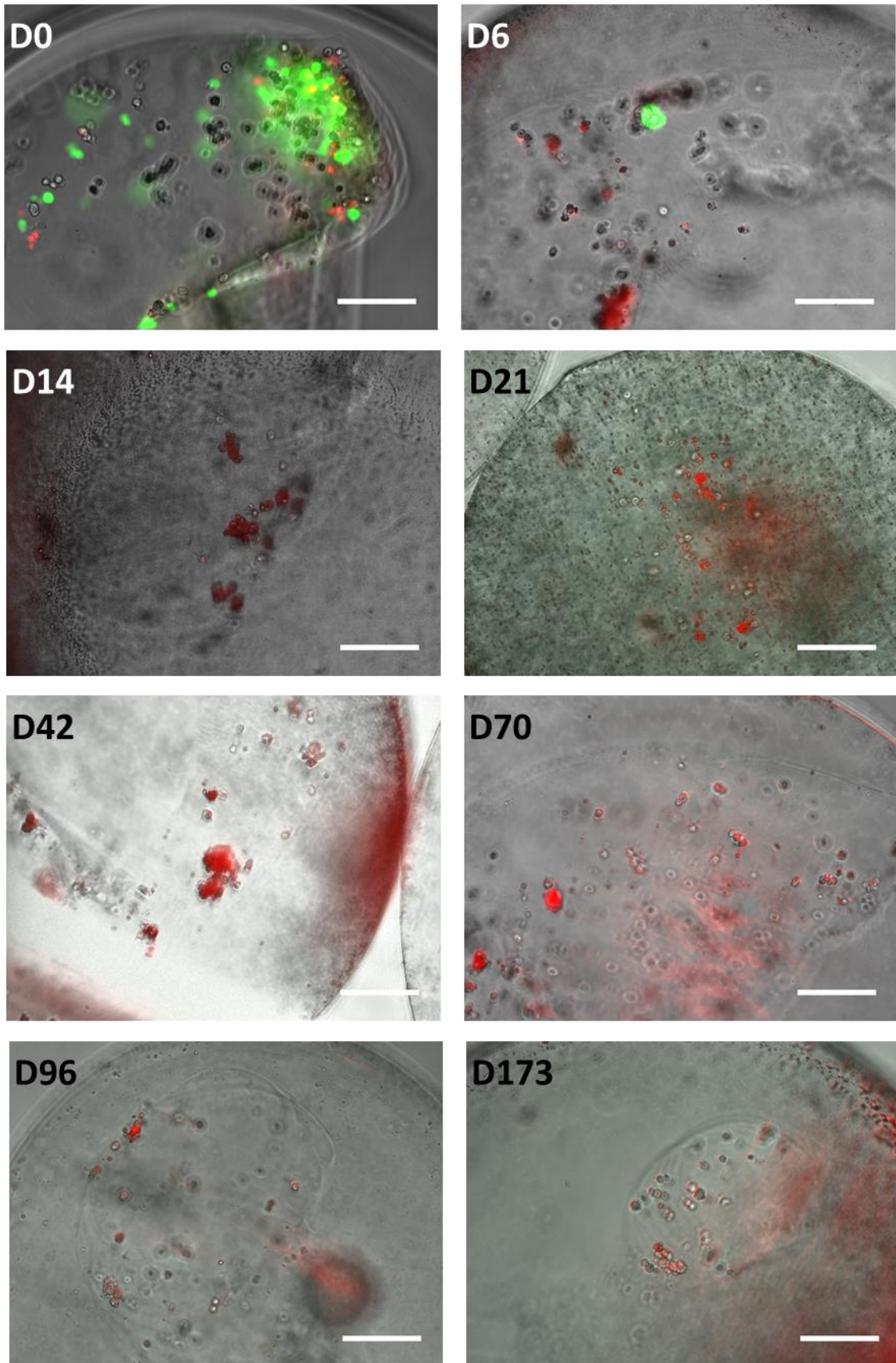


Figure 6.9: Live (green) / dead (red) staining over time on islet cells encapsulated in core-shell beads. The cells were suspended in a CMC solution in the core of Protanal alginate beads, to allow them to aggregate within the bead. Encapsulated islet cells were viable directly after printing but lose viability within days. (Scalebar 100 μm)

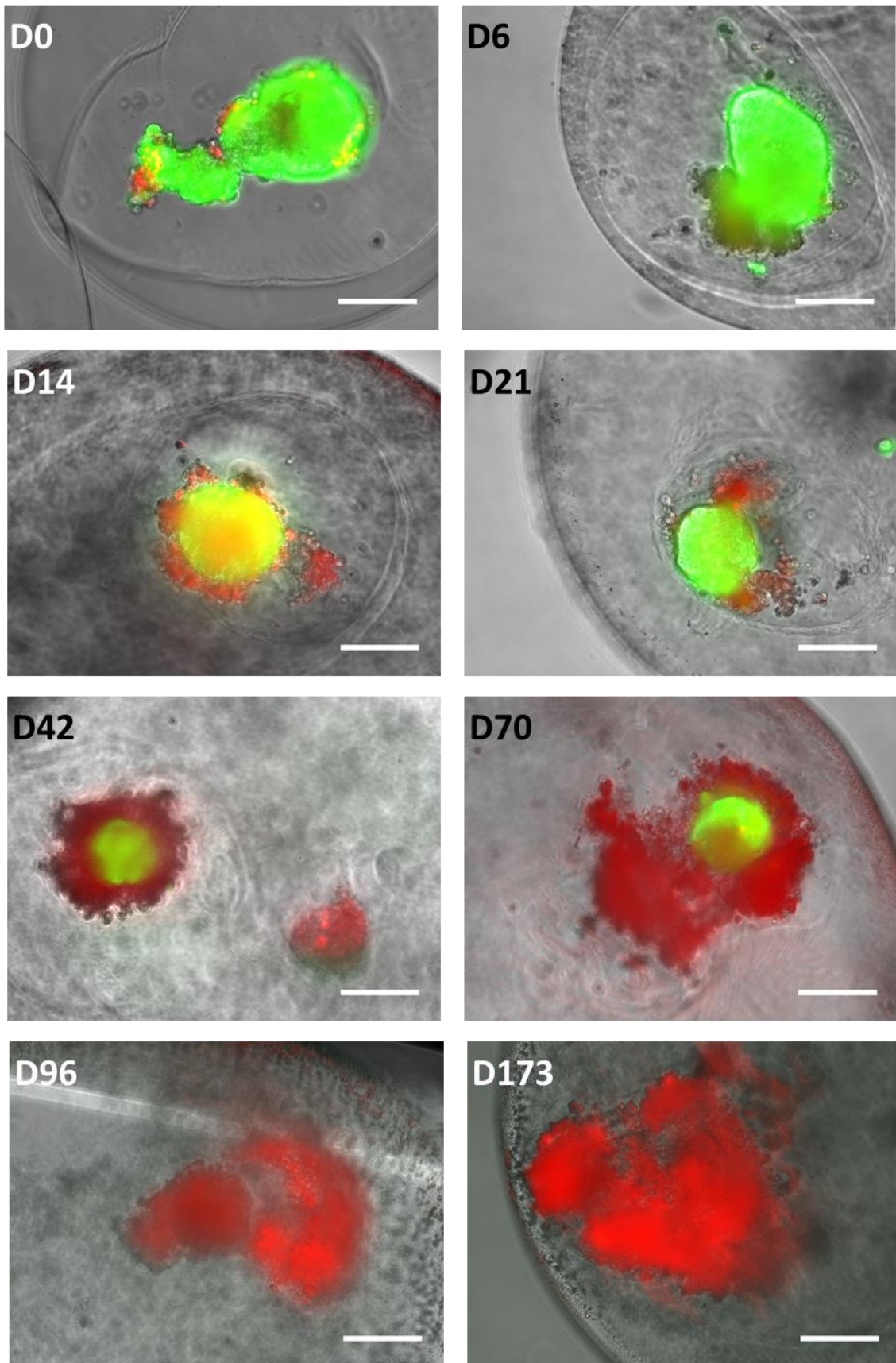


Figure 6.10: Live (green) / dead (red) staining over time on islets encapsulated in core-shell beads. The islets were suspended in a CMC solution in the core of Protanal alginate beads. Encapsulated islets lose morphology and viability over time. (Scalebar 100 μm)

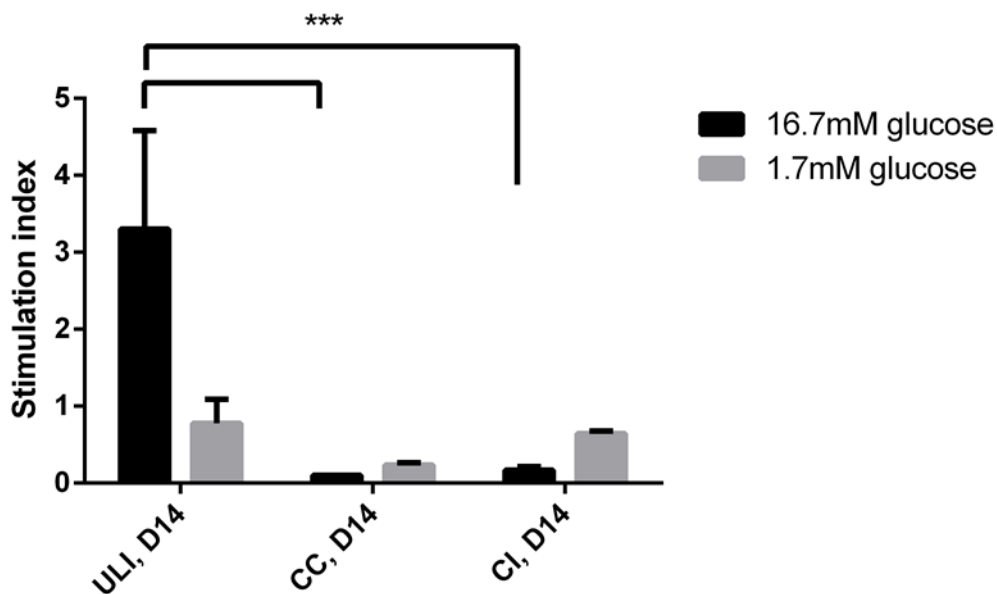


Figure 6.11: Stimulation index of high glucose (16.7 mM) and subsequently low glucose (1.7 mM) normalized to basal insulin secretion levels at 1.7 mM glucose for control islets cultured on ULA-plates (ULI), core-shell encapsulated islet cells (CC) and core-shell encapsulated islets (CI) on day 14 after encapsulation. (stars indicate statistical significant difference between the stimulation index for high glucose only; ***($P < 0.0001$); error bar indicates +SD)

To investigate the idea that the CMC has a toxic effect on the pancreatic islets, a toxicity test was performed with multiple concentrations of CMC (0.5%, 1%, 1.5% and 2% (w/v)), dissolved in islet medium. Furthermore, in case the CMC did turn out to be toxic, a back-up viscosity enhancer had to be tested. Polyethylene-glycol (PEG) is a polymer that is known to be biocompatible and is used for instance as a coating for biomedical devices to make them more biocompatible.^[10, 11] Although it does not enhance the viscosity as much as CMC or alginate (Figure 6.12) a concentration of 20% in water has roughly the same viscosity as 1% Protanal. PEG (95172, Sigma Aldrich) at different concentrations (5%, 10%, 15% and 20% (w/v), dissolved in islet medium) was used as the second material to be tested. The third material that was tested were microcarrier beads (Cytodex 3, GE Helathcare). Although they don't increase the viscosity, they could be useful as islet cells might attach to them, which could help with their aggregation. This group was more of an "out-of-the-box idea" than a

serious combatant. Just as for the other materials, multiple concentrations (1.25%, 2.5%, 3.75% and 5% (w/v) in islet medium) were tested. The last group to be tested was purified Protanal at different concentrations (0.5%, 1%, 1.5% and 2% (w/v) dissolved in islet medium), without crosslinking it. As a control, islets cultured on ULA-plates were used. For each material, at each concentration, 50 islets were handpicked and placed in the well of a 24-wells tissue culture plate in triplicate (for 3 time-points). Using a microscope to ensure no islets were accidentally aspirated, the medium was replaced with the corresponding materials. Medium/materials were replaced every 2/3 days using a microscope to ensure no islets were aspirated. For the microbead group only the medium was removed and replaced, the microbeads were left in the wells.

A live / dead assay was performed before after 1, 3 and 14 days in culture. The 14th day endpoint was chosen as this was the point where some of the islets in the CMC-core beads started to lose their viability.

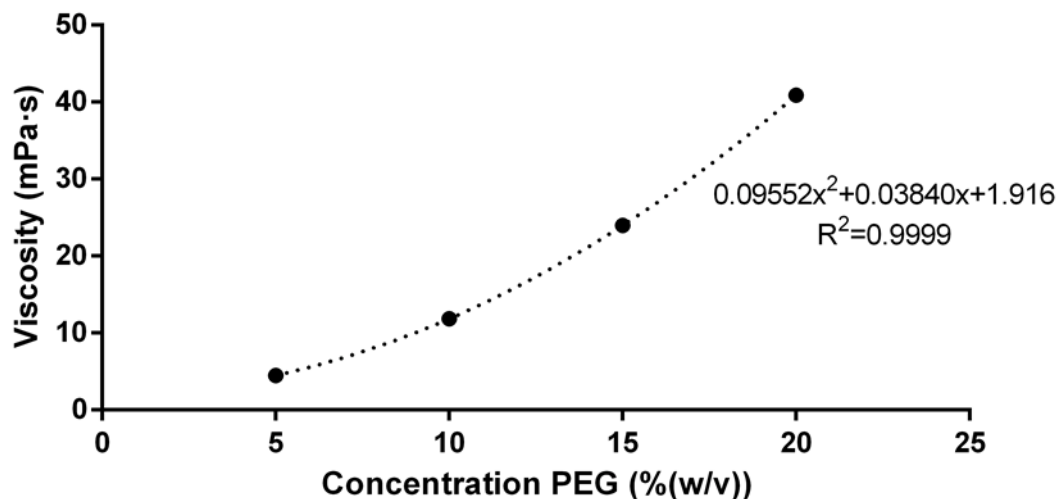


Figure 6.12: Viscosity of PEG plotted against the concentration. Trendline is plotted as a dotted line.

Islets cultured in 2% CMC died within the first 24 hours (Figure 6.13). At 1.5% dying cells could be found on the larger islets after 1 day, whereas the lower concentrations (0.5% and 1.0%) left the islets fully viable. After 3 days the islets cultured in the lowest concentration were still viable, while the islets cultured in 1.0% CMC started to show dead cells on the islets. After 14 days, islets in all concentrations were dead. It is important to note that the islets had started to attach to the tissue culture plastic and started to spread out over the bottom of the tissue culture plate, with the exception of the islets cultured in 2% CMC, as they had already died before they could attach. This experiment suggests that CMC is toxic for pancreatic islets, and that the toxicity is more severe at higher concentrations.

Islets cultured in PEG actually performed worse than the islets cultured in CMC (Figure 6.14). After 1 day in culture, only islets cultured in 5% PEG showed any cells that were still alive, all islets cultured in higher concentrations of PEG were completely dead. After 3 days the islets cultured in 5% PEG had also lost all viability, indicating that PEG is not a suitable replacement for CMC as the core material for coaxial pancreatic islet encapsulations. Especially not at the concentrations necessary to increase the viscosity of the medium enough to make it useful for the coaxial encapsulation.

The islets cultured together with the microcarrier beads were very different compared to the other materials. The microcarriers did not dissolve in the medium but were just added to the wells. Therefore, even though the live / dead staining shows that at the higher concentrations (3.75% and 5%) the islets die after 3 days (Figure 6.15), it is not necessarily connected with toxicity created by the concentration of the beads. It is more likely that it is the weight of the beads piled upon the islets which is killing the islets, not the toxicity, as one islet laying more on top of the beads than on the bottom of the well was still alive after 14 days in the 5% well

(Supplementary Data S3). Islets cultured with less beads (1.25% and 2.5%) remained viable throughout the 14 days, most likely as they were not crushed.

The last group involves islets cultured in a non-crosslinked alginate solution (Figure 6.16). although it is already shown that islets can remain viable and functional in crosslinked alginate (Figure 6.7), the influence of non-crosslinked alginate on pancreatic islets was unknown. After 1 day in culture, islets cultured in 2% purified Protanal alginate were already dead, and islets cultured in 1% and 1.5% showed some dead cells. After 3 days in culture, all the islets cultured in the 1.5% alginate solution were dead, while islets cultured in 1% were dying. After 14 days in culture only the islets cultured in 0.5% alginate were still viable, with islets cultured in 1.0% predominantly dead, with just a few life cells. This indicates that non-crosslinked alginate is also toxic for islets at higher concentrations. It is interesting to note that unlike the islets cultured in CMC, the islets cultured in alginate did not attach to the bottom of the tissue culture wells.

From these experiments it was concluded that both CMC and PEG could not be used as a viscosity enhancer, as they were toxic to the islets. Encapsulating with the microcarrier beads was tried, but unfortunately did not work as the beads would get stuck in the needle, coming out in big clumps at a time (Supplementary Data S4). Using alginate as both the core and the shell material was also deemed to not be a good solution, as there was no easy way to ensure the core to remain liquid with only the shell crosslinking in the gelling bath.

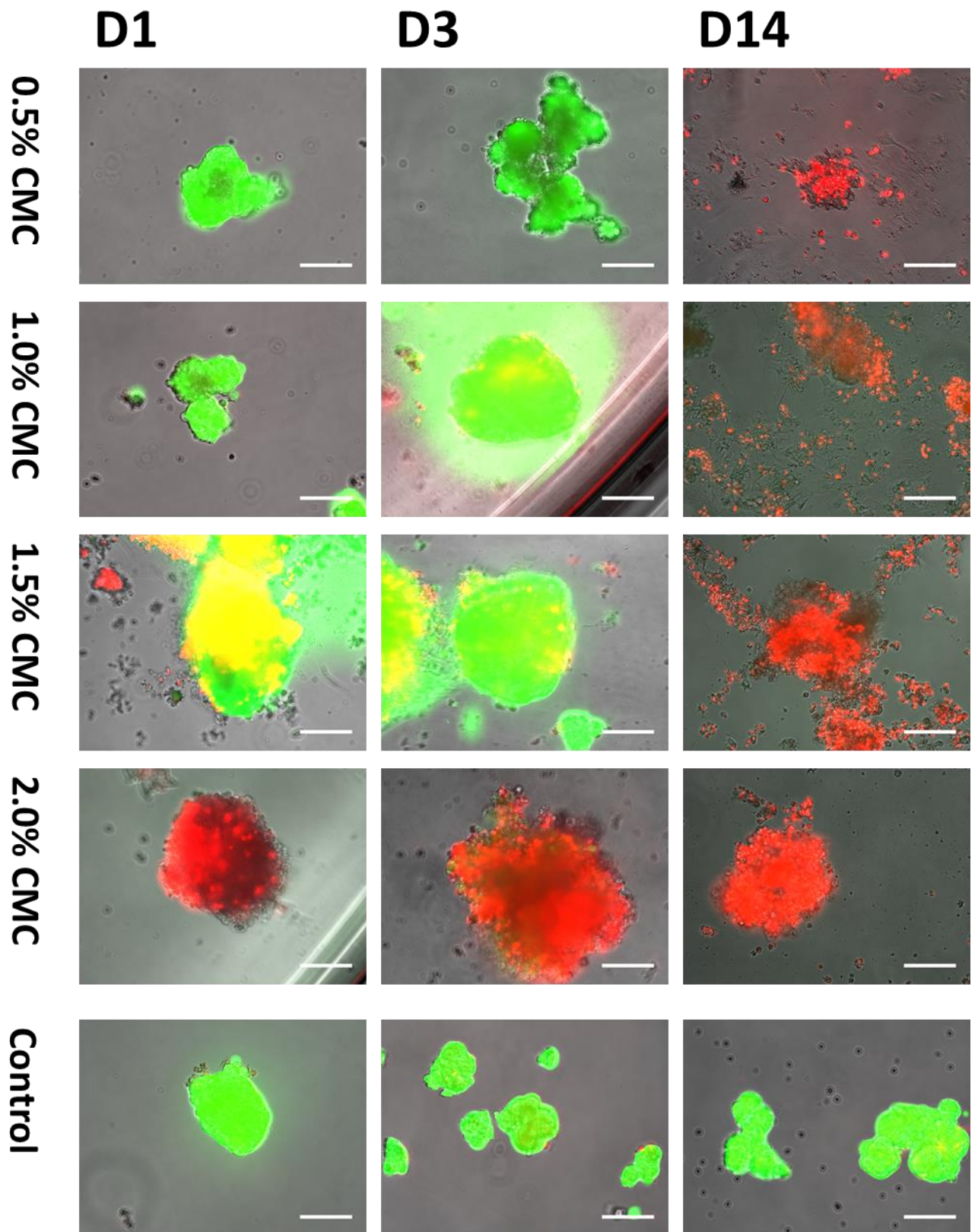


Figure 6.13: Live (green) / dead (red) staining over time on islets cultured in different concentrations of CMC. Control islets were cultured in islet medium on ULA-plates. CMC appears to be toxic to pancreatic islets, with higher concentrations killing the islets in less time. (Scalebar 100 μ m)

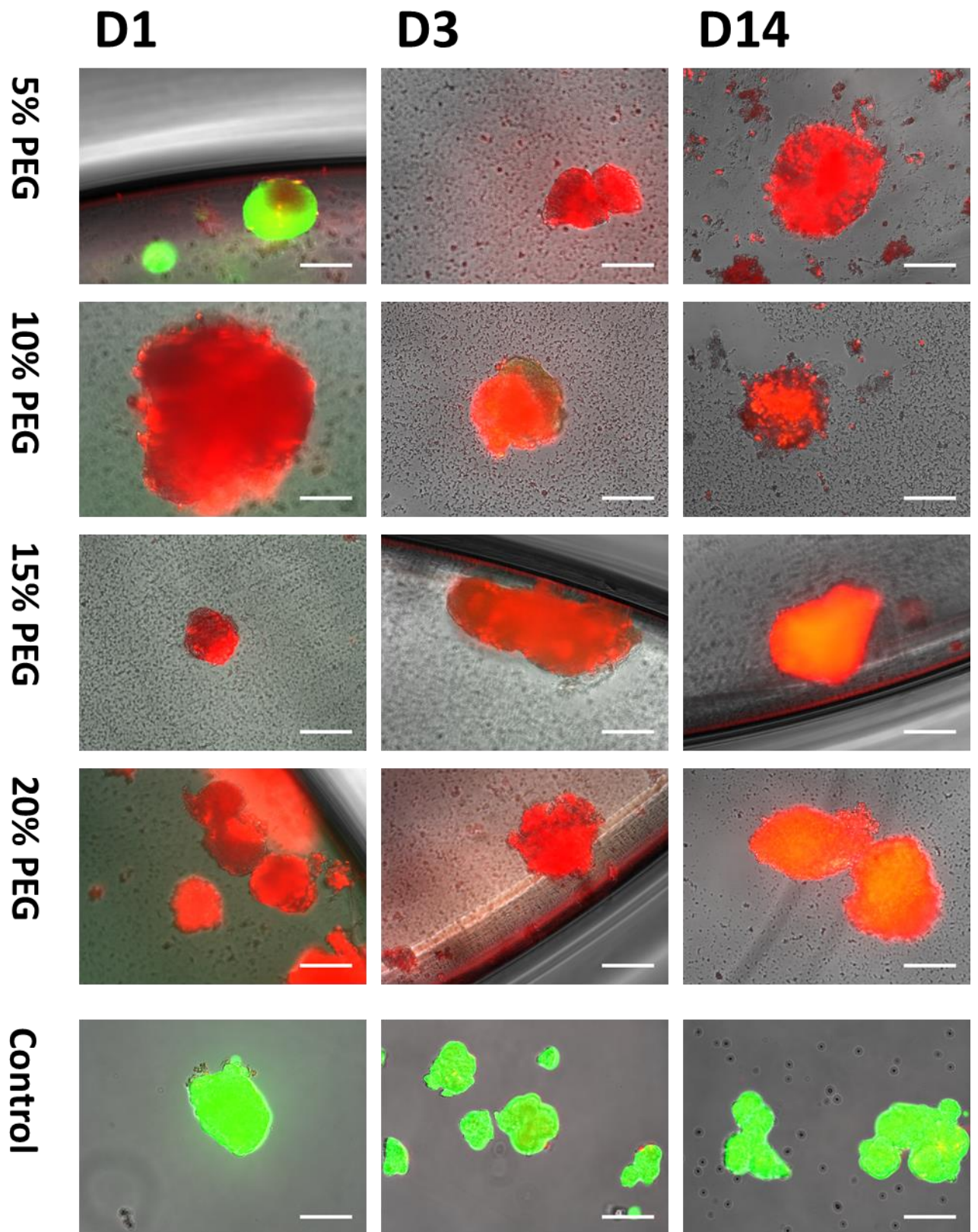


Figure 6.14: Live (green) / dead (red) staining over time on islets cultured in different concentrations of PEG. Control islets were cultured in islet medium on ULA- plates. PEG appears to be toxic to pancreatic islets, killing islets within 3 days for all concentrations. (Scalebar 100 μm)

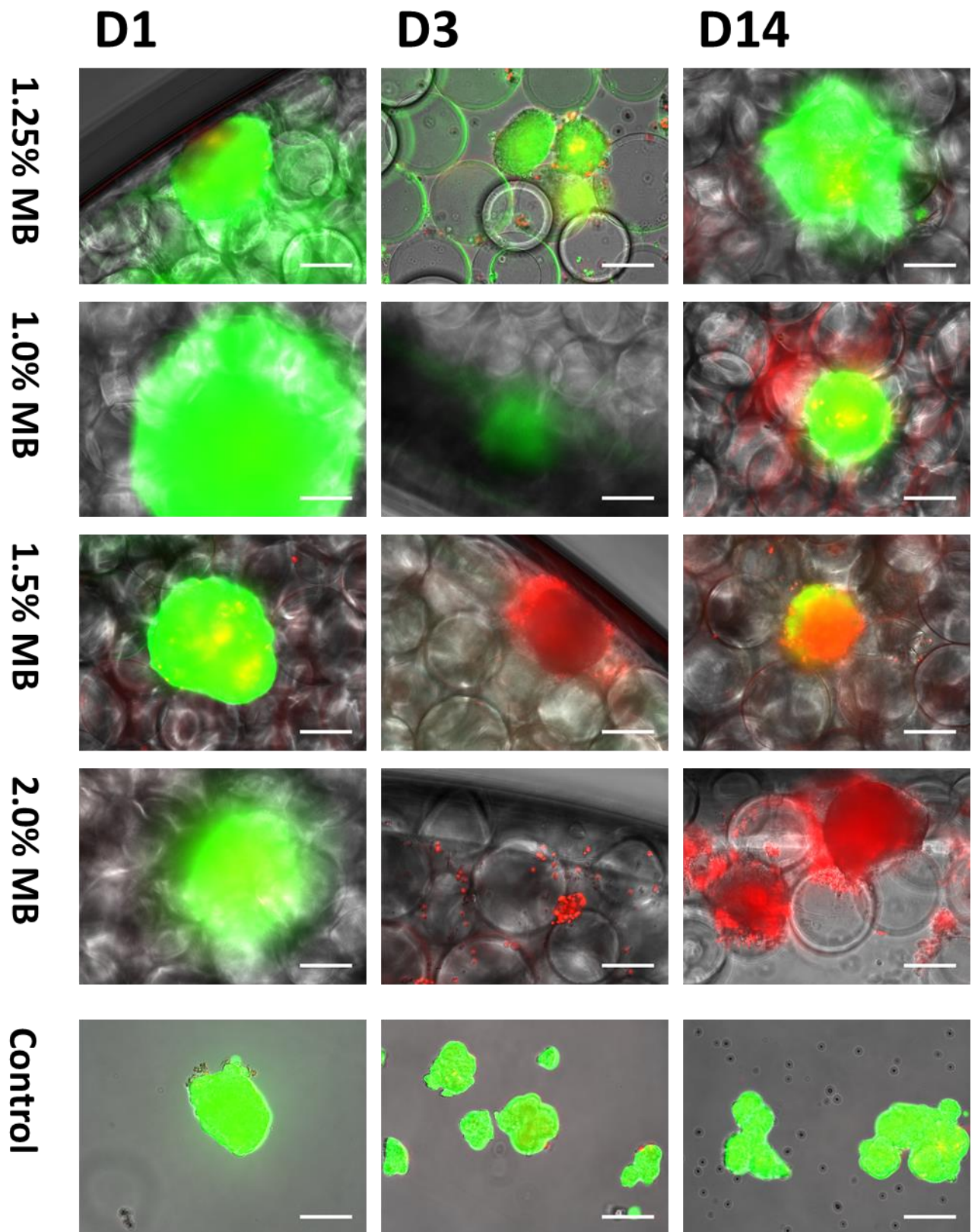


Figure 6.15: Live (green) / dead (red) staining over time on islets cultured in different concentrations of microcarrier beads (MB). Control islets were cultured in islet medium on ULA-plates. At higher concentrations islets cultured with the microcarrier beads died over time, but this could be due to the pressure of the beads on the islets, rather than toxicity.

(Scalebar 100 μ m)

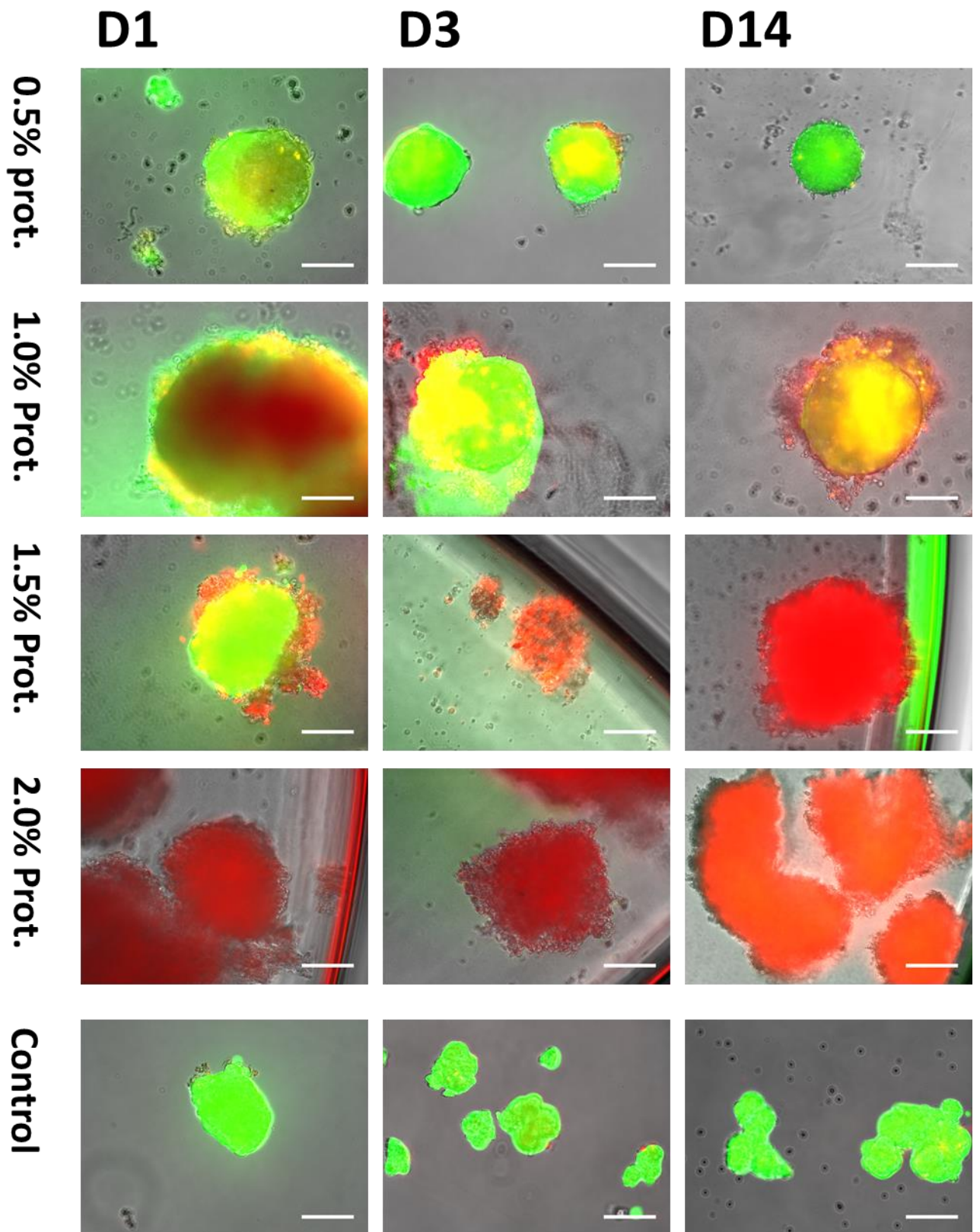


Figure 6.16: Live (green) / dead (red) staining over time on islets cultured in different concentrations of purified Protanal alginate. Control islets were cultured in islet medium on ULA- plates. Non-crosslinked alginate appears to be toxic to pancreatic islets at higher concentrations. (Scalebar 100 μ m)

6.5. Conclusion

In this chapter the use of the micro-encapsulator to encapsulate pancreatic islets was investigated. It was found that this method of encapsulation is an easy way to create encapsulated pancreatic islets with uniform encapsulations. Islets encapsulated in this way were viable and functional for at least 3 months *in vitro*. It was found that islets can be dissociated gently by using Trypsin+EDTA to create a single cell suspension of pancreatic islet cells. When these single cells are encapsulated in Protanal alginate, they also remain viable for a few weeks, but they are not functional and eventually lose their viability.

The core-shell encapsulation method was used on (dissociated) islets to test whether this method could be used to produce more, smaller, encapsulated islets out of dissociated bigger islets in a one step process. Unfortunately, this encapsulation method was not successful with the pancreatic islets. It was found that the viscosity enhancer CMC that was used for the core material was toxic to them. A small toxicity test was performed including a different viscosity enhancer (PEG), microcarrier beads and non-crosslinked Protanal. All these were toxic at high concentrations, but the Protanal and microcarrier beads provided viable environments at lower concentrations for the pancreatic islets to survive for at least 14 days. However, neither of these were useful to be used in a liquid core system, as the beads blocked up the needle and it was deemed nearly impossible to time the crosslinking process in such a way that a core of alginate would maintain liquid while only the shell would be crosslinked.

More research should be done towards viscous materials that can be used as a core material, while maintaining a viable environment for the islet cells.

6.6. References

- [1]. Benhamou PY, Oberholzer J, Toso C, Kessler L, Penfornis A, Bayle F, *et al.* Human islet transplantation network for the treatment of Type I diabetes: first data from the Swiss-French GRAGIL consortium (1999–2000). *Diabetologia*. **2001**;44(7):859-64.
- [2]. Konstantinova I, Nikolova G, Ohara-Imaizumi M, Meda P, Kučera T, Zarbalis K, *et al.* EphA-Ephrin-A-Mediated β Cell Communication Regulates Insulin Secretion from Pancreatic Islets. *Cell*. **2007**;129(2):359-70.
- [3]. Smolen P, Rinzel J, Sherman A. Why pancreatic islets burst but single beta cells do not. The heterogeneity hypothesis. *Biophysical Journal*. **1993**;64(6):1668-80.
- [4]. Rackham CL, Jones PM, King AJF. Maintenance of Islet Morphology Is Beneficial for Transplantation Outcome in Diabetic Mice. *PLoS One*. **2013**;8(2):e57844.
- [5]. Hammar E, Parnaud G, Bosco D, Perriraz N, Maedler K, Donath M, *et al.* Extracellular Matrix Protects Pancreatic β -Cells Against Apoptosis. *Role of Short- and Long-Term Signaling Pathways*. **2004**;53(8):2034-41.
- [6]. Jun Y, Kang AR, Lee JS, Jeong GS, Ju J, Lee DY, *et al.* 3D co-culturing model of primary pancreatic islets and hepatocytes in hybrid spheroid to overcome pancreatic cell shortage. *Biomaterials*. **2013**;34(15):3784-94.
- [7]. Luca G, Calafiore R, Basta G, Ricci M, Calvitti M, Neri L, *et al.* Improved function of rat islets upon co-microencapsulation with Sertoli's cells in alginate/poly-L-ornithine. *AAPS PharmSciTech*. **2001**;2(3):48-54.
- [8]. Perez - Basterrechea M, Esteban MM, Vega JA, Obaya AJ. Tissue - engineering approaches in pancreatic islet transplantation. *Biotechnology and Bioengineering*. **2018**.
- [9]. Vaithilingam V, Evans MDM, Lewy DM, Bean PA, Bal S, Tuch BE. Co-encapsulation and co-transplantation of mesenchymal stem cells reduces pericapsular fibrosis and improves encapsulated islet survival and function when allografted. *Scientific Reports*. **2017**;7(1):10059.
- [10]. Manzoli V, Villa C, Bayer AL, Morales LC, Molano RD, Torrente Y, *et al.* Immunoisolation of murine islet allografts in vascularized sites through conformal coating with polyethylene glycol. *American Journal of Transplantation*. **2018**;18(3):590-603.
- [11]. Rao L, Zhou H, Li T, Li C, Duan YY. Polyethylene glycol-containing polyurethane hydrogel coatings for improving the biocompatibility of neural electrodes. *Acta Biomaterialia*. **2012**;8(6):2233-42.

Chapter 7

Towards a Pancreatic Islet Patch

7.1. Introduction

The current transplantation method of pancreatic islets injects the islets into the portal vein, delivering them to the liver.^[1] The main advantages of transplantation in this manner is the ease of access, which allows for minor invasive surgery and the resulting low morbidity rate, with rates of bleeding and/or thrombosis <10%.^[3] However, the liver might not be the optimal transplantation site, with some researchers reporting more than 50% islet mortality within minutes after transplantation.^[4] Drawbacks of using the liver as the transplantation location are the low oxygen tension compared to that of the pancreas (3-8 mmHg vs. ~30 mmHG),^[5] increased levels of immunosuppressants in the liver hampering the function of beta cells,^[6] and the immediate blood mediated immune reaction (IBMIR), which is characterized by activation of the coagulation and rapid binding of platelets to the infused islets.^[7] Furthermore, after the islets are injected they spread throughout the liver, making it impossible to check on them by doing a puncture, or retrieve them,^[6] something that is especially important when introducing foreign materials to the body (for instance, encapsulations). Therefore, extrahepatic transplantation sites have been reviewed,^[8] such as intramuscular^[9] or subcutaneous,^[10] with macro-devices to retrieve the islets to assess beta cell survival after transplantation. A disadvantage of macro-devices is the large diffusion distance, resulting in a lack of nutrition and oxygen for the cells^[11] and a delay in reaction on changes in blood sugar levels.^[12] Using 3D bioprinting techniques, macro-devices made from hydrogels can be designed with a shape and porosity that decreases diffusion distance and increases the surface area/volume ratio compared to traditional fabricated macro-devices, carrying a clinically relevant amount of islets that can be transplanted as a single device.^[13]

Endogenous pancreatic islets are highly vascularized tissues, with a capillary network that is five to ten times denser than that of the exocrine pancreas,^[14] ensuring that every cell within

the islet is not more than 1 cell separated from arterial blood.^[15] However, after isolation pancreatic islets are no longer vascularized and encapsulation of the islets prevents any revascularisation.^[16] Therefore, encapsulated islets are completely depended on diffusion to get their nutrients and oxygen. Transplantation in a highly vascularized area is therefore a must. These highly vascularised areas can even be created artificially (pre-transplantation) with the aid of localized growth factors.^[17, 18]

In this chapter the use of 3D bioprinting methods to create a “pancreatic islet patch” (Figure 7.1) is investigated. The idea behind the patch is to localize the islets in one certain area, making it easier to transplant as a single construct and easier to retrieve them after transplantation. If possible, the patch should increase vascularization locally and thereby create a better environment for the transplanted islets. Since most of this chapter is a “proof of concept”, most experiments were only performed once, with the exception of the experiments in 7.4, which were performed three times.

Initial printing was done using alginate as the patch material, but as this material is not known for its vascularization properties, a patch made from collagen was created. To allow the use of the less printable collagen, moulds were printed out of a sacrificial Pluronic hydrogel, which could be dissolved and removed after the patch material had fully gelled. This was used to create patches of both alginate and collagen, with or without vascular endothelial growth factor (VEGF). These patches were then investigated for their ability to increase vascularisation surrounding potential encapsulated islets within the patch, using the chicken egg chorioallantoic membrane (CAM) assay.

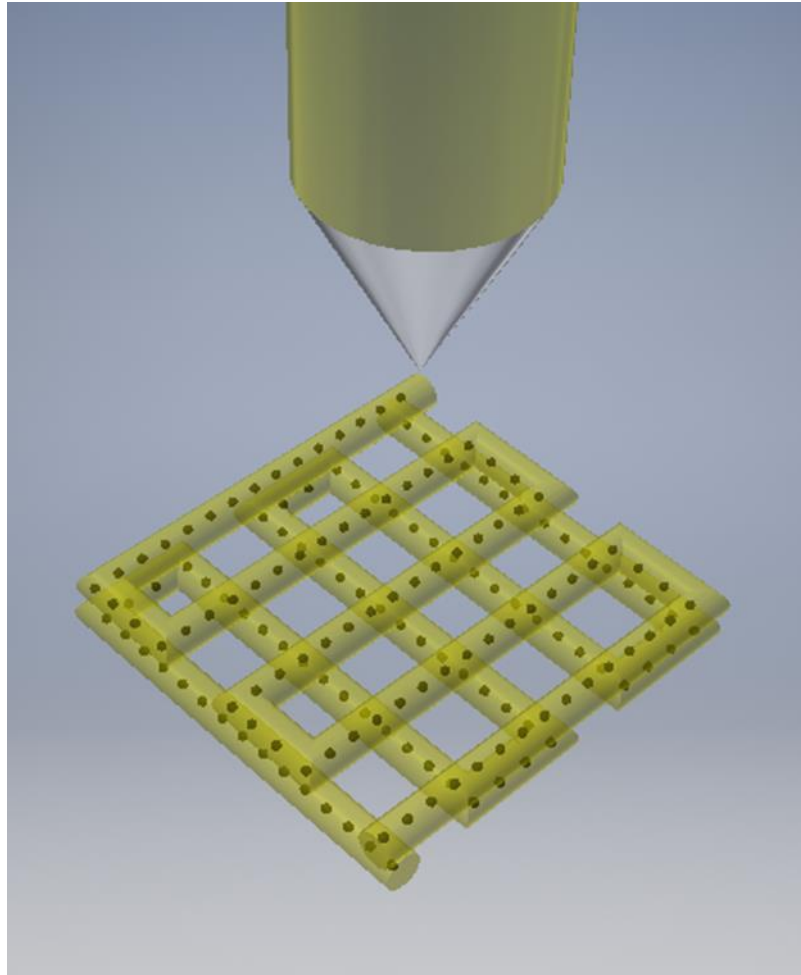


Figure 7.1: In this chapter the use of 3D bioprinting technologies to create a patch of clinically relevant size, that will hold all the encapsulated islets for transplantation, and might even aid in creating a highly vascularized environment surrounding the islet is investigated.

7.2. 3D Bioprinting Patches

The field of 3D bioprinting has undergone rapid development in the past few years for applications in tissue engineering and regenerative medicine.^[19] A variety of 3D bioprinting techniques has been developed for the 3D deposition of cell-laden hydrogels, such as inkjet bioprinting,^[20] valve based bioprinting^[21] and extrusion based bioprinting.^[22] It has been shown that 3D bioprinting of porous structures has been beneficial and enhanced cell viability and metabolic activity compared to bulk constructs.^[23] In this section extrusion bioprinting was investigated as a method to fabricate 3D constructs with a clinically relevant

size. Initially, alginate was used as the hydrogel of choice for the creation of these “patches”. As alginate is liquid until it is crosslinked, it is hard to print with pure alginate. Using high concentrations is a possibility,^[13] but a pre-crosslink alginate as described by Ghanizadeh et al.^[24] was preferred to create a paste like material.

To create the pre-crosslinked bio-ink, 2% purified Protanal was mixed 1:1 with 20 mM CaCl₂ to form a paste like consistency with a final concentration of 1% alginate and 10 mM CaCl₂. This pre-crosslinked bio-ink was thick enough to print a large patch in a “wood stack” pattern (Figure 7.2). After every second layer the structure was sprayed (by hand) with a 100 mM

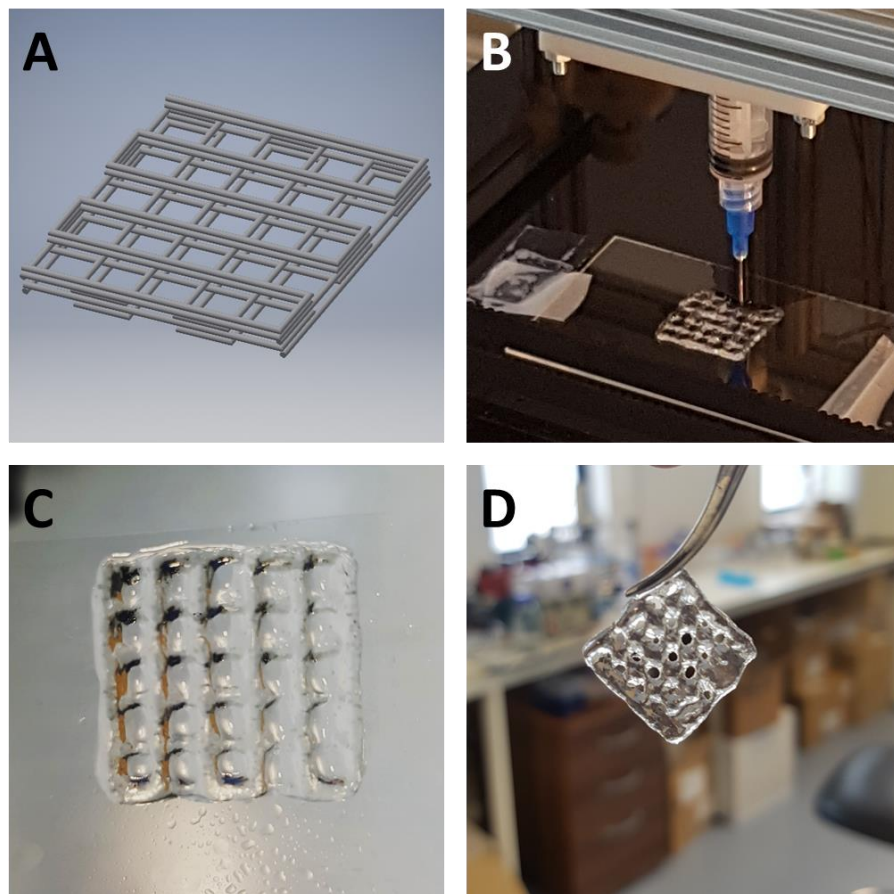


Figure 7.2: Alginate was used to bioprint larger, mechanically stable structures. A: The 3D model recreated by the 3D bioprinter. B: The 3D Bioprinter depositing the pre-crosslinked alginate in the defined shape. C: The patch directly after printing and submerging in the crosslinking solution. D: The resulting structure is mechanically stable and strong enough to be picked up.

CaCl₂ solution, to further crosslink the alginate and provide the structure with more mechanical stability. After the print was completed the entire structure was immersed in a 100 mM CaCl₂ solution to fully crosslink the entire structure. The result was a mechanically stable (Figure 7.2 D) patch made from alginate.

After proving the concept of bioprinting the patches, a few things had to be investigated; first of all, does the printing still work when encapsulated islets are mixed in with the bio-ink, and does the alginate allow for the survival (and preferably, mobility) of cells?

To answer the first question, empty alginate beads were mixed in with the bio-ink to see how it would print. 1.2% Protanal alginate mixed with activated charcoal for visibility was electro-sprayed through a 30G needle at a speed of 1 ml/h, at a distance of 1 cm to the 25 mM Isotonic BaCl₂ gelling bath, with an electric potential of 7 kV. The beads were thoroughly washed with PBS and were kept in PBS overnight to fully wash away any loose ions before suspending them in the 1% purified Protanal/ 10 mM CaCl₂ bio-ink at a concentration of 10.000 beads/ml. The thorough washing was necessary to ensure that the bio-ink will not crosslink further as soon as it comes in contact with the beads. The bio-ink containing the beads was loaded into the bioprinter and used to print the same “wood stack” figure as before, without any problem (Figure 7.3), showing that the creation of a patch to localize the encapsulated islets to one particular area is possible.

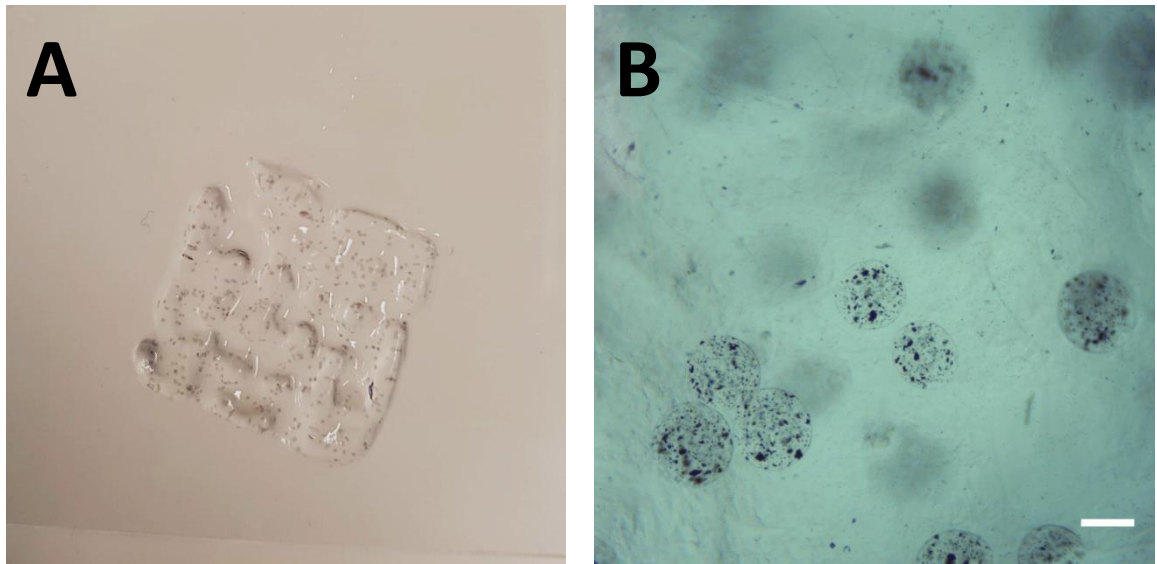


Figure 7.3: Adding alginate beads to the bio-ink doesn't influence the printability of the bio-ink. A: The patch directly after printing and submerging in the crosslinking solution. B: Microscopic image of beads within the patch. (Scalebar 200 μm)

To see if the patch would allow the survival (and preferable, mobility) of cells, a set of patches was printed with HepaRG cells incorporated into the bio-ink, and a live / dead staining was performed at different time points to check on the viability of the cells. HepaRG cells were resuspended at a concentration of $10 \cdot 10^6$ cells in the 1% purified Protanal/ 10 mM CaCl_2 bio-ink. The bio-ink was loaded into the bioprinter and used to print the same “wood stack” figure as before, but this time with cells incorporated (Figure 7.4). When doing a live / dead staining, part of the patches would be cut off using a sterile scalpel and transferred into a different plate before doing the staining. The live / dead staining shows that the HepaRG cells are viable directly after printing and maintain their viability for 2 weeks (Figure 7.4). However, they do not seem to be able to move through the alginate and after 3 weeks in culture the viability went down significantly. It is hypothesized that the alginate restricts the cells so much that they can not migrate or have room to proliferate, which in turn results in apoptosis over time. Since these HepaRG cells are not able to migrate through the patch, it seems very

unlikely that blood vessels will be able to migrate in. Furthermore, in the research done by Marchioli et al.^[13] it was shown that islets bioprinted in alginate were no longer functional, although this could be due to the CaCl_2 needed for crosslinking, not the alginate itself.

It was found that alginate was not suitable as a material for the creation of these patches and collagen was looked into as a replacement. However, it was found almost impossible to directly print using a collagen solution. Collagen solutions can be kept liquid at cold temperatures, but start gelling at higher temperatures. When trying to print with liquid collagen, it was too liquid to keep any form when printed. (Figure 7.5 A) However, when allowing the collagen to gel before trying to print it, it was either too inhomogeneous to print (Figure 7.5 B), or the collagen would clog up the needle and only the liquid within the hydrogel would be squeezed out. Therefore, another solution had to be found to use collagen as the patch material.

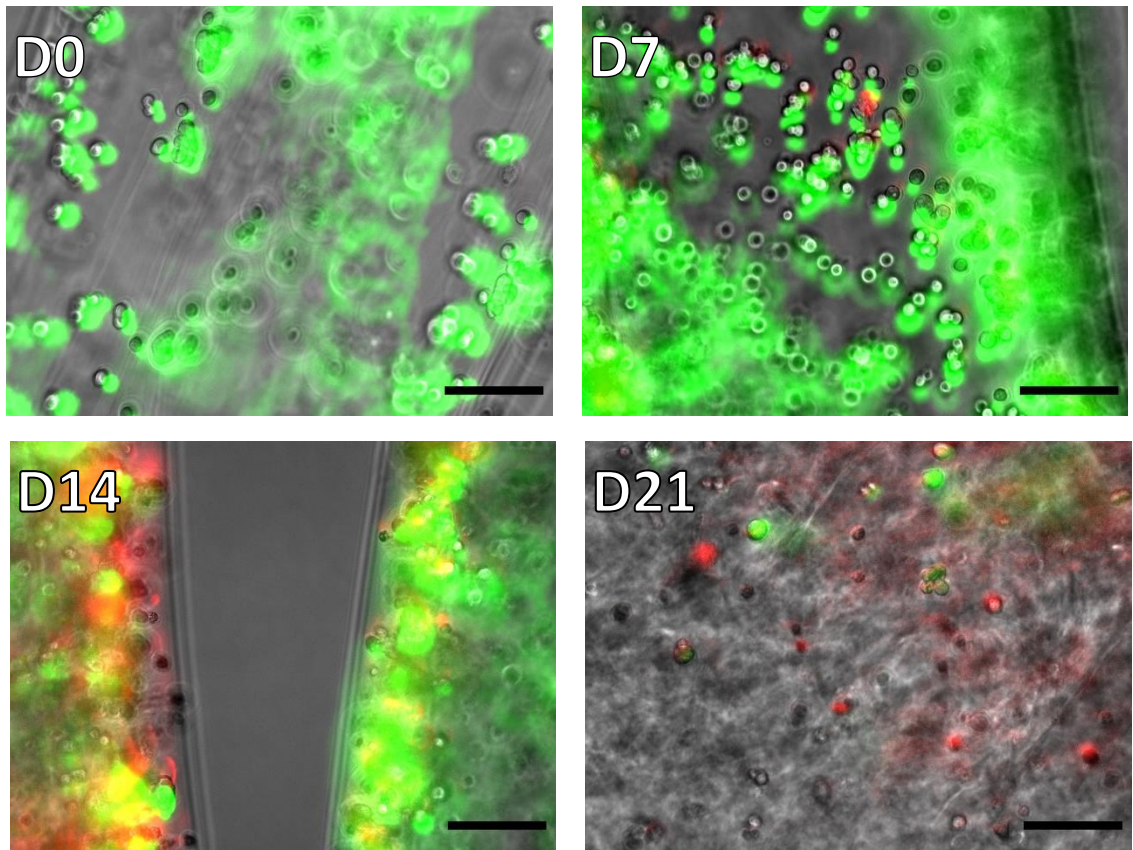


Figure 7.4: Live (green) / dead (red) staining on pieces of 3D bioprinted HepaRG cells in Protanal alginate. Although the bioprinting did not seem to have a negative influence on the viability of the HepaRG cells, they start losing their viability over time in the alginate. (Scalebar 100 μm)

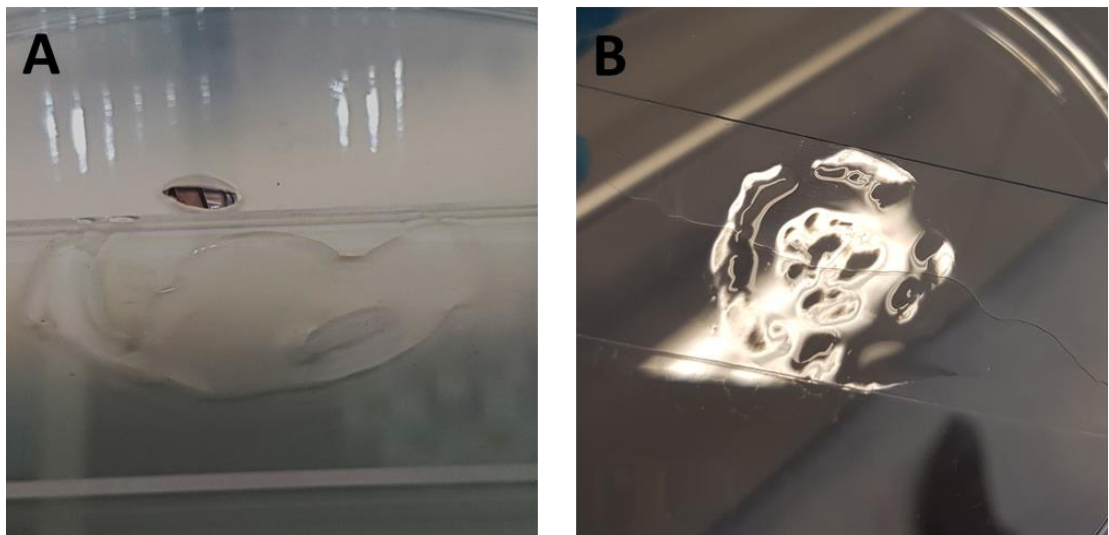


Figure 7.5: Trials with printing collagen in a concentric circle pattern. A: 4 mg/ml collagen printed when it is cold and still liquid. The collagen was too liquid to form any structure B: 4 mg/ml collagen printed after it was allowed to gel in the syringe. The collagen came out in small lumps instead of a continuous material, and eventually blocked the nozzle.

7.3. 3D Moulding Patches

To use collagen as a material for the creation of the patches, a different fabrication method had to be used. Instead of printing collagen directly, a Pluronic hydrogel was used to print moulds which were then used to fabricate the collagen patches. Pluronic (a triblock copolymer consisting of poly(ethylene oxide) - poly(propylene oxide) – poly(ethylene oxide) (PEO-PPO-PEO)) is a thermo-sensitive hydrogel, that will undergo a sol-gel transformation when the temperature gets above its lower critical gelling temperature.^[25] This is a reversible process, which means that once the gels temperature is lowered beneath this transition temperature, it will turn liquid again. Furthermore, this transition temperature can be tailored by changing the concentration of the Pluronic in the hydrogel.^[25] At lower concentrations (up to 5%) Pluronic is not cytotoxic but at higher concentration its membrane penetrating properties do make it toxic for cells.^[26] Pluronic hydrogels are among the best printable hydrogels around due to the nature of their micellar-packing gelation, which allows it to be moved and shifted easily, but its poor mechanical strength, toxicity and its tendency to dissolve in aqueous solutions make it unsuitable as material to be used as a scaffold for tissue engineering or cell encapsulation.^[27] However, its good printability in combination with its thermo-reversible gelation, makes it a perfect material to be used as a sacrificial material (for instance, to make channels in a larger construct),^[28] or as temporary mould.^[29]

In this section the use of Pluronic hydrogel as a mould to create collagen hydrogel patches is investigated. In this research a Pluronic hydrogel with added CaCl₂ was used so it could also be utilized for moulding alginate structures, where the liquid alginate solution would start crosslinking as soon as it was placed in the mould. Through trial and error (Supplemental Data S5) it was found that the collagen gelled more evenly in the Pluronic moulds with added CaCl₂ compared to their gelling in moulds made with just Pluronic.

Pluronic moulds were made by 3D printing 30% (w/v) Pluronic with 100 mM CaCl₂ in a petri dish in an array consisting out of an outer enclosure and multiple pillars, leaving a “lattice” to be filled with either collagen or alginate (Figure 7.6). A smaller lattice was used for these moulds compared to the bioprinted structures, as the mould needed larger gaps between the pillars than the actual desired width so the pillars would not to fuse together during the printing process. Solutions of either 1% purified Protanal alginate or 4 mg/ml collagen were then pipetted into the moulds and allowed to gel in the incubator for 30 minutes. The Pluronic mould would then be washed away by using either a cold (4° C) isotonic 100mM CaCl₂ solution (for the alginate patches) or a cold PBS solution (for the collagen patches). After swirling the petri dishes around a few times (putting them on ice if necessary) the Pluronic moulds were dissolved, and the patches could be transferred to a 6 well plate with fresh, preheated medium. While it was impossible to directly bioprint collagen in the desired form, the moulding process allowed for the creation of custom shaped collagen patches (Figure 7.6).

To see if HepaRG cells would thrive better in collagen than in alginate structures, they were added to the collagen hydrogel (10*10⁶ cells/ml) before moulding. Initially, the HepaRG cells did not do as well as with the bioprinting (Figure 7.7), which could be due to a multitude of reasons. First of all, the cells undergo a lot of very rapid temperature changes in a small amount of time. They are taken from the plate at 37°C, to be mixed into collagen that was kept on ice, followed by incubation at 37°C, followed by a wash in 4°C PBS before they finally are cultured at 37°C. On top of this they are in close proximity to a high concentration of Pluronic, which is known to be toxic at high concentrations. However, due to the fact that the cell death is not solely restricted to the edges of the collagen (where cells would be in contact with the pluronic hydrogel) but can be seen throughout the structure, the Pluronic hydrogel is probably not the main culprit.

After only a few days, the HepaRG cells are no longer rounded in the biomaterial, but show a variety of shapes. This would indicate that the cells can attach to their surroundings. Furthermore, within a week a few clusters of cells can be seen. Since the cells were printed as a single cell

suspension, this seems to indicate that they either migrate towards each other or can proliferate within the structure. Furthermore, the cells start to show extensions in different direction, which could not be seen for the cells in the alginate hydrogel and indicates that these cells can at least attach to the matrix and might migrate through the material. This means that any in grow of endothelial cells (blood vessels) may be possible.

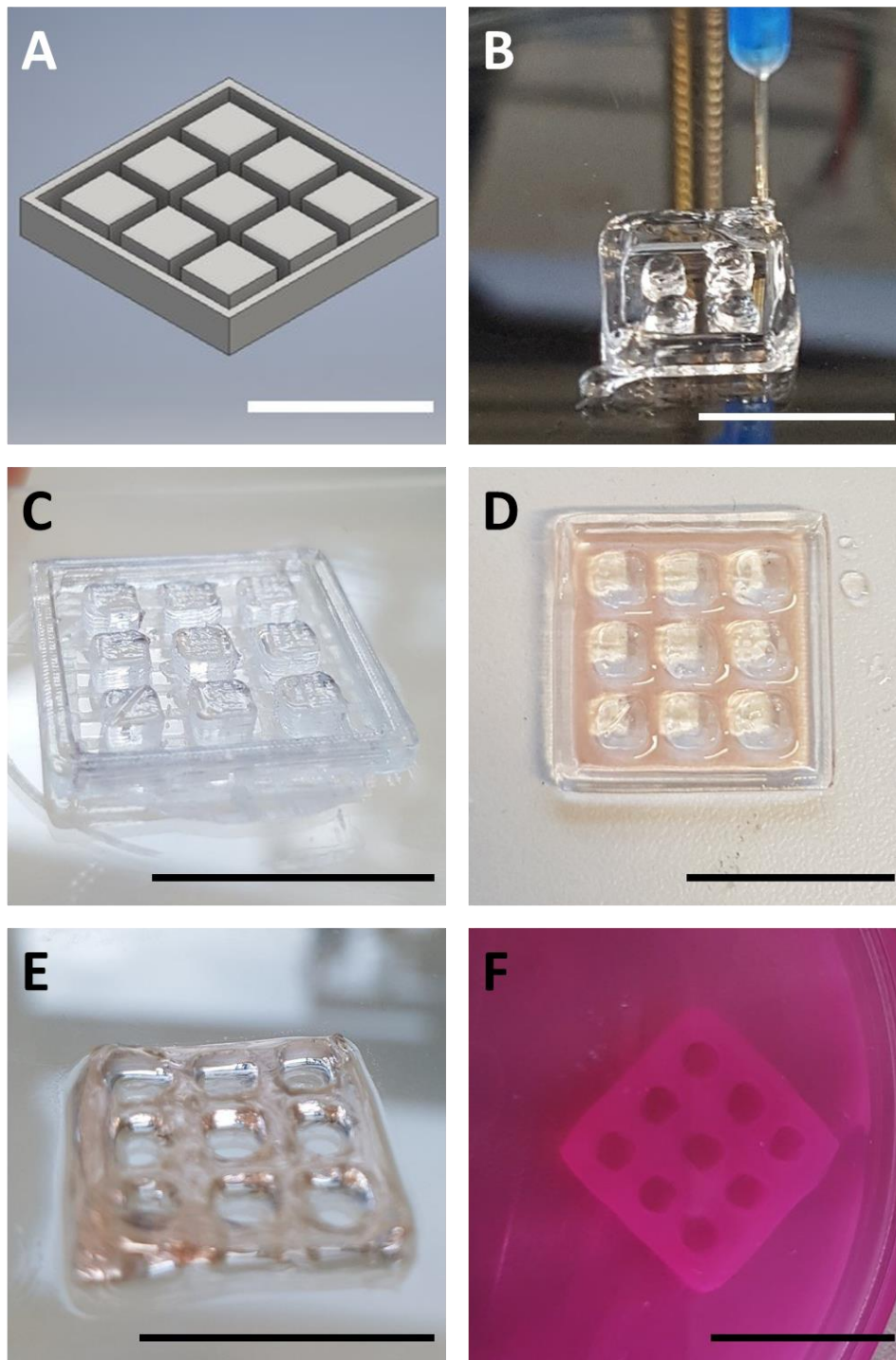


Figure 7.6: Using Pluronic as a sacrificial mould, collagen could be used to create structures in custom shapes. A: A 3D model of a mould to be printed by the 3D printer, consisting of an outer enclosure and multiple pillars. B: The 3D bioprinter printing the mould out of Pluronic. C: The finished Pluronic mould. D: 4 mg/ml collagen was pipetted into the mould and allowed to set in the incubator for 30 minutes. E: After washing away the Pluronic with cold PBS, the collagen structure is left. F: After washing away the Pluronic, the collagen structure can be transferred into prewarmed media. (Scalebar 1cm)

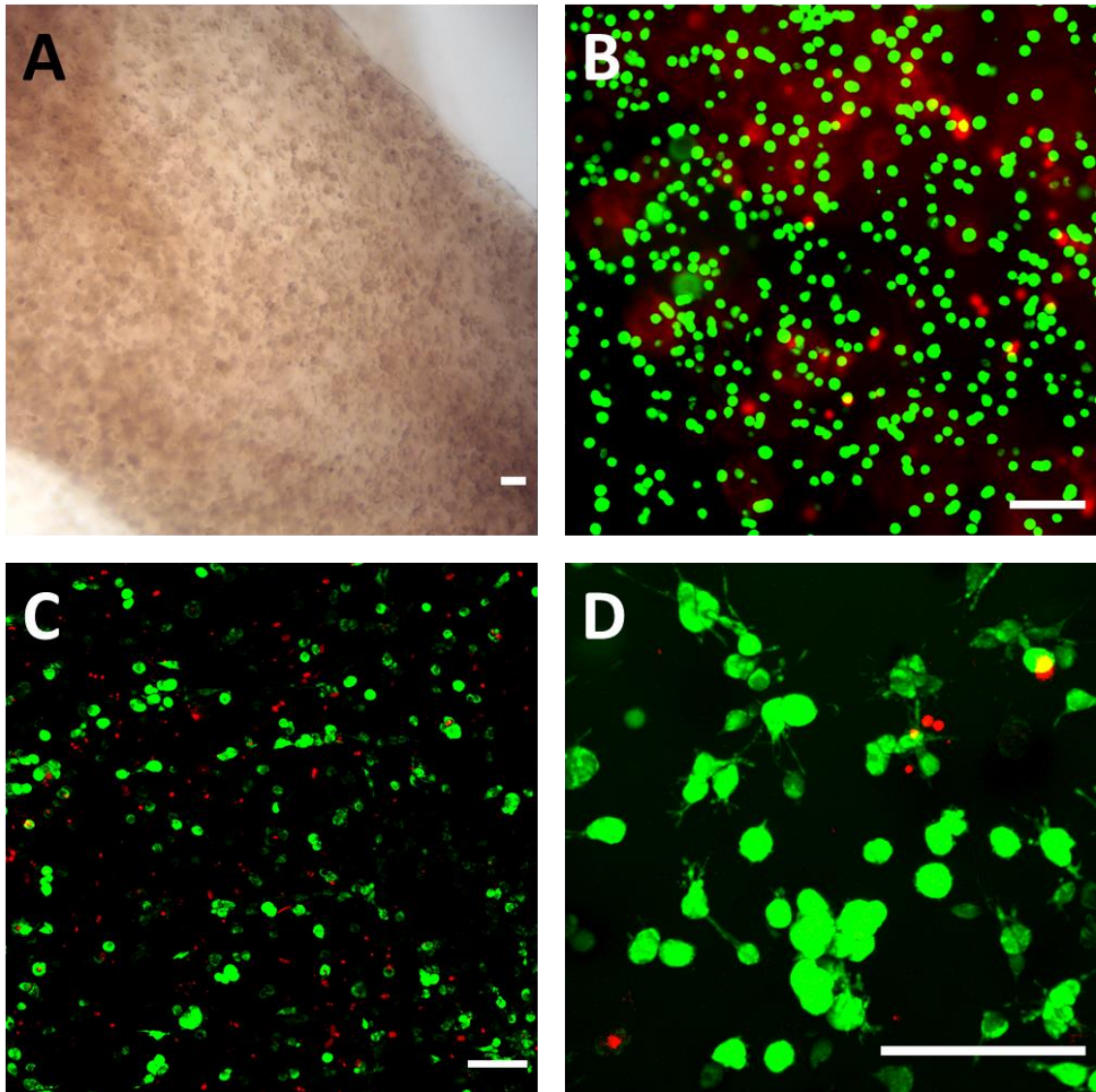


Figure 7.7: A collagen solution with HepaRG cells was pipetted into a Pluronic mould to form a 3D patch.

A: Brightfield microscopic picture of the collagen patch with the HepaRG cells B-D: Life(green)/dead(red) staining on pieces of the patch. B: Epifluorescent microscopic picture of the patch, D0. Unlike the bioprinted sample, a few dead cells could be seen from the onset of the experiment. C: Confocal microscopic picture of the patch, D3. Although a lot of dead cells can be seen, most cells appear to be viable. Cells are not rounded as in the bioprinted structure but have different shapes. D: Confocal microscopic picture of the patch, D7. This zoomed in picture shows both clusters of cells and extensions coming out of the cells. (scalebar 100 μ m)

7.4. Testing Vascularization Using the CAM Model

To test the possibility of vascularizing these patches, the CAM-model was used. Although first used as a tool for embryology, the CAM-model was adapted as an angiogenesis assay by Judah Folkman in 1974^[30]. The CAM of a chicken egg acts as a placenta or a lung for the chick embryo, allowing gas exchange between its blood supply and the surrounding atmosphere. The CAM is formed during day 3-5 of the embryonic development, when the chorion (outermost membrane), and the allantois (membrane sac responsible for collecting liquid waste and gas exchange) merge and a network of blood vessels is formed between them (Figure 7.8). Between day 8 and 10 the central part of the CAM (right above the embryo) is fully developed and the influence of (anti)angiogenic substances (in our case, the patches) can be researched. At day 12 the entire CAM is fully developed.^[2, 31] The CAM of a chicken egg is useful for angiogenesis research due to the combination of ample angiogenic activity and an immature immune system, which is unable to reject foreign cells or other substances.^[32]

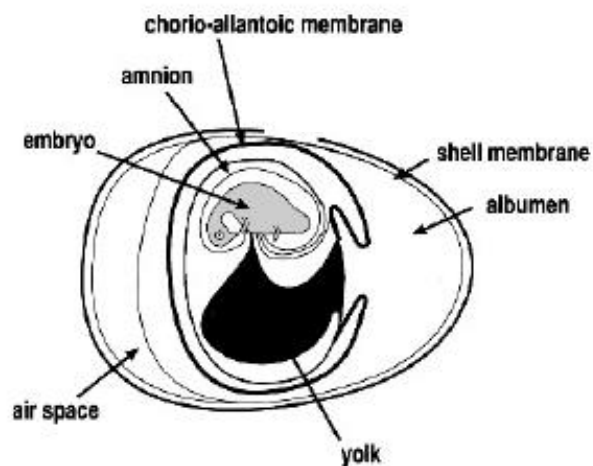


Figure 7.8: Schematic of the various anatomical structures of a fertilized chicken egg, showing the relative location of the chorioallantoic membrane (CAM).^[2]

The use of a chicken egg instead of testing animals has multiple advantages. First of all, a chicken egg is not a testing animal, so the researcher doesn't need to be qualified to work with testing animals. When the chicken egg is discarded before the 14th day after incubation, UK law allows the use of this model without the need of a personal or project licence.^[33] Another advantage are the costs, a simple egg costs a lot less (60p per egg) than a testing animal (tens of pounds per mouse), which must also be fed and cared for. A third advantage is that most of the tests done on the CAM only involve placing a test subject on top of the CAM, which does not require any surgical operations at all, making this model very user friendly.^[34] In this section the CAM model is used to investigate whether the patches would allow, or even increase, vascularisation to surround the encapsulated pancreatic islets.

Pluronic hydrogel moulds were created on day 8 of the egg incubation. Small, 2x2 grid moulds were printed using the Pluronic hydrogel (Figure 7.6 B) on petri-dishes, in batches of 3-4 per petri dish. These moulds were kept in the incubator until creating the patches on day 9 of the egg incubation. The small moulds were filled with 100 µl of one of 4 solutions; either a 1% purified Protanal solution, or a 4 mg/ml collagen solution, with or without 10 ng/ml VEGF (Figure 7.9). The patches were allowed to gel for 30 minutes in the incubator, before washing the moulds away with either cold PBS or a cold 100 mM CaCl₂ solution, for the collagen or alginate patches respectively. Patches were transferred into prewarmed medium and kept in the incubator until placement. The patches containing VEGF were placed in medium that also contained 10 ng/ml VEGF, to balance any VEGF leaching out. At day 10 of egg incubation, the patches were placed on the eggs (Figure 7.10). On day 13, the egg experiment was terminated by injecting the eggs with a fluorescent dye and euthanizing them. The patches were cut from the CAM, fixed in 10% formalin and kept in PBS until imaging with a confocal microscope (Figure 7.11). Collagen patches had shrivelled up and become fully opaque, while

alginate structures maintained their shape, but lost a bit of their translucency. This is most likely due to the patches drying out, as they are no longer in an aqueous surrounding.



Figure 7.9: The 4 different types of patches after releasing them from the mould, but before placing them in medium. Top: alginate patches without (Left) or with 10 ng/ml VEGF (right). Bottom: Collagen patches without (left) or with 10 ng/ml VEGF (right)

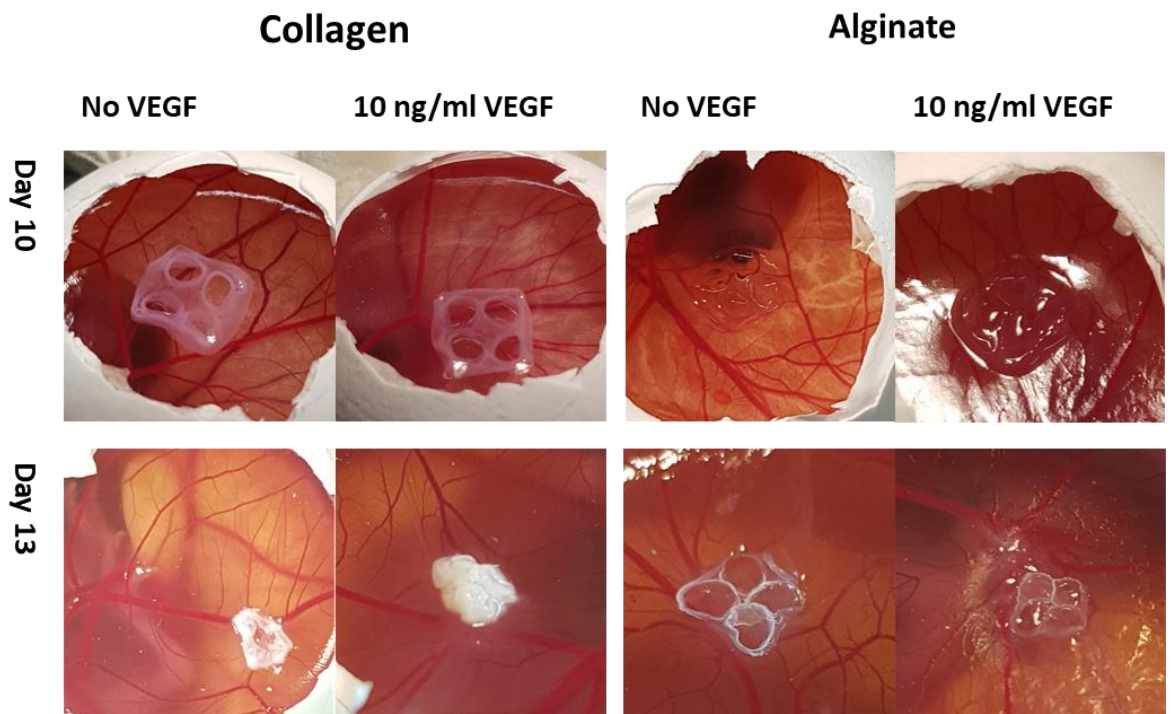


Figure 7.10: patches were placed on top of the CAM of chicken eggs on day 10 of egg incubation. On day 13 of incubation eggs were injected with a fluorescent dye and euthanized, before removing the patches. Collagen patches shrivelled up during the experiment and went from mostly translucent to fully opaque. Alginate patches maintained their shape but went from fully translucent to a little bit opaque. This is most likely due to the patches drying out.

Over the course of 3 experiments, 90 eggs in total were used. Out of these 90 eggs, 59 survived up to the point where a structure could be placed. This low survival rate is most likely due to the fact that in 2 out of 3 experiments, the eggs were not fresh but refrigerated for at least 1.5 weeks. In the experiment where fresh eggs were used, 29 out of 30 eggs were given a structure. Out of the 46 eggs that survived the entire experiment, only 1 was found to have a blood vessel growing into the structure (Figure 7.11). This was into a collagen patch without added VEGF. Since in the other 15 collagen-only patches no ingrowth could be seen, this can not be considered a representative result, but does show the possibilities of this type of experiments.

Even though almost no ingrowth of blood vessels could be observed, a notable difference could be seen in the vascular network on the CAM from the different groups (Figure 7.11). Where the alginate group without VEGF only shows rather large blood vessels, all the other groups show smaller networks. The patches loaded with VEGF show an increase in the density of the vascular network closer to the patch. This is in line with expectations, as VEGF encourages angiogenesis. Even though there is no in growth of blood vessels, the increase of blood vessel density near the patches would increase the concentration of oxygen and nutrients available to the islets within the patches.

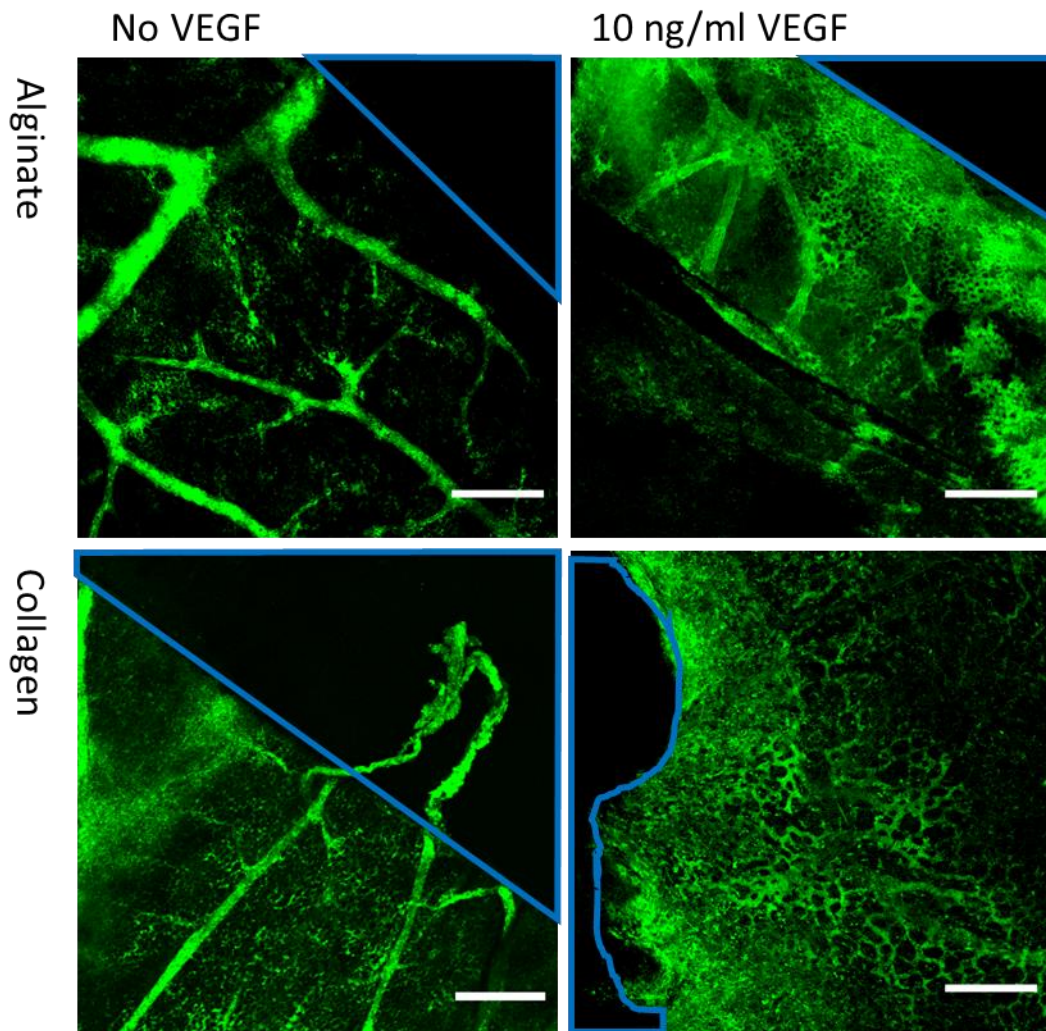


Figure 7. 11: Fluorescent images of blood vessel on the CAM of the chicken egg. Blue lines indicate location of patch. In only 1 patch (collagen) a clear ingrowth of blood vessels could be detected. For patches loaded with VEGF an increase of vascular density can be seen closer to the patch.

7.5. Conclusion

In this chapter a proof of concept was given for the pancreatic islet patch.

Alginate can be used to directly print patches with alginate beads (encapsulated islets) in them, to create a patch than can easily be manipulated and keep the encapsulated islets localized to one certain area. However, due to the bad survival rate of HepaRG cells in these patches, it is thought that they will not support cells migrating through the patch, which would effectively stop any blood vessel at the edge of the patch. This means that the diffusion distance between the islets and their main source of oxygen/nutrients is not only defined by the diameter of the encapsulation, but also the added material of the patch.

Therefore, a second type of material was used to create patches, collagen. Collagen could not be 3D bioprinted, so a moulding process was used. Pluronic hydrogels were 3D printed in the shape of a mould, which was then used to cast the collagen (or alginate) patch. Once the collagen had set, the mould could simply be washed away by using cold solutions. The collagen solution was able to provide a matrix for HepaRG cells to attach to and stay viable, which gives good hope that blood vessels would also be able to grow into these patches.

To check if blood vessels are capable of growing into the structures, the CAM model was used. Even though this experiment did not give any definite proof of blood vessels growing into the constructs, an increase of vessel density could be seen for patches that were loaded with VEGF.

Other materials should be tried for the creation of these patches, as well as maybe some other growth factors, such as basic fibroblast growth factor, as this seems to help create vascularized areas.^[17] Furthermore, experiments should be performed with actual cells (encapsulated aggregates) incorporated into the patches, as cells themselves can release growth factors continuously, inducing angiogenesis.^[35]

Finally, the concentration of encapsulations within the material should be increased to get clinically relevant patches. The bio-ink used to create the patch in Figure 7.3 had a concentration of 10,000 beads/ml, and it took 400 μ l to print the entire patch. This means that around 4000 beads were present in the patch. If every bead would be 1 encapsulated islet, 100 of those patches would be needed to transplant all of the 400,000 IEQ that are needed to treat a patient (based on a 80 Kg patient and the 5000 IEQ per Kg criteria used in current transplantations).^[1, 36]

In this chapter the way was paved for further research to create a patch that will enhance the microenvironment of the encapsulated islets. It was shown that 3D bioprinting methods can be used to create moulds to create patches in any shape desired, even when using slow gelling materials that could otherwise not be used for bioprinting. The quick solvability of Pluronic hydrogels as a mould allows for a quick and easy release of the final patch. Using a moulding approach allows for wide array of materials to be used to create patch, as well as different additives (such as growth factors, or even oxygenating compounds to bridge the time needed for vascularization),^[37] without being bound by the printability of the material.

7.6. References

- [1]. Shapiro AM, Ricordi C, Hering BJ, Auchincloss H, Lindblad R, Robertson RP, *et al.* International trial of the Edmonton protocol for islet transplantation. *New England Journal of Medicine*. **2006**;355(13):1318-30.
- [2]. Valdes T, Kreutzer D, Moussy F. The chick chorioallantoic membrane as a novel in vivo model for the testing of biomaterials. *Journal of Biomedical Materials Research: An Official Journal of The Society for Biomaterials, The Japanese Society for Biomaterials, and The Australian Society for Biomaterials and the Korean Society for Biomaterials*. **2002**;62(2):273-82.
- [3]. Delaune V, Berney T, Lacotte S, Toso C. Intraportal islet transplantation: the impact of the liver microenvironment. *Transplant International*. **2017**;30(3):227-38.
- [4]. Eich T, Eriksson O, Sundin A, Estrada S, Brandhorst D, Brandhorst H, *et al.* Positron Emission Tomography: A Real-Time Tool to Quantify Early Islet Engraftment in a Preclinical Large Animal Model. *Transplantation*. **2007**;84(7):893-8.
- [5]. Carlsson P-O, Palm F, Andersson A, Liss P. Markedly decreased oxygen tension in transplanted rat pancreatic islets irrespective of the implantation site. *Diabetes*. **2001**;50(3):489-95.
- [6]. Harlan DM, Kenyon NS, Korsgren O, Roep BO. Current Advances and Travails in Islet Transplantation. *Diabetes*. **2009**;58(10):2175-84.
- [7]. Bennet W, Sundberg B, Groth CG, Brendel MD, Brandhorst D, Brandhorst H, *et al.* Incompatibility between human blood and isolated islets of Langerhans: a finding with implications for clinical intraportal islet transplantation? *Diabetes*. **1999**;48(10):1907-14.
- [8]. Merani S, Toso C, Emamaullee J, Shapiro AMJ. Optimal implantation site for pancreatic islet transplantation. *British Journal of Surgery*. **2008**;95(12):1449-61.
- [9]. Rafael E, Tibell A, Rydén M, Lundgren T, Sävendahl L, Borgström B, *et al.* Intramuscular Autotransplantation of Pancreatic Islets in a 7-Year-Old Child: A 2-Year Follow-Up. *American Journal of Transplantation*. **2008**;8(2):458-62.
- [10]. Scharp DW, Swanson CJ, Olack BJ, Latta PP, Hegre OD, Doherty EJ, *et al.* Protection of Encapsulated Human Islets Implanted Without Immunosuppression in Patients With Type I or Type II Diabetes and in Nondiabetic Control Subjects. *Diabetes*. **1994**;43(9):1167-70.
- [11]. Vériter S, Gianello P, Dufrane D. Bioengineered sites for islet cell transplantation. *Current diabetes reports*. **2013**;13(5):745-55.
- [12]. de Vos P, Spasojevic M, Faas MM. Treatment of diabetes with encapsulated islets. *Therapeutic Applications of Cell Microencapsulation: Springer*; **2010**. p. 38-53.

- [13]. Marchioli G, Gurr Lv, Krieken PPv, Stamatialis D, Engelse M, Blitterswijk CAv, *et al.* Fabrication of three-dimensional bioplotting hydrogel scaffolds for islets of Langerhans transplantation. *Biofabrication*. **2015**;7(2):025009.
- [14]. El-Gohary Y, Sims-Lucas S, Lath N, Tulachan S, Guo P, Xiao X, *et al.* Three-Dimensional Analysis of the Islet Vasculature. *The Anatomical Record*. **2012**;295(9):1473-81.
- [15]. Olsson R, Carlsson P-O. Better vascular engraftment and function in pancreatic islets transplanted without prior culture. *Diabetologia*. **2005**;48(3):469-76.
- [16]. Vériter S, Mergen J, Goebbels R-M, Aouassar N, Grégoire C, Jordan B, *et al.* In Vivo Selection of Biocompatible Alginates for Islet Encapsulation and Subcutaneous Transplantation. *Tissue Engineering Part A*. **2010**;16(5):1503-13.
- [17]. Komatsu H, Rawson J, Barriga A, Gonzalez N, Mendez D, Li J, *et al.* Posttransplant oxygen inhalation improves the outcome of subcutaneous islet transplantation: A promising clinical alternative to the conventional intrahepatic site. *American Journal of Transplantation*. **2018**;18(4):832-42.
- [18]. Farina M, Ballerini A, Fraga DW, Nicolov E, Hogan M, Demarchi D, *et al.* 3D Printed Vascularized Device for Subcutaneous Transplantation of Human Islets. *Biotechnology Journal*. **2017**;12(9):1700169.
- [19]. Cornelissen D-J, Faulkner-Jones A, Shu W. Current developments in 3D bioprinting for tissue engineering. *Current Opinion in Biomedical Engineering*. **2017**;2:76-82.
- [20]. Gudapati H, Dey M, Ozbolat I. A comprehensive review on droplet-based bioprinting: Past, present and future. *Biomaterials*. **2016**;102:20-42.
- [21]. Faulkner-Jones A, Greenhough S, King JA, Gardner J, Courtney A, Shu W. Development of a valve-based cell printer for the formation of human embryonic stem cell spheroid aggregates. *Biofabrication*. **2013**;5(1):015013.
- [22]. Ozbolat IT, Hospodiuk M. Current advances and future perspectives in extrusion-based bioprinting. *Biomaterials*. **2016**;76:321-43.
- [23]. Wang X, Yan Y, Pan Y, Xiong Z, Liu H, Cheng J, *et al.* Generation of Three-Dimensional Hepatocyte/Gelatin Structures with Rapid Prototyping System. *Tissue Engineering*. **2006**;12(1):83-90.
- [24]. Atabak Ghanizadeh T, Miguel AH, Nicholas RL, Wenmiao S. Three-dimensional bioprinting of complex cell laden alginate hydrogel structures. *Biofabrication*. **2015**;7(4):045012.
- [25]. Gioffredi E, Boffito M, Calzone S, Giannitelli SM, Rainer A, Trombetta M, *et al.* Pluronic F127 hydrogel characterization and biofabrication in cellularized constructs for tissue engineering applications. *Procedia CIRP*. **2016**;49:125-32.
- [26]. Khattak SF, Bhatia SR, Roberts SC. Pluronic F127 as a cell encapsulation material: utilization of membrane-stabilizing agents. *Tissue Engineering*. **2005**;11(5-6):974-83.

- [27]. Suntornnond R, Tan EYS, An J, Chua CK. A highly printable and biocompatible hydrogel composite for direct printing of soft and perfusable vasculature-like structures. *Scientific Reports*. **2017**;7(1):16902.
- [28]. Kolesky DB, Truby RL, Gladman AS, Busbee TA, Homan KA, Lewis JA. 3D Bioprinting of Vascularized, Heterogeneous Cell-Laden Tissue Constructs. *Advanced Materials*. **2014**;26(19):3124-30.
- [29]. Au - Müller M, Au - Becher J, Au - Schnabelrauch M, Au - Zenobi-Wong M. Printing Thermo-responsive Reverse Molds for the Creation of Patterned Two-component Hydrogels for 3D Cell Culture. *JoVE*. **2013**(77):e50632.
- [30]. Folkman J. Tumor angiogenesis factor. *Cancer Research*. **1974**;34(8):2109-13.
- [31]. Deryugina EI, Quigley JP. Chick embryo chorioallantoic membrane models to quantify angiogenesis induced by inflammatory and tumor cells or purified effector molecules. *Methods in enzymology*. **2008**;444:21-41.
- [32]. Ribatti D. The chick embryo chorioallantoic membrane in the study of tumor angiogenesis. *Rom J Morphol Embryol*. **2008**;49(2):131-5.
- [33]. Home-Office. Animals (Scientific Procedures) Act 1986. In: Office H, editor. <https://www.gov.uk/government/publications/consolidated-version-of-aspa-1986>: UK Government; 2012.
- [34]. Nowak-Sliwinska P, Segura T, Iruela-Arispe ML. The chicken chorioallantoic membrane model in biology, medicine and bioengineering. *Angiogenesis*. **2014**;17(4):779-804.
- [35]. Morfoisse F, Renaud E, Hantelys F, Prats A-C, Garmy-Susini B. Role of hypoxia and vascular endothelial growth factors in lymphangiogenesis. *Molecular & cellular oncology*. **2014**;1(1):e29907-e.
- [36]. Tatum JA, Meneveau MO, Brayman KL. Single-donor islet transplantation in type 1 diabetes: patient selection and special considerations. *Diabetes, metabolic syndrome and obesity : targets and therapy*. **2017**;10:73-8.
- [37]. Farris AL, Rindone AN, Grayson WL. Oxygen Delivering Biomaterials for Tissue Engineering. *Journal of materials chemistry B*. **2016**;4(20):3422-32.

Chapter 8

Summary and Future Work

8.1. Research Assessment

The initial aim of this research was to develop a novel method of quickly encapsulating pancreatic islets for clinical transplantation. After the initial literature review it was evident that the electro-spraying method could produce mono-sized encapsulations on a smaller scale than the conventional air-based droplet generator. This method has been used previously on rat islets,^[1, 2] but never before on human islets (to our best knowledge). However, this encapsulation method would have the same problems as other encapsulation methods, with the main problem being the vascularization. If islets can not be vascularized, they must get their nutrients and oxygen through diffusion, and any islets that are too big will develop a necrotic core.^[3] Apart from that, a foreign material is added to the body, so it has to be as biocompatible as possible so it will not trigger the immune system. After the encapsulation method was developed, the research focused on overcoming the problems involved with encapsulation. To diminish the diffusion distance to the islets as much as possible, a choice was made to try to create beads that are small and uniform. Secondly, the material used for encapsulation was purified, so it will not set off the immune response. Care was taken to ensure that islets would be able to survive and be functional in the material without any problem. To overcome the necrotic core problem, research was performed to create a one-step encapsulation method in which a liquid core would allow cells to aggregate after encapsulation. That way bigger islets could be broken up and reassembled into smaller, functional islets, maybe even with the addition of other beneficial cells. Finally, the use of 3D bioprinting techniques was researched for the creation of pancreatic islet patches, that would localize the extrahepatic transplantation of the encapsulated islets and could enhance the environment of the islets by promoting angiogenesis, creating a higher vascularized area.

8.2. Conclusions Summary

The overall aim of this thesis was to enhance islet encapsulation for clinical transplantation.

Although an encapsulation method was developed that can create uniform, small encapsulations, further research is necessary to truly enhance the encapsulations of islets.

Key findings of this thesis are summarized below

- An electro-spray encapsulation device was quickly created using rapid prototype methods, including syringe pumps that outperformed an off-the-shelve syringe pump. Six parameters (concentration of alginate, distance between needle and gelling bath, extrusion speed, gelling bath, needle size and voltage) were defined and tested, to create uniform small encapsulations.

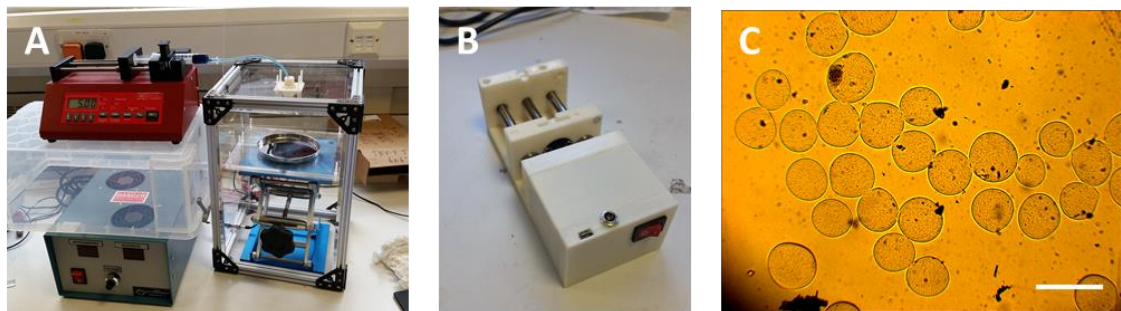


Figure 8.1 Pictorial summary of the development of the encapsulator. A: the encapsulator in its first stage. B: The development of the home-made syringe pump. C: Testing the encapsulator for size and uniformity. (Scalebar 500 μm)

- A purification protocol was adapted to shorten it from a 10-day protocol to a 2-day protocol. Endotoxins, proteins and polyphenols were successfully removed by 99.99%, 63% and 91%, respectively, making this a successful protocol.
- The permeability of alginate hydrogels was measured using fluorescent dyes of different sizes and confocal microscopy. It was found that alginate concentration, alginate purifity and the cations used in the crosslinking all have an influence on the permeability of the formed hydrogel.

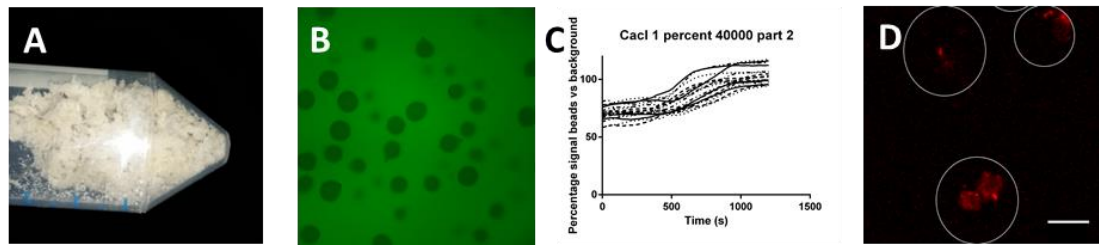


Figure 8.2: A pictorial summary of the purification of the alginate and testing it for permeability. A: alginate was purified using a shortened protocol. B: Using confocal microscopy and FITC-conjugated dextran molecules of different size, the permeability of alginate beads was measured. C: By measuring the fluorescent signal over time, permeability of alginate for different sized molecules could be established. D: When testing the encapsulation with ADSC aggregates, it was found they could prevent attachment of IGM antibodies for at least 24 hours.

- A coaxial needle was used to create alginate encapsulations with a liquid core. To successfully create these encapsulations, the viscosity of both shell and core material must be similar. Furthermore, the speed at which the outer material is dispensed must be larger than that of the inner material. Good results were begotten with a ratio of 4.10 between outer and inner speed.
- HepaRG cells encapsulated using this method aggregated and formed organoids. These organoids showed hepatic function and stained positive for albumin (an adult hepatocyte marker) and patches of CK19 (a bile duct endothelial cell marker)

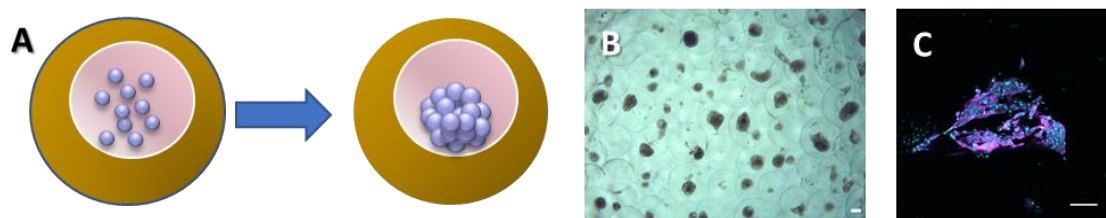


Figure 8.3: A pictorial summary of the core-shell encapsulation. A: Beads with a fluid core but an alginate hydrogel shell were created using coaxial needles. The fluid core allows cells to come together and aggregate. B: This method was successfully used to create HepaRG organoids encapsulated in alginate. C: HepaRG cells self-organized into intricate structures. (Scalebar 100 μm)

- Islet encapsulated in alginate kept their morphology, viability and functionality for over 3 months. In contrast, control islets kept on tissue culture plates lost their morphology within less than a month, and control islets kept on ultra-low attachment plates aggregated into larger islets and did not survive for more than a few weeks.
- When using the core-shell encapsulation method with dissociated islets to form smaller, functional islets, the cells did not survive. When using the system with whole islets, the islets slowly died within 3 months, most likely due to the toxicity of the CMC-solution needed for this method.
- No suitable replacement for CMC as a viscosity enhancer was found in this research, as most of the viscosity enhancer did not maintain viable islets for more than 2 weeks.

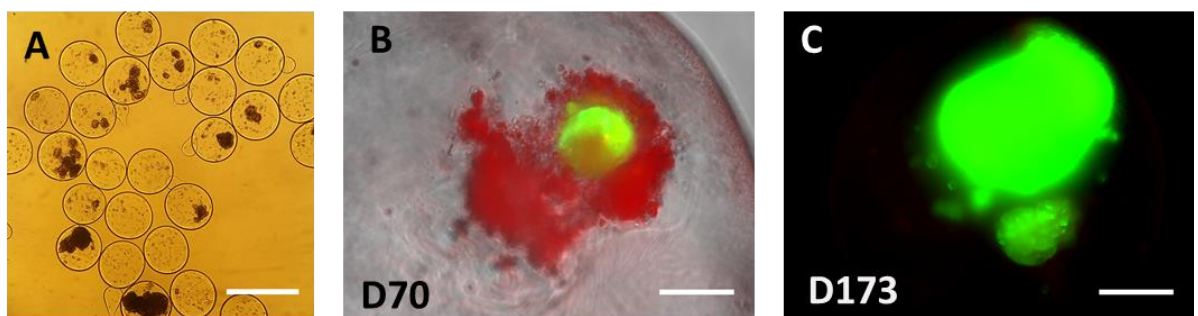


Figure 8.4: A pictorial summary of the encapsulation of pancreatic islets. A: A brightfield microscopy picture of islets encapsulated in purified Protanal alginate B: Islets encapsulated in the core-shell beads did not survive culturing for prolonged periods of time and were not functional. C: Islets encapsulated in purified Protanal alginate only did remain viable and functional for a prolonged period of time. (Scalebar A 500 μm ; Scalebar B&C 100 μm)

- 3D patches containing encapsulations could be 3D bioprinted using pre-crosslinked alginate, but not collagen. The pre-crosslinked alginate had enough mechanical stability to keep its shape until fully crosslinked. However, collagen was either too liquid or too inhomogeneous to be used as a bio-ink for 3D bioprinting.

- Using Pluronic as a sacrificial material, moulds in intricate designs could be created to fabricate both collagen and alginate patches. It was found that cells survived and attached better in the collagen patch than in the alginate patch.
- When placed on the CAM of a chicken egg, almost no patches showed any form of blood vessel ingrowth. However, when looking at the smaller blood vessels using confocal microscopy, it could be seen that the blood vessels surrounding collagen or VEGF loaded alginate structures appeared to be more dense than those surrounding alginate only structures.

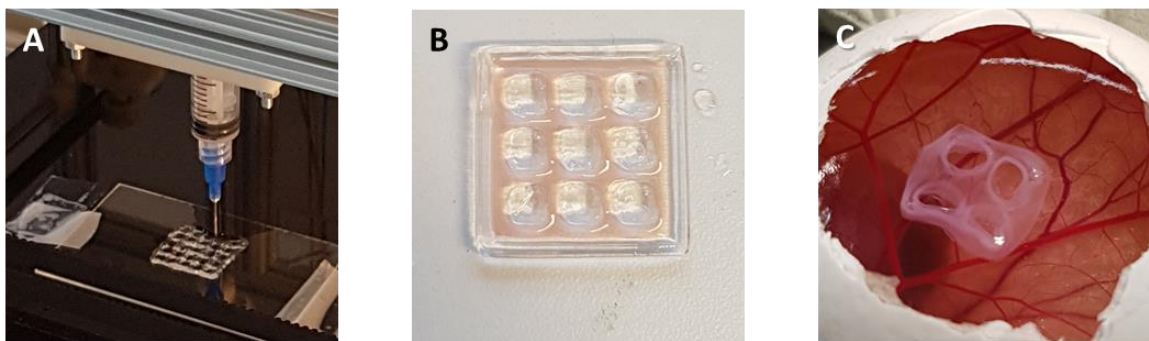


Figure 8.5: Pictorial summary of the creation and testing of patches. A: Alginate patches can be directly 3D bioprinted in large structures, using a pre-crosslinked alginate gel. B: Collagen patches could not be directly bioprinted but can be moulded in 3D printed Pluronic moulds. C: The patches were tested to see if any blood vessels would grow in by using the CAM-model.

8.3. Recommendations and Future Work

In this thesis, a lot of different aspects of the encapsulation of islets or cells have been touched upon. The development of a micro-encapsulation machine, the purification of the encapsulation material, encapsulating and testing the function of multiple cell types and combining the encapsulation method with other biofabrication methods were all addressed. However, due to the broad nature of this work, some interesting research areas were not further investigated. In this section some other ideas, which were not (fully) investigated are presented, which could be used for further research.

8.3.1. The Micro-encapsulator

Although the micro-encapsulator went through a number of improvements, there is still room for further work. The first thing that could be improved is the ground electrode. The final electrode used in this research gave reproducible results, but due to the fact that it is “dunked” into the gelling bath, it does present a risk for (cross) contaminations. It has to be carefully cleaned with a disinfectant before and after every use and then rinsed in PBS to ensure no toxicity of the disinfectant would harm the cells. This was very time consuming, and probably would not be the best option for a machine intended to be used clinically. Although it was not thought of when developing the machine, there is a very easy solution to the problem. The entire baseplate on which the gelling bath is standing could be made into a ground electrode (Figure 8.6).^[4] That way nothing needs to be inserted into the gelling liquid, there is no difference in field strength when the petri dish or dispensing needle are not in the exact same place, and determining the distance between the ground electrode and the dispensing needle is just as easy as with the dunking electrode.

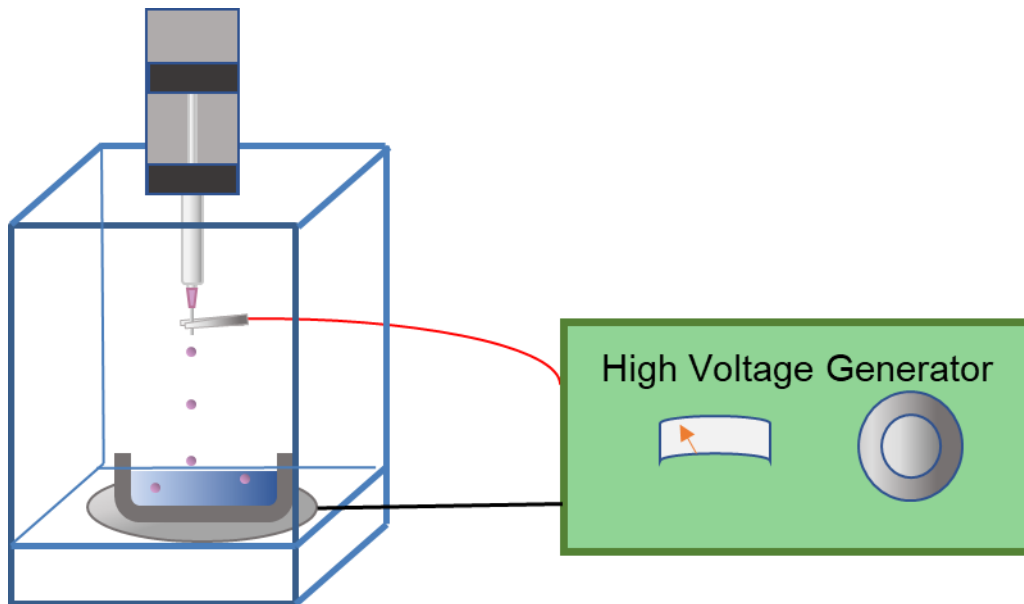


Figure 8.6 One improvement that could be made for the micro-encapsulator is creating a plate underneath the petri dish that would act as the ground electrode.

8.3.2. Core-shell Encapsulation of Pancreatic Islets

Although the core-shell encapsulations worked well to encapsulate and aggregate HepaRG cells, the method was not useful in combination with islets, or islet cells. The main reason for this was the fact that the CMC necessary to increase the viscosity of the core-material turned out to be toxic for the islet cells. It would be interesting to test more viscosity increasing substances to see if any would support pancreatic islet cells. For instance, a look could be taken at different proteins, like collagen^[5], gelatine^[6] or laminin.^[7] When a suitable replacement for CMC is found, the coaxial encapsulation of islet cells could be repeated.

Furthermore, only the core-shell method was investigated to create smaller, functional islets, as a one-step protocol was sought after. It would have been interesting to also use the micro-well assay to create smaller islets, with or without additional cells like hepatic cells or stem cells, to investigate their function without any encapsulation and the influence of the added cells on the pseudo-islets.

Another subject that could be investigated, is the creation of a multicore bead (Figure 8.7). In this thesis the focus was put on creating small, uniform encapsulations to minimize the diffusion distance. However, it is known that islet can survive (*in vitro*) in alginate beads up to 1.5mm in diameter, as long as the islets themselves are not too big.^[3] Furthermore, it has been shown that bigger beads actually induce less fibrotic overgrowth after transplantation,^[1] so going small might not have been the optimal idea. When bigger encapsulations would be produced, it would be very interesting to see whether it would be able to create multiple liquid compartments within the bigger bead, creating multiple aggregates (Figure 8.7 B).

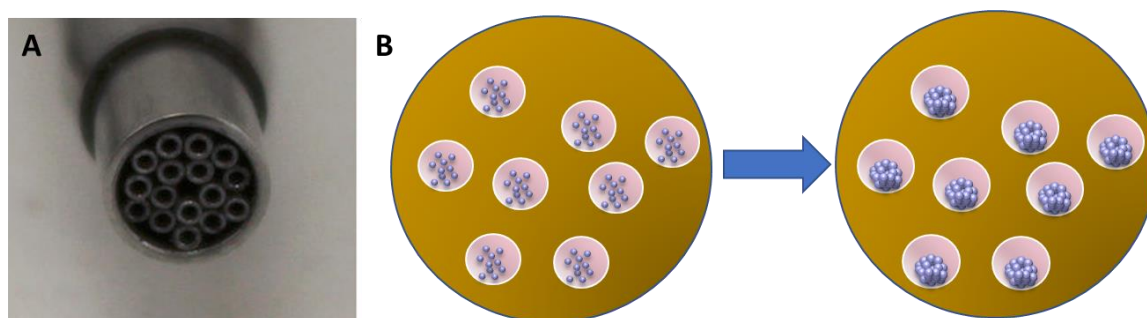


Figure 8.7 A multilumen coaxial needle could be used to create alginate beads with multiple liquid cores, to create larger beads with multiple aggregates inside. A: An example of a multilumen coaxial needle.^[8] B: A schematic overview of the multicore-shell bead idea.

8.3.3. Pancreatic Islet Patch

The islet patch has a large potential to truly enhance islet transplantation. However, more time should be spent in choosing a good biomaterial to create that patch.

The alginate did not support cell attachment or migration, making it a bad choice for the creation of these patches. Furthermore, Marchioli et al. show us that islets in bioprinted alginate structures are no longer responsive to glucose.^[9] This could be due to the high concentration of alginate used, or the fact that they used CaCl_2 as their crosslinking agent. Using the Pluronic mould method, these patches could be created using lower

concentrations of alginate and with other crosslinking agents (like BaCl₂), which could bring back the function of the islets, but it still would not allow the ingrowth of blood vessels.

The collagen used in this research also did not have a lot of success with ingrowth of blood vessels using the CAM-assay. It is therefore really interesting to look into other materials to see whether they would promote the ingrowth of blood vessels. One of the first materials that could be investigated is Matrigel, whose plug-assay is one used a lot for *in vivo* angiogenesis research.^[10] However, a synthetic material tailor made for cell adhesion and migration^[11] could also be interesting, or materials that release growth factors over time to further induce angiogenesis.^[12] However, this kind of work could be an entire PhD on its own, and fell outside the scope of this research.

8.3.4. *In Vivo* Testing

The logical next step for this research would be to start doing *in vivo* assays. Most of the research done in this thesis were *in vitro* approximations, indicating how the body would respond to the encapsulated islets. However, *in vivo* testing could supply us with better indications of whether the encapsulations would be successful.

The first thing that should be tested is how the immune response of a testing animal would react to the purified alginate. Alginate beads of both purified and non-purified alginate could be transplanted subcutaneous in mice and retrieved after 14 days. Histological investigation could be done into fibrotic overgrowth and cellular deposition (for instance macrophages and neutrophils) on the beads. This test could further proof whether purification of the material helps to make it more biocompatible.

After testing the material, the encapsulated islets must be tested to see whether they are as good as non-encapsulated islets for the treatment of diabetes. Human (encapsulated) islets should be transplanted in diabetic, immune-incompetent mice. By checking blood glucose

levels over time (and maybe even human c-peptide levels in the blood) the function of the islets can be measured. If both the mice with encapsulated islets and the group of mice with non-encapsulated islets manages to return to normoglycemia, this test could be marked as a success.

Once the function of encapsulated islets has been shown, the added value of the encapsulation should be confirmed. Just as in the previous experiment, human (encapsulated) islets should be transplanted in diabetic mice, this time with a working immune system. If the encapsulations are capable of shielding the islets from the immune system, the mice with the encapsulated islets will maintain normoglycemia, while those with the non-encapsulated islets will develop hyperglycemia over time, when they are being destroyed by the immune system.

The final thing that could be interesting to test *in vivo* would be the pancreatic islet patches. Although the CAM-assay is a cheap, easy way to investigate angiogenesis, blood vessels are only capable of growing into the constructs from one side. Furthermore, the constructs can dry out quickly on the CAM. When transplanting the patches subcutaneous, blood vessels can grow in from all different directions, and the body fluids can prevent the constructs from drying out. The final step would be to incorporate the encapsulated islets into the patch, and see whether the patch is capable of reversing diabetes in the mice.

8.4. References

- [1]. Veisheh O, Doloff JC, Ma M, Vegas AJ, Tam HH, Bader Andrew R, *et al.* Size- and shape-dependent foreign body immune response to materials implanted in rodents and non-human primates. *Nature Materials*. **2015**;14:643.
- [2]. Ma M, Chiu A, Sahay G, Doloff JC, Dholakia N, Thakrar R, *et al.* Core–shell hydrogel microcapsules for improved islets encapsulation. *Advanced Healthcare Materials*. **2013**;2(5):667-72.
- [3]. de Vos P, Lazarjani HA, Poncelet D, Faas MM. Polymers in cell encapsulation from an enveloped cell perspective. *Adv Drug Deliv Rev*. **2014**;67-68:15-34.
- [4]. Gasperini L, Maniglio D, Migliaresi C. Microencapsulation of cells in alginate through an electrohydrodynamic process. *Journal of Bioactive and Compatible Polymers*. **2013**;28(5):413-25.
- [5]. Chao S-H, Peshwa MV, Sutherland DER, Hu W-S. ENTRAPMENT OF CULTURED PANCREAS ISLETS IN THREE-DIMENSIONAL COLLAGEN MATRICES. **1992**;1(1):51-60.
- [6]. Del Guerra S, Bracci C, Nilsson K, Belcourt A, Kessler L, Lupi R, *et al.* Entrapment of dispersed pancreatic islet cells in CultiSpher-S macroporous gelatin microcarriers: Preparation, in vitro characterization, and microencapsulation. *Biotechnology and Bioengineering*. **2001**;75(6):741-4.
- [7]. Weber LM, Anseth KS. Hydrogel encapsulation environments functionalized with extracellular matrix interactions increase islet insulin secretion. *Matrix Biology*. **2008**;27(8):667-73.
- [8]. Ramehart, *Multilumen Spinnerets*, <https://www.customspinnerets.com/multichannel>, **2018**
- [9]. Marchioli G, Gurr Lv, Krieken PPv, Stamatialis D, Engelse M, Blitterswijk CAv, *et al.* Fabrication of three-dimensional bioplotting hydrogel scaffolds for islets of Langerhans transplantation. *Biofabrication*. **2015**;7(2):025009.
- [10]. Akhtar N, Dickerson EB, Auerbach R. The sponge/Matrigel angiogenesis assay. *Angiogenesis*. **2002**;5(1-2):75-80.
- [11]. Lutolf MP, Raeber GP, Zisch AH, Tirelli N, Hubbell JA. Cell - responsive synthetic hydrogels. *Advanced Materials*. **2003**;15(11):888-92.
- [12]. Zisch AH, Schenk U, Schense JC, Sakiyama-Elbert SE, Hubbell JA. Covalently conjugated VEGF–fibrin matrices for endothelialization. *Journal of Controlled Release*. **2001**;72(1):101-13.

Supplementary data

```

#include <AccelStepper.h>
AccelStepper stepper(1, 9, 10); //driver, step, direction

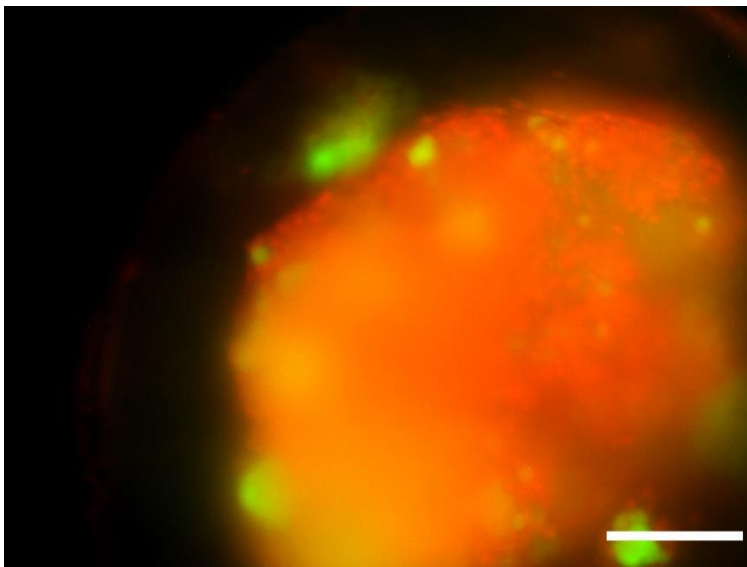
const int buttonPin = 2; //this pin is connected to the endstop
int buttonState = 0;
void setup() {
  Serial.begin(9600);
  stepper.setMaxSpeed(3000.0); // maximum steps/second
  stepper.setSpeed(31.5);      // speed at which the stepper motor will run (steps/second; 6.3 steps/second=1ml/h)

  pinMode(buttonPin, INPUT);
}

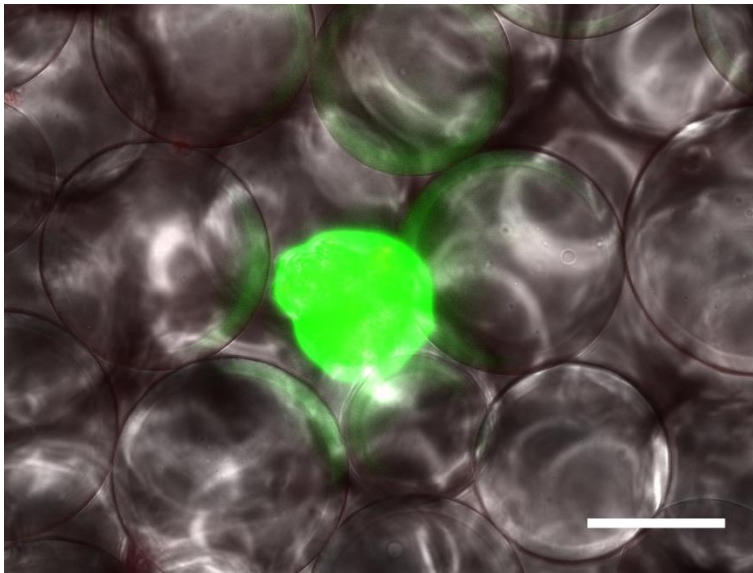
void loop() {
  buttonState = digitalRead(buttonPin);
  if (buttonState == HIGH) {      //If the endstop is not pushed in, buttonstate will be high
    stepper.runSpeed();           //actual code that runs the stepper motor at the set speed
    Serial.println("Hi DJ, this is syringe pump 2, 5mlh"); //When connected to a laptop, this message will appear
  }
  else {
    Serial.println("I'm turned off"); // when the endstop is reached, this message will appear
  }
}

```

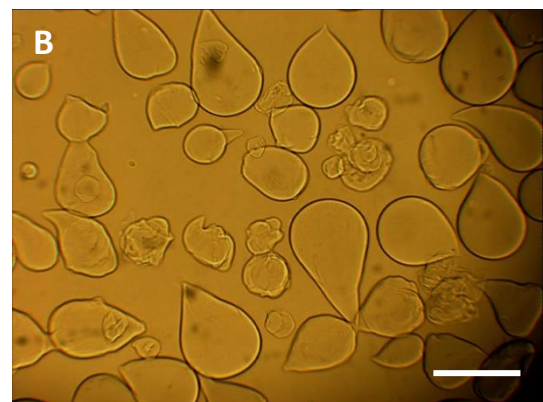
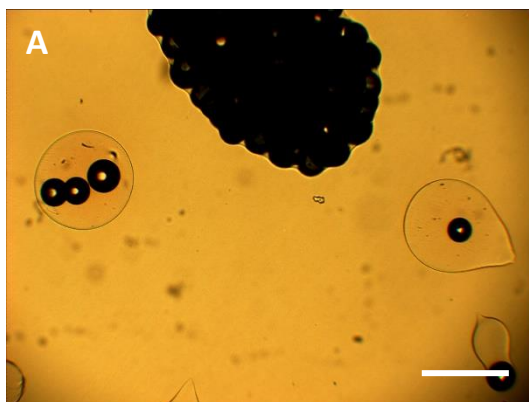
S 1: The code used to run the stepper motor of the syringe pump using an Arduino Micro.



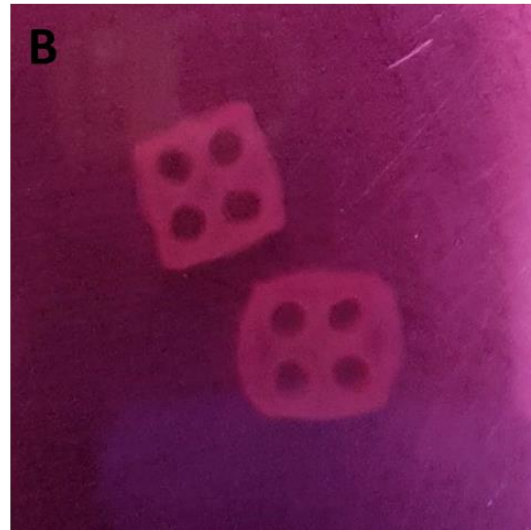
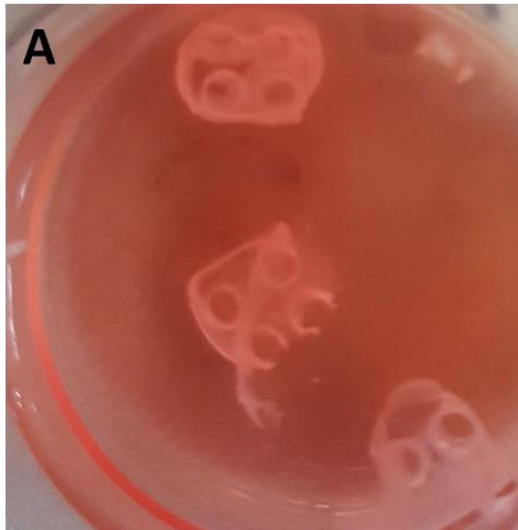
S 2: Live (green) / dead (red) staining of an encapsulated pancreatic islets (D14). Extreme large pancreatic islets did not survive the encapsulation process. (Scalebar 100 μ m)



S 3: Live (green) / dead (red) staining on D14 on islets cultured in 2% microcarrier beads. Although most of the islets near the bottom of the plate had died by this point (Figure 7.15), this islet that lay on top had survived for 14 days.



S 4: Microscopic pictures of a trial where microcarrier beads were encapsulated. The beads would get stuck in the nozzle, and come out in big clumps (A) or not come out at all, while the alginate was pushed past them (B). (Scalebar 500 μ m)



S 5: A: The first few collagen structures that were moulded in Pluronic moulds without added CaCl_2 were mechanically weak, and it appeared as if the collagen concentrated itself around the edges of the construct. When handled, these structures fell apart easily. B: When the Pluronic moulds made for alginate (with added CaCl_2) were used to create collagen patches, more evenly crosslinked structures were formed, that were easier to handle. Therefore, Pluronic moulds with added CaCl_2 were used to create both alginate and collagen structures for the experiments.